IL

NUOVO CIMENTO

ORGANO DELLA SOCIETÀ ITALIANA DI FISICA

SOTTO GLI AUSPICI DEL CONSIGLIO NAZIONALE DELLE RICERCHE

Vol. VI, N. 5 | *Serie decima* | 1° Novembre 1957

Dispersion Relations for Heavy Meson-Nucleon Interaction in a Fixed Source Theory - I.

D. Amati

Istituto di Fisica Teorica - Università di Napoli
Istituto Nazionale di Fisica Nucleare - Sezione di Roma

B. Vitale (*)

Istituto di Fisica dell'Università - Catania
Centro Siciliano di Fisica Nucleare - Catania

(ricevuto il 8 Giugno 1957)

Summary. — Dispersion relations for K-N and $\overline{\mathrm{K}}$-N interactions are obtained in a fixed source approximation. The simultaneous presence of K and $\overline{\mathrm{K}}$ in the heavy meson field is taken into account, as well as the interaction of the pion field with the barions. The dispersion relations for the forward scattering amplitudes are obtained without specifying the Hamiltonian in detail. The results are applied to the special cases of « scalar » and « pseudo-scalar » heavy mesons. For these special cases, a simpler method similar to that of Chew and Low is developed. Results are analyzed and compared formally to those obtained in previous work where rather stringent approximations were done. The neglect of $\overline{\mathrm{K}}$ in K-N scattering (and the inverse) seems unjustifiable. The presence of the pion field is effective in the definition of the K-N-Λ and K-N-Σ renormalized coupling constants, and gives raise to unphysical regions in the dispersion integrals.

Introduction.

Growing experimental information has brought in the last months a considerable interest in the theory of heavy meson-nucleon interaction. Some

(*) Now at Istituto di Fisica Teorica - Università di Napoli.

non-perturbative approaches were done for K-N [1,2] and $\overline{\text{K}}$-N [3] scattering, but in all of them some rather stringent hypotheses were made: the K particles were considered alone without $\overline{\text{K}}$ (or viceversa) coupled to a fixed barion. The problem immediately arises of how the actual presence of both K and $\overline{\text{K}}$ particles in the heavy meson field and the pion field interacting with the barions will influence the K-N and $\overline{\text{K}}$-N interactions. A problem of several interacting fields is obviously rather complicated: nevertheless we shall see that an insight in this problem can be given with rather general methods.

We shall restrict ourselves, however, to the fixed source theory. Owing to the rather large mass of the heavy mesons, the neglected recoil effects will be more important here than in the pion nucleon scattering; nevertheless it is to be expected that their inclusion would not alter essentially the characteristic features of the theory.

In Sect. **1** we shall derive the dispersion relations for heavy meson-nucleon scattering on rather general grounds, following a method similar to that developed by A. KLEIN [4] for the π-N scattering. Here we shall not specify the form of the Hamiltonian, but only assume for it some general properties. In Sect. 2 we shall apply the results obtained in Sect. 1 to the Salam Hamiltonian [5] in its fixed source limit, and to the corresponding one for « pseudoscalar » heavy mesons. For these particular Hamiltonians we shall develop in Sect. 3 the dispersion relations obtained with the Chew-Low method [6]. They present some simplifications with respect to dispersion relations obtained in the more general way but the integrals appearing there are surely less rapidly convergent and then probably more difficult to handle.

1. – Fixed source dispersion relations.

First of all we shall establish the general properties that we assume for the Hamiltonian H. We shall consider here only strong interactions, this meaning that H will conserve strangeness and isobaric spin [7]. Besides, being H the Hamiltonian of all the strong interacting particles, (N, Λ, Σ, π, K, $\overline{\text{K}}$), we shall have the spectrum of eigenvalues given by the real particles. This

(1) H. P. STAPP: *Phys. Rev.*, **106**, 134 (1957). This author treats also the direct K-π interaction as preposed by SCHWINGER (*Phys. Rev.*, **104**, 1164 (1956)).

(2) D. AMATI and B. VITALE: *Proc. of the VII Rochester Conference*; and *Nuovo Cimento*, **5**, 1533 (1957).

(3) D. AMATI and B. VITALE: *Nuovo Cimento*, **6**, 261 (1957).

(4) A. KLEIN: *Phys. Rev.*, **104**, 1131 (1956).

(5) A. SALAM: *Nuclear Physics*, **2**, 173 (1956-57).

(6) G. F. CHEW and F. E. LOW: *Phys. Rev.*, **104**, 235 (1956), we shall refer to this paper with the abbreviation C.L.

(7) M. GELL-MANN and A. PAIS: *Proc. of the Glasgow Conference* (1954), p. 342; B. D'ESPAGNAT and J. PRENTKY: *Nuclear Physics*, **1**, 33 (1956).

2874

means that we have discrete eigenvalues at m_N, m_Λ and m_Σ (measured masses of N, Λ and Σ particles respectively), i.e.

$$(1) \qquad H|\boldsymbol{N}_{r,t}\rangle = m_N|\boldsymbol{N}_{r,t}\rangle\,, \qquad H|\boldsymbol{\Lambda}_r\rangle = m_\Lambda|\boldsymbol{\Lambda}_r\rangle\,, \qquad H|\boldsymbol{\Sigma}_{r,t}\rangle = m_\Sigma|\boldsymbol{\Sigma}_{r,t}\rangle\,,$$

where the kets are the true (dressed) particle eigenfunctions, r and t the indices of spin and isobaric spin respectively. Following the usual procedure we substract m_N from the barion masses i.e. we put equal to 0 the nucleon mass; we shall then call $E_\Lambda = m_\Lambda - m_N$, $E_\Sigma = m_\Sigma - m_N$. From $E = m_\pi$ there will be a continuous set of eigenvalues, another one from $E_\Lambda + m_\pi$ and so on from $2m_\pi$, $E_\Sigma + m_\pi$, ..., m_K, $m_K + m_\pi$, etc.

Let

$$(2) \qquad A_i = \sum_k \frac{1}{\sqrt{2\omega}}\left[a_{k_i}\exp\left[i\boldsymbol{k}\cdot\boldsymbol{r}\right] + b^+_{k_i}\exp\left[-i\boldsymbol{k}\cdot\boldsymbol{r}\right]\right],$$

be the heavy meson field operator where a_{k_i} and b_{k_i} ($a^+_{k_i}$, $b^+_{k_i}$) are the destruction (creation) operators of K and $\overline{\text{K}}$ particles, respectively, with momentum $\boldsymbol{k}$ and isobaric spin index i ($\frac{1}{2}$ for K^+ and K^-, and $-\frac{1}{2}$ for K^0 and $\overline{K}^0$). $\omega = \sqrt{k^2 + m_K^2}$ is the heavy meson total energy ([8]). In the subindex k we include possible spin indices. We shall assume that the heavy meson field operator A_i is coupled to the source function with the same high energy cut-off factor $v(\omega)$ for all the couplings.

The other assumption we shall make is on the behaviour of the matrix elements at high energy; this is essentially a restriction on the order of the derivatives that can be present in the interaction Hamiltonian.

We now define

$$(3) \qquad V_{k_i} = [H', a^+_{k_i}]\,, \qquad \overline{V}_{k_i} = [H', b^+_{k_i}]\,,$$

$$(4) \qquad U_{k_i} = [a_{k_i}, [H', a^+_{k_i}]]\,, \qquad \overline{U}_{k_i} = [b_{k_i}, [H', b^+_{k_i}]]\,,$$

(where H' is the complete interaction Hamiltonian) and from the form of the heavy meson operator given in (2) we note that:

$$(5) \qquad V^+_{k_i} = \overline{V}_{-k_i}\,, \qquad U^+_{k_i} = \overline{U}_{-k_i}\,.$$

Being $|\boldsymbol{N}_{r+}\rangle$ a physical proton state, we define

$$(6) \qquad \begin{cases} T_i(\omega, n) = \langle \Psi_n^{(-)}|V_{k_i}|\boldsymbol{N}_{r+}\rangle\,, & \overline{T}_i(\omega, n) = \langle \Psi_n^{(-)}|\overline{V}_{k_i}|\boldsymbol{N}_{r+}\rangle\,, \\ Y_i(\omega) = \langle \boldsymbol{N}_{r+}|U_{k_i}|\boldsymbol{N}_{r+}\rangle\,, & \overline{Y}_i(\omega) = \langle \boldsymbol{N}_{r+}|\overline{U}_{k_i}|\boldsymbol{N}_{r+}\rangle\,, \end{cases}$$

([8]) We shall use $\hbar = c = 1$.

2875

where $\Psi_n^{(-)}$ is an eigenfunction of H with eigenvalue E_n, belonging to a complete orthonormal set of incoming wave functions. Using (5) we find easily the Low equation for the forward scattering matrix element of the heavy meson of index i on proton:

$$T_i(\omega) = \sum_n \left(\frac{T_i^+(\omega, n) T_i(\omega, n)}{(\omega + i\varepsilon) - E_n} + \frac{\overline{T}_i^+(\omega, n) \overline{T}_i(\omega, n)}{-(\omega + i\varepsilon) - E_n} \right) + Y_i(\omega) , \tag{7a}$$

$$\overline{T}_i(\omega) = \sum_n \left(\frac{\overline{T}_i^+(\omega, n) \overline{T}_i(\omega, n)}{(\omega + i\varepsilon) - E_n} + \frac{T_i^+(\omega, n) T_i(\omega, n)}{-(\omega + i\varepsilon) - E_n} \right) + \overline{Y}_i(\omega) , \tag{7b}$$

where ε is a vanishing small positive number.

If we separate, in V, $\overline{V}$, U and $\overline{U}$ the explicit dependence on ω given by A and the cut-off function $v(\omega)$ by writing

$$\left\{ \begin{aligned} V_{k_i} &= \frac{v(\omega)}{\sqrt{\omega}} W_i(\omega) , &\qquad \overline{V}_{l_i} &= \frac{v(\omega)}{\sqrt{\omega}} \overline{W}_i(\omega), \\ Y_i(\omega) &= \frac{v^2(\omega)}{\omega} X_i(\omega) , &\qquad \overline{Y}_i(\omega) &= \frac{v^2(\omega)}{\omega} \overline{X}_i(\omega), \end{aligned} \right. \tag{8}$$

we can easily see that W_i, $\overline{W}_i$, X_i and $\overline{X}_i$ can be functions of ω only through k, coming from eventual derivatives in the interaction Hamiltonian, so that they are even functions of ω. Then from (7)

$$T_i(-\omega) = -\overline{T}_i^+(\omega) . \tag{9}$$

It is also clear that W_i, $\overline{W}_i$ X_i and $\overline{X}_i$ are regular at $\omega = 0$ so that $T_i(\omega)$ and $\overline{T}_i(\omega)$ have simple poles at $\omega = 0$.

Owing to the conservation of strangeness we see that

$$T_i(\omega, n) = 0 \qquad \text{for} \qquad E_n < m_K , \tag{10}$$

while $\overline{T}_i(\omega, n)$ is different from 0 also for $E_n = E_\Lambda$, $E_n = E_\Sigma$ and from $E_n \geqslant \mu$ where

$$\mu = E_\Lambda + m_\pi . \tag{11}$$

We now define:

$$Q_i(z) = \frac{z T_i(z)}{v^2(z)(z - m_K)(z^2 - \omega^2)} , \tag{12a}$$

$$\overline{Q}_i(z) = \frac{z \overline{T}_i(z)}{v^2(z)(z - m_K)(z^2 - \omega^2)} , \tag{12b}$$

where z is a complex variable. From (7) we see that $T_i(z)$ and $\overline{T}_i(z)$ are analytic functions of z in the upper half plane; then also $Q_i(z)$ and $\overline{Q}_i(z)$ are analytic there.

According to what was said at the beginning of this section, we shall suppose that $T_i(z)/v^2(z)$ and $\overline{T}_i(z)/v^2(z)$ have, at infinity, at most a pole of the first order.

If we now chose the contour integration C given in Fig. 1 we have

$$\oint_C Q_i(z)\,\mathrm{d}z = 0\,, \qquad \oint_C \overline{Q}_i(z)\,\mathrm{d}z = 0 \tag{13}$$

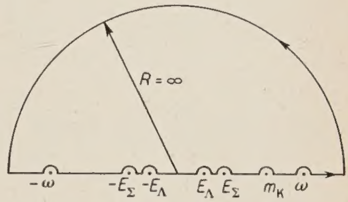

Fig. 1.

and then

$$-i\mathcal{P}\int_{-\infty}^{+\infty}\frac{\omega' T_i(\omega')\,\mathrm{d}\omega'}{v^2(\omega')(\omega'-m_{\mathrm{K}})(\omega'^2-\omega^2)} = \tag{14a}$$

$$=\pi\left[P_i^\Lambda + P_i^\Sigma - \frac{m_{\mathrm{K}}T_i(m_{\mathrm{K}})}{v^2(m_{\mathrm{K}})k^2} - \frac{T_i(-\omega)}{2v^2(\omega)(\omega+m_{\mathrm{K}})} + \frac{T_i(\omega)}{2v^2(\omega)(\omega-m_{\mathrm{K}})}\right],$$

and

$$-i\mathcal{P}\int_{-\infty}^{+\infty}\frac{\omega' \overline{T}_i(\omega')\,\mathrm{d}\omega'}{v^2(\omega')(\omega'-m_{\mathrm{K}})(\omega'^2-\omega^2)} = \tag{14b}$$

$$=\pi\left[\overline{P}_i^\Lambda + \overline{P}_i^\Sigma - \frac{m_{\mathrm{K}}\overline{T}_i(m_{\mathrm{K}})}{v^2(m_{\mathrm{K}})k^2} - \frac{\overline{T}_i(-\omega)}{2v^2(\omega)(\omega+m_{\mathrm{K}})} + \frac{\overline{T}_i(\omega)}{2v^2(\omega)(\omega-m_{\mathrm{K}})}\right],$$

where $\mathcal{P}$ stands for the principal values of the integrals. We have defined $v(-z) = v(z)$.

$P_i^{\mathrm{H}}(\omega)$, where H stays for Λ or Σ, are the poles of $Q_i(\omega)$ at $\omega = -E_{\mathrm{H}}$; $\overline{P}_i^{\mathrm{H}}(\omega)$ those of $\overline{Q}_i(\omega)$ at $\omega = E_{\mathrm{H}}$ and are given by:

$$P_i^{\mathrm{H}}(\omega) = -\frac{|\langle \boldsymbol{H}|W_i^+(E_{\mathrm{H}})|\boldsymbol{N}_+\rangle|^2}{(m_{\mathrm{K}}+E_{\mathrm{H}})(\omega^2-E_{\mathrm{H}}^2)}\,, \tag{15a}$$

$$\overline{P}_i^{\mathrm{H}}(\omega) = \frac{|\langle \boldsymbol{H}|W_i^+(E_{\mathrm{H}})|\boldsymbol{N}_+\rangle|^2}{(m_{\mathrm{K}}-E_{\mathrm{H}})(\omega^2-E_{\mathrm{H}}^2)}\,. \tag{15b}$$

We shall now introduce the forward scattering amplitudes $f_i(\omega)$ and $\bar{f}_i(\omega)$ related to the T matrix elements by

$$f_i(\omega) = -\frac{\omega}{2\pi}\,T_i(\omega)\,, \qquad \bar{f}_i(\omega) = -\frac{\omega}{2\pi}\,\overline{T}_i(\omega)\,. \tag{16}$$

Taking now the real parts of eq. (14a) and (14b), making suitable combinations between them and making use of (9) in order to eliminate negative energies,

we arrive to the dispersion relations.

$$
(17a)\qquad \operatorname{Re}\frac{f_i(\omega)}{v^2(\omega)} = C_i^{\Lambda}(\omega) + C_i^{\Sigma}(\omega) + \frac{1}{2v^2(m_{\mathrm{K}})}\left(1+\frac{\omega}{m_{\mathrm{K}}}\right)\operatorname{Re} f_i(m_{\mathrm{K}}) +
$$
$$
+\frac{1}{2v^2(m_{\mathrm{K}})}\left(1-\frac{\omega}{m_{\mathrm{K}}}\right)\operatorname{Re}\bar{f}_i(m_{\mathrm{K}}) + \frac{k^2}{\pi}\,\mathcal{P}\int_{\mu}^{\infty}\frac{\mathrm{d}\omega'}{v^2(\omega')k'^2}\left(\frac{\operatorname{Im} f_i(\omega')}{\omega'-\omega}+\frac{\operatorname{Im}\bar{f}_i(\omega')}{\omega'+\omega}\right),
$$

$$
(17b)\qquad \operatorname{Re}\frac{\bar{f}_i(\omega)}{v^2(\omega)} = \bar{C}_i^{\Lambda}(\omega) + \bar{C}_i^{\Sigma}(\omega) + \frac{1}{2v^2(m_{\mathrm{K}})}\left(1+\frac{\omega}{m_{\mathrm{K}}}\right)\operatorname{Re}\bar{f}_i(m_{\mathrm{K}}) +
$$
$$
+\frac{1}{2v^2(m_{\mathrm{K}})}\left(1-\frac{\omega}{m_{\mathrm{K}}}\right)\operatorname{Re} f_i(m_{\mathrm{K}}) + \frac{k^2}{\pi}\,\mathcal{P}\int_{\mu}^{\infty}\frac{\mathrm{d}\omega'}{v^2(\omega')k'^2}\left(\frac{\operatorname{Im}\bar{f}_i(\omega')}{\omega'-\omega}+\frac{\operatorname{Im} f_i(\omega')}{\omega'+\omega}\right),
$$

where

$$
(18)\qquad C_i^{\mathrm{H}}(\omega) = -\frac{k^2}{2\pi}\frac{|\langle \boldsymbol{H}|W_i^{+}(E_{\mathrm{H}})|\boldsymbol{N}_{+}\rangle|^2}{(\omega+E_{\mathrm{H}})(m_{\mathrm{K}}^2-E_{\mathrm{H}}^2)},\qquad \bar{C}_i^{\mathrm{H}}(\omega) = \frac{k^2}{2\pi}\frac{|\langle \boldsymbol{H}|W_i^{+}(E_{\mathrm{H}})|\boldsymbol{N}_{+}\rangle|^2}{(\omega-E_{\mathrm{H}})(m_{\mathrm{K}}^2-E_{\mathrm{H}}^2)}\,.
$$

The optical theorem states that

$$
(19a)\qquad \begin{cases} \operatorname{Im} f_i(\omega) = \dfrac{k}{4\pi}\,\sigma_i(\omega)\,, & \text{for } \omega \geqslant m_{\mathrm{K}},\\ \qquad\qquad\; = 0\,, & \text{for } \omega < m_{\mathrm{K}},\end{cases}
$$

$$
(19b)\qquad \begin{cases} \operatorname{Im} \bar{f}_i(\omega) = \dfrac{k}{4\pi}\,\bar{\sigma}_i(\omega)\,, & \text{for } \omega \geqslant m_{\mathrm{K}},\\ \qquad\qquad\; = 0\,, & \text{for } \omega < \mu,\end{cases}
$$

where $\sigma_i(\omega)$ $(\bar{\sigma}_i(\omega))$ is the total cross-section of meson K_i $(\bar{\mathrm{K}}_i)$ on proton. It is then possible to restrict the integration interval in (17) from μ to ∞. We see nevertheless that it remains a domain of unphysical values of the total energy i.e. that from μ to m_{K} in which the part of the integral that contains $\operatorname{Im}\bar{f}_i(\omega)$ is different from 0. This fact is due to the possible exoergic reactions $\bar{\mathrm{K}}+\mathrm{p}\to\pi+\Lambda$ and $\bar{\mathrm{K}}+\mathrm{p}\to\pi+\Sigma$. In the unphysical region $\operatorname{Im}\bar{f}_i(\omega)$ must be obtained from a continuation of $(k/4\pi)\bar{\sigma}_i(\omega)$ from physical values of the energy.

Subdividing the physical states in eigenstates of the total isobaric spin of the K-N or $\bar{\mathrm{K}}$-N system we find

$$
(20a)\qquad f_{\frac{1}{2}}(\omega) = f^1(\omega)\,,\qquad\qquad f_{-\frac{1}{2}}(\omega) = \tfrac{1}{2}\left(f^0(\omega)+f^1(\omega)\right),
$$
$$
(20b)\qquad \bar{f}_{\frac{1}{2}}(\omega) = \tfrac{1}{2}\left(\bar{f}^0(\omega)+\bar{f}^1(\omega)\right),\qquad \bar{f}_{-\frac{1}{2}}(\omega) = \bar{f}^1(\omega)\,,
$$

where $f^{\alpha}(\omega)$ and $\bar{f}^{\alpha}(\omega)$ $(\alpha = 0$ or $1)$ are the forward scattering amplitudes for total isobaric spin states. The total cross-sections are obviously related in

the same way, i.e.

(21*a*) $\sigma_{\frac{1}{2}}(\omega) = \sigma^1(\omega)\,, \qquad \sigma_{-\frac{1}{2}}(\omega) = \frac{1}{2}(\sigma^0(\omega) + \sigma^1(\omega))\,,$

(21*b*) $\bar{\sigma}_{\frac{1}{2}}(\omega) = \frac{1}{2}(\bar{\sigma}^0(\omega) + \bar{\sigma}^1(\omega))\,, \qquad \bar{\sigma}_{-\frac{1}{2}}(\omega) = \bar{\sigma}^1(\omega)\,.$

We can now find from (17) the dispersion relation for f^α and $\bar{f}^\alpha$:

(22*a*)
$$\mathrm{Re}\,\frac{f^\alpha(\omega)}{v^2(\omega)} = \Gamma_\alpha^\Lambda(\omega) + \Gamma_\alpha^\Sigma(\omega) + \frac{1}{2v^2(m_\mathrm{K})}\left(1+\frac{\omega}{m_\mathrm{K}}\right)\mathrm{Re}\,f^\alpha(m_\mathrm{K}) +$$
$$+\frac{1}{2v^2(m_\mathrm{K})}\left(1-\frac{\omega}{m_\mathrm{K}}\right)\sum_\beta A_{\alpha\beta}f^\beta(m_\mathrm{K}) + \frac{k^2}{\pi}\mathcal{P}\int_\mu^\infty \frac{\mathrm{d}\omega'}{v^2(\omega')k'^2}\left(\frac{\mathrm{Im}\,f^\alpha(\omega')}{\omega'-\omega} + \frac{\sum_\beta A_{\alpha\beta}\,\mathrm{Im}\,f^\beta(\omega')}{\omega'+\omega}\right),$$

(22*b*)
$$\mathrm{Re}\,\frac{\bar{f}^\alpha(\omega)}{v^2(\omega)} = \bar{\Gamma}_\alpha^\Lambda(\omega) + \bar{\Gamma}_\alpha^\Sigma(\omega) + \frac{1}{2v^2(m_\mathrm{K})}\left(1+\frac{\omega}{m_\mathrm{K}}\right)\mathrm{Re}\,\bar{f}^\alpha(m_\mathrm{K}) +$$
$$+\frac{1}{2v^2(m_\mathrm{K})}\left(1-\frac{\omega}{m_\mathrm{K}}\right)\sum_\beta A_{\alpha\beta}f^\beta(m_\mathrm{K}) + \frac{k^2}{\pi}\mathcal{P}\int_\mu^\infty \frac{\mathrm{d}\omega'}{v^2(\omega')k'^2}\left(\frac{\mathrm{Im}\,\bar{f}^\alpha(\omega')}{\omega'-\omega} + \frac{\sum_\beta A_{\alpha\beta}\,\mathrm{Im}\,f^\beta(\omega')}{\omega'+\omega}\right),$$

where the matrix A is given by

(23)
$$A = \frac{1}{2}\begin{pmatrix} -1 & 3 \\ 1 & 1 \end{pmatrix},$$

the first column (row) corresponding to $\alpha = 0$ $(\beta = 0)$ and the second to $\alpha = 1$ $(\beta = 1)$. The quantities Γ_α^H are given by

(24*a*) $\Gamma_0^\mathrm{H}(\omega) = 2C_{-\frac{1}{2}}^\mathrm{H}(\omega) - C_{\frac{1}{2}}^\mathrm{H}(\omega)\,, \qquad \Gamma_1^\mathrm{H}(\omega) = C_{\frac{1}{2}}^\mathrm{H}(\omega)\,,$

(24*b*) $\bar{\Gamma}_0^\mathrm{H}(\omega) = 2\bar{C}_{\frac{1}{2}}^\mathrm{H}(\omega) - \bar{C}_{-\frac{1}{2}}^\mathrm{H}(\omega)\,, \qquad \bar{\Gamma}_1^\mathrm{H}(\omega) = \bar{C}_{-\frac{1}{2}}^\mathrm{H}(\omega)\,.$

It is easily seen that the « crossing » matrix A has the usual properties

(25) $\sum_\beta A_{\alpha\beta}A_{\beta\gamma} = \delta_{\alpha\gamma}\,, \qquad \sum_\beta A_{\alpha\beta} = 1\,.$

2. – Special interactions.

We shall now specify the K-N-Λ and K-N-Σ parts of the interaction Hamiltonian. We shall call « scalar » case that in which the parity of the heavy meson-hyperon system is assumed to be equal to the parity of nucleons, sup-

posing spin zero for the heavy meson, and for the Λ and Σ equal parity and spin $\frac{1}{2}$. This is the case to which Salam Hamiltonian applies [5]. The case of opposite parity for the heavy meson hyperon system will be called « pseudo-scalar » (p.s.).

For the scalar case we shall consider:

$$ {}_sH'_{\mathrm{KN}\Lambda} = g_\Lambda \int (\overline{\psi} A \chi + \overline{\chi} A^+ \psi) v(\boldsymbol{x}) \, \mathrm{d}\boldsymbol{x} \,, \tag{26a} $$

$$ {}_sH'_{\mathrm{KN}\Sigma} = g_\Sigma \int (\overline{\psi} \tau^\gamma A \varphi_\gamma + \overline{\varphi}_\gamma A^+ \tau_\gamma \psi) v(\boldsymbol{x}) \, \mathrm{d}\boldsymbol{x} \,, \tag{26b} $$

where ψ, χ and φ ($\overline{\psi}$, $\overline{\chi}$, $\overline{\varphi}$) are destruction (creation) operators of fixed N, Λ and Σ particles (considered isospinors, isoscalars and isovectors respectively); g_Λ and g_Σ are the rationalized unrenormalized coupling constants. It is clear that (26) will give only s-wave heavy meson-nucleon interaction.

For the p.s. case we have:

$$ {}_{p.s.}H'_{\mathrm{KN}\Lambda} = \frac{f_\Lambda}{m_{\mathrm{K}}} \int (\overline{\psi} \boldsymbol{\sigma} \cdot \nabla A \chi + \overline{\chi} \boldsymbol{\sigma} \cdot \nabla A^+ \psi) v(\boldsymbol{x}) \, \mathrm{d}\boldsymbol{x} \,, \tag{27a} $$

$$ {}_{p.s.}H'_{\mathrm{KN}\Sigma} = \frac{f_\Sigma}{m_{\mathrm{K}}} \int (\overline{\psi} \tau^\gamma \boldsymbol{\sigma} \cdot \nabla A \varphi_\gamma + \overline{\varphi}_\gamma \boldsymbol{\sigma} \cdot \nabla A \tau^\gamma \psi) v(\boldsymbol{x}) \, \mathrm{d}\boldsymbol{x} \,. \tag{27b} $$

The operators V defined in (4) are clearly given by

$$ {}_sV_k^\Lambda = \frac{g_\Lambda v(\omega)}{\sqrt{2\omega}} \overline{\psi} \chi \,, \qquad {}_sV_k^\Sigma = \frac{g_\Sigma v(\omega)}{\sqrt{2\omega}} \overline{\psi} \tau^\gamma \varphi_\gamma \,, \tag{28} $$

$$ {}_{p.s.}V_k^\Lambda = \frac{i f_\Lambda v(\omega)}{m_{\mathrm{K}} \sqrt{2\omega}} \overline{\psi} \boldsymbol{\sigma} \cdot \boldsymbol{k} \chi \,, \qquad {}_{p.s.}V_k^\Sigma = \frac{i f_\Sigma v(\omega)}{m_{\mathrm{K}} \sqrt{2\omega}} \overline{\psi} \boldsymbol{\sigma} \cdot \boldsymbol{k} \tau^\gamma f \varphi_\gamma \,, \tag{29} $$

from which the $\overline{V}$ can be obtained using (5). We can then calculate the matrix elements of W_i^+ between physical barion states in terms of the renormalized coupling constants: as usually we observe that from general invariance properties

$$ \langle \boldsymbol{H} | W_i^+ | \boldsymbol{N} \rangle = Z_{\mathrm{H}}^{\frac{1}{2}} \langle H | W_i^+ | N \rangle \,, \tag{30} $$

where $Z_{\mathrm{H}}^{\frac{1}{2}}$ is a proportionality constant and $|N\rangle$ and $|\boldsymbol{H}\rangle$ are the bare particle functions (spin and isobaric spin functions). Defining than the renormalized (rationalized) coupling constants

$$ G_{\mathrm{H}} = Z_{\mathrm{H}}^{\frac{1}{2}} g_{\mathrm{H}} \qquad \text{and} \qquad F_{\mathrm{H}} = Z_{\mathrm{H}}^{\frac{1}{2}} f_{\mathrm{H}} \,, \tag{31} $$

we have

$$(32a)\qquad |\langle\boldsymbol{\Lambda}|{}_sW^+_{\frac12}|\boldsymbol{N}\rangle|^2 = \frac{G^2_\Lambda}{2}\,,\qquad |\langle\boldsymbol{\Lambda}|{}_sW^+_{-\frac12}|\boldsymbol{N}\rangle|^2 = 0\,,$$

$$(32b)\qquad |\langle\boldsymbol{\Sigma}|{}_sW^+_{\frac12}|\boldsymbol{N}\rangle|^2 = |\langle\boldsymbol{\Sigma}|{}_sW^+_{-\frac12}|\boldsymbol{N}\rangle|^2/2 = \frac{G^2_\Sigma}{2}\,,$$

$$(33a)\qquad |\langle\boldsymbol{\Lambda}|{}_{p.s.}W^+_{\frac12}(\omega')|\boldsymbol{N}\rangle|^2 = \frac{k'^2}{m^2_{\mathrm{K}}}\frac{F^2_\Lambda}{2}\,,\qquad |\langle\boldsymbol{\Lambda}|{}_{p.s.}W^+_{-\frac12}(\omega')|\boldsymbol{N}\rangle|^2 = 0\,,$$

$$(33b)\qquad |\langle\boldsymbol{\Sigma}|{}_{p.s.}W^+_{\frac12}(\omega')|\boldsymbol{N}\rangle|^2 = |\langle\boldsymbol{\Sigma}|{}_{p.s.}W^+_{-\frac12}(\omega')|\boldsymbol{N}\rangle|^2/2 = \frac{k'^2}{m^2_{\mathrm{K}}}\frac{F^2_\Sigma}{2}\,.$$

These matrix elements must be introduced in (18) and (24) with $\omega' = E_{\mathrm{H}}$ in order to find the quantities $C^{\mathrm{H}}_i(\omega)$ and $\Gamma^{\mathrm{H}}_i(\omega)$ for the special cases here considered, and so the dispersion relations in terms of the renormalized couplign constants. In particular we obtain for the scalar case:

$$(34a)\qquad \left\{\begin{aligned} &{}_s\Gamma^\Lambda_0(\omega) = -\,{}_s\Gamma^\Lambda_1(\omega) = +\frac{k^2}{4\pi}\frac{G^2_\Lambda}{(\omega+E_\Lambda)(m^2_{\mathrm{K}}-E^2_\Lambda)}\,,\\ &\frac13\,{}_s\Gamma^\Sigma_0(\omega) = {}_s\Gamma^\Sigma_1(\omega) = -\frac{k^2}{4\pi}\frac{G^2_\Sigma}{(\omega+E_\Sigma)(m^2_{\mathrm{K}}-E^2_\Sigma)}\,,\end{aligned}\right.$$

$$(34b)\qquad \left\{\begin{aligned} &{}_s\overline{\Gamma}^\Lambda_0(\omega) = -\frac{k^2}{2\pi}\frac{G^2_\Lambda}{(\omega-E_\Lambda)(m^2_{\mathrm{K}}-E^2_\Lambda)}\,; &&{}_s\overline{\Gamma}^\Lambda_2(\omega) = 0\,,\\ &{}_s\overline{\Gamma}^\Sigma_1 = +\frac{k^2}{2\pi}\frac{G^2_\Sigma}{(\omega-E_\Sigma)(m^2_{\mathrm{K}}-E^2_\Sigma)}\,; &&{}_s\overline{\Gamma}^\Sigma_0(\omega) = 0\,,\end{aligned}\right.$$

and the same formulae for the p.s. quantities with $G^2_{\mathrm{H}}/(m^2_k - E^2_{\mathrm{H}})$ replaced by $-F^2_{\mathrm{H}}/m^2_{\mathrm{K}}$. We note here that the result that G^2_Λ (G^2_Σ) is absent in the $\overline{\mathrm{K}}$-N interaction when $T=1$ ($T=0$), result that was already found by us using approximate methods (see (3)), is here derived indipendently of the form of the Hamiltonian.

The terms with $f(m_{\mathrm{K}})$ and $\bar f(m_{\mathrm{K}})$ in the right hand side of the dispersion relations (17) or (22) complicate the expressions making it more difficult to apply approximate methods or iteration procedures in order to extract indications from dispersion relations (we shall discuss in the following paper the possibility of such approximations). We see that the form of eq. (17) and (22) is such that they are identically satisfied for $\omega = m_{\mathrm{K}}$. We shall obtain in the next section, for the particular interaction Hamiltonians ((26) and (27)) dispersion relations that will not contain the terms with $f(m_{\mathrm{K}})$ and $\bar f(m_{\mathrm{K}})$; this will considerably reduce the complexity of the equations.

3. – Chew-Low approach to dispersion relations.

With the interaction Hamiltonians given in (26) and (27) all the terms present in the V_{k_i}'s and $\bar{V}_{k_i}$'s defined by (4) have the same dependence on the energy ω of the heavy meson. Being this the case, we can use a different approach to dispersion relations, analogous to that used by CHEW and LOW [6] for the p-wave pion-nucleon fixed source interaction. We shall work in the first part of this paragraph with the interaction Hamiltonian corresponding to the « scalar » case (in the sense stated in Sect. 2); the extension of the formalism to the « p.s. » case will be briefly indicated in the last part of this section.

Making use of the known energy dependence of $T_i(\omega, n)$ and $\bar{T}_i(\omega, n)$ we obtain

$$T_i^+(\omega', n)T_i(\omega', n) = \frac{\omega' v^2(\omega')}{\omega v^2(\omega)}\, T_i^+(\omega, n)T_i(\omega, n)\,, \tag{35a}$$

and an analogous relation for $\bar{T}_i^+(\omega, n)\,\bar{T}_i(\omega, n)$.

We can express now the total cross-sections for K-N and $\bar{\text{K}}$-N interaction in terms of the T-matrices as follows:

$$\sigma_i(\omega') = \frac{2\pi}{k'}\,\omega' \sum_n \delta(E_n - \omega')T_i^+(\omega', n)T_i(\omega', n)\,, \tag{36a}$$

$$\bar{\sigma}_i(\omega') = \frac{2\pi}{k'}\,\omega' \sum_n \delta(E_n - \omega')\bar{T}_i^+(\omega', n)\bar{T}_i(\omega', n)\,, \tag{36b}$$

and use (35) in order to obtain

$$\sum_n{}'' \frac{T_i^+(\omega, n)T_i(\omega, n)}{\mp(\omega + i\varepsilon) - E_n} = -\frac{1}{2\pi}\,\frac{v^2(\omega)}{\omega}\int\limits_m^\infty \frac{k'\,\mathrm{d}\omega'}{v^2(\omega')}\,\frac{\sigma_i(\omega')}{(\omega' \pm (\omega + i\varepsilon))}\,, \tag{37a}$$

$$\sum_n{}'' \frac{\bar{T}_i^+(\omega, n)\bar{T}_i(\omega, n)}{\mp(\omega + i\varepsilon) - E_n} = -\frac{1}{2\pi}\,\frac{v^2(\omega)}{\omega}\int\limits_\mu^\infty \frac{k'\,\mathrm{d}\omega'}{v^2(\omega')}\,\frac{\sigma_i(\omega')}{(\omega' \pm (\omega + i\varepsilon))}\,, \tag{37b}$$

where $\sum_n''$ indicates summation from $E_n = \mu$ up to infinity. We note that also here we have integrations over the unphysical region from μ to m_{K}.

The first part of the summation present in the Low equations (7), going from 0 to μ, can be now evaluated in terms of the matrix elements already discussed in Sect. 2, by making use of our knowledge of the spectrum of the

interaction Hamiltonian; this allows us, as we have seen, to renormalize the K-N-Λ and K-N-Σ coupling constants. Formulae (32) of the previous paragraph give:

$$(38a)\qquad -\frac{\omega}{2\pi}\sum_n{}' \frac{\overline{T}_i^+(\omega, n)\overline{T}_i(\omega, n)}{-\omega - E_n} = I_i(\omega) = \frac{v^2(\omega)}{4\pi}\left[\frac{G_\Lambda^2}{\omega + E_\Lambda}\,\delta_{i,\frac{1}{2}} + \frac{G_\Sigma^2}{\omega + E_\Sigma}\,(1 + \delta_{i,-\frac{1}{2}})\right],$$

$$(38b)\qquad -\frac{\omega}{2\pi}\sum_n{}' \frac{\overline{T}_i^+(\omega, n)\overline{T}_i(\omega, n)}{\omega - E_n} = \bar{I}_i(\omega) = -\frac{v^2(\omega)}{4\pi}\left[\frac{G_\Lambda^2}{\omega - E_\Lambda}\,\delta_{i,\frac{1}{2}} + \frac{G_\Sigma^2}{\omega - E_\Sigma}\,(1 + \delta_{i,-\frac{1}{2}})\right].$$

We note the following relation between $I_i(\omega)$ and $\bar{I}_i(\omega)$

$$(39)\qquad I_i(-\omega) = \bar{I}_i(\omega)\,.$$

By introducing now the scattering amplitude given in (16) we can express the Low equations (7) in the form of dispersion relations:

$$(40a)\qquad \operatorname{Re} f_i(\omega) = I_i(\omega) + \frac{v^2(\omega)}{4\pi^2}\,\mathcal{P}\!\int_\mu^\infty \frac{k'\,\mathrm{d}\omega'}{v^2(\omega')}\left[\frac{\sigma_i(\omega')}{\omega' - \omega} + \frac{\bar{\sigma}_i(\omega')}{\omega' + \omega}\right],$$

$$(40b)\qquad \operatorname{Re} \bar{f}_i(\omega) = \bar{I}_i(\omega) + \frac{v^2(w)}{4\pi^2}\,\mathcal{P}\!\int_\mu^\infty \frac{k'\,\mathrm{d}\omega'}{v^2(\omega')}\left[\frac{\bar{\sigma}_i(\omega')}{\omega' - \omega} + \frac{\sigma_i(\omega')}{\omega' + \omega}\right],$$

where the lowest limit of the integral over the σ_i has been shifted from m_K to μ for simplicity of notation, using the fact that the $\sigma_i(\omega)$ are identically zero in the range μ to m_K.

We go now to the dispersion relations for isobaric spin states; by making use of (20) and (21) we obtain:

$$(41a)\qquad \operatorname{Re} f^\alpha(\omega) = I^\alpha(\omega) + \frac{v^2(\omega)}{4\pi^2}\,\mathcal{P}\!\int_\mu^\infty \frac{k'\,\mathrm{d}\omega'}{v^2(\omega')}\left(\frac{\sigma^\alpha(\omega')}{\omega' - \omega} + \frac{\sum_\beta A_{\alpha\beta}\bar{\sigma}_\beta(\omega')}{\omega' + \omega}\right),$$

$$(41b)\qquad \operatorname{Re} \bar{f}^\alpha(\omega) = \bar{I}^\alpha(\omega) + \frac{v^2(\omega)}{4\pi^2}\,\mathcal{P}\!\int_\mu^\infty \frac{k'\,\mathrm{d}\omega'}{v^2(\omega')}\left(\frac{\bar{\sigma}^\alpha(\omega')}{\omega' - \omega} + \frac{\sum_\beta A_{\alpha\beta}\sigma_\beta(\omega')}{\omega' + \omega}\right),$$

where the matrix A is given in (23) and

$$(42a)\qquad I^0(\omega) = 2I_{-\frac{1}{2}}(\omega) - I_{\frac{1}{2}}(\omega) = \frac{v^2(\omega)}{4\pi}\left(\frac{G_\Sigma^2\cdot 3}{\omega + E_\Sigma} - \frac{G_\Lambda^2}{\omega + E_\Lambda}\right); \qquad I^1(\omega) = I_{\frac{1}{2}}(\omega),$$

$$(42b)\qquad \bar{I}^0(\omega) = 2\bar{I}_{\frac{1}{2}}(\omega) - \bar{I}_{-\frac{1}{2}}(\omega) = -\frac{v^2(\omega)}{4\pi}\left(\frac{2G_\Lambda^2}{\omega - E_\Lambda}\right); \qquad \bar{I}^1(\omega) = \bar{I}_{-\frac{1}{2}}(\omega).$$

We note that there is no relation between I^0 and $\bar{I}^0$ analoguos to (39); and that while I^1 is defined positive and $\bar{I}^0$ and $\bar{I}^1$ are defined negative, I^0 can assume both signs depending on the relative weight of the K-N-Λ and K-N-Σ coupling constants.

Quite analogous considerations can be developed in the p.s. case. Apart from the differences in the energy spectrum and for the presence of an unphysical region, the interaction Hamiltonian given in (27) does not differ in a significant way from that used by CHEW and LOW [6]. The only difference with what has been done in the first part of this section will consist in the presence of a k^2/m_K^2 factor, coming out from the different momentum dependence of the $T(\omega, n)$ in the p.s. case. We get therefore in a straightforward way for the dispersion relations for physical states in the p.s. case:

$$(43a)\qquad \operatorname{Re} f_i(\omega) = J_i(\omega) + \frac{k^2v^2(\omega)}{4\pi^2}\mathcal{P}\int_\mu^\infty \frac{d\omega'}{k'v^2(\omega')}\left(\frac{\sigma_i(\omega)}{\omega' - \omega} + \frac{\bar{\sigma}_i(\omega)}{\omega' + \omega}\right),$$

$$(43b)\qquad \operatorname{Re} \bar{f}_i(\omega) = \bar{J}_i(\omega) + \frac{4\pi^2}{k^2v^2(\omega)}\mathcal{P}\int_\mu^\infty \frac{d\omega'}{k'v^2(\omega')}\left(\frac{\bar{\sigma}_i(\omega')}{\omega' - \omega} + \frac{\sigma_i(\omega')}{\omega' + \omega}\right),$$

where

$$(44a)\qquad J_i(\omega) = \frac{k^2v^2(\omega)}{4\pi\omega_K^2}\left(\frac{F_\Lambda^2}{\omega + E_\Lambda}\,\delta_{i,\frac{1}{2}} + \frac{F_\Sigma^2}{\omega + E_\Sigma}\cdot(1 + \delta_{i,-\frac{1}{2}})\right),$$

$$(44b)\qquad \bar{J}_i(\omega) = \frac{k^2v^2(\omega)}{4\pi m_K^2}\left(\frac{F_\Lambda^2}{\omega - E_\Lambda}\,\delta_{i,\frac{1}{2}} + \frac{F_\Sigma^2}{\omega - E_\Sigma}\cdot(1 + \delta_{i,-\frac{1}{2}})\right),$$

and F_H are the p.s. renormalized coupling constants introduced already in the previous section.

4. – Discussion.

We want, first, to compare eq. (17) and (22) with eq. (40) and (43); that is the dispersion relations for the interaction Hamiltonians (26) and (27) obtained with the general method of Sect. 2 and with that of C.L. We see easily

2884

that if eq. (40) or (43) is satisfied then the eq. (17), with the corresponding C_i quantities calculated in Sect. 3, is also valid. But the reverse is not true, and this appears obvious from the analysis of the method used in Sect. 3. There we used the special form of the K-N-Λ and K-N-Σ interaction Hamiltonians in order to compute the terms C_i and $\bar{C}_i$ (or Γ_i and $\bar{\Gamma}_i$) that appear in the general dispersion relations (17) (or (22)), that is those representing the contributions of the poles of $T_i(\omega)$ and $\bar{T}_i(\omega)$ at $\pm E_\Lambda$ and $\pm E_\Sigma$. It is then clear that all other possible interactions that give no contributions to the poles, even containing heavy meson operators, are automatically and implicitly contained in the dispersion relations of Sect. 3. For instance, we can have contribution of angular momentum waves different from those contained explicitly in the interaction Hamiltonians (26) or (27). In Sect. 4 we based instead all the calculations on the explicit form of the interaction Hamiltonian so that the results are strictly valid only for the treated case.

For the « scalar » case, the integral of eq. (17) is more rapidly convergent than that of eq. (40), so that the dispersion relations of eq. (17) or (22) can be valid even if those obtained with the C.L. method would diverge. The extra factor k'^2 in the denominator of the integrand of (17) can also help in future comparison with experiments by cutting down the high energy contributions to dispersion relations.

From an insight in the dispersion relations we see that the particle and antiparticle scattering amplitudes are connected in a non separable way. This fact complicates approximate solutions or developments for the scattering amplitudes (or phase shifts), specially because of the possibility of absorption of $\bar{\text{K}}$ (that must be dominant on scattering at very low energies, and causes the non physical contributions to the integrals).

The other fields (pions) and interactions are also present, implicitly, in the renormalized coupling constants: the renormalization procedure takes into account all the possible fields in interaction.

As it ought to be expected, the cut-off factor v^2 is essential in the p.s. case to preserve the unitary condition for the scattering matrix. For the « scalar » problem this is not the case: the renormalizability of the fixed point source field theory gives us the possibility to put $v^2 = 1$ without obtaining any divergent result after renormalization has been performed. We see, for instance, that there is no problem in putting $v^2 = 1$ in our dispersion relations for the scalar case. However, we know, from studies of simplified models, that inconsistencies (ghosts) can arise even if results are meaningful and finite [9]. Then, also if it is not yet established whether ghost's inconsistencies arise in

---

[9] G. KÄLLÉN and W. PAULI: *Kgl. Danske Vid. Selskab. Mat. Fys. Medd.*, **30**, no. 7 (1955). See also K. W. FORD: *Phys. Rev.*, **105**, 320 (1957).

2885

the scalar fixed source theory, care must be taken in neglecting the high energy cut-off function in the dispersion relations.

* * *

We should like to express our gratitude to Prof. M. Cini for his kind interest in this work and for many enlightening discussions.

RIASSUNTO

Si ottengono relazioni di dispersione per la diffusione K-N e $\overline{\text{K}}$-N in teoria di sorgente fissa. È considerata la presenza simultanea di K e K nel campo dei mesoni pesanti e si tiene anche conto dell'interazione dei mesoni π con i barioni. Le relazioni di dispersione sono ottenute con un metodo generale che non si basa sulla forma esplicita dell'Hamiltoniana ma bensì su alcune sue proprietà generali. I risultati così ottenuti sono poi applicati al caso di mesoni « scalari » e « pseudoscalari »; per questi particolari casi si trovano poi relazioni di dispersione con un metodo più semplice analogo a quello di Chew e Low. I risultati sono analizzati e confrontati con quelli ottenuti in precedenti lavori. Si vede che nelle relazioni di dispersione per l'interazione K-N il contributo dei mesoni K sembra non trascurabile. Si osserva pure che i mesoni π contribuiscono alla definizione delle costanti di accoppiamento rinormalizzate e danno luogo a zone non fisiche negli integrali che compaiono nelle relazioni di dispersione.

The Binding Energy of Sigma Hyperons with Nucleons.

F. Ferrari and L. Fonda

Istituto Nazionale di Fisica Nucleare - Sezione di Padova
Istituto Nazionale di Fisica Nucleare - Sottosezione di Trieste
Istituto di Fisica dell'Università - Padova
Istituto di Fisica dell'Università - Trieste

(ricevuto l'11 Giugno 1957)

Summary. — The binding of Σ hyperons with single nucleons is discussed assuming that the interaction takes place either through pions, or K-mesons or both. It appears that in order to obtain a bound system, the most reasonable assumption is to consider both the pion- and the K-forces.

1. – The possibility that Σ-hyperons may be bound with one or more nucleons has recently been discussed (1). The discovery of a possible example of a (Σ^+, proton) compound (2), has made it interesting to attempt a theoretical description of the binding mechanism. In this note the binding of a positive Σ with a proton and of a negative Σ with a neutron are considered.

We have started from a simple field-theoretical model assuming that binding takes place by means of the exchange of pions and of K-mesons. We assume that both Λ and Σ hyperons have spin $\frac{1}{2}$, while the K-meson is taken to have spin zero.

2. – We shall first consider the case of interaction through the pion field. If we accept that the Λ and the Σ have the same parity, as certain experimental

(1) W. G. Holladay: quoted by R. G. Sachs: *Phys. Rev.*, **99**, 1573 (1955); R. H. Dalitz: *Nuclear Physics*, **1**, 372 (1956).

(2) M. Baldo-Ceolin, W. F. Fry, W. D. Greening, H. Huzita and S. Limentani: *Nuovo Cimento* **6**, 130 (1957).

evidences seem to suggest (3), then the interaction lagrangian for the pion-nucleon-hyperon field can be written in the following form:

$$L_\pi = ig_{n\pi}\bar{n}\gamma_5(\boldsymbol{\tau\pi})n + g_{\Lambda\pi}(i\bar{\Lambda}\gamma_5\boldsymbol{\pi\Sigma} + \text{h. c.}) - ig_{\Sigma\pi}(i\bar{\boldsymbol{\Sigma}}\gamma_5 \times \boldsymbol{\Sigma})\boldsymbol{\pi}\,. \tag{1}$$

The (Σ^+, proton) and the (Σ^-, neutron) potentials arising from this lagrangian, taking into account the second and fourth order processes, have been obtained following a method similar to that of Brueckner and Watson (4), and are given by:

$$\begin{aligned} V_\pi = &-\frac{g_{n\pi}}{2M_n}\frac{g_{\Sigma\pi}}{2M_\Sigma}\frac{1}{(2\pi)^3}\int d^3k(\boldsymbol{\sigma}_1\boldsymbol{k})(\boldsymbol{\sigma}_2\boldsymbol{k})\frac{\exp[i\boldsymbol{kr}]}{\omega^2} - \\ &-\left(\frac{g_{n\pi}}{2M_n}\right)^2\frac{1}{(2\pi)^6}\int d^3k\, d^3k'\,\frac{\exp[i(\boldsymbol{k}+\boldsymbol{k}')\cdot\boldsymbol{r}]}{\omega^3\omega'}\cdot \\ &\cdot\left\{(\boldsymbol{kk}')^2\left[\left(\frac{g_{\Lambda\pi}}{M_\Sigma + M_\Lambda}\right)^2\left(\frac{1}{\omega+\omega'}+\frac{1}{\omega'}\right) + \left(\frac{g_{\Sigma\pi}}{2M_\Sigma}\right)^2\left(\frac{1}{\omega+\omega'}+\frac{2}{\omega'}\right)\right] + \right. \\ &\left. -\boldsymbol{\sigma}_1\boldsymbol{k}\wedge\boldsymbol{k}'\,\boldsymbol{\sigma}_2\boldsymbol{k}\wedge\boldsymbol{k}'\left[\left(\frac{g_{\Lambda\pi}}{M_\Sigma + M_\Lambda}\right)^2\left(\frac{1}{\omega+\omega'}+\frac{1}{\omega'}\right) + \left(\frac{g_{\Sigma\pi}}{2M_\Sigma}\right)^2\left(\frac{2}{\omega+\omega'}+\frac{1}{\omega'}\right)\right]\right\}. \end{aligned} \tag{2}$$

This potential is expressed by the same formula as the nucleon-nucleon potential when we put $\boldsymbol{\tau}_1\boldsymbol{\tau}_2 = 1$ and assume $M_\Sigma = M_\Lambda$ and $g_{\Lambda\pi} = g_{\Sigma\pi}$ (i.e. that the pion-hyperon coupling constant is always the same).

3. – Let us now consider the K field: in this case only the lowest order processes will be taken into account (5)

$$\Sigma_1 + n_2 \to \left\{\begin{matrix} n_1 + \bar{K} + n_2 \\ \\ \Sigma_1 + K + \Sigma_2 \end{matrix}\right\} \to n_1 + \Sigma_2\,.$$

Since the parity of the K-meson, relative to the Σ hyperon, can be the same or different, the only lagrangians which contribute are

$$L^{s}_{\Sigma K} = g^{s}_{\Sigma K}\bar{n}\boldsymbol{\tau\Sigma}K + \text{h. c.} \tag{3a}$$

for the scalar case, and

$$L^{ps}_{\Sigma K} = ig^{ps}_{\Sigma K}\bar{n}\gamma_5\boldsymbol{\tau\Sigma}K + \text{h. c.} \tag{3b}$$

(3) M. Gell-Mann: *Phys. Rev.* (in course of publication); D. Lichtenberg and M. Ross (private communication); N. Dallaporta and F. Ferrari: *Nuovo Cimento* **5**, 111 (1957).

(4) K. A. Brueckner and K. W. Watson: *Phys. Rev.*, **92**, 1023 (1953).

(5) G. Wentzel: *Phys. Rev.*, **101**, 835 (1956).

for the pseudoscalar case. The corresponding potentials are (see Appendix)

$$V_{\mathrm{K}}^{\mathrm{s}}=\frac{(g_{\Sigma\mathrm{K}}^{\mathrm{s}})^2}{2\pi}\,\frac{\exp\left[-\mu_{\mathrm{K}}r\right]}{r}\,P_xP_\sigma \tag{4a}$$

and

$$V_{\mathrm{K}}^{\mathrm{ps}}=-\frac{1}{3}\,\frac{(g_{\Sigma\mathrm{K}}^{\mathrm{ps}})^2}{2\pi}\,\mu_{\mathrm{K}}\left(\frac{\mu_{\mathrm{K}}}{2M_{\mathrm{n}}}\right)^2 P_xP_\sigma\left[\boldsymbol{\sigma}_1\boldsymbol{\sigma}_2+\frac{3+3x'+x'^2}{x'^3}\,S_{12}\right]\frac{\exp\left[-x'\right]}{x'} \tag{4b}$$

where $x'=\mu_{\mathrm{K}}r$; $P_\sigma=1$ for parallel spins and -1 for antiparallel spins; $P_x=1$ for even states.

4. – It has however to be pointed out that besides the limiting cases considered above, a large contribution to the Σ-nucleon potential can arise also from processes in which one pion and one K-meson are exchanged between hyperons and nucleons. The diagrams representing these processes are given in Fig. 1. The relative lagrangians for the scalar and the pseudoscalar cases are respectively:

$$L_{\mathrm{s}}=L_\pi+L_{\Sigma\mathrm{K}}^{\mathrm{s}}+g_{\Lambda\mathrm{K}}^{\mathrm{s}}(\bar{\mathrm{n}}\Lambda\mathrm{K}+\mathrm{h.\,c.}) \tag{5a}$$

and

$$L_{\mathrm{ps}}=L_\pi+L_{\Sigma\mathrm{K}}^{\mathrm{ps}}+ig_{\Lambda\mathrm{K}}^{\mathrm{ps}}(\bar{\mathrm{n}}\gamma_5\Lambda\mathrm{K}-\mathrm{h.\,c.})\,. \tag{5b}$$

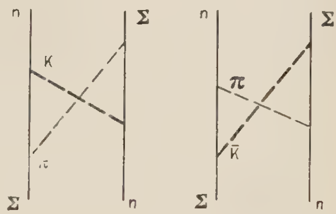

Fig. 1.

The explicit potentials associated to the processes of Fig. 1 are:

Scalar case:

$$\begin{aligned}V_{\mathrm{K}\pi}^{\mathrm{s}}=\frac{g_{\mathrm{Y}\pi}^2}{4\pi}\,\frac{(g_{\mathrm{YK}}^{\mathrm{s}})^2}{4\pi}\left(\frac{\mu_\pi}{2M_{\mathrm{n}}}\right)^2\mu_\pi\,\frac{4}{3\pi}\,P_xP_\sigma\cdot\frac{1}{x}\,\cdot\\ \cdot\Big\{\boldsymbol{\sigma}_1\boldsymbol{\sigma}_2\Big[-K_0(x')\,e^{-x}+e^{-x'}\Big(\frac{K_1(x)}{x}-K_0(x)\Big)\Big]-\\ -S_{\sigma 2}\Big[K_0(x')\,e^{-x}\,\frac{x^2+3x+3}{x^2}+e^{-x'}\Big(2\,\frac{K_1(x)}{x}+K_0(x)\Big)\Big]\Big\}\,,\end{aligned} \tag{6a}$$

where $x=\mu_\pi r$ and $x'=\mu_{\mathrm{K}}r$.

Pseudoscalar case (*):

$$V_{\mathrm{K}\pi}^{\mathrm{ps}}=\frac{g_{\mathrm{Y}\pi}^2}{4\pi}\,\frac{(g_{\mathrm{YK}}^{\mathrm{ps}})^2}{4\pi}\left(\frac{\mu_\pi}{2M_{\mathrm{n}}}\right)^4\mu_\pi\,\frac{4}{\pi}\,P_xP_\sigma\,\frac{e^{-x'}}{x^3}\,. \tag{6b}$$

(*) In evaluating the last term of $V_{\mathrm{K}\pi}^{\mathrm{ps}}$ the following approximation has been used:

$$\frac{\omega\Omega'}{\omega+\Omega'}\sim\frac{\mu_\pi\mu_{\mathrm{K}}}{\mu_\pi+\mu_{\mathrm{K}}}\,,$$

where $\omega=\sqrt{k^2+\mu_\pi^2}$ and $\Omega'=\sqrt{k'^2+\mu_{\mathrm{K}}^2}$.

$$\cdot\left\{\left[\left[K_0(x)(2+2x'+x'^2)+\frac{K_1(x)}{x}(4+4x'+x'^2)\right]-\right.\right.$$

$$-\frac{2}{3}\boldsymbol{\sigma}_1\boldsymbol{\sigma}_2\left[K_0(x)(1+x')+\frac{K_1(x)}{x}(2+2x'+x'^2)\right]+$$

$$\left.\left.+\frac{1}{3}S_{12}\left[K_0(x)(1+x')+\frac{K_1(x)}{x}(5+5x'+x'^2)\right]\right]\right\}+$$

$$+\text{ the same expression with }\mu_\pi\leftrightarrow\mu_K+$$

$$+\frac{g^2_{Y\pi}}{4\pi}\frac{(g^{ps}_{YK})^2}{4\pi}\left(\frac{\mu_\pi}{2M_n}\right)^4\frac{\mu_K^3}{\mu_\pi(\mu_\pi+\mu_K)}\frac{16}{\pi^2}P_xP_\sigma\cdot$$

$$\cdot\left\{\frac{2}{3}\boldsymbol{\sigma}_1\boldsymbol{\sigma}_2\left[\frac{K_1(x)}{x}\cdot\frac{K_1(x')}{x'}+K_0(x)\frac{K_1(x')}{x'}+K_0(x')\frac{K_1(x)}{x}\right]-\right.$$

$$\left.-\frac{1}{3}S_{12}\left[4\frac{K_1(x)}{x}\frac{K_1(x')}{x'}+K_0(x)\frac{K_1(x')}{x'}+K_0(x')\frac{K_1(x)}{x}\right]\right\}.$$

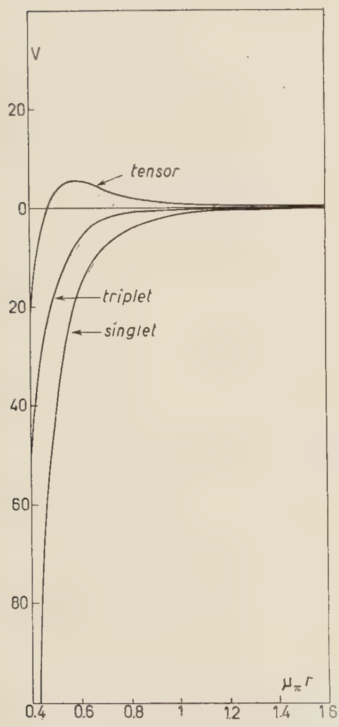

Fig. 2. – The calculated Σ-nucleon singlet, triplet and tensor pion potentials. The ordinate is in units of $\mu_\pi(\mu_\pi/2M_\Sigma)^2\cdot(g^2_{\Sigma\pi}/4\pi)$.

Both these potentials $V^s_{K\pi}$ and $V^{ps}_{K\pi}$ have been calculated assuming

$$g_{\Lambda\pi}=g_{\Sigma\pi}=g_{n\pi}\qquad\text{and}\qquad g_{\Sigma K}=g_{\Lambda K}\,.$$

We point out that all the potentials given in eqs. (2), (4) and (6) show that the lowest level is the singlet state. The singlet potentials are plotted in Fig. 2 and 3.

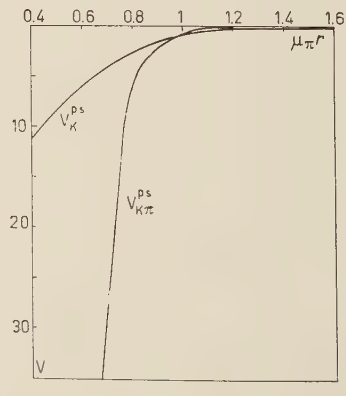

Fig. 3. – The calculated Σ-nucleon singlet V^{ps}_K and $V^{ps}_{K\pi}$ potentials. The ordinate is in units of $(g^{ps}_{YK})^2/4\pi$ MeV. It has been assumed $g^2_{Y\pi}/4\pi=13.3$.

5. – We will now try to obtain the binding energy by the usual variational method, assuming the trial wave function (4):

$$u = \frac{12}{7}[4\pi r_0]^{-\frac{1}{2}}\{\exp[-(r-r_c)/r_0] - \exp[-8(r-r_c)/r_0]\}\frac{1}{r} \qquad \text{for } r > r_c,$$

$$u = 0 \qquad \text{for } r < r_c,$$

where r_c is the core radius and r_0 is considered as a free parameter. Three cases have been considered:

a) Interactions by means of pions only. – In this case, if one assumes that $g^2_{\Lambda\pi}/4\pi = g^2_{\Sigma\pi}/4\pi = g^2_{n\pi}/4\pi = 13.3$ and takes for r_c the value necessary to ensure the virtual state of the deuteron and which also gives the nucleon-nucleon singlet scattering length $r_c = 0.328(\hbar/\mu_\pi c)$ (4), it is found that the (Σ^+, proton) and the (Σ^-, neutron) compounds are not bound (the Coulomb potential for the (Σ^+, proton) system contributes less than 2% to the total potential). In order to obtain a bound state with these values of r_c and $g^2_{n\pi}/4\pi$ it is necessary that $g^2_{\Lambda\pi}/4\pi = g^2_{\Sigma\pi}/4\pi \gtrsim 15$.

b) Interactions by means of K*-mesons only.* – In order to obtain a bound system, assuming a repulsive core at $r_c = 0.2(\hbar/\mu_\pi c)$, the coupling constant must be $(g^s_{\Sigma K})^2/4\pi \gtrsim 0.7$ in the scalar case and $(g^{ps}_{\Sigma K})^2/4\pi \gtrsim 11$ in the pseudoscalar case. However, the values of the coupling constants are very sensitive to the choice of the repulsive core radius. As an indication, assuming $r_c = 0.15(\hbar/\mu_\pi c)$ the coupling constants are respectively $(g^s_{\Sigma K})^2/4\pi \gtrsim 0.6$ and $(g^{ps}_{\Sigma K})^2/4\pi \gtrsim 9$.

c) Interactions by means of both pions and K*-mesons.* – If we assume that the pion-hyperon coupling constant is equal to that for pion-nucleon, i.e. that $g^2_{\Lambda\pi}/4\pi = g^2_{\Sigma\pi}/4\pi = g^2_{n\pi}/4\pi = 13.3$, and assume the same repulsive core at $r_c = 0.328(\hbar/\mu_\pi c)$ for both the nucleon-nucleon and nucleon-hyperon potential, we can obtain a bound state for the (Σ^+, proton) and the (Σ^-, neutron). systems when $(g^{ps}_{\Sigma K})^2/4\pi \sim 1$ (pseudoscalar case) or $(g^s_{\Sigma K})^2/4\pi \sim 0.6$ (scalar case).

It would therefore appear that by combining both kinds of interactions one obtains binding with more reasonable values for the interaction coupling constants that with one kind of interaction alone. Of course one must bear in mind that the binding could be explained not only with the interaction constants here proposed, but also by decreasing the pion binding and increasing the K binding. Until now no strong and well-cut evidence is available relative to the values of the pion-hyperon and K-meson-hyperon coupling constants independently of each other. One may hope that the value of the K-meson-hyperon coupling constant will soon be available from photo-

production reactions, as already pointed out by GELL-MANN [3]. If the present incomplete experimental values for the differential cross-section could be extrapolated to obtain the total cross-section by assuming an isotropical angular distribution, one would obtain $(g^{ps}_{K\Lambda})^2/4\pi \sim 1$ which is in quite good agreement with those given in case *c*). It may be observed that a similar value of the $(g^{ps}_{K\Lambda})^2/4\pi$ constant has been obtained by CEOLIN and TAFFARA [6] for the K^+N scattering.

* * *

The authors wish to thank Prof. N. DALLAPORTA, Prof. W. FRY and the members of the Plate Group of Padua for discussions, and also Drs. D. LICHTENBERG and M. ROSS for an exchange of views relative to the pion-hyperon interaction.

APPENDIX

In this appendix we give a simple account of the derivation of the exchange operators P_σ and P_x used in formulae (4*a*) and (4*b*), (6*a*) and (6*b*).

Consider the matrix element:

$$\langle 0 | P_\alpha(x_1)\Sigma^+_\beta(x_2) V | \boldsymbol{P}\rangle \, ,$$

where V specifies the potential for the system (Σ^+, proton) which is described by the state vector $|\boldsymbol{P}\rangle$; α and β are spin indices.

When the scalar interaction through the K-field is taken into account up o the second order of approximation, then in the non-relativistic limit the matrix element becomes:

$$\langle 0 | P_\alpha(x_1)\, \Sigma^+_\beta(x) V_{2K} | \boldsymbol{P}\rangle = \langle 0 | P_\alpha(x_1)\, \Sigma^+_\beta(x_2) 2 g^2_{\Sigma K} \cdot$$
$$\cdot \left\{ \int P^*_\varrho K^d_0 \Sigma^+_\varrho \, d^3x \, \frac{1}{A} \int \Sigma^{+*}_\sigma K^{*c}_0 P_\sigma \, d^3x + \int \Sigma^{+*}_\sigma K^{*d}_0 P_\sigma \, d^3x \, \frac{1}{A} \int P^*_\varrho K^c_0 \Sigma^+_\varrho \, d^3x \right\} | \boldsymbol{P}\rangle \, .$$

A is simply $-H^k_0$ in the static approximation. The indices c and d denote the creation and annihilation of particles.

Operating on this matrix element with the usual anticommutation relations:

$$[P_\varrho(x),\, P^*_\sigma(x')]_+ = [\Sigma^+_\varrho(x),\, \Sigma^{+*}_\sigma(x')]_+ = \delta^3(\boldsymbol{x} - \boldsymbol{x}')\,\delta_{\varrho\sigma}$$
$$[P_\varrho(x),\, \Sigma^+_\sigma(x')]_+ = [P_\varrho(x),\, P_\sigma(x')]_+ = [\Sigma^+_\varrho(x),\, \Sigma^+_\sigma(x')]_+ = \dots = 0$$

(6) C. CEOLIN and L. TAFFARA: *Nuovo Cimento*, 5, 435 (1957).

and disregarding self-energy effects, one obtains:

$$\langle 0 | P_\alpha(x_1)\, \Sigma^+_\beta(x_2) V_{2K} | \boldsymbol{P} \rangle = \frac{2g^2_{\Sigma K}}{(2\pi)^3} \int \frac{d^3k}{\omega^2} \exp[i\boldsymbol{k}\cdot\boldsymbol{r}] \psi_{\beta\alpha}(x_2, x_1)\,,$$

where $\psi_{\beta\alpha}(x_2, x_1) = \langle 0 | P_\beta(x_2)\, \Sigma^+_\alpha(x_1) | \boldsymbol{P} \rangle$ is the wave function of the system. Finally we have that:

$$\psi_{\beta\alpha}(x_2, x_1) = {}_{\alpha\beta}[P_x P_\sigma \psi(x_1, x_2)\,,$$

with

$$P_\sigma = \frac{1 + \boldsymbol{\sigma}_1\boldsymbol{\sigma}_2}{2}\,.$$

Suppressing spin indices and integrating over k we have

$$\langle 0 | P(x_1)\, \Sigma^+(x_2) V_{2K} | \boldsymbol{P} \rangle = \frac{(g^s_{\Sigma K})^2}{2\pi} \frac{\exp[-\mu_K r]}{r} P_x P_\sigma \psi(x_1, x_2)\,.$$

The generalization to the other cases is straightforward.

RIASSUNTO

Si discute il legame degli iperoni Σ con nucleoni, assumendo che l'interazione avvenga per scambio di mesoni π, di mesoni K o di entrambi. Si dimostra che quest'ultimo è il caso più probabile.

IL NUOVO CIMENTO Vol. VI, N. 5 1° Novembre 1957

On the Quantization of Tensor Fields with Zero Mass.

C. G. Bollini

Comisión Nacional de la Energía Atómica - Argentina

(ricevuto il 17 Giugno 1957)

Summary. — A general formulation of quantum field theory for massless tensor fields, compatible with the supplementary conditions, is given. The free field (or the interacting field in the interaction representation) is expressed in terms of its components « along » the transversal polarization tensors defined in the text. These components are taken as canonical co-ordinates, on which the canonical commutation relations are imposed. The corresponding commutation relations of the field components are given.

1. – Introduction.

The field of an elementary particle with vanishing mass, satisfies the equations [1]:

$$\partial_\nu \partial_\nu A_{\nu_1 \dots \nu_s} = 0 \,, \tag{1.1}$$

$$\partial_{\nu_1} A_{\nu_1 \dots \nu_s} = 0 \,, \tag{1.2}$$

$$A_{\nu_1 \nu_1 \nu_3 \dots \nu_s} = 0 \,. \tag{1.3}$$

The field quantities $A_{\nu_1 \dots \nu_s}$ are the components of a symmetric tensor of rank s. (1.1) is the field equation and (1.2), (1.3) are the supplementary conditions which ensure that the theory is based on an irreducible representation of a unique spin s.

In the usual quantization procedure, the field components are taken as canonical variables and the canonical commutation relations are imposed.

---

(1) H. Umezawa: *Quantum Field Theory* (1956).

However, these commutation relations will not be compatible with the supplementary conditions (1.2) and (1.3). Therefore, a subsidiary condition on the state vector is adopted instead of equations (1.2) and (1.3). Nevertheless, this procedure is not universally adhered to [2].

We want to approach the problem of the quantization from a different point of view. We intend to take (1.2) and (1.3) as constraint equations and so we are going to extract the independent components from the field tensor. As a consequence, a generalization of a method for the vectorial field due to J. G. VALATIN [3] will result. Of course, the commutation relations between the independent components of the field will be compatible with the supplementary conditions.

2. – Decomposition of the field tensor.

Starting with the symmetric and traceless tensor of rank s, $\boldsymbol{A}$, satisfying the equations (1.1), (1.2), (1.3), let us define by recurrence the following tensors:

$$A^{(0)} = n_{\nu_1} \dots n_{\nu_s} A_{\nu_1 \dots \nu_s}$$

$$A^{(0)}_{\nu_1 \dots \nu_s} = \partial^{-s} \partial_{\nu_1} \dots \partial_{\nu_s} A^{(0)}$$

$$A^{(r)}_{\nu_1 \dots \nu_r} = n_{\nu_{r+1}} \dots n_{\nu_s} \Big(A_{\nu_1 \dots \nu_s} - \sum_{t=0}^{r-1} A^{(r)}_{\nu_1 \dots \nu_s}\Big) \tag{2.1}$$

$$A^{(r)}_{\nu_1 \dots \nu_s} = \partial^{-(s-r)} \partial_{\nu_{r+1}} \dots \partial_{\nu_s} A^{(r)}_{\nu_1 \dots \nu_r} + (\text{symm}) \tag{2.2}$$

n_ν is an arbitrary time-like unit vector: $n_\nu n_\nu = -1$. « (symm) » means terms necessary to obtain a symmetric tensor. $\partial = n_\nu \partial_\nu$ and ∂^{-1} is the inverse operator (COESTER and JAUCH [4]).

All these tensors satisfy (1.1), (1.2) and (1.3). We also have:

$$n_{\nu_1} A^{(r)}_{\nu_1 \dots \nu_r} = 0 \qquad r \neq 0 \tag{2.3}$$

$$n_{\nu_{r+1}} \dots n_{\nu_s} A^{(r)}_{\nu_1 \dots \nu_s} = A^{(r)}_{\nu_1 \dots \nu_r} . \tag{2.4}$$

From (2.1) with $r = s$, we have:

$$A_{\nu_1 \dots \nu_s} = \sum_{t=0}^{s} A^{(t)}_{\nu_1 \dots \nu_s} . \tag{2.5}$$

---

(2) See, for example: T. KIMURA: *Prog. Theor. Phys.*, **16**, 555 (1956); S. OZAKI: *Prog. Theor. Phys.*, **14**, 511 (1955).

(3) J. G. VALATIN: *Danske Vidensk. Selsk. Mat. Fys. Medd.*, **26**, No. 13 (1951).

(4) F. COESTER and J. M. JAUCH: *Phys. Rev.*, **78**, 149 and 827 (1950).

The tensor $A^{(r)}_{\nu_1...\nu_r}$ ($r \neq 0$) being orthogonal to ∂_ν and to n_ν, has the same number of independent components as a symmetric and traceless tensor in two dimensions. This number is two. Of course, $A^{(0)}$ being scalar, has only one component. From (2.2), we deduce that $A^{(r)}_{\nu_1...\nu_s}$ posseses the same number of independent components as $A^{(r)}_{\nu_1...\nu_r}$. Then, equation (2.5) is a decomposition of the field tensor in $s+1$ tensors with a total of $2s+1$ independent components. The tensor $A^{(0)}_{\nu_1...\nu_s}$ is purely longitudinal, while $A^{(s)}_{\nu_1...\nu_s}$ is purely transversal.

3. – Polarization tensors.

Let us take two derivation operators α_ν and β_ν, in such a way that:

$$n_\nu \alpha_\nu = 0 \qquad n_\nu \beta_\nu = 0$$

$$\alpha_\nu \partial_\nu = 0 \qquad \beta_\nu \partial_\nu = 0$$

$$\alpha_\nu \alpha_\nu = 1 \qquad \beta_\nu \beta_\nu = 1$$

$$\alpha_\nu \beta_\nu = 0 \, .$$

(They are not unique).

Now, let us define by recurrence, the following tensor operators

$$\alpha_{\nu_1...\nu_{r+1}} = \alpha_{\nu_1...\nu_r} \alpha_{\nu_{r+1}} - \beta_{\nu_1...\nu_r} \beta_{\nu_{r+1}} \tag{3.1}$$

$$\beta_{\nu_1...\nu_{r+1}} = \alpha_{\nu_1...\nu_r} \beta_{\nu_{r+1}} + \beta_{\nu_1...\nu_r} \alpha_{\nu_{r+1}} \, . \tag{3.2}$$

They are symmetric and traceless. Furthermore, they are orthogonal to n_ν and ∂_ν, and

$$\alpha_{\nu_1...\nu_r} \beta_{\nu_1...\nu_r} = 0 \, .$$

Let us call them the transversal polarization tensors.

Two independent components of $A^{(r)}_{\nu_1...\nu_r}$ ($r \neq 0$) may be obtained by means of

$$\alpha_{\nu_1...\nu_r} A^{(r)}_{\nu_1...\nu_r} \quad \text{and} \quad \beta_{\nu_1...\nu_r} A^{(r)}_{\nu_1...\nu_r} \, .$$

Then, we can put:

$$A^{(r)}_{\nu_1...\nu_r} = \alpha_{\nu_1...\nu_r} Q^{(2r)} + \beta_{\nu_1...\nu_r} Q^{(2r+1)} \tag{3.3}$$

$$A^{(0)} = Q^{(1)} \, . \tag{3.4}$$

By means of (2.2) we can obtain the tensors $A^{(r)}_{\nu_1...\nu_s}$.

The $2s+1$ scalar quantities $Q^{(\varrho)}$ ($\varrho = 1, ..., 2s+1$) are free variables which may be taken as canonical co-ordinates of the field. They satisfy the equation

$$\partial_\nu \partial_\nu Q^{(\varrho)} = 0 \,, \tag{3.5}$$

without any supplementary condition.

4. – Gauge transformations.

If the tensor $A_{\nu_1 .. \nu_{s-1}}$ satisfies (1.1), (1.2) and (1.3), then it follows from

$$G_{\nu_1 .. \nu_s} = \partial_{\nu_s} A_{\nu_1 ... \nu_{s-1}} + (\text{symm}) \tag{4.1}$$

that

$$B_{\nu_1 .. \nu_s} = A_{\nu_1 ... \nu_s} + G_{\nu_1 .. \nu_s} \,, \tag{4.2}$$

also satisfies the same equations. The transformation $\boldsymbol{A} \to \boldsymbol{B}$ is called a Gauge transformation.

The decomposition of $\boldsymbol{A}$ is (cf. eq. (2.5))

$$A_{\nu_1 .. \nu_{s-1}} = \sum_{t=0}^{s-1} A^{(t)}_{\nu_1 .. \nu_{s-1}} \,.$$

Then

$$G_{\nu_1 .. \nu_s} = \sum_{t=0}^{s-1} G^{(t)}_{\nu_1 ... \nu_s} \,. \tag{4.3}$$

The tensor $\boldsymbol{G}$ has no totally transversal component:

$$G^{(s)}_{\nu_1 ... \nu_s} = 0 \,.$$

Thus, if a gauge transformation is made on $\boldsymbol{A}$, all but one of its tensor components are changed. The part unaffected by a gauge transformation is $A^{(s)}_{\nu_1 .. \nu_s}$, i.e. $Q^{(2s)}$ and $Q^{(2s+1)}$. They are actually the free components of $\boldsymbol{A}$. The other components are needed to describe the « direct » or « longitudinal » interaction between the sources of the field.

5. – Quantization.

The quantities $Q^{(\varrho)}$ form a system of independent co-ordinates satisfying (3.5). Therefore, we impose on them the « canonical » commutation relations

$$[Q^{(\varrho)}(x), Q^{(\varrho')}(x')] = i \cdot \delta^{\varrho\varrho'} \cdot D(x - x') \,, \tag{5.1}$$
$$\delta^{\varrho\varrho'} = 0 \quad \varrho \neq \varrho' \,; \qquad \delta^{\varrho\varrho} = \pm 1 \,.$$

(We leave open the assignment of sign. See [3] for the electromagnetic field) (3.3), (3.4) and (5.1) give

$$(5.2)\qquad [A^{(r)}_{\nu_1\ldots\nu_r}(x),\, A^{(r')}_{\mu_1\ldots\mu_{r'}}(x')] = i\cdot\delta^{rr'}\cdot(\alpha_{\nu_1\ldots\nu_r}\alpha_{\mu_1\ldots\mu_r}+\beta_{\nu_1\ldots\nu_r}\beta_{\mu_1\ldots\mu_r})\cdot D(x-x') = i\cdot\delta^{rr'}\cdot d_{\nu_1\ldots\nu_r;\,\mu_1\ldots\mu_r}D(x-x')\,.$$

It is easily seen that $d_{\nu_1\ldots\nu_r;\,\mu_1\ldots\mu_r}$ is independent of the choice of the polarization vectors α_ν and β_ν. In fact, from (3.1) and (3.2) we can derive the recurrence relations:

$$d_{\nu_1\ldots\nu_{r+1};\,\mu_1\ldots\mu_{r+1}} = d_{\nu_1\ldots\nu_r;\,\mu_1\ldots\mu_r}\, d_{\nu_{r+1};\,\mu_{r+1}} - e_{\nu_1\ldots\nu_r;\,\mu_1\ldots\mu_r}\, e_{\nu_{r+1};\,\mu_{r+1}}$$

$$e_{\nu_1\ldots\nu_{r+1};\,\mu_1\ldots\mu_{r+1}} = d_{\nu_1\ldots\nu_r;\,\mu_1\ldots\mu_r}\, e_{\nu_{r+1};\,\mu_{r+1}} + e_{\nu_1\ldots\nu_r;\,\mu_1\ldots\mu_r}\, d_{\nu_{r+1};\,\mu_{r+1}}\,.$$

With

$$e_{\nu_1\ldots\nu_r;\,\mu_1\ldots\mu_r} = \alpha_{\nu_1\ldots\nu_r}\beta_{\mu_1\ldots\mu_r} - \beta_{\nu_1\ldots\nu_r}\alpha_{\mu_1\ldots\mu_r}\,,$$

$d_{\nu;\mu}$ and $e_{\nu;\mu}$ are actually independent of α_ν and β_ν; they are the fundamental tensors (symm. and antisymm. resp.) in a plane perpendicular to n_ν and ∂_ν.

Defining now,

$$(5.3)\qquad d^{(r)}_{\nu_1\ldots\nu_s;\,\mu_1\ldots\mu_s} = \partial^{-2(s-r)}\partial_{\nu_{r+1}}\ldots\partial_{\nu_s}\partial_{\mu_{r+1}}\ldots\partial_{\mu_r} d_{\nu_1\ldots\nu_r;\,\mu_1\ldots\mu_r} + (\text{symm})$$

we have (cf. (2.2) and (5.2)):

$$(5.4)\qquad [A^{(r)}_{\nu_1\ldots\nu_s}(x),\, A^{(r')}_{\mu_1\ldots\mu_s}(x')] = i\cdot\delta^{rr'}\cdot d^{(r)}_{\nu_1\ldots\nu_s;\,\mu_1\ldots\mu_s}D(x-x')\,.$$

Finally, summing over r and r' we obtain

$$(5.5)\qquad [A_{\nu_1\ldots\nu_s}(x),\, A_{\mu_1\ldots\mu_s}(x')] = i\cdot\bar d_{\nu_1\ldots\nu_s;\,\mu_1\ldots\mu_s}D(x-x')\,,$$

$$(5.6)\qquad \bar d_{\nu_1\ldots\nu_s;\,\mu_1\ldots\mu_s} = \sum_r \delta^{rr} d^{(r)}_{\nu_1\ldots\nu_s;\,\mu_1\ldots\mu_s}\,,$$

(5.4) are the commutation relations to be imposed on the field tensor. They are compatible with the supplementary conditions (1.2) and (1.3).

6. – Examples.

In the case $s=1$, taking $-\delta^{00}=\delta^{11}=1$, the commutation relations (5.5) are reduced to those of J. VALATIN [3] for the electromagnetic field,

$$(6.1)\qquad \begin{cases} d^{(0)}_{\mu;\,\nu} = \partial^{-2}\partial_\mu\partial_\nu\,, \\ d^{(1)}_{\mu;\,\nu} = \delta_{\mu\nu} - \partial^{-2}\partial_\mu\partial_\nu - n_\mu\partial_\nu\partial^{-2} - n_\nu\partial_\mu\partial^{-1}\,, \\ \bar d_{\mu;\,\nu} = \delta_{\mu\nu} - 2\partial^{-2}\partial_\mu\partial_\nu - n_\mu\partial_\nu\partial^{-1} - n_\nu\partial_\mu\partial^{-1}\,. \end{cases}$$

In the case $s=2$, we have

$$A^{(0)}_{\mu\nu}=\partial^{-2}\partial_\mu\partial_\nu A^{(0)}\,;\qquad A^{(0)}=Q^{(1)}$$

$$A^{(1)}_{\mu\nu}=\partial^{-1}\partial_\mu A^{(1)}_\nu+\partial^{-1}\partial_\nu A^{(1)}_\mu\,;\qquad A^{(1)}_\mu=\alpha_\mu Q^{(2)}+\beta_\mu Q^{(3)}$$

$$A^{(2)}_{\mu\nu}=\alpha_{\mu\nu}Q^{(4)}+\beta_{\mu\nu}Q^{(5)}$$

$$A_{\mu\nu}=\partial^{-2}\partial_\mu\partial_\nu Q^{(1)}+\partial^{-1}(\partial_\mu\alpha_\nu+\partial_\nu\alpha_\mu)Q^{(2)}+ \\ +\partial^{-1}(\partial_\mu\beta_\nu+\partial_\nu\beta_\mu)Q^{(3)}+\alpha_{\mu\nu}Q^{(4)}+\beta_{\mu\nu}Q^{(5)}\,, \tag{6.2}$$

$$[A^{(0)}_{\mu\nu}(x),\,A^{(0)}_{\varrho\sigma}(x')]=i\cdot\delta^{00}\partial^{-4}\partial_\mu\partial_\nu\partial_\varrho\partial_\sigma D(x-x')\,, \tag{6.3}$$

$$[A^{(1)}_{\mu\nu}(x),\,A^{(1)}_{\varrho\sigma}(x')]=i\cdot\delta^{11}\partial^{-2}\big(\partial_\mu\partial_\nu d^{(1)}_{\varrho;\sigma}+(\text{symm})\big)D(x-x')\,, \tag{6.4}$$

$$[A^{(2)}_{\mu\nu}(x),\,A^{(2)}_{\varrho\sigma}(x')]=i\cdot\delta^{22}(\alpha_{\mu\nu}\alpha_{\varrho\sigma}+\beta_{\mu\nu}\beta_{\varrho\sigma})D(x-x')= \\ =i\cdot\delta^{22}(d^{(1)}_{\mu;\varrho}d^{(1)}_{\nu;\sigma}+d^{(1)}_{\mu;\sigma}d^{(1)}_{\nu;\varrho}-d^{(1)}_{\mu;\nu}d^{(1)}_{\varrho;\sigma})D(x-x')\,. \tag{6.5}$$

The last commutation relation coincides with that of T. KIMURA ([5]) for the incoming transversal field if the trace part is substracted from his result.

([5]) T. KIMURA: *Prog. Theor. Phys.*, **16**, 555 (1956), p. 566, eq. (4.10).

RIASSUNTO (*)

Si dà una formulazione generale della teoria quantistica dei campi, per campi di tensori privi di massa, compatibili con le condizioni supplementari. Il campo libero (o il campo interagente nella rappresentazione per mezzo dell'interazione) si esprime in termini delle sue componenti «secondo» i tensori di polarizzazione trasversali definiti nel testo. Tali componenti si prendono come coordinate canoniche alle quali si impongono le relazioni di commutazione canoniche. Si danno le corrispondenti relazioni di commutazione delle componenti del campo.

(*) *Traduzione a cura della Redazione.*

General Theory of Particle Mixtures.

Ko Aizu

Department of Physics, Rikkyo University - Ikebukuro, Tokyo

(ricevuto il 18 Giugno 1957)

Summary. — The general theory of particle mixtures is developed and their remarkable time behavior at decay is shown to be a natural consequence of degeneracy of the initial state. Applications to several simple cases, positronium in a magnetic field, K^0 and $\overline{K}^0$ particle mixture and a possible θ-τ doublet are discussed. In particular it is shown that, if the K^0 has two lifetimes, the mass difference between K^0 and $\overline{K}^0$ caused by a possible non-invariance of strong interaction under charge-conjugation can not exceed much the value 10^{-5} eV.

1. – Introduction.

In connection with the θ^0 and $\overline{\theta}^0$ decay, Gell-Mann and Pais (1) proposed the notion of « particle mixture » and discussed their remarkable time behavior at decay. Then Pais and Piccioni (2) pointed out a possible experiment which shows the regeneration of the θ_1 component after traversal in matter. Snow (3) discussed similar problems in the case of τ^0 and $\overline{\tau}^0$ particle mixtures. Treiman and Sachs (4) pointed out the existence of an interference phenomenon in the θ^0 and $\overline{\theta}^0$ decay, if one considers $e^++\pi^-+\nu$ and $e^-+\pi^++\overline{\nu}$ decay modes besides $\pi^++\pi^-$ and $\pi^++\pi^-+\gamma$ modes, and takes into account the initial mass difference. Arnowitt and Teutsch (5) discussed the θ-τ problem, including a

(1) M. Gell-Mann and A. Pais: *Phys. Rev.*, **47**, 1387 (1955).
(2) A. Pais and O. Piccioni: *Phys. Rev.*, **100**, 1487 (1955).
(3) G. Snow: *Phys. Rev.*, **103**, 1111 (1956).
(4) S. B. Treiman and R. G. Sachs: *Phys. Rev.*, **103**, 1545 (1956).
(5) R. Arnowitt and W. B. Teutsch: *Phys. Rev.*, **105**, 285 (1957).

possible mixing interaction between them. More recently LEE, OEHME and YANG ([6]) discussed a more complicated time behavior of K^0 and K^0 particle mixture in connection with a possible non-invariance of time reversal and charge conjugation of weak interaction.

Although in this way the properties of particle mixtures seem to have been discussed thoroughly, there remains a point worth discussing. So far the following elementary question has not been explicitly answered; particle mixtures decay with several decay modes. On the other hand as is well known there are many examples of β and γ decays with several decay modes in nuclear physics. Why the former cases have several lifetimes and the latter only one lifetime? What is the fundamental reason for appearance of such a remarkable time behavior of particle mixtures at decay?

To answer these questions, it is important to notice that a particle mixture is a degenerate system. The usual WEISSKOPF and WIGNER ([7]) theory on decay of quantum mechanical systems is confined implicitly to a non-degenerate initial system. If one extends the WW theory to a degenerate system, it is found that the remarkable time behavior of particle mixtures at decay is a natural consequence of their degeneracy and the usual exponential decay of degenerate systems is a rather special case which is simplified by some selection rules.

In Sect. 2 we start from the fundamental equations in the usual time dependent perturbation theory and will show that the assumption on time variation of initial amplitudes is not only unnecessary but can be also proved from the fundamental equations. This point is important because for the case of degenerate systems we do not know how to assume a priori time behavior of initial amplitudes except for special cases. In solving the fundamental equations, we meet a matrix which we call a decay rate matrix. The eigenstates of this matrix are just « particle states » with a single lifetime, which is the eigenvalue of this matrix. In this way the whole time behavior at decay is characterized by the decay matrix. Applications to several simple cases are discussed and some points assumed by previous authors are shown to be correct.

However the discussion in Sect. 2 is incomplete in that the mass (energy) shift was neglected. In Sect. 3 we shall discuss the effect of mass shift together with the case where the energy of initial states is different. It is necessary to treat carefully the mass shift effect on the initial energy and the energy dependence of decay and mass shift matrix. The general formulas for lifetime and decay rate are complicated, but in the usual decay problems, these expressions can be further simplified. Applications to several examples are dis-

---

([6]) T. D. LEE, R. OEHME and C. N. YANG: *Phys. Rev.*, **106**, 340 (1957).

([7]) V. WEISSKOPF and E. WIGNER: *Zeits. f. Phys.*, **63**, 54 (1932).

cussed. In particular, for K^0 and $\bar{K}^0$ particle mixtures an important conclusion is obtained. If the initial mass difference between K^0 and $\bar{K}^0$ is larger than the line breadhts due to decay, they decay practically with a single lifetime.

2. – Elementary theory.

To clarify the essential features of our problem, let us consider it in the frame of elementary time dependent perturbation theory as in WEISSKOPF and WIGNER's paper. In the case where the degenerate initial states have the same energy, the initial amplitudes $a_r(t)$, $(r=1, 2, \ldots)$ and the final amplitudes $f_n(t)$, $(n=1, 2, \ldots)$ are connected by a set of the following equations (*)

$$i\dot{a}_r(t) = \sum_n H_{rn} f_n(t) \exp[-i\omega_n t], \tag{1}$$

$$i\dot{f}_n(t) = \sum_r H_{nr} a_r(t) \exp[+i\omega_n t], \tag{2}$$

where $\omega_n = E_n - E_0$, i.e. the final energy minus the initial energy, and the choice of the set of eigenfunctions may be arbitrary. Since we abandon Weisskopf and Wigner's assumption on the time behavior of initial states, it seems desirable to find equations containing only the initial amplitudes. Integrating Eq. (2) formally and substituting it in Eq. (1), we get after interchanging the order of time integration,

$$a_r(t) = a_r^0 - i \sum_n H_{rn} H_{ns} \int_0^t \mathrm{d}t' a_s(t') (\exp[-i(t-t')\omega_n] -)/\omega_n, \tag{3}$$

Now we divide the summation $\sum_n$ in two parts

$$\sum_n = \int_Q^\infty \mathrm{d}\omega_n \varrho(E_n) \sum_n{}',$$

where $\sum_n{}'$ means the summation over the freedoms other than energy, $\varrho(E_n)$ is the density of energy levels, and Q is the Q value of the decay process (if there are several decay modes with different Q values, we must integrate separately over the energy for each decay mode). As in WEISSKOPF and WIGNER, we consider the behavior of the system after a long time t, or more precisely $t \gg Q^{-1}$, which is the case for « ordinary » strange particles, where the lifetime is of the

(*) $\hbar = c = 1$.

order of 10^{-9} s and $Q \geqslant 1$ MeV. After integration over energy, Eq. (3) becomes

$$a_r(t) = a_r^0 - \frac{1}{2}\sum_s \Gamma_{rs}\int_0^t \mathrm{d}t' a_s(t') , \tag{4}$$

where (*)

$$\begin{cases} \Gamma_{rs} = \Lambda_{rs}(E_0) + 2i\Delta_{rs}(E_0) , \\ \Lambda_{rs}(E_n) = 2\pi \sum' \varrho(E_n) H_{rn} H_{ns} , \\ \Delta_{rs}(E) = \mathfrak{P}\int_{-Q}^{\infty} \mathrm{d}\omega_n \, \varrho(E_n) \sum' H_{rn} H_{ns}/(E - E_n) . \end{cases} \tag{5}$$

The matrix Γ_{rs} consists of two Hermitian matrices: decay matrix Λ_{rs} and mass shift matrix Δ_{rs}. Eq. (5) can be converted into a differential equation

$$\dot{a}_r(t) = \tfrac{1}{2}\sum_s \Gamma_{rs} a_s(t) . \tag{6}$$

Here we would like to make a few remarks.

a) If there are several decay modes denoted by i where $n = (i, m)$, one can express the above matrices as sums of similar matrices referring to only one decay mode, for example,

$$\begin{cases} \Lambda_{rs} = \sum \Lambda_{rs}^{(i)}(E_0) , \\ \Lambda_{rs}^{(i)}(E_n) = 2\pi \sum_m' \varrho(E_n) H_{rim} H_{ims} . \end{cases} \tag{7}$$

b) If we start from the usual point interaction and calculate the mass shift matrix Δ_{rs}, it will generally diverge. As at the present stage of our knowledge we have not any method to treat this divergence other than the cut-off method or renormalization technique, it will be better to treat this matrix phenomenologically, and assume that it is finite and is at most of the same order of magnitude as Λ_{rs}.

c) However it is to be noted that in deriving Eqs. (4) and (5) we tacitly assume that $a_r(t)$ and $f_n(t)$ do not contain an oscillating term due to energy shift. In order to be consistent with this assumption, we must drop the mass shift and postpone the discussion on its effect to the next section.

(*) The author is indebted to Dr. M. L. Good for drawing the author's special attention on the mass shift term.

Then Eq. (6) becomes

$$\dot{a}_r(t) = -\tfrac{1}{2} \sum_s \Lambda_{rs} a_s(t) \tag{8}$$

and its general solution is easily written down by the aid of real eigenvalues λ_α and orthonormal eigenstates χ^α of the decay matrix Λ_{rs} as follows,

$$a_r(t) = \sum_\alpha c_\alpha \chi_r^\alpha \exp[-\lambda_\alpha t/2]\,, \tag{9}$$

where c_α are determined by initial conditions. This solutions shows that *a*) only the eigenstates χ^α which are definite linear combinations of initial bases, can have a single lifetime and are just « particle states » in the terminology of GELL-MANN and PAIS ([1]). *b*) The initial state decays generally with several lifetimes.

The physical reason why there appear eigenstates χ^α which are defined by the decay process, is the same as in the case of the usual steady perturbation theory of degenerate systems. In fact, the eigenvalue problem of the matrix (5) is essentially the diagonalization of the first order energy matrix with complex energy, the imaginary part of which is the reciprocal of lifetime. In order to get not only the lifetime and eigenfunction, but also the time variation of various amplitudes, it is necessary to use non-steady perturbation theory as is done in this note.

Now, Eq. (9) gives the time dependence of the probability of initial states

$$P(t) = \sum_r |a_r(t)|^2 = \sum_\alpha |c_\alpha|^2 \exp[-\lambda_\alpha t]\,. \tag{11}$$

The decay rate of a certain mode i,

$$R^{(i)}(t) = (\partial/\partial t) \sum_n |f_n(t)|^2 = 2\Re \sum_m f_{im}^*(f)\, \dot{f}_{im}(t)$$

is calculated by means of Eqs. (2), (3) and (9) as follows:

$$R^{(i)}(t) = \sum a_r^*(t) \Lambda_{rs} a_s(t) = \sum_\alpha \lambda_\alpha |c_\alpha|^2 \exp[-\lambda_\alpha t]\,. \tag{12}$$

Thus as long as the mass shift is neglected there appears no interference term in the probability of initial state and the decay rate.

Thus the remarkable time behavior of particle mixture is a natural consequence of the degeneracy of the initial system and the usual exponential character of the decay is, in the degenerate system, a special case caused by some selection rules.

Now we shall apply the above theory to several decay processes. There is no new result, but it is of some interest to review diverse cases from a general point of view.

A) The case where the initial state is not degenerate. This is, for example, the case where the decaying particle has spin 0 and no other internal degree of freedom as in $\pi \to \mu + \nu$ decay. The decay matrix is simply a decay constant and the initial amplitude decays with a simple exponential law as was assumed by WEISSKOPF and WIGNER.

B) The case where the initial state is degenerate but can be treated as if it were not degenerate. This is, for example, the case where the initial degeneracy is due only to the spin of the decaying particle, as in β or γ decay in nuclear physics. We assume, for simplicity, the decaying particle to have spin $\frac{1}{2}$ and denote the spin up and down states by suffixes 1 and 2 respectively. Due to the conservation law of angular momentum we have $\Lambda_{11}=\Lambda_{22}$, $\Lambda_{12}=\Lambda_{21}=0$. Then there is only one lifetime and the degeneracy does not give rise to any complication in this case. We can treat the spin polarization of the initial state as usually.

C) The θ^0 and $\bar{\theta}^0$ problem of Gell-Mann and Pais. θ^0 and $\bar{\theta}^0$ are a particle mixture of θ_1 and θ_2 which are eigenstates of charge conjugation and decay, for example, into $\pi^+ + \pi^-$ and $\pi^+ + \pi^- + \gamma$ respectively. We shall denote the θ_1 and θ_2 states by suffixes 1 and 2. If the decay process is invariant under charge conjugation, $\Lambda_{12} = \Lambda_{21} = 0$ but not necessarily $\Lambda_{11} = \Lambda_{22}$. Then the θ_1 and θ_2 states are quite appropriate linear combinations of θ^0 and $\bar{\theta}^0$ so that each state θ_1 and θ_2 has only one decay constant Λ_{11} and Λ_{22} respectively. If the initial state is θ^0 we may have $c_1 = c_2 = 1/\sqrt{2}$ and the decay rates (12) become

$$R(\theta^0 \to \pi^+ + \pi^-) \qquad = (\Lambda_{11}/2) \exp [- \Lambda_{11} t] ,$$

$$R(\theta^0 \to \pi^+ + \pi^- + \gamma) = (\Lambda_{22}/2) \exp [- \Lambda_{22} t] ,$$

3. – General theory and its applications.

Although the essential features of particle mixtures are clarified in the preceeding paragraph, two points remain to be further discussed: *a*) the mass shift due to decay should be taken into account. *b*) It is desirable to treat the case where the energies of the states of the initial system are different, for example, owing to some process other than decay. There are several examples of this case: 1) singlet and triplet positronium in magnetic field; 2) K^0 and K^0 particle mixture if their masses are different because of possible non-invariance under charge conjugation in strong interactions; 3) θ and τ particle mixture with different masses.

Now we start from the following fundamental equations:

$$(13)\qquad i\dot{a}_r = \sum_n H_{rn} f_n \exp\left[-i(E_n - E_r)t\right],$$

$$(14)\qquad i\dot{f}_n = \sum_s H_{ns} a_s \exp\left[-i(E_s - E_n)t\right].$$

It is not allowed to apply the method used in the preceeding section, because, as was pointed out in Sect. **1**, $a_r(t)$ must contain an oscillating term which expresses the effect of mass shift. Instead of intending to arrive at an equation similar to Eq. (6), we start from an assumption that $a_r(t)$ is of the form:

$$(15)\qquad a_r(t) = \sum_\alpha c_\alpha \chi_r^\alpha \exp\left[-i(E_\alpha - E_r)t - \lambda_\alpha t/2\right],$$

where c_α, E_α, λ_α and normalized vectors χ^α are constants to be determined. This assumption means that the initial amplitudes are linear combinations of states χ^α with some definite energy E_α and single lifetime $1/\lambda_\alpha$.

Then one can easily obtain from Eqs. (13), (14) and (15) an equation which determines the above unknown constants E_α, λ_α and χ^α,

$$(16)\qquad \sum_s \left[\Gamma_{rs}(E_\alpha - i\lambda_\alpha/2) + 2i\delta_{rs}E_r - \delta_{rs}(\lambda_\alpha + 2iE_\alpha)\right]\chi_s^\alpha = 0,$$

where Γ_{rs} are defined by Eq. (5) with complex argument $E_\alpha - i\lambda_\alpha/2$. This is a non-linear and non-Hermitian eigenvalue problem, and the existence and nature of its solution is not clear. For the time being we assume that a sufficient number of solutions exist and the eigenvectors χ^α are linearly independent. Thus, as in the simple theory in Sect. **1**, *a*) only the eigenstates χ^α, which are definite linear combination of bases initially chosen, can have a definite energy and a single lifetime and are «particle states» by Gell-Mann and Pais. *b*) If the weak decay interaction is taken into account, the initial state has no definite mass and decays with several lifetimes.

The probability of the initial state $P(t)$ and the decay rate of a certain decay mode $iR^{(i)}(t)$ are easily calculated as follows,

$$(17)\qquad \begin{cases} P(t) = \sum_r \left|\sum_\alpha c_\alpha \chi_r^\alpha \exp\left[-iE_\alpha t - \lambda_\alpha t/2\right]\right|^2, \\ R^{(i)}(t) = \sum_{r,s}\sum_{\alpha,\beta} \Re\left[c_\alpha^* \chi_r^{\alpha *}\{\exp\left[iE_\alpha t - \lambda_\alpha t/2\right]\}\Gamma_{rs}(E_\beta - \lambda_\beta/2)\cdot \right. \\ \qquad\qquad \left. \cdot c_\beta \chi_s^\beta \exp\left[-iE_\beta t - \lambda_\beta t/2\right]\right]. \end{cases}$$

In the above equations, contrary to the case treated in Sect. 2, appear interference terms.

Although the characteristic equation (16) and the formula for the decay rate (17) have a rather complicated expression, they can be replaced by simpler forms in most of the decay problems where the following conditions are satisfied:

a) The mass difference of the initial system of the order of Δ and the line breadth of the order of Λ are much smaller than the mass itself.

b) The characteristic matrix elements are smooth function of E. This is the case in the usual perturbation calculation based on point interaction, provided the mass shift terms are properly treated.

Then the small energy dependence of Γ_{rs} can be neglected in Eqs. (16) and (17). To see this we develop $\Gamma_{rs}(E_\alpha - i\lambda_\alpha/2)$ in power series about some mean initial mass E_0 and note that the first order terms are estimated as $\Gamma' \sim \Gamma/E_0$. In the matrix element in Eq. (16), these first order terms are neglected compared with the other terms. Then Eq. (16) becomes a linear eigenvalue problem

$$\sum_{n} [\Gamma_{rs}(E_0) + 2i\delta_{rs}E_r - \delta_{rs}(\lambda_\alpha + 2iE_\alpha)]\chi_s^\alpha = 0 \,. \tag{18}$$

and the formula for the decay rate becomes

$$R^{(i)}(t) = \sum_{r,s}\sum_{\alpha,\beta} \Re[c_\alpha^* \chi_r^{\alpha *} \exp[iE_\alpha t - \lambda_\alpha t/2]\Lambda(E_0) c_\beta \chi_s^\beta \exp[-iE_\beta t - \lambda_\beta t/2)]$$

or analogously to Eq. (12)

$$R^{(i)}(t) = \sum_{\alpha,\beta} \Re[c_\alpha^* c_\beta (\chi^\alpha, \chi^\beta)\{(\lambda_\alpha + \lambda_\beta)/2 - i(E_\alpha - E_\beta)\}\cdot \\ \cdot \exp[-(\lambda_\alpha + \lambda_\beta)t/2 - i(E_\alpha - E_\beta)t]] \,. \tag{19}$$

We shall confine ourselves to these approximation of Γ_{rs} in the following applications.

Before entering into the application, we will make one remark; the matrix elements in (18) consist of two terms of different nature, the mass shift term and the line breadth. Then the character of the solutions is strongly dependent on whether the mass shift terms are larger than the line breadth terms or not. This point is important in the applications.

Now we shall apply the above theory to the following three problems: *A*) Positronium in a magnetic field. *B*) K^0 and K^0 particle mixture. *C*) θ-τ parity doublet with mixing interactions. These problems were discussed by many authors, but to examine the various cases from a general point of view is of some interest and adds some new information to the results already obtained.

A) Singlet and triplet positronium in a uniform magnetic field. As is well known [8], in a uniform magnetic field in the z-direction, singlet positronium ^1S and triplet positronium ^3S with 0 z-spin component are mixed. We denote by ^1E and ^3E the energies of the mixed states. As long as the magnetic field is not too strong, the mixing is not large and the energy difference $^1E - {}^3E$ is, in the first approximation, $\Delta E \simeq \frac{7}{2} m\alpha^4$, where m is the electron mass and $\alpha \simeq 1/137$. The decay rates of free ^1S and ^3S positronium are $^1\lambda = \frac{1}{2}\alpha^5 m$ and $^3\lambda \simeq 11\alpha^6 m$, which are much smaller than the energy difference $^1E - {}^3E$. The characteristic matrix $\Gamma_{rs} + 2i\delta_{rs}E_r$ in the representation where the energy in a magnetic field is diagonal, is given by

$$(20) \qquad \begin{pmatrix} {}^1\lambda a^2 + {}^3\lambda b^2 + 2i\,{}^3E & ({}^3\lambda - {}^1\lambda)ab \\ ({}^3\lambda - {}^1\lambda)ab & {}^1\lambda b^2 + {}^3\lambda a^2 + 2i\,{}^1E \end{pmatrix}$$

where $\begin{pmatrix} a & b \\ -b & a \end{pmatrix}$ is a transformation matrix from the representation where free energy is diagonal to the representation where the energy in a field is diagonal. Let $x = 2\mu H/\Delta E$ and μ be the magnetic moment of the electron. In the approximation $x \ll 1$, the eigenvalues of the matrix (20) are ${}^3\lambda + {}^1\lambda x^2 + 2i\,{}^3E$ and ${}^1\lambda + 2i\,{}^1E$. Thus the positronium in a magnetic field has two decay constants ${}^3\lambda + {}^1\lambda x^2$, ${}^1\lambda$ and contains an interference term oscillating with frequency ΔE. The lifetime of the short lived component is too small to be observed and also, if the initial state is in the upper level, the amplitude of this component is very small compared with the amplitude of the long lived component, so that to retain only the latter component is a good approximation. We obtain the decay rates for 3γ decay and 2γ decay

$$R(3\gamma) = {}^3\lambda \exp\left[-({}^3\lambda + {}^1\lambda x^2)t\right],$$

$$R(2\gamma) = {}^1\lambda x^2 \exp\left[-({}^3\lambda + {}^1\lambda x^2)t\right].$$

The ratio of these rates has been measured but up to present there seems to be no measurement of this lifetime which is somewhat shorter than that of the pure ^3S state.

B) K^0 *and* K^0 *particle mixture.* As this problem was rather fully treated by LEE, OEHME and YANG [6] (LOY), we shall only give one remark about the relation between mass difference and lifetime. We denote the masses

[8] For example, summary report, S. DE BENEDETTI and H. C. CORBEN: *Ann. Rev. of Nucl. Sci.*, 4, 191 (1954).

of K⁰ and $\bar{K}^0$ by E_1 and E_2 and let $E_1+E_2=2E_0$ and $E_1-E_2=\Delta$. We may consider that this mass difference is connected with a possible non-invariance under charge conjugation. Even in this case we have $\Lambda_{11}=\Lambda_{22}$ and $\Delta_{11}=\Delta_{22}$ as is noted by LOY. Then, dropping the trivial diagonal terms, we obtain the characteristic matrix essentially as follows:

$$\begin{pmatrix} \Lambda_{11}+2i(\Delta_{11}+\Delta/2) & \Lambda_{12}+2i\Delta_{12} \\ \Lambda_{21}+2i\Delta_{21} & \Lambda_{22}+2i(\Delta_{11}-\Delta/2)\,. \end{pmatrix} \tag{21}$$

In the case where the initial mass difference Δ is smaller than the line breadths Λ_{rs}, and mass shift Δ_{rs}, the general conclusion by LOY holds. If, on the other hand, $\Delta \gg \Lambda_{rs}=\Delta_{rs}$, there arises a remarkable simplification. The eigenvalues of the matrix are, in this approximation, $\Lambda_{11}+2i(\Delta_{11}\pm\Delta/2)$, which shows that K⁰ has only one lifetime. Thus if K⁰ has two distinct lifetimes as is indicated by some experiments [9], the mass difference between K⁰ and K⁰ can not exceed much the values $\Lambda\sim 10^{-9}$ s or $\sim 10^{-5}$ eV.

C) θ-τ doublet with mixing interaction. This problem was discussed by ARNOWITT and TEUTSCH [5]. The above general theory allows us to extend their result to more general cases; they confine themselves to the case where the mass difference between a parity doublet is much larger than the line widths due to decay, but we like to omit this restriction. In the representation where θ and τ are eigenstates, the decay matrix is also diagonal with diagonal elements λ_θ and λ_τ. We denote by φ_a and φ_b the eigenstates and by E_a and E_b the eigenstates of energy in the presence of mixing interaction. In this representation the characteristic matrix is

$$\begin{pmatrix} \lambda_a+2iE_a & \lambda \\ \lambda & \lambda_b+2iE_b \end{pmatrix}, \tag{22}$$

where $\lambda_a=\lambda_\theta|c_1|^2+\lambda_\tau|c_2|^2$, $\lambda_b=\lambda_\theta|c_2|^2+\lambda_\tau|c_1|^2$ and $\lambda=(\lambda_\theta-\lambda_\tau)c_1^*c_2$ and the unitary matrix $\begin{pmatrix} c & c_2 \\ -c_2^* & c_1^* \end{pmatrix}$ is a transformation matrix from (θ, τ) to (*a*, *b*). The eigenvalues of this matrix are

$$\tfrac{1}{2}[\{\lambda_a+\lambda_b+2i(M_a+M_b)\pm[\{(\lambda_a-\lambda_b+2i(M_a-M_b)\}^2+4|\lambda|^2]\}^{\frac{1}{2}}\,.$$

If the mass difference E_a-E_b is much larger than the line widths λ_θ, λ_τ, these eigenvalues are reduced to λ_a+2iE_a and λ_b+2iE_b and eigenstates become

---

(9) K. LANDE *et al.*: *Phys. Rev.*, **103**, 1901 (1956); W. F. FRY, J. SCHNEPS and M. S. SWAMI: *Phys. Rev.*, **103**, 1904 (1956)..

approximately φ_a, φ_b. Although ARNOWITT and TEUTSCH write in their paper that the states a and b decay with a simple exponential law even in the presence of mixing interactions, as long as $\Delta E \gg \lambda$, it holds only in some approximation as we explained in the above discussion.

4. – Conclusions.

The main results of this paper are summarized as follows:

A) The Weisskopf and Wigner theory of decaying systems was extended to the cases where the initial state fully is or nearly degenerate. The existence and the remarkable time behavior of particle mixtures in contrast with the usual β or γ decay in nuclear physics are natural consequences of the degeneracy of the initial system.

B) This theory allows us to consider the various examples of particle mixtures from a general point of view, and to prove some assumptions, for example, an assumption on the time variation of the initial amplitude made by many authors, and also that of the approximate « particle » character of « a » and « b » particles in the discussion by ARNOWITT and TEUTSCH.

C) An important relation between the mass difference between K^0 and K^0 and their lifetimes is obtained. If the mass difference is much larger than the line breadhts due to decay, K^0 and K^0 have practically only one lifetime. If the experimental result that there is a long life component of the K^0 meson (9) is correct, the mass difference can not exceed too much the value of 10^{-5} eV. This result does not depend on special models of K^0 particle.

At the end of this paper we would like to point out some related problems which have not been discussed but seem to be interesting from the point of view of our theory.

A') The refinement of the general theory in Sect. 2, so that the assumption of the perturbation treatment is to be removed, can be done easily along the line developed by ARNOUS and ZIENAU (10), LOW (11), ARNOUS and HEITLER (12), NAMIKI and MUGIBAYASHI (13).

(10) E. ARNOUS and S. ZIENAU: *Helv. Phys. Acta*, **24**, 279 (1951).
(11) F. LOW: *Phys. Rev.*, **88**, 53 (1952).
(12) E. ARNOUS and W. HEITLER: *Proc. Roy. Soc.*, A **220**, 290 (1953).
(13) M. NAMIKI and N. MUGIBAYASHI: *Prog. Theor. Phys.*, **10**, 474 (1953).

B') If we apply our general theory to the problem discussed by PAIS and PICCIONI (2), WEINSTEIN (14), CASE (15) and GOOD (16) i.e., the interaction of decaying particle mixtures with matter or with external fields, we may be able to obtain a clearer insight in this phenomena.

* * *

The author would like to thank Dr. S. TANAKA for his suggestion of the importance of this problem and helpful discussions.

(14) R. M. WEINSTEIN: *The Proceedings of 6-th Rochester Conference*, VIII-9 (1956).
(15) K. CASE: *Phys. Rev.*, **103**, 1449 (1956).
(16) M. L. GOOD: *Phys. Rev.*, **105**, 1120 (1957).

RIASSUNTO (*)

Si sviluppa la teoria generale delle miscele di particelle e si dimostra che il loro notevole comportamento rispetto al tempo nel decadimento è una conseguenza naturale della degenerazione dello stato iniziale. Si discutono applicazioni a vari casi semplici: positronio in un campo magnetico, miscela di particelle K^0 e $\overline{K}^0$ e un possibile doppietto θ-τ. Si dimostra in particolare che se il K^0 ha due vite medie la differenza di massa tra K^0 e $\overline{K}^0$ dovuta a una possibile non-invarianza dell'interazione forte nella coniugazione della carica non può eccedere di molto il valore 10^{-5} eV.

(*) *Traduzione a cura della Redazione.*

IL NUOVO CIMENTO Vol. VI, N. 5 1° Novembre 1957

The 24 Hour Intensity Variations of the Primary Cosmic Rays (*).

A. M. Conforto (+) and J. A. Simpson

Enrico Fermi Institute for Nuclear Studies, The University of Chicago - Chicago, Illinois

(ricevuto il 21 Giugno 1957)

Summary. — The data from nucleonic component detectors (neutron intensity monitors) are analysed for the amplitude and phase of maximum intensity of the 24 h variation at the geomagnetic equator and at 48° N. The same analysis is performed on selected charged particle detectors. The analysis covers 1953-55, which includes the time of solar cycle (sunspot) minimum in 1954. During 1954 it is known that the 24 h variation possesses an anomalous behaviour. It is shown that during 1954 there is an interval of 9 months or more when the solar daily variation appears to undergo a progressive phase shift whose time of maximum lies in the range of 0800-1000 h on a sidereal time scale. This anisotropy certainly exists in the radiation falling upon the atmosphere, and it is likely, although not proven, that the anisotropy prevails even outside the terrestrial field. The question of whether this sidereal effect is spurious or real is discussed in relationship to the recent results on the modulation of cosmic ray intensity within the solar system.

1. – Introduction.

From the many studies already reported on the subject of 24 hour cosmic-ray intensity variations, it is clear that the effect is complicated by the superposition of geophysical and solar effects tending to produce intensity changes

(*) Assisted in part by the Office of Scientific Research and the Geophysics Research Directorate, Air Force Cambridge Research Center, Air Research and Development Command, U. S. Air Force.

(+) On leave from Department of Physics, Istituto di Fisica dell'Università, Roma, Italy, 1955-1956,

of the measured radiation recurring in 24 hour intervals [1,2]. Counter telescope and ion chamber data are difficult to correct for meteorological effects but, even by the measurement of intensity changes using the nucleonic component where we may eliminate atmospheric effects, the 24 hour variation is still observed to change in amplitude and phase with time. Thus these changes in the 24 hour variation, even at low energies, exist in the primary radiation incident upon the atmosphere. If we restrict ourselves to the low energy end of the spectrum ($E < 40$ GeV), the evidence points qualitatively to an indirect solar origin for the effect, and to an association with geomagnetic disturbance.

Specifically, we may summarize some of the results as follows:

a) There exists a world-wide mean daily cycle of amplitude approximately 0.2% for ion chambers [1,2], and approximately 0.5-1% for the nucleonic component [3].

b) Both the amplitude and the phase of the variation changes from day to day, the effect is recurring and not diurnal [3]. On some occasions, the time of maximum may even occur near local midnight [4-7].

c) The variation takes place in the primary radiation falling upon the atmosphere and extends in energy from the lowest energy particles in the beam up to energies in excess of 30 GeV [1,2]. There is a slight indication that the amplitude of the effect is greater at low energies [3].

d) There is a weak correlation of these cosmic ray variations with solar activity and geomagnetic disturbances [1,2,8].

e) The average time of maximum intensity for each year changes with an apparent 22 year cycle [9].

f) As yet, there is no clear physical interpretation for the phenomenon.

In this paper we have studied the 24 hour variation over a three year p riod which includes the decline of solar activity to a minimum and the subsequent

---

(1) For a review of the problem prior to 1951 see H. Elliot in *Progress in Cosmic Ray Physics* (Amsterdam, 1952).

(2) For a review of the problem since 1951 see V. Sarabhai and N. W. Nerurkar in *Annual Review of Nuclear Science*, vol. VI (1956).

(3) J. Firor, W. Fonger and J. A. Simpson: *Phys. Rev.*, **94**, 1031 (1954).

(4) M. Possener and I. J. Van Heerden: *Phil. Mag.*, **1**, 253 (1956).

(5) R. Steinmaurer and H. Gheri: *Naturwiss.*, **42**, 10, 204 (1955).

(6) Y. Miyazaki: *Journ. Sci. Res. Instr.*, **49**, 267 (1955).

(7) T. Yagi and H. Ueno: *Journ. Geomag. and Geoelect.*, **3**, 93 (1956).

(8) R. P. Kane: *Phys. Rev.*, **98**, 130 (1955).

(9) T. Thambyahpillai and H. Elliot: *Nature*, **171**, 918 (1953).

beginning of the new solar cycle; namely, the years 1953, 1954 and 1955. This period was of special interest since we had noticed that the 24 hour variations undergo large phase shifts during the time of solar minimum. This anomalous effect was reported by several observers [4-7]. Recently POSSENER and VAN HEERDEN have reported a study of this variation covering a period ending in early 1955. They have observed these anomalous phase changes for meson counter telescopes, but found that the amplitude of this anomalous effect was negligible for the nucleonic component [4].

Our studies are primarily devoted to data from neutron intensity monitors, in order to study the intensity changes as a function of the primary particle energy and to avoid unknown meteorological effects. Even though the atmospheric temperature effect is known to be insignificant for the nucleonic component, however we have corrected all neutron data in this paper for the well established atmospheric pressure effect. For the high energy observation, we use the neutron monitor at Huancayo, Peru ($E > 15$ GeV) where the counting rate is approximately 360 counts per minute. For the integration down to low energy particles, we use the Climax, Colorado, neutron pile ($E \gtrsim 3$ GeV), where the counting rate for each half of the pile is ~ 3400 counts per minute.

We have defined a vector to represent the amplitude and phase of the daily variation. This is equivalent to the first harmonic of the 24 hour variation. With this vector representation we have studied the long term changes in phase of the day to day variation and the average variation for each month.

We shall show that:

a) During 1953 and 1955, the phase of the vectors, except for short periods, was nearly constant when plotted on a solar time base.

b) During 1954, the phase of the vector was drifting counter-clockwise in time with respect to the solar time base, but was nearly constant on a sidereal time scale. The amplitudes of the variation at this time were not greatly different from the amplitudes for 1953 or 1955.

c) It is undecided as to whether the effect is spurious or real. However, it is likely that the observed sidereal effect is not produced by terrestrial phenomena but is an anisotropy in the cosmic radiation during 1954.

In view of these results we have investigated whether this effect persists for different kinds of charged particle detectors even though there are meteorological effects present. The main effect was observed in the Freiburg ion chamber data, and in counter telescopes at Rome, even though there are large scale distorsions.

2. – Representation of 24 hour intensity variations by vectors.

2·1. *Day to day variations.* – For each day the *amplitude* of the intensity variation is determined by the ratio of the sum of deviations in the twelve consecutive hour interval of maximum intensity, divided by the standard deviation (see Fig. 1). The standard deviation is constant for each station and is equal to $\sqrt{\text{mean count rate}}$.

As one examines an intensity variation over a 24 hour period and picks the 12 hour interval which has the highest intensity, the *phase* is determined by the hour at the center of the 12 hour time interval (see Fig. 1). To carry out the analysis where there are occasional hours of missing data, the days with 20 hours or more data are accepted by interpolating the missing data.

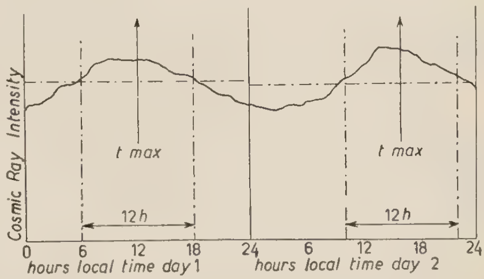

Fig. 1. – Description of the method for determining amplitude and phase of the solar daily vector.

2·2. *Month to month averaged variations.* – The definition of a vector for the month to month variations is similar to that above for the day to day variations. However, the standard deviation is not kept constant, but is computed for each month separately. Only the available data are taken into account. Missing data are not interpolated but replaced by an average daily vector for that month. The amplitude of a monthly vector is equivalent to the average daily vector multiplied by the total number of days in that month, or if

F_{ki} = the counting rate for hour i on day k,

N_d = number of days of available data in a month,

N_t = total number of days in each month,

$$\bar{F} = \frac{\sum_{1}^{N_d}{}_k \sum_{1}^{24}{}_i F_{ki}}{24\, N_d}, \qquad \mu_d = \sqrt{\text{mean count rate}} = \sqrt{\frac{\sum_{1}^{24}{}_i F_{ki}}{24}}, \qquad \mu_m = \frac{\mu_d}{N_d},$$

then,

$$\text{Vector Amplitude} = \frac{\dfrac{1}{12}\sum_{\max}{}_i \left(\dfrac{\sum_{1}^{N_d}{}_k F_{ki}}{N_d} - \bar{F}\right)}{\mu_m}\cdot N_t\,.$$

2915

This vector method for representing the 24 hour intensity variations has been subjected to a number of tests to verify that it represents the principal physical features of the 24 hour variation. *a*) The daily vectors were obtained independently for the two sections (A and B) of the Climax neutron pile: the amplitudes agree and the phases differ by $\pm$ 1 hour. *b*) For periods in which the average intensity is changing over several days, the amplitude and phase were determined by taking into account the preceding and following days, and compared with the vector method outlined above: the amplitudes and phases were in agreement. *c*) It was shown that, when the amplitude is very small and the phase indefinite, the distribution of deviations is nearly gaussian.

3. – Vector summation dials for 1953-1954-1955.

3·1. *Solar time scale.* – In order to eliminate unknown seasonal and meteorological effects, the nucleonic component intensity was measured near the equator at Huancayo, Peru ($\lambda \approx 0°$). The results of the analysis for the Huancayo neutron pile are shown in Fig. 2 using the monthly average vectors on a solar time scale. There is a preferred phase for the maximum of a solar 24 hour variation in 1953 and 1955. The time of maximum intensity is near

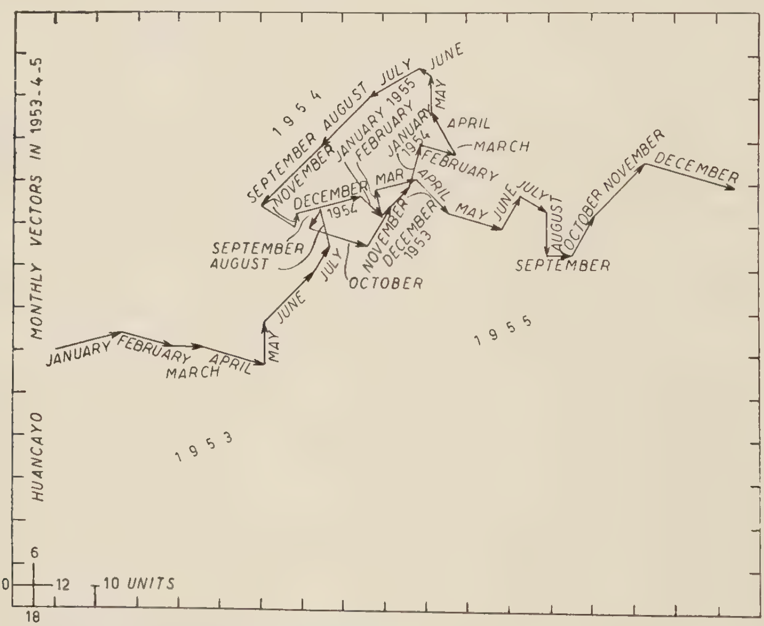

Fig. 2. – Data from the equatorial nucleonic component detector (neutron monitor) at Huancayo, Peru. The monthly average vectors are shown for the years 1953-55 plotted on a *solar* time scale. 10 units = 0.12 % amplitude.

1000 hour local solar time. However, during approximately twelve months in 1954 the monthly vectors rotate counter-clockwise through nearly 2π radians.

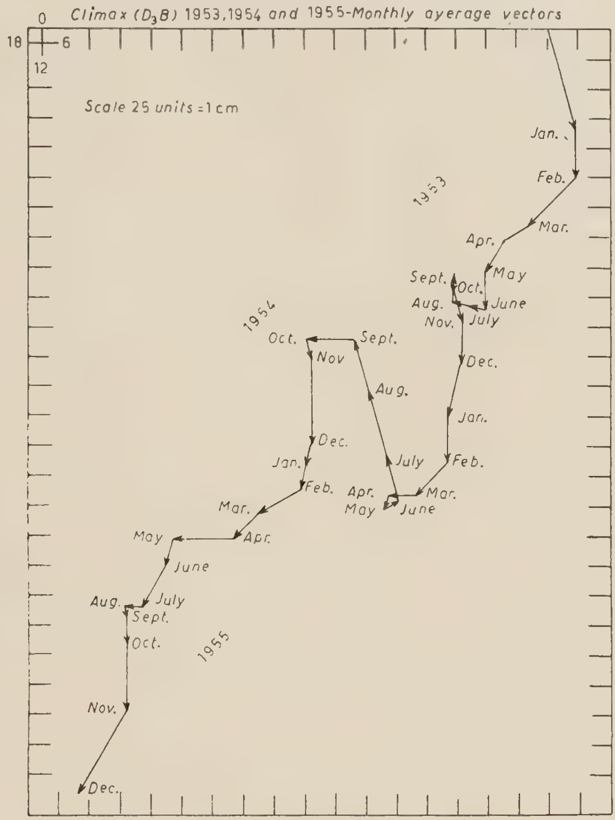

Fig. 3. - Data from geomagnetic latitude 48° N for the Climax neutron monitor. The monthly average vectors are shown for 1953-55 plotted on a solar time scale. Length of 1 coordinate division = 0.036 % amplitude.

We investigated the same three year period at lower primary particle energies, and for entirely different local geophysical conditions, by using the data from the neutron pile at Climax, Colorado ($\lambda \approx 48°$). Both Huancayo and Climax are at approximately the same atmospheric depths (i.e. 670-690 g cm² air). The monthly vector summation dial is given in Fig. 3. The counter clockwise rotation of the monthly vectors during 1954 is again evident although the vectors do not form a closed loop like at Huancayo. The maximum in the solar daily variations occurs at about 1500 hour local solar time during 1953 and 1955.

To compare these nucleonic component intensity results with the meson

intensity for the same period we have selected the ion chamber data of A. SITTKUS at Freiburg (10) ($\lambda \approx 48°$). These data are corrected by

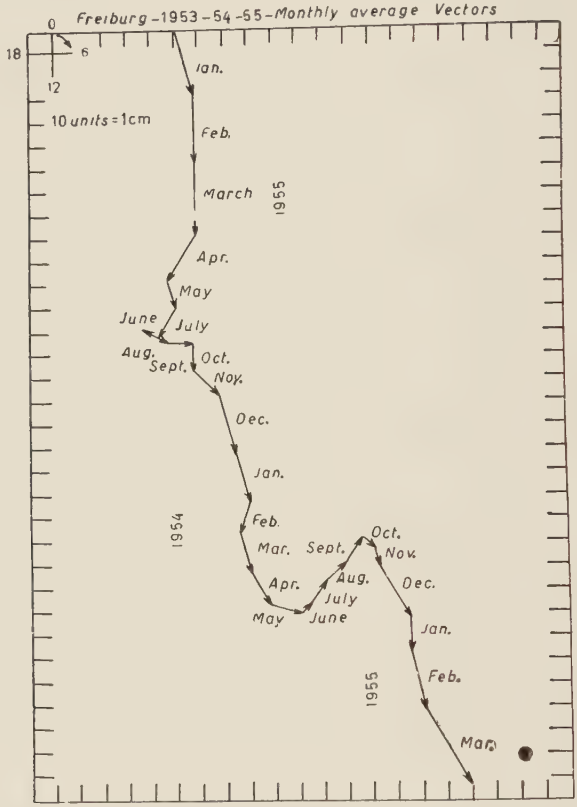

Fig. 4. – The ionization chamber data from Freiburg, Germany (10), are shown after correction by A. SITTKUS for pressure and temperature. The data are plotted on a *solar* time scale.

SITTKUS for the major temperature and pressure effects. The results are shown in Fig. 4. There is evidence for a solar 24 hour variation in 1954 and 1955, and the counter-clockwise shift of vectors in a 7-8 month period in 1954 is the oustanding feature of the data. We do not know to what extent meteorological effects may still be present in these data.

The data from both the vertical and inclined charged particle telescopes

(10) A. SITTKUS as published in *Sonnen Zirkular*. Fraunhofer Institute, Germany, 1953, 1954, 1955.

which are operating in Rome [11], were combined and analyzed for the vector amplitude and phase after correcting for atmospheric pressure variations. The counter-clockwise shift of vectors is evident in Fig. 5 for a period of not less than 9 months in 1954.

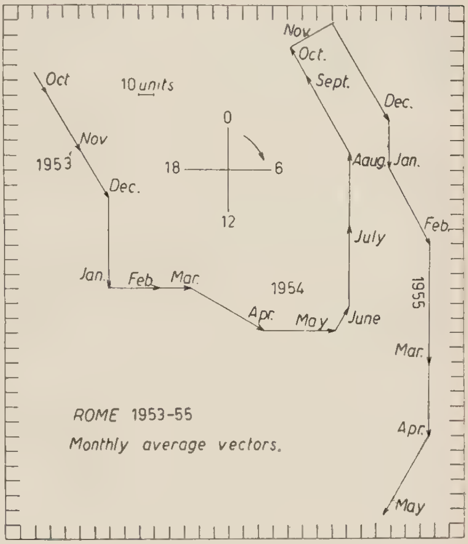

Fig. 5. – The charged particle counter telescope data from Rome, Italy, are shown after pressure corrections. The data are plotted on a *solar* time scale. 10 units = 0.04 % amplitude.

3·2. *Sidereal time scale.* – It is clear, especially from Fig. 2, that a variation of phase which simulates a dependence on sidereal time occurs in 1954. To examine this possibility in more detail we converted the phases of all vectors to sidereal time by assuming that solar and sidereal time are identical on 21 March and that there is one more sidereal day than the number of solar days in one year.

The neutron intensity data are shown in Fig. 6 and 7 for Huancayo and Climax, respectively. The spread in time of maximum between these two ranges of primary particle energies is 08 00-10 00 hour. The corresponding

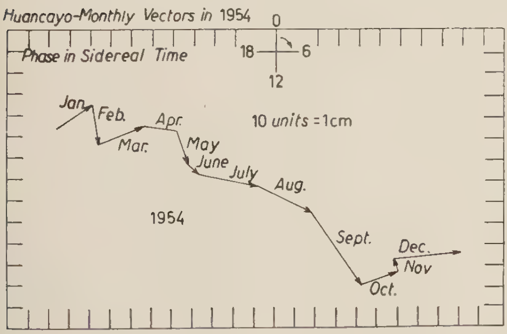

Fig. 6. – The data from Fig. 2 have been replotted on a *sidereal* time scale for 1954.

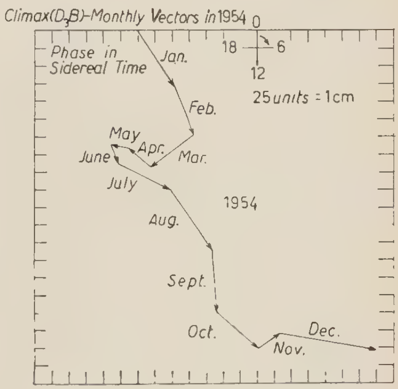

Fig. 7. – The data from Fig. 3 have been replotted on a *sidereal* time scale for 1954.

([11]) For a description of this instrument see F. BACHELET and A. M. CONFORTO: *Nuovo Cimento*, **12**, 923 (1954).

hour of maximum intensity for Freiburg is 1000÷1200 hour sidereal time: Fig. 8. For Rome, Fig. 9, the time of maximum is approximately 0900 hour sidereal time.

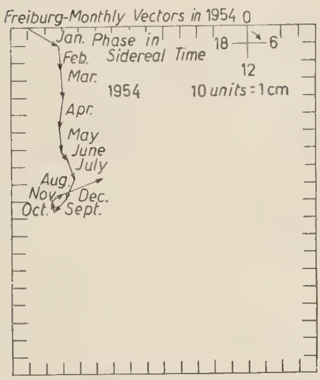

Fig. 8. – The data from Fig. 4 have been replotted on a *sidereal* time scale for 1954.

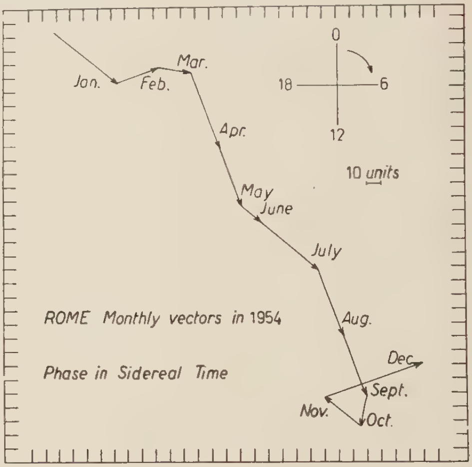

Fig. 9. – The data from Fig. 5 have been replotted on a *sidereal* time scale for 1954.

4. – Discussion.

The questions now arise:

Does this anisotropy during 1954 exist for the cosmic radiation outside the terrestrial atmosphere and the geomagnetic field, or is it the result of a modulation effect within the earth system? Is the observed sidereal effect spurious or real?

We shall first consider the possibility that the cosmic radiation approaching the earth's magnetic field is completely isotropic and undergoes a modulation effect at the earth which yields a local time dependence. In earlier discussions it has been pointed out that, for observations obtained with the nucleonic component, meteorological effects are negligible after correction for pressure variations. Thus, we have conclusive evidence from both the nucleonic and meson components that the 24 hour intensity variations do not have their origin in the atmosphere. For example, entirely different meteorological conditions exist at Huancayo and Climax, even though the main effect in 1954 is of the same character at both sites.

It is well known that the geomagnetic field undergoes a daily variation of intensity as a result of ionospheric currents developed by solar effects. This variation is a solar daily variation changing with season and position of ob-

servation on the earth ([12]). We shall leave open in this paper the question of whether these geomagnetic field effects may produce part or all of the cosmic ray 24 hour variation observed on solar time, for example, in 1953 and 1955.

For the phase shift occurring in 1954 it is obvious that no geomagnetic effects, which have a seasonal dependence, could be associated with a progressive counter-clockwise shift of 9 months, or more, as observed at Huancayo and Climax. Likewise, no progressive changes in the geomagnetic field with a time scale in any way comparable to this effect are known in geomagnetism at present ([12]). Neither does a superposition of two or more solar modulation effects produce a spurious sidereal effect.

We are then left with the alternatives that either the external geomagnetic field undergoes significant changes during the solar cycle which are not so far detected at the earth, or the radiation was anisotropic before entering the terrestrial field.

The most direct evidence that the 24 hour variation was an anisotropy in the incident primary radiation in 1954 is the fact that the time of maximum intensity in sidereal time lies in the narrow range of 08 00 ÷ 10 00 hour sidereal time, *independently for each detector* (The only exception is Freiburg at 12 00 hours). The spread in the time of maximum may arise from the deflection of particles with different ranges of energies in the geomagnetic field.

On the other hand, if the primary particles responsible for this effect are charged then the particle energies are mostly below ~ 30 GeV for protons, and it is unlikely that an anisotropy in the galaxy, no matter how close to our solar system, will be preserved within the solar system because of the expected stray magnetic fields which effectively randomize the trajectories of these low energy particles.

If we assumed that there existed a neutral radiation from the galaxy which is anisotropic and which could generate a charged particle secondary component in the atmosphere, the expected 24 our intensity variations would display a larger amplitude at the equator, where the charged primary background is a minimum, than at the intermediate latitudes of Climax. Such an effect is contrary to the observations reported here.

We are left with the tentative conclusion that if the observed sidereal effect really exists in the primary radiation, then the solar system must be remarkably free of disordered magnetic fields at the time of minimum solar activity (1954). There is increasing evidence that this may be so, since there were special conditions for the cosmic radiation at this time.

First, all cosmic ray intensity variations of solar origin other than the 24 hour variation became trivially small. *Second*, the low energy cosmic ray

([12]) S. Chapman and J. Bartels: *Geomagnetism* (Oxford, 1940).

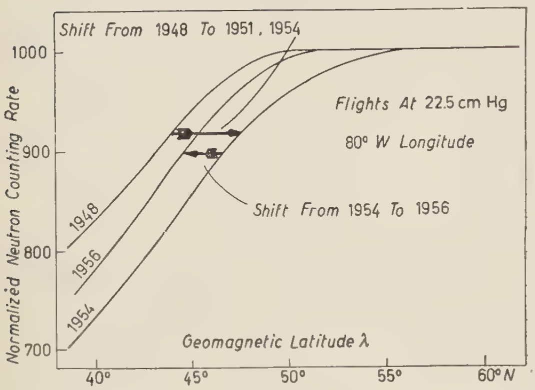

Fig. 10. – The change in the value of the low energy cut-off in the cosmic ray particle spectrum is shown, including the reversal of the effect in 1954. For details see ref. [13].

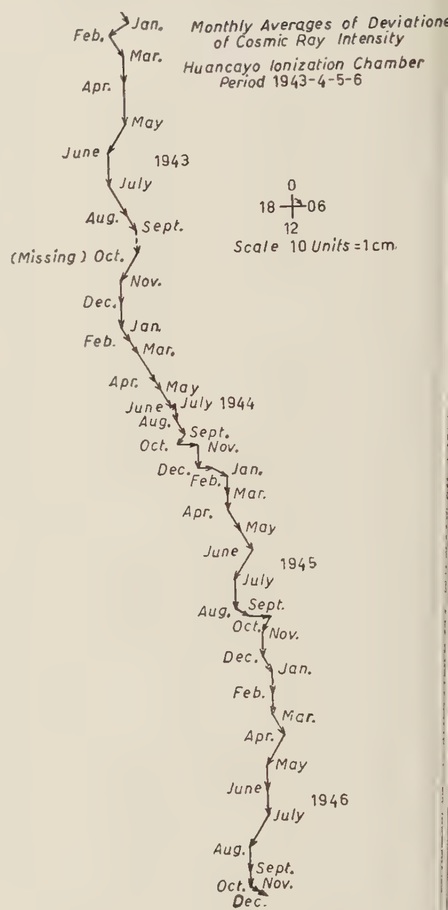

Fig. 11. – The data covering the period of the earlier solar sunspot minimum (1944) is shown using ionization chamber data near the geomagnetic equator [14] plotted on a *solar* time scale.

spectrum attained its highest exponent for the power law spectrum. *Third*, the total intensity of cosmic radiation reached its greatest average value. *Fourth*, the low energy cut-off shifted to attain a very small or negligible value and then became re-established again at ~ 1 GeV when the new solar cycle began to develop [13]. See Fig. 10.

If, as we have reason to believe, these effects represent the absence of solar ion beams and solar ejected plasma clouds containing magnetic fields at the time of minimum in the solar activity cycle, then it is likely that the system was relatively free of strong cosmic ray scattering regions in 1954. These results suggested the possibility that we only observ[e] the galactic distribution of low energy particles at that portion of the solar cycle when the sun does not introduce transient magnetic properties in the solar system [13]. At other times evidence for sidereal effects must surely be concealed by the solar daily variations.

---

[13] P. Meyer and J. A. Simpson: *Phys. Rev.*, **106**, 568 (1957).

[14] S. E. Forbush and I. Lange: *Carnegie Institution of Washington Publication* V, no. 175.

2922

The solar minimum of 1944 was not as free of solar active regions (15) as the 1954 minimum and an investigation of the monthly vectors obtained from the Carnegie Institution ion chamber (14) at Huancayo, Peru, shows that only a solar 24 hour variation persisted through 1943 ÷ 1946 as shown in Fig. 11. This result is in agreement with the first harmonic analysis by POSSENER and VAN HEERDEN (4). The hour for time of maximum intensity during 1943 ÷ 1946 is also in agreement with the results of THAMBYAHPILLAI and ELLIOT (9). However, it is interesting to note from figures 2 and 11 that the phase of the 24 hour variation both in 1943 ÷ 1946, 1953 and 1955 is substantially the *same*. These results suggest that the apparent 22 year cycle (9) for phase changes in the first harmonic of the 24 hour variation is not valid for equatorial observations.

In summary, we believe that since the results reported in this paper appear to be free from terrestrial effects, we are observing a sidereal effect, either spurious or real, which existed across the entire low energy primary cosmic ray spectrum for $\gtrsim 9$ months during 1954. We emphasize, however, that these results are in no way a proof for the existence of a sidereal effect upon cosmic ray intensity, and many more years of data may be required before this problem is settled.

* * *

For assistance in preparaing the data we wish to thank Mr. P. K. S. RAJA and the Enrico Fermi Institute Cosmic Ray Group Computing staff. For co-operation in operating the Counter Telescopes at the University of Rome we thank Dr. F. BACHELET.

RIASSUNTO

I dati di rivelatori della componente nucleonica dei raggi cosmici (« pila » per neutroni) sono analizzati dal punto di vista della variazione diurna all'equatore geomagnetico e a 48° N. L'esame si estende agli anni 1953-54-55, che comprendono l'ultimo periodo di minimo del ciclo delle macchie solari. Si è notato che durante l'anno 1954 la variazione diurna con periodo solare presenta un comportamento anomalo: si mostra qui che essa sembra risentire di uno spostamento progressivo della fase, mentre in tempo sidereo l'ora del massimo si mantiene costantemente nell'intervallo fra le 08 00 e le 10 00. Si è certamente in presenza di una anisotropia della radiazione che incide sull'atmosfera, e sembra molto probabile, sebbene non del tutto provato, che essa si estenda anche al di fuori del campo magnetico terrestre. La questione se tale effetto sia reale o spurio viene discussa alla luce dei recenti risultati sui processi di modulazione dell'intensità dei raggi cosmici.

(15) *The Sun*. Ed. by KUIPER (Chicago, 1953).

IL NUOVO CIMENTO Vol. VI, N. 5 1° Novembre 1957

Parametric Representations of General Green's Functions (*).

Y. Nambu

The Enrico Fermi Institute for Nuclear Studies
The University of Chicago - Chicago, Ill.

(ricevuto il 23 Giugno 1957)

Summary. — Parametric representations for the Green's function of field theory are derived in perturbation theory. These representations are valid for each term in the perturbation series that corresponds to a Feynman diagram, and reflect its analytic property and threshold characteristics. As an example, the three-body (vertex) function is shown to satisfy a dispersion relation when two of the three momenta are fixed, with the correct location of the singularities expected from the thresholds of the competing real processes.

1. – Introduction.

Attempts to investigate the structure of the present field theory have been pursued by various authors making use of only such fundamental properties as causality and unitarity. The so-called Green's functions are of particular interest in this respect as well as for the fact that their asymptotic part gives the S-matrix elements. In previous papers (1) we proposed specific representations of the Green's functions which seemed to follow from simple physical considerations and indicate their analytic property. It has been found, however, that these formulae are not necessarily satisfied by the actual Green's

(*) This work was supported by the United States Atomic Energy Commission.
(1) Y. Nambu: *Phys. Rev.*, **100**, 394 (1955); **101**, 459 (1956).

functions calculated by perturbation theory (2); it seems that although the representations have the correct properties we would expect from physical considerations, they are too restricted to correspond to reality.

In this paper a different, more general kind of representation is proposed and proved in perturbation theory. The main difference is that in the new formula there is only a single denominator determining the dependence of the function on all the momenta, the kind of denominator which one would obtain in actual calculations by combining various denominators according to Feynman's method. In this respect it resembles another formula proposed before for scattering matrices (3). As in the case of scattering matrices, the dispersion relations for general Green's functions are expected to reflect two properties, namely that the functions have certain analyticity in appropriate variables, and that the so-called absorptive part has a spectrum determined by the various reaction thresholds, where branch points or poles are located. The existence of branch points at threshold of the S matrix were shown in general by EDEN (4), and the general dispersion relations for causal amplitudes were recently discussed by POLKINGHORNE (5). The present formulas have properties which seem to be closely related to these points. But an explicit demonstration of the conventional dispersion relations has been possible so far only for the vertex (three-field) function, which will be illustrated in Sect. **3**. The relation of the present representation to the previous more restricted one will be discussed.

2. – Derivation of the representation.

In this section we will derive a representation that applies to every Feynman diagram in the perturbation series of a Green's function or related functions. For definiteness we work with quantum electrodynamics. But we ignore here the problem of ultraviolet as well as infrared divergences, and assume all the integrals are convergent. Renormalization is not an important point in our consideration.

In terms of the interaction representation, the Green's functions, as de-

---

(2) A simplest counter-example wuold be the first radiative correction to the three-body Green's function (vertex function). The main point has to do with the range of the integration parameters which, according to the results of Ref. (1), carried a meaning of the square of the mass of intermediate states, and thus were supposed to take positive values only. The present paper leads only to a much weaker statement.

(3) Y. NAMBU: *Phys. Rev.*, **98**, 803 (1955).

(4) R. J. EDEN: *Proc. Roy. Soc.*, A **210**, 388 (1951).

(5) J. C. POLKINGHORNE: *Nuovo Cimento*, **4**, 216 (1956); *Proc. Camb. Phil. Soc.*, **53** Part I, 260 (1957).

fined in I, can be expressed as

$$
(1)\qquad\left\{\begin{aligned}
\varrho_{2,0}(x|y|) &= \langle T(\psi(x), \overline{\psi}(y), S)\rangle_0\\
\varrho_{0,2}(||zz') &= \langle T(A(z), A(z'), S)\rangle_0\,,\\
\varrho_{2,1}(x|y|z) &= \langle T(\psi(x), \overline{\psi}(y), A(z), S)\rangle_0\,, \quad \text{etc.}\\
S &= T\exp\left[+ie\int i\bar{\psi}\gamma_\mu\psi A_\mu \mathrm{d}^4x\right].
\end{aligned}\right.
$$

Expanding S and rearranging the T-product into a normal product, one gets a series of terms which can be constructed according to the rules of Dyson and corresponds to various Feynman diagrams. The contribution of a Feynman diagram to $\varrho_{2n,m}$ is of the form

$$
(2)\qquad F(x|y|z) = (-e)^R(-1)^l\int\ldots\int\prod_{i,r} S_F(x_i - u_r)\prod_{r,s}\gamma_r S_F(u_k - u_s)\gamma_s\cdot
$$
$$
\cdot\prod_{s,j} S_F(u_s - y_j)\prod_{k,t} D_F(z_k - u_t)\prod_{r,s} D_F(u_r - u_s)\cdot \mathrm{d}^4u_1\ldots\mathrm{d}^4u_R\,,
$$

where R is the number of internal points (vertices), and l the number of closed electron loops. The rules as to the multiplication of γ-matrices are not explicitly indicated. Hereafter the letter x will be used to denote all the external points x, y and z indiscriminately. Our theorems in this section will hold for any quantity if it has the structure shown in Eq. (2), namely if it consists of Δ_F- functions and their derivatives, being integrated over internal points.

We begin by observing that S_F and D_F have the representation

$$
(3)\qquad\left\{\begin{aligned}
D_F(x) &= \frac{-i}{8\pi^2}\int_0^\infty \exp[iax^2/2]\,\mathrm{d}a\,,\\
S_F(x) &= (-\gamma\cdot\partial/\partial x + m)\frac{-i}{8\pi^2}\int_0^\infty \exp[iax^2/2 - im^2/2a]\,\mathrm{d}a\,,
\end{aligned}\right.
$$

while the corresponding Fourier coefficients are

$$
(4)\qquad\left\{\begin{aligned}
\int D_F(x)\exp[-ik\cdot x]\,\mathrm{d}^4x &= \frac{1}{2}\int_0^\infty \exp[-ibk^2/2]\,\mathrm{d}b = -i/(k^2 - i\varepsilon)\,,\\
\int S_F(x)\exp[-ik\cdot x]\,\mathrm{d}^4x &= \frac{1}{2}\int_0^\infty(-i\gamma\cdot k + m)\exp[-ib(k^2+m^2)/2]\,\mathrm{d}b =\\
&= -i(-i\gamma\cdot k + m)/(k^2 + m^2 - i\varepsilon)\,.
\end{aligned}\right.
$$

2926

We will substitute the above representations into Eq. (2), and carry out the integrations one by one. The first integrations to be done will be of the type

$$\int S_F(x_1 - u)\gamma_\mu S_F(u - x_2) D_F(u - x_3)\, \mathrm{d}^4 u\,. \tag{5}$$

We shall make use of the following lemma.

Lemma 1. Let I be a quadratic form in the N vectors x_i:

$$I = \tfrac{1}{2}\sum_{i>j} a_{ij}(x_i - x_j)^2 = \tfrac{1}{2}\sum_{j} A_{ij} x_i \cdot x_j \qquad a_{ij} \geqslant 0, \qquad \sum_{i,j} a_{ij} > 0 \tag{6}$$

a and A are related by

$$A_{ji} = A_{ij} = -a_{ij} \leqslant 0\,, \qquad A_{ii} = \sum_{j=1}^{N} a_{ij} > 0\,, \qquad \sum_{j=1}^{N} A_{ij} = 0\,. \qquad i \neq j \tag{7}$$

Then

$$\exp[iI]\, \mathrm{d}^4 x_1 = i(4\pi^2/A_{11}^2) \exp[iI']\,, \tag{8}$$

with

$$\begin{cases} I' = \tfrac{1}{2}\displaystyle\sum_{i>j>1} a'_{ij}(x_i - x_j)^2 = \sum_{i,j\neq 1} {}'_{ij}A\, x_i \cdot x_j\,, & \\ a'_{ij} = a_{ij} + a_{i1}a_{j1} \Big/ \displaystyle\sum_{k} a_{k1} \geqslant a_{ij}, & i, j > 1 \\ A'_{ij} = A_{ij} - A_{i1}A_{j1}/A_{11}\,, & \displaystyle\sum_{j=2}^{N} A'_{ij} = 0\,. \end{cases} \tag{9}$$

Eq. (8) can be derived by observing

$$\sum_{i=2}^{N} a_{i1}(x_i - x_1)^2 = \Big(\sum_i a_{i1}\Big)\Big(x_1 - \sum_i a_{i1}x_i \Big/ \sum_i a_{i1}\Big)^2 + \tag{10}$$
$$+ \Big(1 \Big/ \sum_i a_{i1}\Big) \sum_{i,j\neq 1} a_{i1}a_{j1}(x_i - x_j)^2$$

and

$$\int \exp[iAx^2/2]\, \mathrm{d}^4 x = 4\pi^2 i/A^2\,, \qquad (A > 0).$$

The above lemma implies that the basic structure of the exponential $\exp[iI]$, as given by Eqs. (6) and (7), is preserved after integration over some

of its co-ordinates. Eq. (5) becomes, for example,

$$
(11)\quad \begin{cases}
(\gamma\cdot\partial/\partial x_1 - m)\gamma_\mu(\gamma\cdot\partial/\partial x_2 - m)[i/(8\pi^2)^3]\int\!\!\int\!\!\int_0^\infty\!\!\int \exp\,[(i/2)\{a_1(x_1-u)^2 + \\
\qquad + a_2(x_2-u)^2 + a_3(x_3-u)^2\}]\cdot\exp\,[(-im^2/2)(1/a_1+1/a_2]\,\mathrm{d}a_1\,\mathrm{d}a_2\,\mathrm{d}a_3\,\mathrm{d}^4u = \\
\qquad\qquad = -(\gamma\cdot\partial/\partial x_1 - m)\gamma_\mu(\gamma\cdot\partial/\partial x_2 - m)(1/128\pi^4)\cdot \\
\cdot\int_0^\infty\!\!\int_0^\infty\!\!\int_0^\infty \exp\,[(i/2)\{a_{12}(x_1-x_2)^2 + a_{33}(x_2-x_3)^2 + a_{31}(x_3-x_1)^2\}]f(a_{ij})\,\mathrm{d}a_{12}\,\mathrm{d}a_{23}\,\mathrm{d}a_{31}, \\
f(a_{ij}) = \int\!\!\int\!\!\int \exp\,[(-im^2/2)(1/a_1+1/a_2)]\cdot \\
\qquad\qquad \cdot\big[\prod_{i>j}\delta\{a_{ij} - a_ia_j/(a_1+a_2+a_3)\}\big](a_1+a_2+a_3)^{-2}\,\mathrm{d}a_1\,\mathrm{d}a_2\,\mathrm{d}a_3\,.
\end{cases}
$$

One can then proceed to the next integration by using Lemma 1 again. It should be noted that, if a differential operator arising from an S_F-function acts on an internal point over which to integrate, it can always be replaced by a linear combination of differential operators with respect to the remaining points. This will be shown in the appendix. One can thus exhaust all the integrations and arrive at the theorem:

Theorem 1. The function $F_{2n,m}$ of Eq. (2), which corresponds to a certain Feynman diagram, has a parametric representation

$$
(12)\quad \begin{cases}
F_{2r,m} = (-i)^{(N+R)/2}\sum_\alpha \int\!\dots\!\int O^{(\alpha)}(\gamma,(1/m)\partial/\partial x)\,\exp\,[iI]f^{(\alpha)}(a_{ij})\prod \mathrm{d}a_{ij}\,, \\
I = \tfrac{1}{2}\sum_{i>j} a_{ij}(x_i-x_j)^2 = \tfrac{1}{2}\sum_{i,j} A_{ij}x_ix_j\,, \qquad i,j = 1,\dots 2n+m = N \\
a_{ij} = -A_{ij} = -A_{ji} \geqslant 0\,, \qquad \sum_{i=1}^{N} A_{ij} = 0\,,
\end{cases}
$$

$O^{(\alpha)}$ here designates a product of Dirac matrices, photon polarization vectors, and a number $n_\alpha \leqslant \mathrm{Min}\,(n+R,\, n(N-1)+m)$ of differential operators with respect to the external points x (see Appendix); $f^{(\alpha)}$ is a complex function of the positive parameters a_{ij}. The power of i in front of the integral is the combined result of all the i's coming from D_F, S_F and integrations over the internal points.

As regards the function $f^{(\alpha)}$ one can further make the following statement.

Theorem 2. Introduce a common scaling factor t with the dimensions of m^2 for all the variables such that

$$
(13)\qquad a_{ij} = t\alpha_{ij}\,, \qquad t > 0.
$$

Then $f_{(\alpha)}(a_{ij})$ of Eq. (12) has the form

$$(14)\qquad f^{(\alpha)}(t\alpha_{ij})t^{N(N-1)/2} = m^{3n+m}\sum_{\nu=0}^{(N+R-N\alpha)/2}\int_0^\infty \exp\left[-iM^2/2t\right] i_\nu \tau_\nu^{(\alpha)}(\alpha_{ij}, M^2/m^2)\cdot$$
$$\cdot(m^2/t)^{((R-N)/2)-\nu}\,\mathrm{d}M^2/m^2\,,$$

where $\tau_\nu^{(\alpha)}(\alpha_{ij}, M^2/m^2)$ is real. In other words, $f^{(\alpha)}$ as a function of t has a continuation which is analytic for $\operatorname{Im} t > 0$.

To prove the theorem, first observe that both sides of the transformation Eq. (9) are homogeneous functions of order one with respect to the variables a'_{ij} or a_{ij} respectively, so that the relation does not depend on t; it simply tells how the ratios $a_{12} : a_{13} : \ldots$ are transformed. Now each S_F in Eq. (1), according to Eq. (4), contributes a factor of the form

$$\exp\left[-im^2/2a_l\right] = \exp\left[-im^2/2t\alpha_l\right]\,, \qquad l = 1, \ldots, (n+R)/2,$$

and after integration over the internal points α_j will eventually be expressed as functions of α_{ij}. Further, one may write

$$(14')\quad \exp\left[(-im^2/2t)\sum 1/\alpha_l\right] = \int_0^\infty \exp\left]-iM^2/2t\right]\delta\left[M^2/m^2 - \sum 1/\alpha_l\right]\mathrm{d}M^2/m^2\,.$$

The factor m^{3n+m} in front of Eq. (14) is put simply for dimensional reasons. The factor $(m^2/t)^{((R-N)/2)-\nu}$ comes from the change of variables and the fact that each integration over a vertex yields a factor of the form $1/A_{ii}^2$ according to Eq. (8), which altogether gives $t^{-2R+3R/2+N/2} = t^{-R/2+N/2}$; in addition, as is shown in the appendix, the differential operators in S_F can bring about extra t's up to $t^{-(n+R-n\alpha)/2}$ when $F_{2n,m}$ is brought into the form Eq. (12).

Let us next introduce the Fourier transform of the function according to

$$(15)\qquad \delta(\sum_i k_i)\, G(k_i) = \frac{1}{(2\pi)^4}\int\ldots\int \exp\left[-i\sum k_i\cdot x_i\right] F(x_i)\prod_i \mathrm{d}^4x_i\,.$$

The conservation law $\sum_i k_i = 0$ is implied in Eq. (12) by the relation $\sum_i A_{ij} = 0$, which also means that the rank of matrix A is $N-1$ (6), and $\det A = 0$. This brings about a little inconvenience in carrying out the integration in

(6) The rank is even smaller if the Feynman diagram contains disconnected graphs, which is not the case here by virtue of the definition of the Green's functions.

Eq. (15). If $\det A \neq 0$, one could use the formula

$$\int \dots \int \exp\left[-i \sum k_i \cdot x_i\right] \exp\left[(i/2) \sum A_{ij} x_i \cdot x_j'\right] \prod d^4 x_i = \frac{(4\pi^2 i)^N}{[\det A]^2} \exp\left[(-i/2) \sum B_{ij} k_i \cdot k_j\right], \tag{16}$$

where B_{ij} is the inverse matrix of A. When $\det A = 0$, there is no unique way of defining an $N \times N$ matrix B. Two matrices B_{ij} and $B'_{ij} = B_{ij} + X_i + X_j$ are equivalent for $\sum k_i = 0$ since

$$\sum B'_{ij} k_i \cdot k_j = \sum B_{ij} k_i \cdot k_j + 2 \left(\sum X_i k_i\right) \cdot \left(\sum k_j\right).$$

We will adopt here a more or less arbitrary prescription. We modify A into $A' = A + \lambda E$, so that $\det A' \neq 0$, and take an appropriate limit $\lambda \to 0$ according to

$$\left\{\begin{aligned} &\lim_{\lambda \to 0} \int \dots \int \exp\left[-i \sum k_i \cdot x_i\right] \exp\left[(i/2) \sum A'_{ij} x_i \cdot x_j\right] \prod d^4 x_i = \\ &= \lim_{\lambda \to 0} \left[(4\pi i)^N / \lambda^2 D^2\right] \exp\left[-i \left(\sum k_i\right)^2 / 2N\lambda\right] \exp\left[(-i/2) \sum B_{ij} k_i \cdot k_j\right] = \\ &\qquad = (2\pi)^4 \delta\left(\sum k_i\right) \left[(4\pi^2 i)^{N-1} / D^2\right] \exp\left[(-i/2) \sum B_{ij} k_i \cdot k_j\right], \\ &D \equiv \left[d(\det A')/d\lambda\right]_{\lambda = 0}, \\ &B_{ij} \equiv \lim_{\lambda \to 0} \frac{\det A_{(ij)}(\lambda) - \det A_{(ij)}(0)}{\det A(\lambda)} = \frac{\sum_k \det A_{(ik,jk)}}{D} \equiv \frac{b_{ij}}{D}. \end{aligned}\right. \tag{17}$$

Here $A_{(ij)}$ and $A_{(ik,jk)}$ mean submatrices of A where the designated rows and columns are omitted. This particular choice of B_{ij} has an interesting feature which will be stated in the following theorem.

Theorem 3. The Fourier transform $G(k)$ of $F(x)$, as defined in Eq. (15), has a representation

$$\left\{\begin{aligned} &G_{2\cdot,m}(k_i) = \sum_\alpha \int \dots \int O^{(\alpha)}_{2n,m}(\gamma, ik/m) \exp\left[-iJ\right] g^\alpha(a_{ij}) \prod da_{ij}, \\ &g^{(\alpha)}(a_{ij}) = (-i)^{(N+E)/2} \left[(4\pi^2 i)^{N-1} / D^2(a_{ij})\right] f^{(\alpha)}(a_{ij}), \\ &J = \tfrac{1}{2} \sum_{i,j-1}^{N} B_{ij} k_i \cdot k_j, \\ &\quad = \tfrac{1}{2} \sum_{\mu=1}^{N(N-1)/2} b_\mu l_\mu^2, \qquad b_\mu \geqslant 0. \end{aligned}\right. \tag{18}$$

2930

l_μ is a sum of up to $[N/2]$ vectors

$$k_i\,,\qquad k_i+k_j\,,\qquad k_i+k_j+k_l\,,\qquad \text{etc.}$$

taken from $k_1, \ldots, k_N$. The summation need be extended only up to $[N/2]$ momenta since any l_μ may be replaced by $-l'_\mu$ where l'_μ is the sum of the complementary momenta.

The last expression for J can be derived by noting that $b_{ij} = \sum_k A_{(ik,jk)}$ is a positive, multi-linear function of the coefficients a_{lm}:

$$b_{ij} = \sum a_{lm} a_{np} \ldots \qquad \text{and} \qquad b_{ii} \geqslant b_{ij} \geqslant 0\,. \tag{19}$$

Each term in the summation is a product of $N-2$ different a_{lm}'s taken appropriately out of $N(N-1)/2$ parameters $a_{12}, \ldots, a_{N,N-1}$. By reason of symmetry, the sum must run over the indices in such a way that it is symmetric in i and j, and that if a particular combination of the a_{lm}'s occurs, it also includes all the terms obtained from it by permutation of the indices except i and j. It is then possible to break up the sum for b_{ij}, $i \neq j$, into various groups:

$$b_{ij} = b_{(ij)} + \sum_l b_{(ijl)} + \sum_{l,m} b_{(ijlm)} + \ldots\,, \tag{20}$$

where $b_{(ij)}$, $b_{(ijl)}$, $b_{(ijlm)}$, etc., are partial sums which are symmetric with respect to the indices ij, ijl, $ijlm$, etc. This means that $b_{(ijl)}$, for example, occurs equally in b_{ij}, b_{jl} and b_{li}. Since furthermore any term in b_{ij}, $i\neq j$, is contained also in b_{ii} and b_{jj}, these partial sums $b_{(ij)}$, $b_{(ijl)}$, $b_{(ijlm)}$, etc., are coefficients of $(k_i+k_j)^2$, $(k_i+k_j+k_l)^2$, $(k_i+k_j+k_l+k_m)^2$, etc., respectively. The remaining part b_i of b_{ii}, which does not belong to any of these terms, will then give the coefficient of k_i^2. In other words

$$J = \frac{1}{2D}\left\{\sum_i b_i k_i^2 + \sum_{(ij)} b_{(ij)}(k_i+k_j)^2 + \sum_{(ijl)} b_{(ijl)}(k_i+k_j+k_l)^2 + \ldots\right\}. \tag{21}$$

Since B is essentially the inverse of the matrix A, it depends on the scaling factor t of Theorem 2 as

$$B_{ij} = \frac{1}{t}\beta_{ij}\,,\qquad J = \frac{1}{2t}\sum \beta_{ij} k_i\cdot k_j = \frac{1}{2t}\sum \beta_\mu l_\mu^2\,,$$

where β_{ij} or β_μ is a function of the variables α_{ij}. Let us now choose t as one of the integration parameters by normalizing α_{ij} or β_{ij} in a suitable way. For example, adopting the convention

$$\sum_{i>j} \alpha_{ij} = 1 \qquad \text{or} \qquad t = \sum_{i>j} a_{ij}\,,$$

2931

one may write for any $\mathcal{F}(a_{ij})$

$$\int_0^\infty\!\!\cdots\!\!\int \mathcal{F}(a_{ij}) \prod \mathrm{d}a_{ij} = \int_0^\infty\!\!\cdots\!\!\int \mathcal{F}(t\alpha_{ij})\, \delta(\textstyle\sum\alpha_{ij}) \prod \mathrm{d}\alpha_{ij} t^{(N(N-1)/2)-1}\mathrm{d}t\,. \tag{22}$$

t will then run from 0 to ∞. Substituting this expression into Eq. (18), the t integration may be carried out first. Noting that

$$\int_0^\infty \exp\,[-ib/t]\,\mathrm{d}t/t^{n+2} = (i\partial/\partial b)^n \frac{-i}{b-i\varepsilon}\,,$$

one gets the following result.

Theorem 4. G has the representation

$$(23)\quad \left\{\begin{aligned} G(k) &= -im^{3n+m}\sum_{\alpha,\nu}\int\!\!\cdots\!\!\int O^{(\alpha)}(\gamma, ik/m)\sigma_\nu^{(\alpha)}(\alpha_{ij}, M^2/m^2)\,\cdot \\ &\qquad\cdot\, m^{R-N-2\nu}(\partial/\partial M^2)^{((3N+R)/2)-\nu-3}\frac{1}{\frac{1}{2}\sum\beta_\mu l_\mu^2 + M^2 - i\varepsilon}\,\mathrm{d}\left(\frac{M^2}{m^2}\right)\prod \mathrm{d}\alpha_{ij}\,, \\ \sigma_\nu^{(\alpha)} &= [(4\pi^2)^{N-1}/D^2(\alpha_{ij})]\,\tau_\nu^{(\alpha)}(\alpha_{ij}, M^2/m^2)\delta(\textstyle\sum\alpha_{ij}-1)\,, \end{aligned}\right.$$

where all the integration variables run only over positive values:

$$\alpha_{ij} \geqslant 0\,, \qquad M^2 \geqslant 0\,.$$

This means that G, regarded as a function of $N(N-1)/2$ *independent* variables l_μ^2, is analytic if all the variables lie in the upper half of the complex plane. If the differential operator in the integrand $((3N+R)/2-\nu-3 \geqslant 0$ always) is incorporated into the weight function, Eq. (23) may also be written

$$(23')\quad \left\{\begin{aligned} G(k) &= -im^{6-5n-3m}\sum_{\alpha}\int\!\!\cdots\!\!\int O^{(\alpha)}(\gamma, ik/m)\sigma^{(\alpha)}(\alpha_{ij}, M^2/m^2)\,\cdot \\ &\qquad\cdot\,\frac{1}{\frac{1}{2}\sum_\mu\beta_\mu l_\mu^2 + M^2 - i\varepsilon}\,\mathrm{d}\left(\frac{M^2}{m^2}\right)\prod \mathrm{d}\alpha_{ij}\,, \\ \sigma^{(\alpha)} &= \sum_\nu \sigma_\nu^{(\alpha)}(\alpha_{ij}, M^2/m^2)m^{R-N-2\nu}(\partial/\partial M^2)^{(3N+R)/2-\nu-3} \\ &= \sum_\nu (-m^2\,\partial/\partial M^2)^{(3N+R)/2-\nu-3}\sigma_\nu^{(\alpha)}(\alpha_{ij}, M^2/m^2)\,. \end{aligned}\right.$$

The last expression obtains if integration by parts is admitted. The fact that the weight functions $\sigma_\nu^{(\alpha)}$ or $\sigma^{(\alpha)}$ are real (with the proper definition of $O^{(\alpha)}$) is

essentially a consequence of the time reveşal invariance of our underlying field theory.

Our next task is to look closely into the range of the variables α_{ij} or β_μ, which is necessary to exhibit the dispersion relations of the desired nature for G. For this purpose some more lemmas have to be introduced

Lemma 2. The contents of lemma 1 can be restated as follows: If one replaces all the vectors x_i by real numbers z_i (or vectors in an Euclidean space of any dimensions), so that $\sum_i z_i^2 > 0$, then I' in Eq. (9) is numerically equal to the minimum of the positive definite form I with respect to the variation of z_1.

This is obvious in view of Eq. (10). But it has also an interesting implication that the factor $\exp[iI]$, which governs the analytic behavior of the Green's functions, is determined by a classical action principle. One may regard $1/a_{ij}$ as a parameter similar to the proper time (or its square) required by a particle to travel between x_i and x_j. One may also adopt the following mechanical model. Take N points $\boldsymbol{z}_1, \ldots, \boldsymbol{z}_N$ (vectors now) in space, and between each pair of points $\boldsymbol{z}_i$ and $\boldsymbol{z}_j$ hook a spring with a force constant a_{ij}. The potential energy of such a system is then equal to I, and as one sets the point $\boldsymbol{z}_1$ free, it will settle down to an equilibrium position $\boldsymbol{z}_1 = \sum a_{i1} z_i \,/\, \sum a_{i1}$ with energy I'.

Lemma 3. Two quadratic forms

$$I = \tfrac{1}{2}a(z_1 - z_2)^2\,, \qquad I' = \tfrac{1}{2}a'(z_1 - z)^2 + \tfrac{1}{2}a''(z - z_2)^2\,, \tag{24}$$

with

$$1/a = 1/a' + 1/a''\,,$$

satisfy the inequality

$$I' \geqslant I\,.$$

This can be establihsed by finding the minimum of I' as a function of z which turns out to be

$$\text{Min}\, I' = (z_1 - z_2)^2 / (1/a' + 1/a'')\,.$$

In terms of the above mechanical model, it means that the energy of the system always increases by picking any point P on a spring stretched between z_1 and z_2, and moving it to any new fixed position z by force. The spring constants of the resulting two sub-springs $z_1 z$ and $z z_2$ are given by the relation

$$\frac{1}{a'} = \frac{|z_1 - P|}{|z_1 - z_2|}\frac{1}{a}\,, \quad \frac{1}{a''} = \frac{|P - z_2|}{|z_1 - z_2|}\frac{1}{a}\,, \quad \frac{1}{a'} + \frac{1}{a''} = \frac{1}{a}\,. \tag{25}$$

This observation immediately leads to the following conclusion.

Lemma 4. Let $I(z_i; a_l)$ and $M^2(a_l)$ correspond to a Feynman diagram $\mathcal{G}$, where all the parameters a_l carried by the lines are fixed. If $\mathcal{G}$ is changed to $\mathcal{G}'$ by inserting an internal photon line (radiative correction), then for any $I'(z_i, a'_l)$ and $M'^2(a'_l)$ for $\mathcal{G}'$ there exist such $I(z_i; a_l)$ and $M^2(a_l)$ for $\mathcal{G}$ that

$$(26) \qquad \begin{cases} I'(z_i; a'_l) \geqslant I(z_i; a_l) & \text{for all } z_i, \\ M'^2(a'_l) \;\; = M^2(a_l)\,, \end{cases}$$

and vice versa. The corresponding quantities $J'(q; a'_l)$ and $J(q; a_l)$ in the momentum space ($z_i \to q_i$) satisfy the relation

$$(26') \qquad J'(q_i; a'_l) \leqslant J(q_i; a_l) \qquad \text{for all } q_i, \quad \sum q_i = 0\,,$$

since they are inverse quadratic forms of I' and I. If we do not insist on fixing M^2 and M'^2, Eqs. (26) and (27) may alternatively be stated respectively as

$$(27) \qquad I'M'^2 \geqslant IM^2 \quad \text{and} \quad J'/M'^2 \leqslant J/M^2\,,$$

since these quantities are scaling-invariant. One can always change the scale of a_l or a'_l according to Theorem 2 to make $M^2 = M'^2$.

In general, radiative corrections to a Feynman diagram are built up by 1) attaching photon lines to electron lines, and 2) inserting electron closed loops in (single or groups of) photon lines. The effect of the first process is covered by the above lemma. The effect of the second process may be understood again in terms of the mechanical model. Take first a diagram with an electron loop correction. We keep temporarily all the vertices on the loop fixed in space, and replace the spring representing the electron loop by a set of photon springs which connect the vertices in pairs, and which have the same potential energy as the former. Then the vertices are set free, and the whole system is allowed to settle down to an equilibrium position that corresponds to a diagram without the radiative correction. It is clear that by this operation both the potential energy I and the mass M^2 decrease. Thus:

Lemma 5. The relations of Lemma 4 hold true also for insertion of an electron loop.

Combining these results, we are led to the important theorem.

Theorem 4. The weight functions $\sigma_v^{(\alpha)}(\alpha_{ij}, M^2/m^2)$ in Eq. (23) have a property such that J/M^2 is not larger than a suitable J_0/M_0^2 for a lower order diagram from which the diagram under consideration can be constructed by

insertion of electron and photon lines:

$$0 < J(q;\,\beta)/M^2 \leqslant J_0(q;\,\beta^{(0)})/M_0^2\,. \tag{28}$$

for all q_i with $\sum\limits_i q_i = 0$, $\sum\limits_i q_i^2 > 0$.

The lemmas and theorems in this section have been derived under the assumption that the Bose field is massless. In case a meson field is considered, most of the results remain essentially unaltered, except that Theorem 4 and the preceding lemmas need a careful examination. Thus if a meson line is inserted, both I and M^2 will increase. In the case of inserting a closed loop in meson lines, it is necessary for the theorem to hold that M^2 does not decrease by the operation. This sets an upper limit $2m/n$ to the meson mass that depends on the number n of the meson lines connected to the loop. For example, if a loop is inserted in a single meson line (meson self-energy), the meson and nucleon masses have to satisfy the relation $\mu \leqslant 2m$. Physically it means that the meson must be energetically stable against decay into a pair. The proof will be given in the appendix.

3. – Application to the three-field Green's function.

We will here apply the results of the preceding section to exhibit the structure of the three-field Green's function or the vertex function.

The three-field Green's function $\varrho_{2,1}(p\,|\,p'\,|\,k)$ may be written in terms of eight scalar functions as

$$\begin{aligned}\varrho_{2,1}(p\,|\,p'\,|\,k) &= i\sum_{\lambda,\lambda'=0}^{1}(ip\cdot\gamma)^{\lambda}[H_{\lambda\lambda'}(pp'k)\gamma_\mu + K_{\lambda\lambda'}(pp'k)\sigma_{\mu\nu}k_\nu](ip'\cdot\gamma)^{\lambda'}\,,\\ \sigma_{\mu\nu} &= (\gamma_\mu\gamma_\nu-\gamma_\nu\gamma_\mu)/2i\,.\end{aligned} \tag{29}$$

In the (lowest) order e,

$$\left|\begin{aligned} H^{(0)}_{\lambda\lambda'} &= eC_{\lambda\lambda'}\frac{1}{p^2+m^2-i\varepsilon}\,\frac{1}{p'^2+m^2-i\varepsilon}\,\frac{1}{k^2-i\varepsilon} =\\ &= 2eC_{\lambda\lambda'}\iiint_0^1\frac{\delta(1-\alpha_0-\beta_0-\gamma_0)\,\mathrm{d}\alpha_0\,\mathrm{d}\beta_0\,\mathrm{d}\gamma_0/(1-\gamma_0)^3}{[(\alpha_0/1-\gamma_0)p^2+(\beta_0/(1-\gamma_0))p'^2+(\gamma_0/(1-\gamma_0))\,k^2+m^2-i\varepsilon]^3}\,,\\ K^{(0)}_{\lambda\lambda'} &= 0\,,\\ C_{\lambda\lambda'} &= \begin{pmatrix} m^2 & -m\\ -m & 1\end{pmatrix}.\end{aligned}\right. \tag{30}$$

Accordingly to Theorem 4, $H_{\lambda\lambda'}$ in general should have a form

$$H_{\lambda\lambda'} = \int \cdots \int \frac{\sigma_{\lambda\lambda'}(\alpha\beta\gamma)\,\mathrm{d}\alpha\,\mathrm{d}\beta\,\mathrm{d}\gamma}{[\alpha p^2 + \beta p'^2 + \gamma k^2 + m^2 - i\varepsilon]^n}, \qquad (n \geqslant 3), \tag{31}$$

where we have normalized M^2 to m^2 instead of normalizing $\alpha+\beta+\gamma$. Theorem 5 then says that there exists such J_0 that

$$J_0 = (\alpha_0/(1-\gamma_0))q_1^2 + (\beta_0/(1-\gamma_0))q_2^2 + (\gamma_0/(1-\gamma_0))q_3^2 \geqslant J = \alpha q_1^2 + \beta q_2^2 + \gamma q_3^2 \geqslant 0, \tag{32}$$

if three real numbers q_1, q_2 and q_3 satisfy $q_1 + q_2 + q_3 = 0$. Writing also

$$\begin{cases} \alpha \equiv (\alpha_0/(1-\gamma_0)) - \xi \geqslant 0, \\ \beta \equiv (\beta_0/(1-\gamma_0)) - \eta \geqslant 0, \\ \gamma \equiv (\gamma_0/(1-\gamma_0)) - \zeta \geqslant 0, \end{cases} \tag{33}$$

Eq. (32) becomes

$$\xi q_1^2 + \eta q_2^2 + \zeta (q_1 + q_2)^2 \geqslant 0, \tag{34}$$

which entails the inequalities

$$\xi + \eta \geqslant 0, \quad \eta + \zeta \geqslant 0, \quad \zeta + \xi \geqslant 0, \quad \xi\eta + \eta\zeta + \zeta\xi \geqslant 0. \tag{35}$$

Eqs. (33) and (35) are the conditions that essentially determine the spectrum of the absorptive part of H. For example, if one makes the electron legs free: $p^2 = p'^2 = -m^2$, then

$$\alpha p^2 + \beta p'^2 + \gamma k^2 = (\xi + \eta - 1)m^2 + \gamma k^2. \tag{36}$$

As a function of $-k^2$, the zero of the denominator $J + m^2$ in Eq. (31) is given by

$$-k^2 = (\xi + \eta) m^2/\gamma \geqslant 0. \tag{37}$$

Thus in this case the singularities of $H(-k^2)$ lie on the positive real axis, and their smallest value is indeed zero, which comes from $H^{(0)}$. In the same way, if $p'^2 = -m^2$, $k^2 = 0$, one can show that the singularities (absorptive part) of $H(-p^2)$ are restricted to $-p^2 \geqslant 0$.

It is possible to recognize the thresholds for various real processes by further classification of the Feynman diagrams. In the case of $p^2 = p'^2 = -m^2$,

the lowest threshold, apart from the incoming single photon state, is at $k^2=0$, corresponding to the creation of three photons. Now if one starts from the lowest order vertex (Eq. (30)) minus the external photon line (a V-shaped graph with electron lines only), and inserts all radiative corrections to it, the above kind of many-photon processes do not occur in such diagrams, but the first reaction that can take place is creation of a pair: $-k \to p+p'$; p_0, $p_0' \geqslant m$, which is possible if $-k^2 \geqslant 4m^2$. That this is indeed so can be seen as follows: The lowest order H is now

$$(38) \qquad \frac{1}{p^2+m^2-i\varepsilon}\,\frac{1}{p'^2+m^2-i\varepsilon}=\iint_0^1 \frac{\delta(1-\alpha_0-\beta_0)\,\mathrm{d}\alpha_0\,\mathrm{d}\beta_0}{[\alpha_0 p^2+\beta_0 p'^2+m^2-i\varepsilon]^2}\,,$$

so that γ_0 of Eq. (33) is zero, and $-\zeta \geqslant 0$. Putting $p^2=p'^2=-m^2$,

$$(39) \qquad J+m^2=(\xi+\eta)m^2-\zeta k^2\,.$$

Its zero corresponds to

$$(40) \qquad -k^2=m^2(\xi+\eta)/(-\zeta)\geqslant m^2(\xi+\eta)(1/\xi+1/\eta)\geqslant 4m^2\,.$$

where use was made of the relation

$$(41) \qquad -1/\zeta \geqslant 1/\xi+1/\eta \geqslant 0\,,$$

a consequence of Eq. (35).

As for the anomalous moment part K of $\varrho_{2,1}$, the lowest order is e^3, which will not be discussed here. But it is obvious that for any diagram all the functions have, in general, the same thresholds unless they vanish accidentally or by selection rules.

It is difficult to generalize these considerations to Green's functions of higher order. In particular, the dispersion relations of the familiar variety for the scattering matrix do not seem to follow in a simple way from our formulas. The main reason is as follows. The lowest order Compton scattering, for example, consists of the familiar uncrossed and crossed diagrams. As a function of $-P\cdot K$, where $P(K)$ is the sum of the initial and final electron (photon) momenta, they have a singularity at $-P\cdot K=-\Delta^2$ and $-P\cdot K=+\Delta^2$ respectively, Δ being the momentum transfer. In higher orders, it is expected that one class of matrix elements has singularities for $-P\cdot K\geqslant-\Delta^2$ and the other $-P\cdot K\leqslant\Delta^2$ so that each can be treated separately. But these classes cannot in general be related to the crossed and uncrossed diagrams. In fact some higher order diagrams contain both branches of the singularities simultaneously, which are difficult to unscramble.

4. – Remarks.

The derivation of the representations in Sect. 2 was made on the assumption that all the parametric integrations converge and the order of integration can be freely interchanged. This is not actually true because of the various divergences. These divergences are hidden in the weight functions $\sigma_\nu^{(\alpha)}(\alpha_{ji}, M^2/m^2)$ of Eq. (23), the explicit evaluation of which was not attempted. To remove the ultraviolet divergences, renormalization has to be carried out by introducing into the Hamiltonian appropriate counter terms. This will not affect the results of Sect. 2 since the counter terms do not destroy the nature of the representation, but the weight functions will be modified in such a way that they themselves are finite and give convergent integrals [7], apart from the infrared divergences characteristic of the radiation field. The presence of the infrared divergences in the Green's functions is a reflection of the fact that these functions do not necessarily correspond to physical quantities. Formally the difficulty is removed by giving a finite mass to the photon, and our theorems will still be valid.

The results of Sect. 2 exhibit the analytic property and characteristic thresholds of each function corresponding to a Feynman diagram; but obviously they cannot be carried over to a complete Green's function which is an infinite sum of such functions. In particular, our approach will certainly fail when bound states of particles exist since they affect the thresholds. It would be interesting if our results, after suitable modifications, could be derived without the use of perturbation. The variational properties of the functions observed in Sect. 2 may offer a clue to this problem.

Finally we will discuss the relation of the present representation to the previously proposed one of more restricted type. The latter had essentially the form

$$G(k_\mu^2) = \int \ldots \int_0^\infty \prod_{\mu=1}^{N(N-1)/2} \frac{1}{l_\mu^2 + s_\mu - i\varepsilon}\, \sigma(s_\mu)\pi\, \mathrm{d}s_\mu\,, \tag{54}$$

which should be compared with the new form

$$G'(k) = \int \ldots \int \frac{1}{[\sum_\mu \beta_\mu l_\mu^2 + M^2 - i\varepsilon]^n}\, \sigma'(M^2, \beta_\mu)\pi\, \mathrm{d}\beta_\mu \mathrm{d}M^2\,, \tag{55}$$

---

(7) The problem of renormalization was discussed in detail by Bogoljubow and Shirkow using the same kind of representation as in the present work. Bogoljubow and Shirkow: *Fortschritte d. Phys.*, 4, 438 (1956).

where the l_μ's are defined in Theorem 3. As was pointed out in Sect. 2, Eq. (55) shows that G' is the boundary value of a function analytic for $\operatorname{Im}(-l_\mu^2) > 0$. Thus it can be expressed as

$$G'(l_\mu^2) = \frac{1}{2\pi i}\int_{-\infty}^{\infty} \frac{G'(-s_1, l_2^2, \ldots)}{l_1^2 + s_1 - i\varepsilon}\, \mathrm{d}s_1 \,. \tag{56}$$

The same procedure can then be applied to $G'(-s_1, l_2^2, \ldots)$ in the integrand with respect to the variable l_2^2, and so on.

One gets finally

$$\begin{cases} G'(l_\mu^2) = \dfrac{1}{(2\pi i)^{N(N-1)/2}}\displaystyle\int \ldots \int_{-\infty}^{\infty} \prod \frac{1}{l_\mu^2 + s_\mu - i\varepsilon}\, G'(-s_\mu)\pi\, \mathrm{d}_\mu s \,, \\[2ex] \qquad = \dfrac{2i}{(2\pi i)^{N(N-1)/2}}\displaystyle\int \ldots \int_{-\infty}^{\infty} \prod \frac{1}{l_\mu^2 + s_\mu - i\varepsilon}\, \operatorname{Im} G'(-s_\mu)\pi\, \mathrm{d}s_\mu \,, \end{cases} \tag{57}$$

where in the last step only the imaginary part was used in the integrand to express $G'(-S_1, \ldots, -S_{N(N-1)/2-1}, l^2_{N(N-1)/2})$. Eq. (57) is similar to Eq. (54), but the parameters S_μ here run all the way from $-\infty$ to $+\infty$. Thus we see that $G(k_i)$ must have an additional special character if it is at all representable in the restricted form Eq. (54).

* * *

The author expresses his gratitude to Prof. M. Gell-Mann for his discussions when the former was staying at the California Institute of Technology in the summer of 1956.

Appendix I.

Take a diagram with $2n$ external electron lines, m photon lines, and R internal vertices. The total number of electron lines is $n+R$, and each electron line connecting two points x_i and x_k contributes a

$$S_F(x_i - x_k) = (-\gamma\cdot\partial/\partial x + m)\Delta_F(x) = \tag{A1}$$

$$= -\frac{i}{8\pi^2}\int_0^\infty \{-ia\gamma\cdot(x_i - x_k) + m\}\exp\left[ia(x_i - x_k)^2/2 - im^2/2a\right]\mathrm{d}a \,.$$

When one is supposed to integrate over x_i or x_k, the differentiation may be regarded as $-\partial/\partial x_k$ or $+\partial/\partial x_i$ respectively, and taken out of the integral sign.

Suppose in general one has a form

$$(x_1 - x_2)_\mu \exp[iI], \qquad I = \tfrac{1}{4}\sum_{i,k=1}^{N} a_{ik}(x_i - x_k)^2, \tag{A2}$$

which has to be integrated over x_1. Our problem is to express $(x_1 - x_2)_\mu$ in terms of derivatives with respect to the other $N-1$ co-ordinates, $x_2, \ldots, x_N$. Each $-i\partial/\partial x_i$ on $\exp[iI]$ gives $r_i = \sum_k a_{ik}(x_i - x_k)$, so that one requires

$$\begin{cases} x_1 - x_2 = \sum_i c_i r_i = \sum_{i,k} x_i(\delta_{ik}\sum_j a_{ij} - a_{ik})c_k \\ \qquad\quad = \sum_{i,k} A_{ik}x_i c_k, \end{cases} \tag{A3}$$

where A_{ik} is the matrix introduced in Eq. (7). Since this equation must hold for all x_i, one gets

$$\begin{cases} \sum_k A_{ik}c_k = C_i, \\ C_i = \begin{cases} 1 & i = 1 \\ -1 & i = 2 \\ 0 & i > 2 \end{cases} \end{cases} \tag{A4}$$

Both sides become zero on summing over i, so that one equation and one c_i is redundant. Thus there exists a solution with $c_1 = 0$, which enables $x_1 - x_2$ to be expressed in terms of the derivatives $\partial/\partial x_2, \ldots \partial/\partial x_N$.

Now each derivative in $S_F(x_i - x_k)$ is accompanied by a γ-matrix so that in our diagram there will be up to $(n+R)$ γ-matrices coupled with derivatives. On the other hand, our Green's function contains $2n$ spinor indices which can span a direct product of n γ-spaces. In each space there are $N-1$ independent scalars $\gamma\cdot r_i$ $(\sum_{i=1}^{N} r_i = 0)$. Thus the number of γ-matrices coupled with derivatives need not exceed $n(N-1)$. Some of the $\gamma\cdot r_i$'s will then be reduced to the scalars $r_i\cdot r_j$ and $r_i\cdot e_k$, where e_k $(k = 1, \ldots, m)$ are the polarization vectors of the radiation field. The number ν of the scalars $r_i\cdot r_j$ will be at most $(n+R)/2$ or $(n+R-1)/2$. Each $r_i\cdot r_j$ can be obtained by a linear combination of $i\partial/\partial a_k$ on $\exp[iI]$ with coefficients which are homogeneous functions of a_k of degree zero. Thus the effect of these scalars arising from γ-matrices will be absorbed into the function $\sigma(\alpha_{ij}, M^2/m^2)$ and an extra factor $(i/t)^\nu$.

Appendix II.

We will consider the effect of inserting a nucleon closed loop in a group of n meson lines spanned between the points x_1x_2; x_3x_4, ...; $x_{2n-1}x_{2n}$ (in a Eucl

space). These lines contribute

$$
\text{(A5)}\quad
\begin{cases}
I = \dfrac{1}{2}a_1(x_1-x_2)^2+\dfrac{1}{2}a_2(x_3-x_4)^2+\ldots+\dfrac{1}{2}a_n(x_{2n-1}-x_{2n})^2\,, \\[2ex]
M^2 = \dfrac{1}{2}\mu^2\left(\dfrac{1}{a_1}+\dfrac{1}{a_2}+\ldots+\dfrac{1}{a_n}\right).
\end{cases}
$$

After the insertion of a closed loop, the meson lines starting from $x_1, \ldots, x_{2n}$ will end on the loop at $y_1, \ldots, y_{2n}$, so that now

$$
\text{(A6)}\quad
\begin{cases}
I' = \dfrac{b_1}{2}(x_1-y_1)^2+\dfrac{b_2}{2}(x_2-y_2)^2+\ldots+\dfrac{b_{2n}}{2}(x_{2n}-y_{2n})^2+ \\[2ex]
\qquad\qquad +\dfrac{c_1}{2}(y'_1-y'_2)^2+\dfrac{c_2}{2}(y'_2-y'_3)^2+\ldots+\dfrac{c_{2n}}{2}(y'_{2n}-y'_1)^2\,, \\[2ex]
M'^2 = \dfrac{1}{2}\mu^2\left(\dfrac{1}{b_1}+\dfrac{1}{b_2}+\ldots+\dfrac{1}{b_{2n}}\right)+\dfrac{1}{2}m^2\left(\dfrac{1}{c_1}+\dfrac{1}{c_2}+\ldots+\dfrac{1}{c_{2n}}\right),
\end{cases}
$$

where $(y'_1, \ldots, y'_{2n})$, being a certain permutation of $(y_1, \ldots, y_{2n})$, is numbered by counting along the loop.

Let us subdivide c_l as

$$
\text{(A7)}\quad
\begin{cases}
c_l = \sum\limits_{i=1}^{n} c_{li}\,, \qquad\qquad l=1, \ldots, 2n;\ c_{li}\geqslant 0, \\[2ex]
\frac{1}{2}\sum\limits_{l=1}^{2n} c_l(y'_l-y'_{l+1})^2 = \frac{1}{2}\sum\limits_{i=1}^{n}\sum\limits_{l=1}^{2n} c_{li}(y'_l-y'_{l+1})^2\,,\ (y'_{2n+1}\equiv y'_1)
\end{cases}
$$

and observe that for any pair y'_a and y'_b $(a>b)$ and fixed i

$$
\begin{aligned}
&\tfrac{1}{2}c_{ai}(y'_a-y'_{a+1})^2+\tfrac{1}{2}c_{a+1,i}(y'_{a+1}-y'_{a+2})^2+\ldots+\tfrac{1}{2}c_{b-1,i}(y'_{b-1}-y'_b)^2\geqslant \\
&\qquad\geqslant\frac{1}{2}\,\frac{(|y'_a-y'_{a+1}|+\ldots+|y'_{b+1}-y'_b|)^2}{(1/c_{ai})+\ldots+(1/c_{b-1,i})}\geqslant\frac{1}{2}\,\frac{(y'_a-y'_b)^2}{1/c_{ai}+\ldots+1/c_{b-1,i}}
\end{aligned}
$$

$$
\begin{aligned}
&\tfrac{1}{2}c_{bi}(y'_b-y'_{b+1})^2+\tfrac{1}{2}c_{b+1,i}(y'_{b+1}-y'_{b+2})^2+\ldots+\tfrac{1}{2}c_{a-1,i}(y'_{a-1}-y'_a)^2\geqslant \\
&\qquad\geqslant\frac{1}{2}\,\frac{(|y'_b-y'_{b+1})+\ldots+|y'_{a-1}+y'_a|)^2}{(1/c_{bi})+\ldots+(1/c_{a-1,i})}\geqslant\frac{1}{2}\,\frac{(y'_b-y'_a)^2}{(1/c_{bi})+\ldots+(1/c_{a-1,i})}\,.
\end{aligned}
$$

Thus

$$
\begin{aligned}
\text{(A8)}\quad &\frac{1}{2}\sum_l c_{li}(y'_l-y'_{l+1})^2\geqslant\frac{1}{2}(y'_a-y'_b)^2\left(\frac{1}{(1/c_{ai})+(1/c_{a+1,i})+\ldots+(1/c_{b-1,i})}\right)+ \\
&\qquad+\left(\frac{1}{(1/c_{bi})+(1/c_{b+1,i})+\ldots+(1/c_{a-1,i})}\right)\geqslant\frac{1}{2}(y'_a-y'_b)^2\frac{4}{\sum\limits_{l=1}^{2n}(1/c_{li})}\,.
\end{aligned}
$$

Identifying (y'_a, y'_b) with (y_{2i-1}, y_{2i}), we obtain from Eq. (A8)

$$\text{(A9)}\qquad \frac{1}{2}\, b_{2i-1}(x_{2i-1} - y_{2i-1})^2 + \frac{1}{2}\, b_{2i}(x_{2i} - y_{2i})^2 + \frac{1}{2}\sum c_{li}(y'_l - y'_{l+1})^2 \geqslant$$

$$\geqslant \frac{1}{2}\,\frac{(|x_{2i-1} - y_{2i}| + |x_{2i} - y_{2i}| + |y_{2i-1} + y_{2i}|)^2}{(1/b_{2i-1}) + (1/b_{2i}) + \frac{1}{4}\sum_{l=1}^{2n}(1/c_{li})} \geqslant$$

$$\geqslant \frac{1}{2}\,(x_{2i-1} - x_{2i})^2 \Big/ \left(\frac{1}{b_{2i-1}} + \frac{1}{b_{2i}} + \frac{1}{4}\sum_{l=1}^{2n}\frac{1}{c_{li}}\right).$$

Summing this over i, the left-hand side becomes I':

$$\text{(A10)}\qquad I' \geqslant \frac{1}{2}\sum_{i=1}^{n}\left[(x_{2i-1} - x_{2i})^2 \Big/ \left(\frac{1}{b_{2i-1}} + \frac{1}{b_{2i}} + \frac{1}{4}\sum_{l=1}^{2n}\frac{1}{c_{li}}\right)\right].$$

In order to compare I, M and I', M', we choose a_i in such a way that

$$\text{(A11)}\qquad \frac{1}{a_i} = \frac{1}{b_{2i-1}} + \frac{1}{b_{2i}} + \frac{1}{4}\sum_{l=1}^{2n}\frac{1}{c_{li}}.$$

Then clearly

$$\text{(A12)}\qquad I' \geqslant I.$$

Also

$$\text{(A13)}\qquad M^2 = \frac{1}{2}\,\mu^2\sum_{i=1}^{n}\left(\frac{1}{b_{2i-1}} + \frac{1}{b_{2i}} + \frac{1}{4}\sum_{l=1}^{2n}\frac{1}{c_{li}}\right) =$$

$$= \frac{1}{2}\,\mu^2\left(\frac{1}{b_1} + \frac{1}{b_2} + \dots + \frac{1}{b_{2n}}\right) + \frac{1}{2}\,\frac{1}{4}\,\mu^2\sum_{l=1}^{2n}\sum_{i=1}^{n}\frac{1}{c_{li}} \geqslant$$

$$\geqslant \frac{1}{2}\,\mu^2\left(\frac{1}{b_1} + \frac{1}{b_2} + \dots + \frac{1}{b_{2n}}\right) + \frac{1}{2}\,\frac{n^2}{4}\,\mu^2\sum_{l=1}^{2n}\frac{1}{c_l},$$

where the inequality

$$\sum_{i=1}^{n}\frac{1}{c_{li}} \geqslant n^2 \Big/ \sum_{i=1}^{n} c_{li} = n^2/c_l$$

was used. Comparing this with M'^2,

$$\text{(A14)}\qquad M^2 - M'^2 \geqslant \frac{1}{2}\left(\frac{n^2}{4}\,\mu^2 - m^2\right)\sum_l \frac{1}{c}.$$

The equality holds if the particular choice

(A15) $$c_{l1} = c_{l2} = \ldots = c_{ln} = c_l/n$$

is made for a given c_l.

Now if $n\mu > 2m$, we have the situation $I' \geqslant I$, $M^2 \geqslant M'^2$, which is not necessarily compatible with

(A16) $$I'M'^2 \geqslant IM^2 .$$

On the other hand, if $n\mu \leqslant 2m$, then with the choice Eq. (A15), $M^2 \leqslant M'^2$ so that the inequality Eq. (A16) follows.

RIASSUNTO (*)

Si derivano, nella teoria delle perturbazioni, delle rappresentazioni parametriche per la funzione di Green della teoria dei campi. Tali rappresentazioni sono valide per ogni termine della serie perturbativa corrispondente a un diagramma di Feynman e rispecchiano la sua proprietà analitica e le sue caratteristiche di soglia. Come esempio si dimostra che quando siano fissati due dei tre impulsi la funzione di tre corpi (di vertice) soddisfa una relazione di dispersione con la corretta localizzazione delle singolarità previste in base alle soglie dei processi reali in competizione.

(*) *Traduzione a cura della Redazione.*

IL NUOVO CIMENTO Vol. VI, N. 5 1° Novembre 1957

On the Mean Life of μ^--Mesons in Elements of Medium and High Atomic Number.

A. Alberigi-Quaranta (*) and F. Pieraccini

Istituto di Fisica dell'Università - Roma
Istituto Nazionale di Fisica Nucleare - Sezione di Roma

D. Broadbent (+)

Istituto Nazionale di Fisica Nucleare - Sezione di Roma

(ricevuto il 25 Giugno 1957)

Summary. — The mean life of μ-mesons stopped in iron has been investigated by means of a new apparatus. The experimental arrangement for the determination of the mean life of μ^- in elements of mean and high atomic number is described. The deflection of the trajectory of a cosmic ray μ-meson passing through two magnetized iron blocks ($B = 1.5$ Wb m^{-2}) indicates the sign of the incoming meson. The deflection is measured by an hodoscope of 90 Geiger counters. A fast syncroscope determines the interval of time between the arrival of the meson and its disappearance in the absorbers due either to capture by nuclei or to the normal process of decay. The error in the reading of the time interval is $\sim 10^{-8}$ s. The mean life of the meson in the element constituting the absorber is directly calculated from the distribution of the delays. The value for the mean life of the μ^--meson in iron was found to be $\tau = (16 \pm 1) \cdot 10^{-8}$ s.

(*) Now at the Istituto Nazionale di Fisica Nucleare, Sezione Acceleratore, Roma.
(+) Now at the University of Manchester, Manchester, Great Britain.

Introduction.

In the last decade the experimental study of the behaviour of μ-mesons coming to rest in the proximity of atomic nuclei has been carried out by several laboratories. It has thus been possible to shed some light on several aspects of the nature of this particle, among which the weak interaction μ^--meson-nucleon and its reaction with the proton according to the scheme

$$\mu^- + P \to N + \nu . \tag{1}$$

It has moreover been possible to obtain interesting information concerning the processes induced in nuclei of different atomic number by the capture of negative μ-mesons. In this connection it is noteworthy to observe that although it does not seem likely that this type of research could provide further information on the nature of the μ-meson (with the obvious exception of capture by hydrogen), it can be assumed that a more accurate investigation of the interactions between negative μ-mesons and nuclei of different atomic numbers Z could give useful information about the structure of the nuclei themselves.

First of all it is important to remember that several experimental approaches to this problem have been adopted; they can be briefly summarized as follows:

1) Direct determination of the mean life τ, of the negative meson in elements of different atomic number (1-10).

2) Determination of the ratio R between the number of negative μ-mesons disintegrated after stopping in a given element and the total number of negative μ-mesons stopped by the same element (1) (11-13).

---

(1) H. K. Ticho: *Phys. Rev.*, **74**, 1337 (1948).
(2) G. E. Valley: *Rev. Mod. Phys.*, **21**, 35 (1949).
(3) W. E. Bell and E. P. Hincks: *Phys. Rev.*, **84**, 1243 (1951).
(4) L. Cathey: *Phys. Rev.*, **87**, 169 (A) (1952).
(5) J. W. Keuffel, F. B. Harrison, T. M. K. Godfrey and G. T. Reynolds: *Phys. Rev.*, **87**, 942 (1952).
(6) W. E. Bell and E. P. Hincks: *Phys. Rev.*, **88**, 1424 (1952).
(7) A. Alberigi-Quaranta and E. Pancini: *Nuovo Cimento*, **9**, 959 (1952).
(8) A. H. Benade: *Phys. Rev.*, **91**, 971 (1953).
(9) A. G. Tenner: *Physica*, **20**, 24 (1954).
(10) A. Alberigi-Quaranta and E. Pancini: *Nuovo Cimento*, **11**, 607 (1954).
(11) M. Conversi, E. Pancini and O. Piccioni: *Nuovo Cimento*, **3**, 372 (1946).
(12) T. Sigurgeirsson and K. A. Yamakava: *Rev. Mod. Phys.*, **21**, 124 (1949).
(13) L. Ledermann and M. Weinrich: *CERN Symposium*, June 1956.

3) Study of the products formed in the process of capture of negative μ-mesons by nuclei (neutrons and γ-rays) [14-28].

4) Radiochemical study of the nuclei produced by the capture of negative μ-mesons in nuclei [29-32].

It is easily shown that both methods 1) and 2) allow a determination of the probability of capture of the negative μ-meson by nuclei. It is well known [33] that the probability p of disappearance per unit of time of the μ^--meson in the proximity of a nucleus is given by the following relation:

$$p = p_d + p_c \,, \tag{2}$$

where p_d is the probability of decay per second of the μ^-meson in vacuum and p_c is the capture probability per second of the μ^-meson by the nucleus. The relation (2) can also be written

$$\frac{1}{\tau} = \frac{1}{\tau_d} + \frac{1}{\tau_c} \,, \tag{3}$$

where τ is the mean life of the meson in the proximity of the nucleus, $\tau_d = 2.22 \cdot 10^{-6}$ s is the mean life of the meson in vacuum ($p_d = 1/\tau_d$) and $\tau_c = 1/p_c$.

---

(14) R. D. Sard, W. B. Ittner III, A. M. Conforto and M. F. Crouch: *Phys. Rev.*, **74**, 97 (1948).
(15) G. Groetzinger and G. M. McClure: *Phys. Rev.*, **74**, 341 (1948).
(16) R. D. Sard, A. M. Conforto and M. F. Crouch: *Phys. Rev.*, **76**, 1134 (1949).
(17) R. D. Sard, M. F. Crouch, D. R. Jones, A. M. Conforto and B. F. Stearn: *Nuovo Cimento*, **8**, 326 (1951).
(18) G. Groetzinger, M. J. Berger and G. W. McClure: *Phys. Rev.*, **81**, 969 (1951).
(19) M. F. Crouch and R. D. Sard: *Phys. Rev.*, **85**, 120 (1952).
(20) A. M. Conforto and R. D. Sard: *Phys. Rev.*, **86**, 465 (1952).
(21) E. J. Althaus and R. D. Sard: *Phys. Rev.*, **91**, 373 (1953).
(22) M. Widgoff: *Phys. Rev.*, **90**, 891 (1953).
(23) L. Niklas and K. H. Lauterjung: *Zeits. f. Naturf.*, **80**, 214 (1953).
(24) H. Morinaga and W. F. Fry: *Nuovo Cimento*, **10**, 308 (1953).
(25) D. R. Jones: *Phys. Rev.*, **105**, 1591 (1957).
(26) W. Y. Chang: *Rev. Mod. Phys.*, **21**, 166 (1949).
(27) W. Galbraith and W. J. Whitehouse: *Phil. Mag.*, **44**, 77 (1953).
(28) G. B. Harris and T. J. B. Shauley: *Phys. Rev.*, **89**, 983 (1953).
(29) T. N. K. Godfrey: *Phys. Rev.*, **92**, 512 (1953).
(30) T. N. K. Godfrey: *Thesis*, Princeton University (Princeton, U.S.A.).
(31) A. Turkevich and S. C. Fung: *Phys. Rev.*, **92**, 521 (1953).
(32) L. Winsberg: *Phys. Rev.*, **95**, 205 (1954).
(33) R. E. Marshak: *Meson Physics* (New York, 1952), p. 191 e segg.

It is therefore evident that

$$R = \frac{p_d}{p_c} = \frac{\tau_c}{\tau_d}\,.$$

As the value of $p_d = 1/\tau_d$ is well known, it is possible to calculate the value of $p_c = 1/\tau_c$ by the measurement of τ or R.

With regard to the method 1) it should be observed that the mean life of the μ^--meson in a given element can be directly calculated either from the distribution of the decay times of the meson or from the distribution of the capture times of the meson by nuclei. Moreover it is obvious that the distribution of the disappearance times of the μ^--meson due both to the decay process and to capture by the nucleus also follows the typical exponential law, with time constant τ.

The mean life obtained by method 1) might not, however, coincide with that ascertained by method 2) if the time distribution were altered as explained below. Method 1), in fact, does not directly measure the time interval between the stopping of the meson and its capture or decay, but determines, instead, the interval between the arrival of the meson in a given absorber and the exit from the absorber of the decay (electron) or capture products (neutrons and γ-rays). Although it can reasonably ([34-39]) be assumed that no appreciable alteration in the time distribution of the decay process occurs it cannot « a priori » be excluded that the capture of the μ-meson by the nucleus and the emission of neutrons and γ-rays by the nucleus itself does not take place simultaneously. In particular a delay in the γ-ray emission can result whenever the mean lives of the isomeric states created by the absorption of the μ^--meson are of the same or of a greater order of magnitude than that of the mean life of the meson.

In order to exclude this possibility two methods can be followed:

a) In the case of method 1), that only the events of the disappearance of the meson by capture in the nucleus are considered, the mean lives obtained by this method can be compared with the capture probability estimated by method 2).

b) The mean life obtained by method 1) for a given element by the distribution of the time intervals between the arrival of the μ^--mesons and

---

([34]) E. Fermi and E. Teller: *Phys, Rev.*, **72**, 399 (1947).
([35]) E. Fermi, E. Teller and V. Weisskopf: *Phys. Rev.*, **71**, 314 (1947).
([36]) J. A. Wheeler: *Phys. Rev.*, **71**, 320 (1947).
([37]) B. Ferretti: *Nuovo Cimento*, **5**, 325 (1948).
([38]) R. Huby: *Phil. Mag.*, **40**, 685 (1949).
([39]) R. E. Marshak: *Meson Physics* (New York, 1952), p. 166 and foll.

the emission of the capture products can be compared with the mean life determined for the same element from the distribution of the time intervals between the arrival and the decay of the meson.

If the results obtained by the different methods are consistent, the determination of the mean life of the μ^--meson in the presence of a given nucleus can safely be compared with the results of the theoretical calculations elaborated by different authors for the interpretation of the dependence of τ on the atomic number Z [40-44].

In particular it cannot be excluded that the remarkable discrepancies observed by KEUFFEL *et al.* [5] between the mean lives, τ, of μ^--mesons for elements of similar atomic numbers (e.g. Hg ($Z=80$), Pb ($Z=82$), Bi ($Z=83$)) can be ascribed not only to variations of the capture probability due to the different nuclear structures but also to delay between the meson capture and the successive emission of γ-rays by the nucleus.

It should therefore be expedient to determine the mean life of the μ^--meson in these elements taking into account only the meson decays even though these measurements in the case of heavy elements, present some difficulties owing to the inherent prevalence of the capture process with respect to the disintegration process.

On the basis of these considerations we have thought convenient to build an apparatus which would allow the determination of the mean life of cosmic ray mesons stopped in elements of different atomic numbers, registering both decay- and nuclear capture events. Unfortunately, a differentiation between these two types of events is not possible, only an approximate evaluation of the rate of either process being permitted. Since our apparatus allows registration of both meson captures and decays, a determination of the mean life in elements both of high atomic number (in which the capture process prevails) and low (in which decay predominates) is permitted. Our apparatus is therefore particularly fit for a verification of the accurate calculations by KENNEDY [42] for the mean lives in Ca ($Z = 20$) and Pb ($Z = 82$).

Iron was the element chosen first for the following reasons. The value for the mean life τ of μ^--mesons in iron has already been determined though not with very high precision in other laboratories; a comparison between these results and those obtained with our apparatus provided therefore the mean to establish its efficiency. Moreover, iron can be considered to occupy

---

(40) W. WHEELER: *Rev. Mod. Phys.*, **21**, 133 (1949).

(41) J. TIOMNO and J. A. WHEELER: *Rev. Mod. Phys.*, **21**, 154 (1949).

(42) J. M. KENNEDY: *Phys. Rev.*, **87**, 953 (1952).

(43) T. EGUCHI and M. OHTA: *Nuovo Cimento*, **10**, 1415 (1953).

(44) H. PRIMAKOFF: *Proceedings of the Fifth Annual Rochester Conference* (1955). p. 174.

an intermediate position between the light elements, which follow the Wheeler law $p_c = (1/\tau_d)(Z_e/Z_0)^K$ (with $Z_0 = 11$, $K = 4$ and Z_e a function of Z) with a good approximation, and the heavy elements, in which the behaviour of p_c differs considerably from that described by the above mentioned law ([45]). Therefore in order to establish the exact value of Z for which the experimental values differ from those obtained from Wheeler's law, it might be of some interest to determine the value of τ for iron with high precision. A further advantage is constituted by the fact that, the value for R in iron being known ([13]), it is possible, as shown below, to make an approximate estimation of the efficiency of our apparatus to register both the capture and decay products of the μ^--mesons.

Our determination of the mean life τ of the μ^--meson in Fe is affected by a standard error which is considerably smaller than that of previous determinations. In this connection it should be observed that cosmic radiation can be favorably compared even with accelerator apparatuses as a source of mesons for the determination of τ by method 1). Cosmic radiation, however, has to be excluded when expensive elements, such as isotopes, are to be studied; in this case, in fact, the supply of sufficiently large absorbers might present serious difficulties.

Finally, it should be noted that, in order to complete our present knowledge of the μ^--meson-nucleus interaction, thorough systematic investigations with method 4) are highly desirable; this requires, however, the use of accelerator apparatuses.

Experimental apparatus.

The longitudinal and lateral sections of our experimental apparatus are shown in Fig. 1. The upper part detects the sign of the incoming μ-mesons and records their arrival into the lower part which measures the life-time of the particle after it has come to rest. A knowledge of the sign of the meson allows a more direct determination of the distribution of the lifet-imes of the μ^--mesons, taking also the disintegrations into account. In fact, if the determination of the sign of the mesons were omitted, the mean life should be calculated from the distribution of the life-time of both μ^+ and μ^--mesons and the known values of τ_d and the positive excess. The uncertainty concerning the last two quantities, however, would affect the determination of τ. For the recognition of the sign of the mesons this apparatus was chosen instead of

([45]) S. DE BENEDETTI: *Suppl. Nuovo Cimento*, **4**, 1209 (1956).

the well known magnetic lens ([46]) because it allows both the simultaneous flux of mesons of either sign, and a much higher intensity of incoming particles.

The 90 Geiger counters (length = 50 cm; diameter = 1 cm) of trays S_1-D_1; S_2-D_2; S_3-D_3 constitute a hodoscope from which information on the curvature of the trajectory of the meson going through the magnetized iron blocks M_1', M_1'', M_2', M_2'' can be obtained. The magnetic induction vector B within the blocks is parallel to the axis of the counters, its sense in $M_1'M_1''$ being opposed

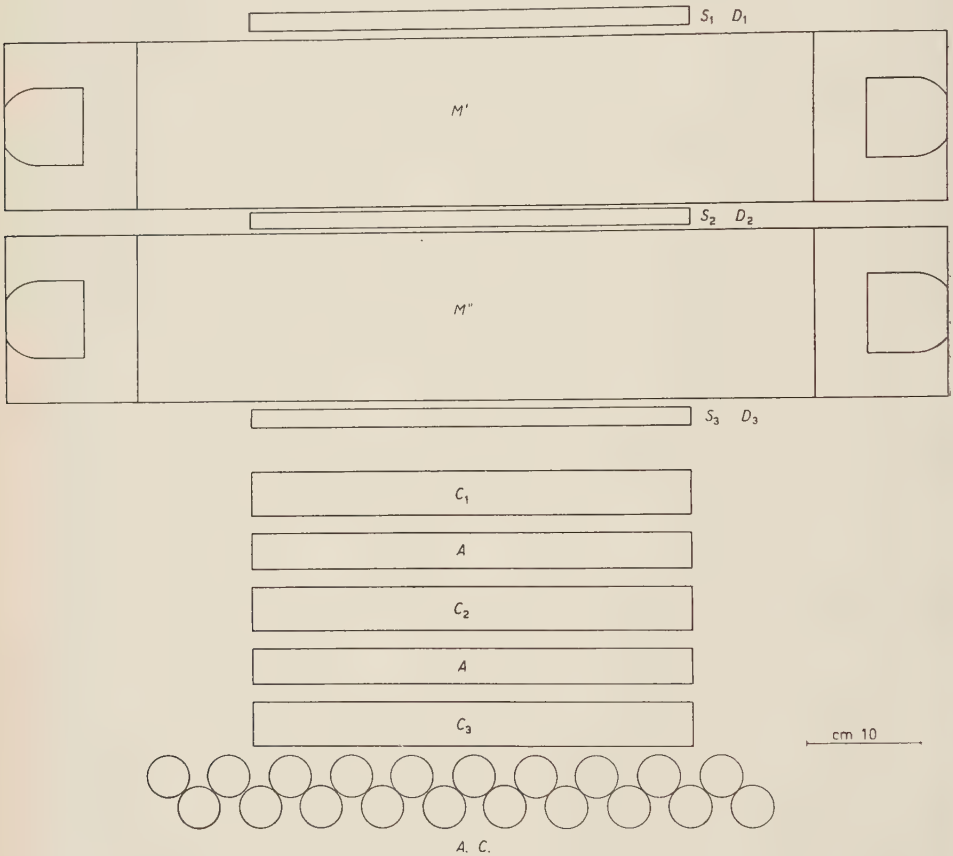

Fig. 1 *a*).

to that in $M_2'M_2''$. This is due to the fact that $M_1'M_2'$ and, separately, $M_1''M_2''$ constitute two identical magnetic (circuits in which the value of B is slightly larger than 1.5 Wb/m²). The error introduced by scattering in the magnetic

([46]) G. Bernardini, M. Conversi, E. Pancini, E. Scrocco and G. C. Wick: *Phys. Rev.*, **68**, 109 (1945).

blocks on the curvatures of mesons stopped by the absorbers placed under blocks $M_1'M_1''M_2'M_2''$ was estimated. It can be forseen that 80% of the incoming mesons will be recognized with the right sign, 19% recognized with

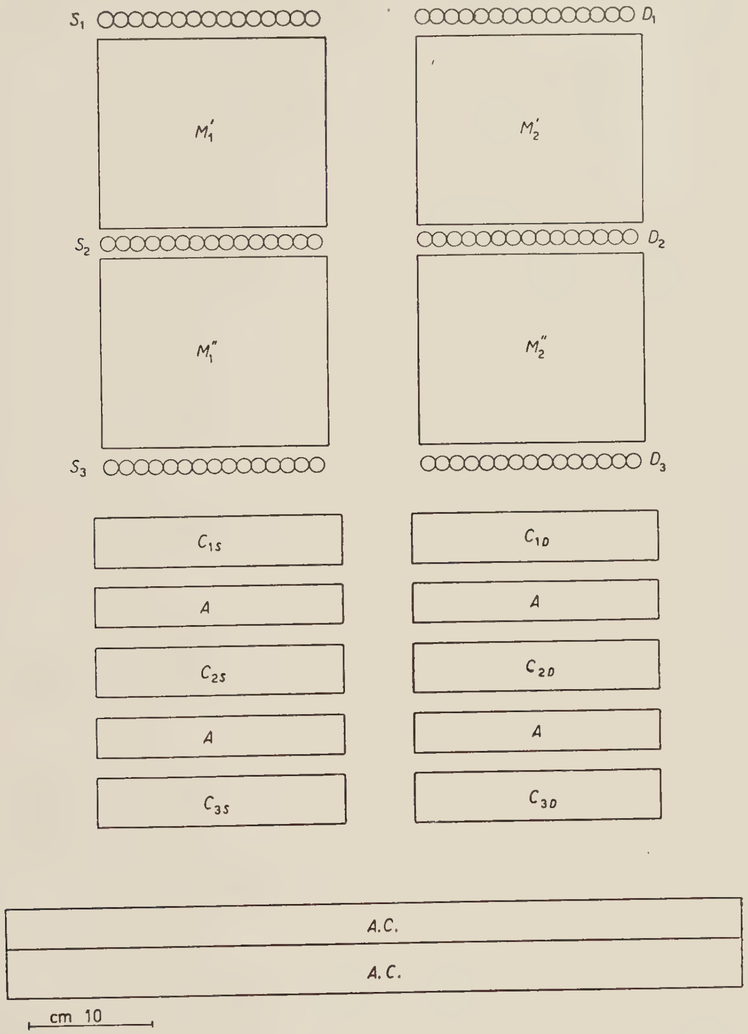

Fig. 1 *b*)

the right sign or not recognized (curvature = zero) and 1% not recognized or recognized with the wrong sign. The lower part of the apparatus consists of six scintillation counters C_{1S} C_{2S} C_{3S} C_{1D} C_{2D} C_{3D} very similar to those employed by KEUFFEL *et al.* (5) size 4 cm × 20 cm × 50 cm. These counters have brass walls polished on the inner surfaces, and are viewed by 4 photomultipliers

each (1 P 21 RCA). The scintillating solution has the following composition: paraterphenyl (5 g/l) and diphenylexatriene (10 mg/l) in toluene. The efficiency of the counters for charged particles at the minimum of ionization crossing the counters along the vertical direction is about 75%. During the measurements, the voltage in each phototube was periodically adjusted so that, when a beam of γ-rays from ^{60}Co crossed the counter in a central position equally distant from the four phototubes, the mean frequency of pulses, with amplitudes greater than a chosen value coming from each of them reached a previously fixed value.

22 Geiger counters in anticoincidence have been placed below the scintillation counters.

The operation of this apparatus can be better understood with the help of its block diagram (Fig. 2).

When the same particle discharges a counter in each of the three trays $S_1\,S_2\,S_3$ or $D_1\,D_2\,D_3$ a coincidence pulse leaves the triple coincidence circuit S or D (resolution time $\sim 1\ \mu$s). The pulse is forwarded to one of the inputs of the double coincidence circuit CS or CD (resolution time $\sim 1\ \mu$s). The other input of circuits CS and CD is connected with the output of the selector circuit that utilizes the information coming from the photomultipliers. The photomultiplier plates of each scintillation counter are joined by a low capacity (30 pF/m) high impedance ($Z_0 = 140\ \Omega$) coaxial cable connected to the input of a rapid amplifier (gain 50; rise-time $T_r = 10^{-8}$ s). Each couple of scintillation counters $C_{1S}C_{1D}$, $C_{2S}C_{2D}$, $C_{3S}C_{3D}$ is connected with a different amplifier $A_1A_2A_3$. The outputs V_1 of these amplifiers are connected to the selector circuit with different delays obtained by low impedance coaxial cable ($Z_0 = 52\ \Omega$).

The pulses coming from A_1 reach the selector with a delay of about 10^{-7} s (with respect to the pulses coming from A_2 and A_3) and are lengthened to 0.6 μs before being forwarded to the input of a rapid double coincidence circuit. To the other input of this double coincidence circuit come pulses of a duration of about $5\cdot10^{-8}$ s, from A_2 and A_3, which, as mentioned above, are in advance of the pulses from A_1 by about 10^{-7} s. When an output pulse from A_1 is followed by a pulse from A_2 or A_3 with a delay of $5\cdot10^{-8} \div 6\cdot10^{-7}$ s a double coincidence occurs and, consequently, a pulse leaves the selector.

No pulse comes out of the selector when pulses from A_2 or A_3 are coincident or delayed less than $5\cdot10^{-8}$ s with respect to pulses from A_1. In this way all delays of less than $5\cdot10^{-8}$ s are eliminated from the analysis and, consequently, all events due to processes of short mean life (mesons π, K, etc) and to other causes discussed in detail by KEUFFEL *et al.* [5] are also excluded.

The upper limit of the delay (0.6 μs) has, instead, been chosen so as to limit the analysis to the time interval in which the greatest part of the events under investigation are presumed to occur.

2952

When a coincidence occurs in CD or CS between a pulse from the selector and a triple coincidence (D or S) pulse, the pulse leaving CD or CS triggers the generator of the master pulse. The master pulse starts the registration cycle, in which the hodoscope ascertains which of the counters in trays S or D

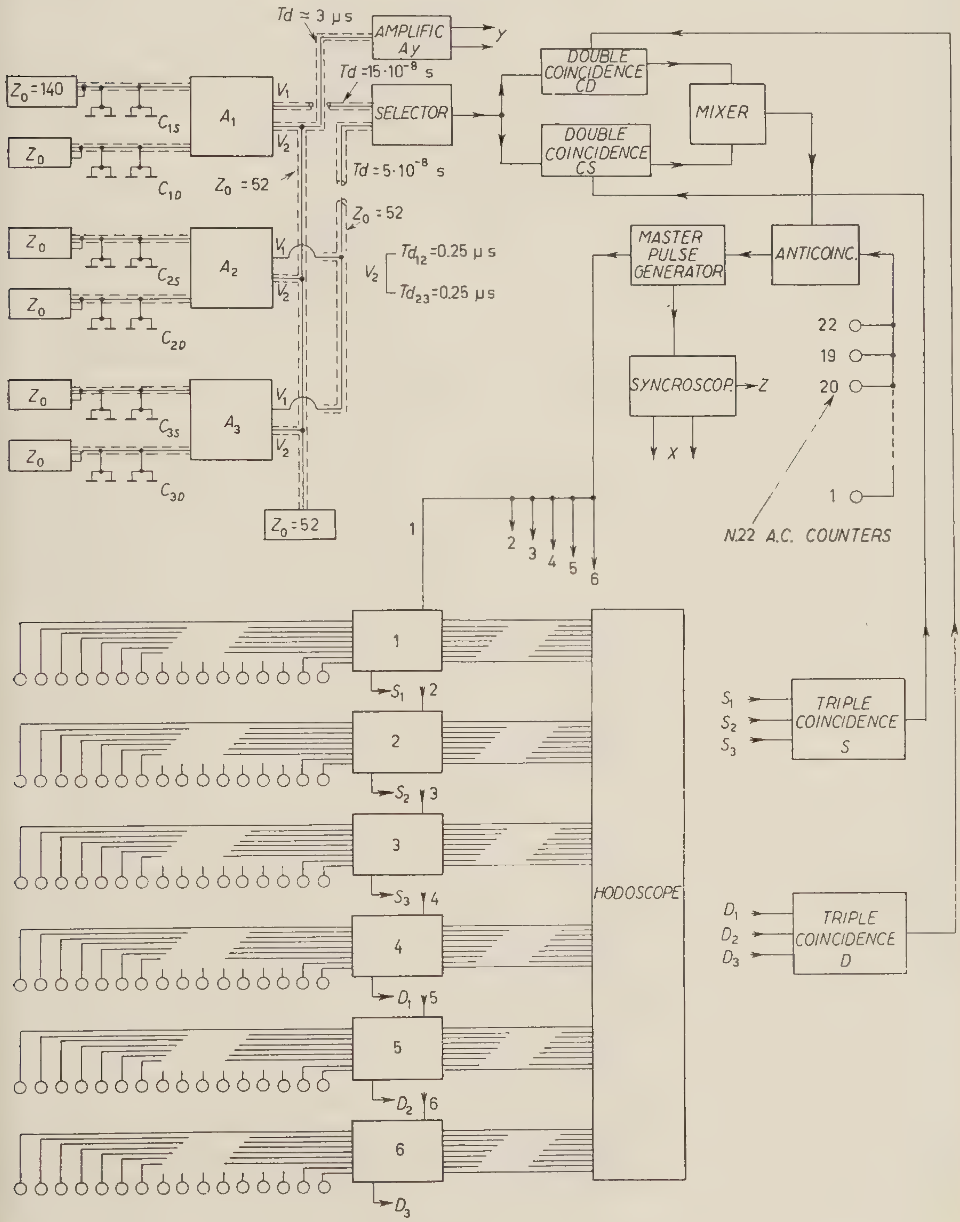

Fig. 2.

have been activated and the synchroscope and camera record the time succession of pulses from $A_1A_2A_3$.

The total length of the sweep of the synchroscope corresponds to 2 μs and the pulses coming from amplifiers $A_1A_2A_3$ are delayed 3 μs by a coaxial cable before they reach amplifier A_y (gain $= 10^2$, rise-time $T_R = 2\cdot10^{-8}$ s) of the synchroscope. This delay is introduced in order to compensate for the time required by the different circuits to produce the master pulse and to start the synchroscope. The three outputs V_2 of amplifiers $A_1A_2A_3$ are joined by 50 m of coaxial cable (delay 0.25 μs) so that pulses from $A_1A_2A_3$ reach A_y in succession. That is, if three pulses start simultaneously from the three amplifiers the pulse from A_2 will reach A_y 0.25 μs later than the pulse from A_1, and the pulse from A_3 will reach A_y 0.25 μs later than the one from A_2 and 0.5 μs later than the pulse from A_1. Moreover each amplifier produces pulses of different shapes at the outputs V_2, so as to make possible a recognition on the photographic record (Fig. 3) of the amplifier from which pulses originate.

Measurements of the oscillograph recording film allow a determination of the delays between pulses with a precision of 10^{-8} s.

It should be observed that pulses coming from the selector are delayed about 1 μs by a delay line, so that they reach *CD* and *CS* only after the arrival of pulses from triple coincidence circuits *D* or *S*.

In this way the master pulse and the start of the synchroscope are separated by a constant delay from the selector pulse and, therefore, from the pulses of the scintillation counters going to the amplifier A_y of the synchroscope. Consequently, the pulses to be recorded on the synchroscope appear at about $\frac{1}{3}$ the distance of the sweep from the origin of the sweep.

The sweep speed is checked at the beginning and at the end of each run. During the measurement a further check of the sweep speed is established by the distance separating simultaneous pulses from the three amplifiers, which, as shown above, are delayed, one from the other, by constant time intervals fixed by the length of the cable connecting the output V_2 of the three amplifiers. The dispersions of these time intervals, due to variations in the delays of the scintillation counters and of the amplifiers, or to uncertainties in the readings, do not exceed, however, 10^{-8} s, and do not, therefore, affect [47] the precision of the mean life determination.

The characteristics of the above described apparatus are briefly summarized as follows:

By means of a synchroscope the time succession of pulses from the scintillation counters is recorded.

The curve of the trajectory of the particles crossing iron blocks $M'_1M''_1M'_2M''_2$ is established. This is possible whenever the following conditions are fulfilled:

---

[47] N. NERESON and B. ROSSI: *Phys. Rev.*, **62**, 417 (1942).

a) Three or more Geiger counters (at least one an each of trays $S_1S_2S_3$ or $D_1D_2D_3$) are simultaneously discharged (resolution time 1 μs).

b) No anti-coincidence counter in A.C. is discharged.

c) A pulse in either of the scintillation counters C_{1S} or C_{1D} is followed by a pulse in counters $C_{2D}C_{2S}$, $C_{3D}C_{3S}$ within a delay range of $5\cdot10^{-8}\div6\cdot10^{-7}$ s.

Experimental results.

By this apparatus a series of measurements for the determination of the mean life of the μ^--meson in iron has been performed.

The absorbers were iron blocks (Fe content $\geqslant 99.5\,\%$) size 3 cm $\times$ 21 cm $\times$ 45 cm and consequently with a vertical thickness of 23.5 g/cm². This value is slightly greater than the mean range ([48]) in iron of decay electrons with maximal energy (17 g/cm²).

The frequency of incoming mesons of both signs is approximately given by the frequency of pulses from triple coincidences S and D, and is, therefore, equal to $\sim 4\,000$/h. The frequency of the events registered when conditions *a*), *b*) and *c*) of the preceding paragraph are fulfilled is about 20/h. From these events are selected only those characterized by the following succession of pulses on the synchroscope, i.e. only these events are considered as disappearances of mesons in the absorbers:

1) A pulse from A_1 is followed by a delayed pulse from A_2 (Fig. 3*a*)

2) A pulse from A_1 is followed by two simultaneous pulses from A_2 and A_3 both delayed with respect to the pulse from A_1 (Fig. 3 *b*).

3) Two simultaneous pulses from A_1 and A_2 are followed by a delayed pulse from A_3 (Fig. 3 *c*).

It is reasonable to think that these three groups of events (see Fig. 3) include only events produced by mesons stopped by the absorbers and not by the scintillation counters; moreover, only the decay and capture products downwards emitted of the stopped mesons are taken into account. The events in which the disintegration or capture products of the stopped mesons are emitted in the upward direction are purposely excluded because they are by no means distinguishable from events occurring in the scintillators (*). More-

([48]) R. D. Sard and J. Althaus: *Phys. Rev.*, **74**, 1366 (1948).

(*) On the other hand it would not be correct to consider all of these events together, and to discard, successively, the contribution of the disappearances of mesons in the scintillators by subtracting the results obtained without absorbers in an equal interval of time. It cannot be assumed, in fact, even in a gross approximation, that the disappearance products of μ^- mesons in the scintillators are registered with equal efficiency both in the presence and absence of the absorbers.

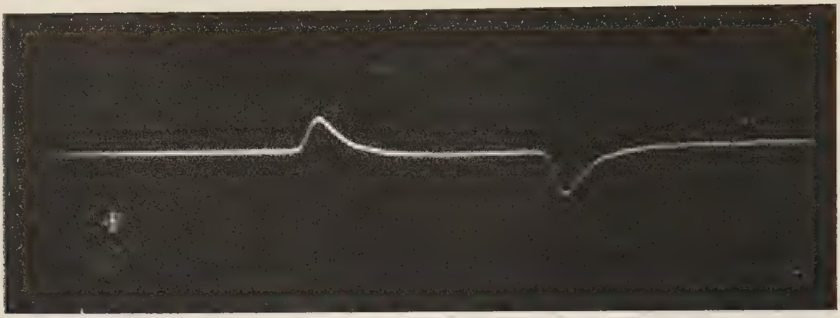

Fig. 3 *a*). – The first pulse comes from amplifier A_1 while the second, having an opposite sign, comes from amplifier A_2; the delay between the two pulses is greater than the artificially introduced delay (0.25 μs). The event is interpreted as due to the disappearance of a μ meson in the upper absorbers. The disappearance product activates only scintillation counters C_2.

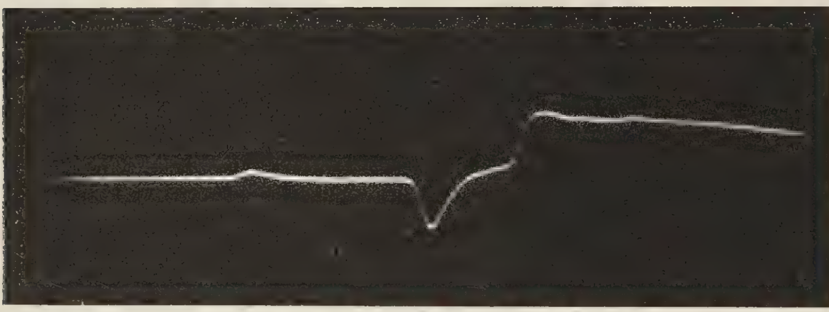

Fig. 3 *b*). – The first pulse coming from amplifier A_1 is followed by two pulses coming from A_2 and A_3 respectively. The delay between the last two pulses is that artificially introduced (0.25 μs). The delay between the pulse from A_1 and the pulses from A_2 and A_3 is, on the contrary, greater than the artificial delay. This event is interpreted as a disappearance of a μ-meson in upper absorbers. The disappearance product has activated counters C_2 and C_3.

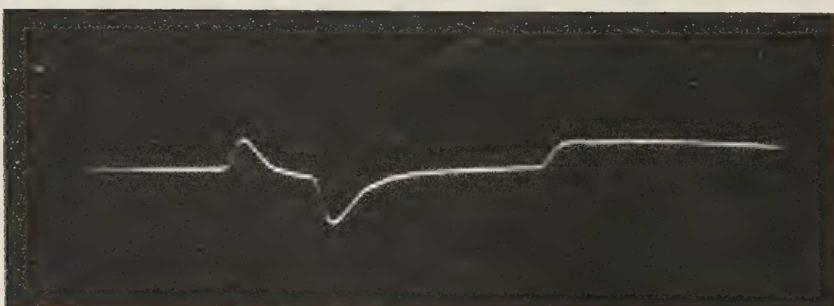

Fig. 3 *c*). – Two coincident pulses from A_1 and A_2 are artificially delayed of 0.25 μs. and are followed by a pulse from A_3 with a delay greater than the artificial delay. The event is interpreted as a disappearance of a μ-meson in lower absorbers. The disappearance product has activated scintillation counters C_3.

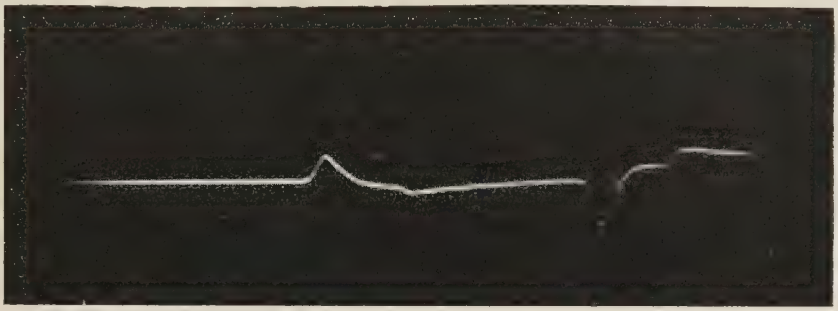

Fig. 3 *d*). – Two coincident pulses from A_1 and A_2 (the latter a very weak one) are artificially delayed, two coincident pulses from A_2 and A_3 follow. The event is interpreted as a disappearance of a μ-meson in one of the C_2 scintillation counters.

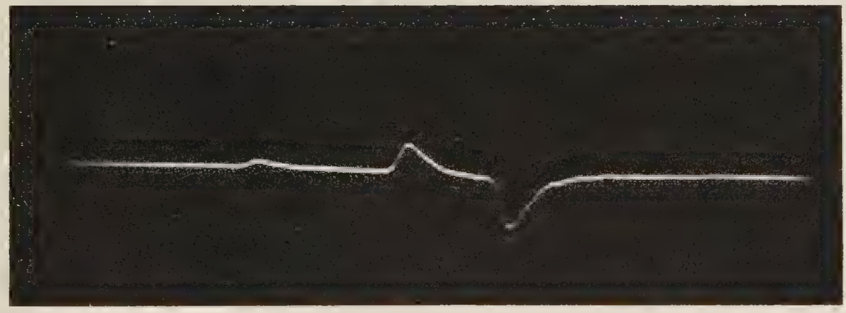

Fig. 3 *e*). – A pulse from A_1 is followed by two pulses from A_1 and A_2. The delay between the two pulses corresponds to the artificial delay. The event is interpreted as a disappearance of a μ-meson in one the C_1 counters.

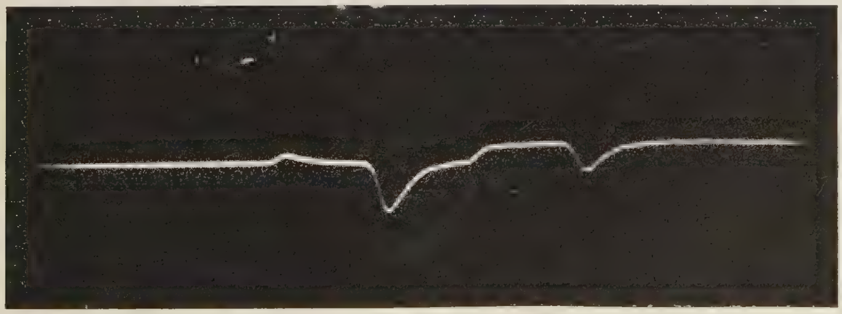

Fig. 3 *f*). – Three contemporary pulses from A_1, A_2, A_3 artificially delayed one in respect of the other. A pulse from A_2 follows, probably an afterpulse.

over, owing to photomultiplier afterpulses, it is absolutely necessary to discard events in which only one delayed pulse from a counter crossed by a meson is registered. It is well known, in fact, ([49,50]) that pulses produced by a photomultiplier excited by light are often followed by after-pulses with a delay within the range analyzed by ours apparatus (Fig. 3 *f*). Conversely, events of type I and II can be taken into account even when after-pulses appear; in this case, in fact, it is possible to measure the life time with no uncertainty in the choice of the pulses by considering the first of the two pulses coming from the same amplifier.

The events selected according to the principles described above have a frequency $f^- = 1.3/h$ for μ^- meson and $f^+ = 1.1/h$ for μ^+. A comparison between f^- and f^+ allows us to evaluate, for the meson, the ratio K between the recorded capture—and decay—events. In fact, if f_0^+ is the frequency for μ^+ mesons and f_0^- that for μ^- mesons stopped in the absorbers, and e_d and e_c are the detection efficiencies for decay—and capture—products respectively ($e_c/e_d = \alpha$), the following relations can be written:

$$
(4) \qquad \left\{
\begin{aligned}
f^+ &= f_0^+ e_d(\exp[-t_1/\tau_d] - \exp[-t_2/\tau_d])\,, \\
f^- &= f_0^-\{e_dR + e_c(1-R)\}(\exp[-t_1/\tau] - \exp[-t_2/\tau])\,,
\end{aligned}
\right.
$$

where R is the ratio previously defined in the introduction (for iron, $R=0.1$ ([13])) and t_1 and t_2 are the limits of the explored time interval ($t_1 = 5\cdot 10^{-8}$ s, $t_2 = 0.6$ μs). Substituting for τ the value found for the mean life and for τ_d the known value 2.22 μs one has

$$\exp[-t_1/\tau_d] - \exp[-t_2/\tau_d] = 0.22$$

$$\exp[-t_1/\tau] - \exp[-t_2/\tau] = 0.71$$

and from relation (4), with $f_0^+/f_0^- = 1.2$ (positive excess)

$$\alpha = \frac{e_c}{e_l} = 0.40\,\frac{f^-}{f^+} - 0.1\,.$$

Substituting the experimental values for f^- and f^+ one obtains

$$\alpha = \frac{e_c}{e_l} \simeq 0.4$$

([49]) Latest developments in scintillation counting, *Nucleonics*, **10**, 3, 33 (1952).
([50]) K. P. MEYER and A. MAIER: *Helv. Phys. Acta*, **27**, 1, 57 (1954).

and, consequently,

$$K = \alpha \frac{1-R}{R} \simeq 3.6 ,$$

which means that about three quarter of the recorded events are due to meson captures by nuclei. The distributions of the delays obtained for μ^- and μ^+ are reproduced in Fig. 4.

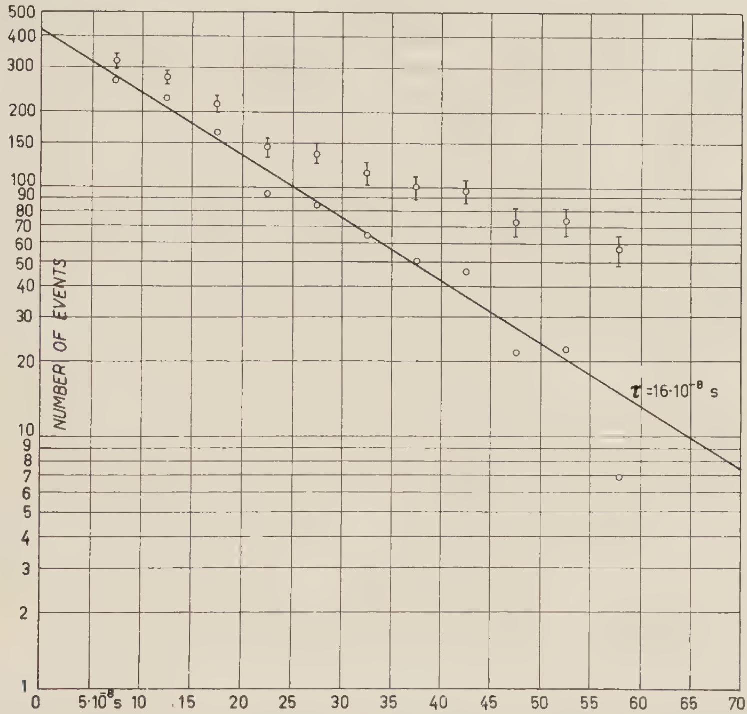

Fig. 4 a). – Points with error represent the observed number of μ^- mesons disappearing in Fe absorbers per $5 \cdot 10^{-8}$ s versus time; the total number of events is 1609. Points without error are obtained subtracting the background.

The fact that the distribution of the experimental points for μ^+-mesons is in good agreement with the mean life $\tau_d = 2.22$ μs, provides conclusive evidence for the efficiency of the apparatus both in separating mesons of opposite signs and in the measurement of time in the interval considered.

The distribution of the life times for μ^- mesons was used for the determination of the mean life τ. The number of recorded events with a delay greater than 0.4 μs is higher than what could be expected for the disappearance in the absorbers of μ^--mesons. This is very probably due to the disintegration

of the μ^--mesons in the lower part of the scintillation counters not recognized as such because the delayed pulse from the counter is of too small an amplitude, and the disintegration electron is recorded only by the underlying counter.

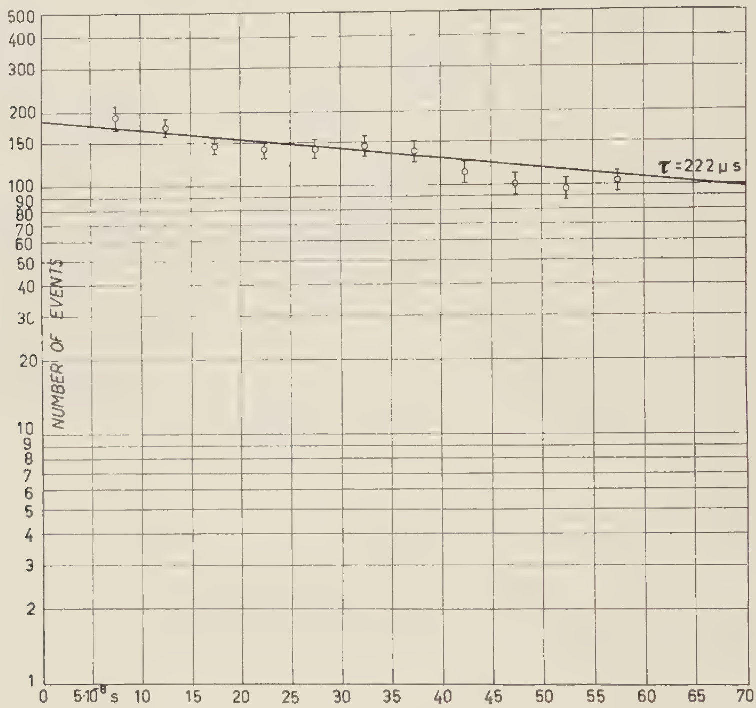

Fig. 4 *b*). – Observed number of μ^+ mesons decaying per $5\cdot10^{-8}$ s versus time. The total number of events is 1492.

Taking into account this background, which can reasonably be considered constant in the time considered, the following value for the mean life calculated according to PEIERLS [51] is obtained,

$$\tau = (16 \pm 1)\cdot 10^{-8}\ \text{s}\ .$$

Conclusion.

The value of the mean life τ of negative μ-mesons in iron determined by our method is practically coincident with the value obtained by KEUFFEL *et al.* $(16.3 \pm 2.7)\cdot 10^{-8}$ s [5]. Our determination, however, is statistically more

[51] R. PEIERLS: *Proc. Roy. Soc.*, A **149**, 467 (1935).

accurate. Moreover the probability p_c of capture of mesons in Fe calculated by equation (2) and (3) from our determination of the mean life is (assuming $\tau_d = 2.22\ \mu s$)

$$p_c = (58 \pm 4)\cdot 10^5\ s^{-1}$$

and is therefore higher than the value found by LEDERMAN *et al.* [13] $(44.3 \pm 3)\cdot 10^5\ s^{-1}$. The results of the two measurements, however, are not in disagreement.

Eventually the comparison of our value for p_c and the value calculated by the above mentioned Wheeler law ($\sim 50\cdot 10^5\ s^{-1}$) suggests that the meson capture by the iron nucleus is satisfactorily interpreted by this law, the validity of which is confirmed for values of $Z \leqslant 26$.

* * *

The authors are indebted to Prof. E. AMALDI for constant encouragement and constructive discussions and to Proff. E. PANCINI and M. L. SANDS for stimulating suggestions concerning the general design of the apparatus. Thanks are due to Dr. F. LEPRI for skilful collaboration in the design of some of the electronic circuits.

RIASSUNTO

Viene descritto un apparato per la determinazione delle vite medie dei mesoni μ negativi in elementi di medio ed elevato numero atomico. Dalla curvatura della traiettoria subita dai mesoni μ della radiazione cosmica in due blocchi di ferro magnetizzato ($B = 1.5\ \mathrm{Wb\ m^{-2}}$) si riconosce il segno dei mesoni incidenti. La curvatura è misurata da un odoscopio di 90 contatori di Geiger. Mediante un sincroscopio rapido vengono misurati i ritardi tra l'arrivo del mesone incidente e la sua susseguente scomparsa in assorbitori sia attraverso processi di cattura da parte dei nuclei che attraverso il normale processo di decadimento. L'incertezza nella lettura dei tempi è di $\sim 10^{-8}$ s. Dalla distribuzione di tali ritardi si determina direttamente la vita media del mesone nell'elemento di cui è costituito l'assorbitore. È stata eseguita una prima determinazione della vita media del mesone negativo nel ferro ottenendo il valore $\tau = (16 \pm 1)\cdot 10^{-8}$ s.

IL NUOVO CIMENTO Vol. VI, N. 5 1° Novembre 1957

Diffusione di radioelementi della famiglia del Th nelle emulsioni nucleari.

N. Marongiu

Istituto di Fisica dell'Università - Cagliari

(ricevuto il 27 Giugno 1957)

Riassunto. — Si descrive un nuovo caso di diffusione di atomi radioattivi nelle emulsioni nucleari. Dalle caratteristiche del fenomeno risulta la particolare importanza del trattamento subito dalla lastra, in relazione alla migrazione di atomi radioattivi di varie specie.

1. – Introduzione.

È noto che le misure di piccolissime quantità di radioelementi basate sul caratteristico fenomeno di formazione di stelle nelle emulsioni nucleari (1,2), richiedono che nel conteggio degli eventi in studio si debba tener conto delle stelle di data molteplicità dissociate in altre di molteplicità inferiore.

Nelle stelle da Ra e RdTh l'attenzione è stata principalmente rivolta alle dissociazioni la cui origine è legata ad un processo di diffusione degli atomi di Rn e Tn nella emulsione (*).

La particolare mobilità di cui sono dotati questi atomi deriverebbe dal fatto che essi sono chimicamente inerti (3,4); agli effetti della entità dei cammini percorsi il Rn è quindi notevolmente favorito rispetto al Tn, in virtù della sua vita media assai più elevata.

Il fenomeno risulta, in generale, influenzato dallo stato della gelatina del-

(1) N. Isaac e E. Picciotto: *Nature*, **171**, 742 (1953).

(2) E. Picciotto e S. Wilgain: *Nature*, **173**, 632 (1954).

(*) Una completa bibliografia sull'argomento è riportata nel lavoro di M. Debeauvais *et al.* (6).

(3) G. G. Eichholz e F. C. Flack: *Journ. Chem. Phys.*, **19**, 363 (1951).

l'emulsione ([4]) e dal trattamento subito dalla lastra ([5]), ma il fattore che ne controlla fortemente gli effetti è la temperatura alla quale avviene l'esposizione.

È risultato ([6]) che a — 85 °C la diffusione del Rn è praticamente arrestata, mentre per il Tn ciò avviene a — 36 °C.

Nella catena che si svolge a partire dal RdTh sono stati osservati, ma in numero pressochè trascurabile, anche altri tipi di dissociazioni ([6,7]): queste mostrano migrazioni del ThA e ThB (o ThC o ThC′).

Ci sembra interessante, perciò, riportare nella presente nota i risultati relativi ad un nuovo caso di dissociazione, i quali dimostrano che per un particolare stato dell'emulsione l'atomo di ThX diffonde facilmente in questa, in proporzione notevolmente superiore allo stesso atomo di Tn.

2. – Procedimento.

La raccolta degli eventi è stata effettuata nel corso di una esplorazione di lastre G5, da 400 μm, tenute per 120 giorni in un ambiente alla temperatura di 4 °C e umidità 30%.

Le lastre non furono preventivamente sottoposte ad alcun processo di arricchimento; le stelle analizzate sono quelle presenti come effetto di fondo, e pertanto estremamente diluite, nella massa dell'emulsione. Ciò facilita enormemente l'osservazione, in quanto ogni eventuale particolarità delle stelle è facilmente avvertita, e risulta quindi praticamente trascurabile la probabilità che quelle particolarità possano essere attribuite alla combinazione di processi multipli, non correlati, originatisi casualmente in punti vicini.

Complessivamente sono state raccolte 3890 stelle a cinque rami; su quelle mostranti un percettibile spostamento dei centri di disintegrazione furono effettuate, con ingrandimento 1300 ×, misure di lunghezza dei rami per un esatto riconoscimento delle stelle di molteplicità inferiore.

Il fattore di correzione per le misure di profondità fu preventivamente determinato utilizzando le tracce α del ThC′.

Si è tenuto conto solo degli spostamenti non inferiori ad 1 μm.

3. – Risultati.

I vari tipi di dissociazioni osservate risultano ripartiti come indicato nella Tabella.

([4]) L. Vigneron, R. Chastel and J. Genin: *Journ. Phys. et Rad.*, **14**, 288 (1953).
([5]) W. Schneider e T. Matisch: *Sitzber. österr. Akad. Wiss. Math. naturw. Klasse*, Abt. II*a*, **161**, 4, 131 (1952).
([6]) M. Debeauvais, E. Picciotto e S. Wilgain: *Nuovo Cimento*, **5**, 260 (1957).
([7]) P. Demers: *Phys. Rev.*, **72**, 536 (1947).

Nel simbolo S usato per contrassegnarli i numeri indicano il grado di molteplicità dei singoli eventi che entrano nelle combinazioni, nell'ordine secondo cui si svolge la catena delle disintegrazioni a partire dal RdTh.

S_5 è una stella a cinque rami non scissa; $S_{1,4}$ è la separazione: (RdTh) + + (ThX + Tn + ThA + ThC o ThC′); $S_{1,1,3}$ è la separazione: (RdTh) + (ThX) + + (Tn + ThA + ThC o ThC′); e così via.

Sono attribuite ad una diffusione del ThB tutte le dissociazioni in cui il ramo separato è costituito dalla traccia α del ThC o ThC′.

Evento	Atomo diffondente	Numero di eventi	Percentuale
S_5	—	1458	37.5
$S_{1.4}$	ThX	1351	34.7
$S_{1.1.3}$	ThX, Tn	752	19.3
$S_{2.3}$	Tn	228	5.9
$S_{1.1.2.1}$	ThX, Tn, ThB	17	0.4
$S_{1.3.1}$	ThX, ThB	30	0.8
$S_{4.1}$	ThB	54	1.4

Risulta che, in rapporto al numero delle stelle osservate, si hanno diffusioni del ThX nella percentuale del 55,2 %, contro il 25,6 % ed il 2,6 % per il Tn ed il ThB rispettivamente.

4. – Conclusione.

Nelle emulsioni trattate con soluzioni di $Th(NO_3)_4$ può verificarsi [6,7] che il ThA ed il ThB diffondano, mentre il ThX, nonostante la sua vita media relativamente lunga, resta completamente fissato.

I presenti risultati mostrano d'altra parte che nelle emulsioni non trattate si può avere una notevole diffusione da parte degli atomi di ThX.

Uno studio approfondito del fenomeno richiederebbe un'analisi correlata tra le medie dei percorsi di migrazione dei diversi atomi diffondenti e le vite medie di questi, tenuto conto eventualmente di un opportuno coefficiente di diffusione caratteristico per ciascuna specie di nuclide e per un dato tipo di emulsione.

Nelle condizioni sperimentali da noi adottate ciò non è possibile, in quanto il massimo percorso di migrazione apparente per il ThX è risultato pari a 30 μm, distanza maggiore della lunghezza della traccia α del RdTh di cui non può pertanto stabilirsi l'origine.

Ci sembra tuttavia che del fenomeno segnalato debba tenersi giusto conto

nel quadro delle indagini sulle cause relative alla migrazione degli atomi radioattivi nelle emulsioni secche.

* * *

Ringrazio sentitamente il Prof. G. FRONGIA per l'interesse con cui ha seguito il presente lavoro.

SUMMARY (*)

We give a description of a new case of diffusion of radioactive atoms in nuclear emulsions. The phenomenic characteristics of the case prove the particular importancs of the plate's treatment in relation with migration of radioactive atoms of varioue kinds.

(*) *Editor's Translation.*

IL NUOVO CIMENTO Vol. VI, N. 5 1° Novembre 1957

Beta-Gamma Directional Correlation in ^{170}Tm.

G. Bertolini (*), E. Lazzarini and M. Mandelli Bettoni

Istituto di Fisica Sperimentale del Politecnico - Milano

(ricevuto il 6 Luglio 1957)

Summary. — The existence has been confirmed of angular correlation between the β-rays belonging to decay of 889 keV maximum energy of ^{170}Tm and the 84 keV γ-rays of ^{170}Yb. The differential angular correlation has been measured. By means of a β magnetic spectrometer and β-γ coincidences the shape of the low energy β spectrum of ^{170}Tm has been studied. The results are in agreement with an assignment 1 — to the ground state of ^{170}Tm. Under this hypothesis we have found the ratios of nuclear matrix elements effective in the β transition which were in best agreement with the experimental data.

1. – Introduction.

Beta-gamma angular correlation in ^{170}Tm between the lower energy β-spectrum and the subsequent γ-ray (Fig. 1) has been subject to three experimental measurements. Novey first [1] reported an anisotropy in the β-γ angular correlation. Assuming the correlation function $W(\theta) = 1 + a(E)\cos^2\theta$ he obtained $a = -0.259 \pm 0.053$ for β-particles of energy ranging between ~ 150 keV and the end point. However, as the same author points out, the scattering of the electrons in the air can distort this result as the experiment was not carried out in vacuum. Moreover about 24% of the electromagnetic radiation of ^{170}Tm not absorbed in the 1 g/cm² copper absorber over the γ counter was due to K-X-rays isotropically correlated with the continuous spectrum electrons. In a later work [2] Novey shows that the asimmetry might be due in part to coincidences between β-rays and inner bremsstrahlung.

(*) Now at CISE Laboratories, Milan.

(1) T. B. Novey: *Phys. Rev.*, **78**, 66 (1950).

(2) T. B. Novey: *Phys. Rev.*, **84**, 145 (1951).

SIEGBAHN (3) finds no anisotropy in the angular correlation between L-conversion electrons of the 84 keV γ-rays and β-rays. Given the very low energy of the L-conversion electrons ($\sim$ 74 keV) a strong scattering in the source, whose thickness was 0.1 mg/cm², cannot be excluded.

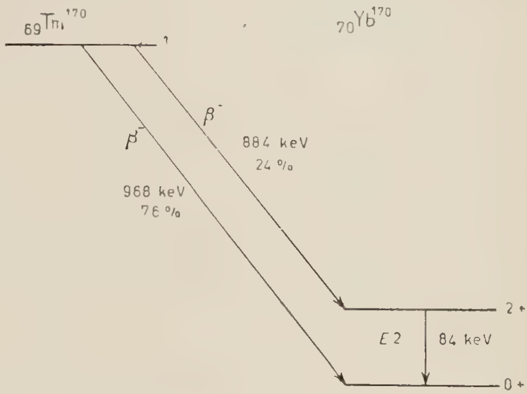

Fig. 1. – Decay scheme of ^{170}Tm.

In the third measurement of this correlation, H. ROSE (4), analizyng the continuous β-spectrum with a magnetic β-spectrograph and detecting the γ-rays with a scintillation counter, measured the β-γ angular correlation for various energy electrons and found a value of $a(E_{\max}) = \sim - 0.3$. In this experiment too, electrons scattering in the source (1 mg/cm²) would be expected to distort the correlation.

A detailed discussions of the β-γ correlation of ^{170}Tm has been presented by FUYITA and coll. (5). They found that both the β-γ angular correlation and the allowed shape of the β-spectrum could be explained by the linear combination of the first forbidden nuclear matrix elements $m(\beta r)$, $m(\beta\alpha)$ and $m(\beta\sigma\times r)$ in ST type interaction of the Fermi theory of the β-decay. The decay ^{170}Tm $\rightarrow$ ^{170}Yb can be explained as occurring between states

$$(1\,-) \xrightarrow{\beta} (2\,+) \xrightarrow{\gamma} (0\,+)\,.$$

As there was little agreement between the results, a further investigation on the shape of the lower β-decay and on the β-γ differential correlation of ^{170}Tm was carried out.

2. – Sources.

The source for the analysis of the β-spectrum was prepared from a solution of $TmCl_3$ with the method of Schafer and Harkev (6) and the uniformity of the active layer was verified with the autoradiographic method. The thickness

(3) K. SIEGBAHN: *Ark. for Phys.*, **4**, 223 (1952).
(4) H. ROSE: *Phil. Mag.*, **43**, 1146 (1952).
(5) J. FUYITA, M. MORITA and M. YAMADA: *Prog. Theor. Phys.*, **11**, 219 (1954).
(6) N. J. SCHAFER and D. HARKRV: *Journ. App. Phys.*, **13**, 427 (1942).

2967

of the source was evaluated at $\sim 14\ \mu g/cm^2$ and the backing consisted of nylon film of $0.1\ mg/cm^2$.

The sources for the β-γ angular correlation were prepared from $TmCl_3$ through electrodeposition of ^{170}Tm on thin copper foil ($\sim 0.5\ mg/cm^2$ thick). The diameter of the sources was about 4 mm.

3. – β-Spectrum.

An intermediate image β spectrometer was used in the investigations involving the spectral shape determination of ^{170}Tm. The lower energy spectrum was observed in a conventional β-γ coincidence arrangment described in a preceding paper (7). The Fermi plot of the gross spectrum and the coincidence spectrum are shown in Fig. 2.

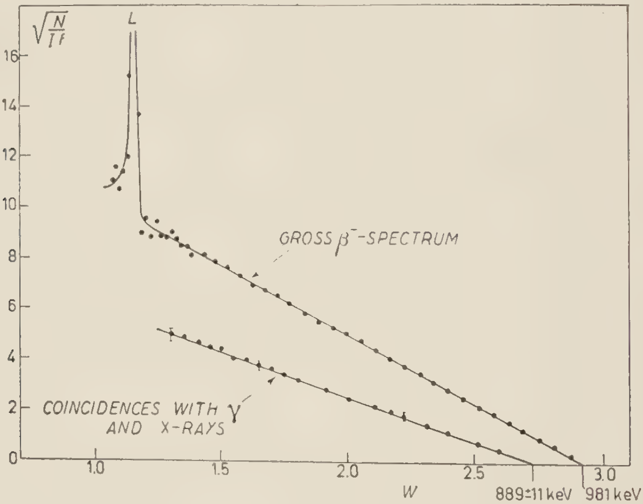

Fig. 2. – Fermi plot of total β-spectrum of ^{170}Tm and Fermi plot of the β-spectrum in coincidence with 84 keV γ-rays.

From the coincidence spectrum it can be deduced that the shape of the spectrum allowed is at least as far as 150 keV. On the coincidence spectrum the standard deviation is indicated by vertical bars.

4. – β-γ-angular correlation.

An anthracene crystal 1 in. in diameter and 0,3 in. high, in optical joint with an EMI 6262 photomultiplier, was used to detect the β-particles. The

(7) G. BERTOLINI, M. BETTONI and E. LAZZARINI: *Nuovo Cimento*, **10**, 273 (1955)

2968

scattering of the electrons in the air was avoided by placing source and detector in a vacuum as shown in Fig. 3.

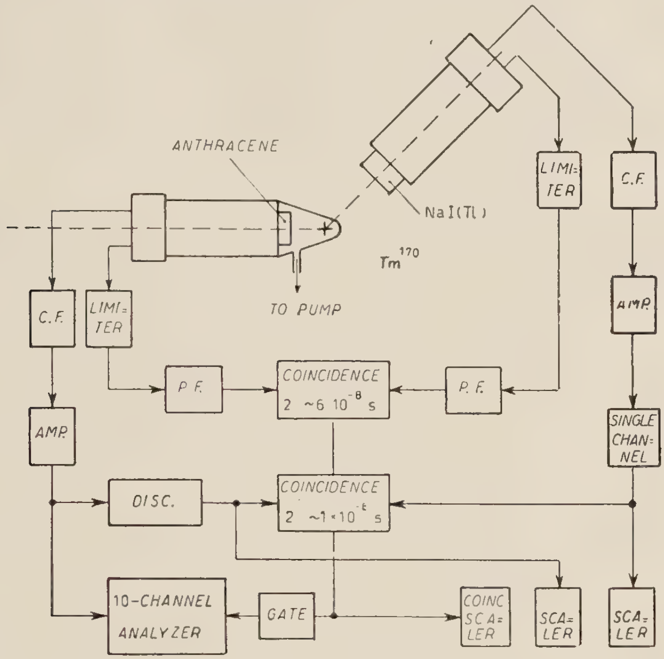

Fig. 3. – Block diagram of the experimental apparatus.

The γ detector consisted of an 1 in. × 1 in. Na(Tl) cylindrical crystal mounted on another EMI 6262 photomultiplier. The spectrum is shown in Fig. 4. A 7 mm thick polythene absorber in front of the crystal absorbed the electrons. The pulses from the anodes of the two photomultipliers were fed into a conventional fast-slow coincidence apparatus as shown in Fig. 3. A ten channel device ([8]) analyzed the pulses from the continuous spectrum gated from the triple coincidences.

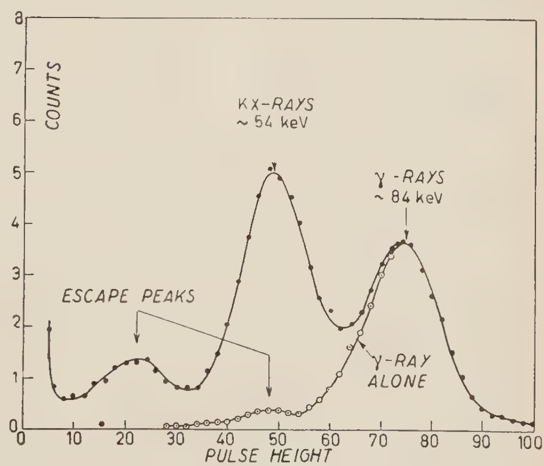

Fig. 4. – γ-spectrum of ^{170}Tm.

([8]) E. Gatti: *Nuovo Cimento*, **11**, 153 (1953).

In the γ-channel a differential discriminator provided the γ or X-rays selection. The energy calibration of the β-analyser was based on the 624 keV conversion line of ^{137}Ba and on the Compton distribution of γ-rays of 0.279 MeV (^{203}Hg), 0.511 (^{22}Na), 0.661 MeV (^{137}Cs), 0.89 and 1.12 MeV (^{46}Sc). For the anthracene crystal a linear relationship between pulse amplitude and β energy was assumed to hold above 200 keV (Fig. 5). The resolution for the conversion line of ^{137}Ba (624 keV) was $\sim 10\%$.

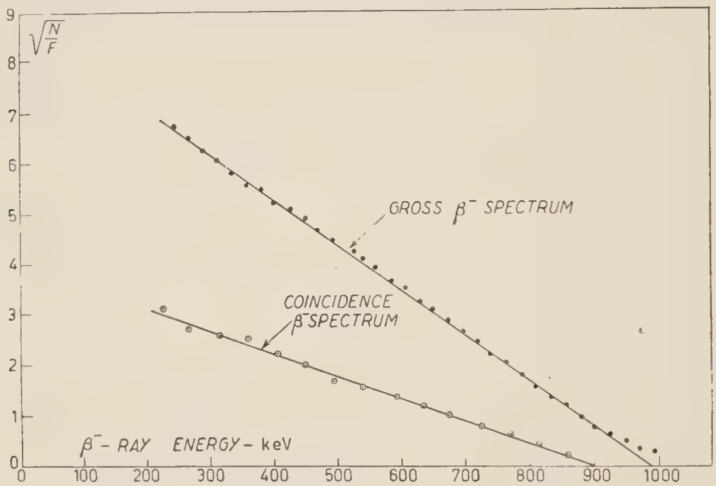

Fig. 5. – Fermi plot of the β-spectrum in coincidence with 84 keV γ-rays with the anthracene crystal.

The β-γ correlation was examined in ~ 70 keV increments of β energy with a channel width of 40 keV. At each energy the anisotropy was measured scanning the sequence 90°, 100°, 270° forward and backward counting 90 minutes at each angle. A total of about 120 000 genuine coincidences was obtained. The measurement of the anisotropy was carried out with two different sources of the same mean thickness of ~ 40 μg/cm^2, in order to reveal a possible anisotropy due to a non uniformity of the source. The two measurements gave the same results within the experimental errors.

To be sure that the experimental apparatus did not give a non-existent correlation, the differential anisotropy between continuous β-spectrum of ^{170}Tm and K-X-rays due to internal conversion of ^{170}Yb was examined with one of the sources used for the correlation. This correlation, as is known, must be isotropic, and it was proved to be so (Table I).

Fig. 6 presents the experimental results of the anisotropy $a(E)$ as a function

TABLE I.

Electron energy	200	280	360	450	520	580	640	700	Total
a	1.022 $\pm$.005	1.003 $\pm$.003	1.012 $\pm$.013	.982 $\pm$.012	.978 $\pm$.005	1.014 $\pm$.012	1.000 $\pm$.019	.991 $\pm$.031	1.001 $\pm$0.001

of the β-energy in keV. The experimental points have been corrected for the finite angular resolution with the method suggestes by FRANKEL [9].

No correction for the finite width of the pulse analyser and for the back-scattering of the electrons from the crystal has been carried out. This correction is expected to be lower than 2% above 200 keV and therefore within our experimental errors. The contribution to β-γ coincidences due to inner bremsstrahlung has been verified to be negligible.

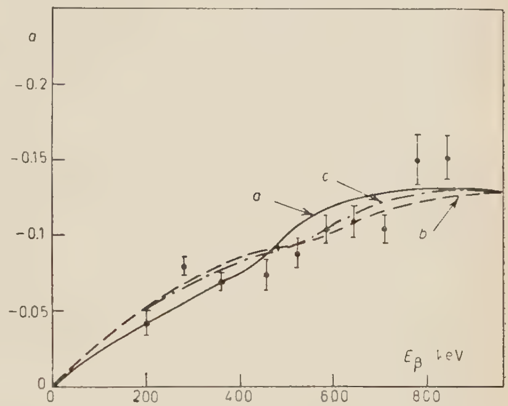

Fig. 6. Experimental points of the angular correlation coefficient $a(E)$. The lines represent the angular correlation function for (1—) (2+) (0+) in the case of three linear combination of the nuclear matrix elements effective in the transition: $z=-0.5$ $x=0.41$ (a line); $z=0$, $x=0.37$ (b line); $z=0.5$, $x=0.32$ (c line).

The observed β-γ directional correlation as a function of the β-energy in ^{170}Tm has been compared with the theoretical expression given by FUYITA and coll. [5]. From this comparison the ratios of nuclear matrix elements effective in the β-transition are obtained. Introducing the x, y and z parameters as defined by FUYITA and coll. the angular correlation coefficient $a(E)$ best agreeing with the experimental data has been found to be for the pair of values $z=-0.5$, $x=0.41$, $z=0$, $x=0.37$ and $z=0.2$, $x=0.32$ in the hypothesis of a spin and parity sequence (1 —) (2+) (0+).

A comparison of our results with the previous experimental data shows that our anisotropy is lower than that found by NOVEY and ROSE. It is difficult to understand such difference inasmuch as the source of ROSE was ~ 25 times thicker than ours while NOVEY measured the correlation in the air, two conditions that would have caused a reduction of the correlation. More-

(9) S. FRANKEL: *Phys. Rev.*, **83**, 673 (1951).

over, it was ascertained during the measurement of the angular efficiency of the detector, determined by a well collimated γ-ray beam from a strong ^{170}Tm source in vacuum, that a 5 mg/cm^2 alluminium foil placed at the end of the collimator was enough to eliminate the collimation of the electron beam.

In conclusion, the existence of an angular correlation in ^{170}Tm decay was confirmed, though an uncertainty about the anisotropy value remains. It is pointed out that all the measurements have been carried out with a coincidence apparatus of $\sim 6\ 10^{-8}$ resolving power, and some reduction of angular correlation may have occurred in our measurements on account of the long life of the first excited level of ^{170}Yb (about $1.5 \cdot 10^{-9}$ s). Moreover one should keep in mind that the possibility of a perturbation by the chemical nature of the source cannot be excluded and also that in the mentioned works the chemical form of the sources used is not specified.

* * *

Thanks are due to Prof. G. BOLLA, Director of the Institute, for his constant encouragement.

RIASSUNTO

Con uno spettrografo magnetico e coincidenze β-γ è stata studiata la forma dello spettro β del ^{170}Tm di energia massima 889 keV. È stata confermata l'esistenza di una correlazione fra gli elettroni appartenenti al decadimento di energia massima 889 keV e i raggi γ di 84 keV del ^{170}Tm con l'uso di rivelatori a scintillazione. I risultati ci permettono di attribuire spin e parità 1 — allo stato fondamentale del ^{170}Tm. In questa ipotesi sono stati ricavati i miscelamenti degli elementi di matrice della transizione β che meglio interpretano i risultati sperimentali.

IL NUOVO CIMENTO Vol. VI, N. 5 1° Novembre 1957

The Effect of the Angular Variation of Intensity on Scattering Distributions of μ-Mesons Underground at a Depth of 40 m w.e.

J. E. Cousins, W. F. Nash and A. J. Pointon

Physical Laboratories, University of Nottingham

(ricevuto il 9 Luglio 1957)

Summary. — The interpretation of experiments carried out underground to investigate the large angle scattering of μ-mesons depends on the assumed form of the underground spectrum and the geometrical bias introduced by the counter selection system. The form of the angular variation of intensity at 40 m w.e. has been obtained. The effect of introducing this into the calculation of the geometrical correction factors is discussed. It is shown that previous workers who assumed normal incidence of all particles have underestimated the expected number of large angle scatters.

1. – Introduction.

Experiments carried out to investigate the scattering of μ-mesons in absorbers have indicated that the large angle scattering can not be interpreted purely in terms of Coulomb interactions (for summary see Lloyd and Wolfendale (1)). In experiments performed underground it is necessary to know the spectrum of the μ-mesons undergoing scattering in the apparatus. Two main factors affect this spectrum; namely the momentum spectrum underground and the limitations imposed by the geometry of the apparatus. The appropriate momentum spectrum to be used has already been considered by Nash and Pointon (2) and it is the purpose of this paper to consider the second factor.

(1) J. L. Lloyd and A. W. Wolfendale: *Proc. Phys. Soc.*, A **68**, 1045 (1955).
(2) W. F. Nash and A. J. Pointon: *Proc. Phys. Soc.*, A **69**, 725 (1956).

Since in the experiments of GEORGE, REDDING and TRENT (3), MCDIARMID (4), NASH and POINTON (to be published), and others, only the projected angles of scattering were measured, the limitations imposed by the geometry of the counter system depend on the theoretical scattering distribution used. This may be seen as follows, the total angle of scattering, α, is composed of the projected angle, φ, and the perpendicular projection, ψ. Thus the acceptance, by the counter system, of a particle scattered through a projected angle φ will depend on the acceptance of the corresponding angle ψ and hence the observed distribution in φ will depend on the allowable distribution in ψ. Thus the resulting correction to be applied to the distribution in φ will depend on the chosen theoretical scattering distribution.

Corrections for this effect have been made by previous workers but they assumed that all the particle were incident vertically. The effect of including angular distribution of the particles shows that previous correction factors have underestimated the expected number of large angle scatters.

2. – The angular distribution of the underground particles.

To perform a calculation of this nature, the form of the angular distribution of the underground particles will be required. The situation at 40 m w.e. has been considered since this is the depth at which NASH and POINTON have carried out their observations, and lies within the range in which most experiments have been performed, namely between 23 and 60 m.w.e.

In order to calculate the variation of the intensity of μ-mesons underground with angle of incidence and momentum, it is first necessary to consider the situation at sea level. Since we will be considering the variation at a depth equivalent to 40 m of water, only momenta greater than about 8 GeV/c at sea level are of direct interest.

Various experimenters have shown that the variation of intensity « I » with the angle of inclination to the vertical « θ », for the whole of the penetrating component can be expressed in the form

$$I = I_0 \cos^n \theta ,$$

where I_0 is the vertical intensity at sea level and « n » has a value close to 2; e.g. GREISEN (5) gives $n = 2.1$. Counter experiments on low momentum me-

(3) E. P. GEORGE, J. L. REDDING and P. T. TRENT: *Proc. Phys. Soc.*, A **66**, 533 (1953).

(4) I. B. MCDIARMID: *Phil. Mag.*, **45**, 933 (1954); **46**, 177 (1955).

(5) K. GREISEN: *Phys. Rev.*, **61**, 212 (1942).

sons have been performed by KRAUSHAAR ([6]), ZAR ([7]), and QUERCIA and RISPOLI ([8]); these have shown that values of « n » of the order 3 are obtained. BUDINI and MOLIÈRE ([9]) have calculated « n » as a function of momentum for μ-mesons and part of their curve is shown in Fig. 1. At present, experimental comparison can only be made satisfactorily using the results of MORONEY and PARRY ([10]) who assumed the validity of the $\cos^n \theta$ form for individual momenta and determined the various values of « n ». They found that for 10 GeV/c mesons, $n = 0.95$ and 1.25 in the eastern and western azimuths respectively. The mean value is plotted in Fig. 1. These experimental results are based on measurements in the vertical direction and at angles of 30° and 60° only in each azimuth. The sparse experimental data available are in fair agreement with the curve in Fig. 1. Values of « n » are taken from this curve in the following calculations.

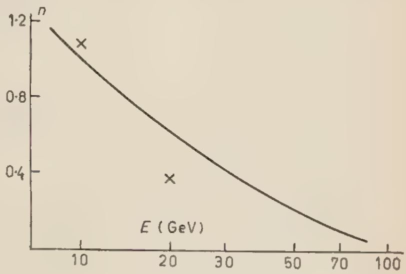

Fig. 1.

To obtain the intensity of the underground particles of any particular momentum value arriving at a given angle to the vertical, the value of the momentum of the particles at sea level was calculated assuming a constant energy loss. NASH and POINTON ([2]) found that, at 40 m w.e., the vertical spectrum could be derived from the sea level spectrum assuming a constant average energy loss of 2.3 MeV g/cm² for particles arriving underground in the range 0.3÷1.5 GeV/c, which is in good agreement with the value obtained from a range-energy relationship of the type given by GEORGE ([11]). The intensity at sea level was then calculated using the differential spectrum of HOLMES *et al.* and the curve of Fig. 1. Calculations were made up to 45° and it was found that the $\cos^n \theta$ form was valid. The form of the variation of « n » is shown in Fig. 2.

These results do not take into account scattering in the 40 m v.e. of rock. Calculations have been performed taking into account the effect of scattering using the expression given by ROSSI and GREISEN (1941) and assuming that the rock has an average atomic number 10 and atomic weight 20. At the lowest momentum considered, 0.5 GeV/c, it was found that the scattering

([6]) W. L. KRAUSHAAR: *Phys. Rev.*, **76**, 1045 (1949).
([7]) J. L. ZAR: *Phys. Rev.*, **83**, 761 (1951).
([8]) I. F. QUERCIA and B. RISPOLI: *Nuovo Cimento*, **10**, 357 (1953).
([9]) P. BUDINI and G. MOLIÈRE: *New Research Techniques in Physics*, (1952), pag. 59.
([10]) J. R. MORONEY and J. K. PARRY: *Aust. Journ. Phys.*, **7**, 423 (1954).
([11]) E. P. GEORGE: *Progress in Cosmic Ray Physics*, I (Amsterdam, 1952).

increased the intensity at 45° to the vertical by 4% and decreased the vertical intensity by 1%. It can therefore be seen that above 1.5 GeV/c the effect will be negligible at this depth.

It may also be noted that, since at sea level « n » varies only slowly at high momenta, the underground variation of intensity for a particular momentum « p » with « θ » will be nearly of the form

$$I(p, \theta) \simeq \frac{1}{(p + P_h/\cos\theta)^3} \cdot \cos^n \theta \,,$$

where $P_h = 9.2$ GeV/c at 40 m w.e. and « n » can be taken as the value for the momentum $p + \frac{1}{2}(P_h + P_h/\cos\theta)$ at sea level. So for $p \gg P_h/\cos\theta$ the value of « n » approaches the sea level value. This tendency is shown in Fig. 2.

Finally, the value of « n » for all μ-mesons with momentum greater than 0.5 GeV/c was calculated and found to be 1.8. This may be compared with the experimental results at similar depths of FOLLET and CRANSHAW ([12]) and GEORGE and SHRIKANTIA ([13]). FOLLET and CRANSHAW using a counter arrangement found that $n = 2$; while using nuclear emulsion at 57 m w.e. GEORGE and SHRIKANTIA found that $n = 2.7 \pm 0.25$ for slow particles and $n = 1.7 \pm 0.2$ for fast particles. This value for fast particles is close to our calculated value for momenta greater than 0.5 GeV/c at 40 m w.e. as would be expected. The validity of Fig. 2 has been assumed in the following discussion.

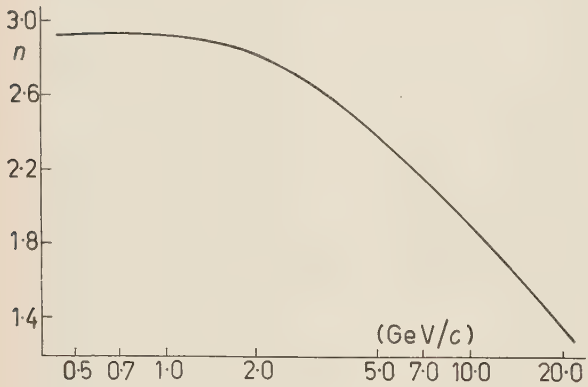

Fig. 2.

3. – Corrections to the theoretical scattering distributions.

The required correction function is composed of two parts which will be termed $c_1(\varphi)$ and $c_2(\varphi)$. $c_1(\varphi)$ is the correction imposed by the geometry of the system in the plane of observation of the angles (the front plane) and gives

([12]) D. H. FOLLET and J. D. CRAWSHAW: *Proc. Roy. Soc.*, A **155**, 546 (1936).
([13]) E. P. GEORGE and G. S. SHRIKANTIA: *Nuclear Physics*, **1**, 54 (1956).

the probability that, if there is no limitation imposed other than in the plane of observation, an angle of scatter φ will be observed. $c_2(\varphi)$ is the corresponding function perpendicular to the plane of observation.

A schematic representation of the type of arrangement considered is shown in Fig. 3 *a*).

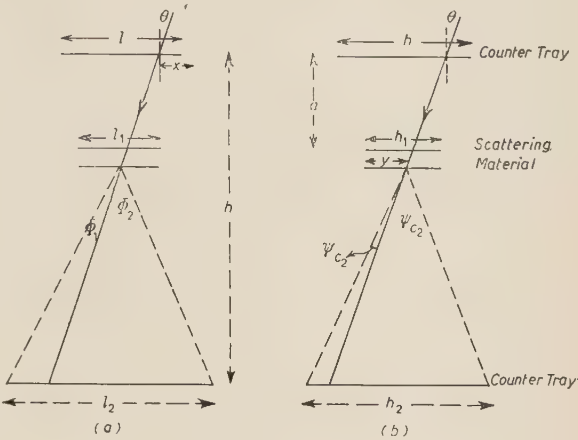

Fig. 3.

3·1. *Calculation of* $c_1(\varphi)$. – If a particle is incident on the apparatus at an angle θ, and is scattered through an angle φ, then a length, b, of the top counter tray, total length l, may be found such that if the particle is incident in this length it will also cross the bottom tray l_2.

From the preceeding section it can be seen that the probability that a particle will be incident between θ and $\theta+\mathrm{d}\theta$ to the vertical is approximately proportional to $\cos^2\theta\,\mathrm{d}\theta$. This will be adopted at present to maintain an analytic form independent of the momentum of the particle. Then the relative probability for observing the angle φ is given by $(b\cos^2\theta\,\mathrm{d}\theta)/l$. The total relative probability of observing φ is,

$$P(\varphi) = \frac{1}{2}\int_0^{\mathrm{tg}^{-1}(l+l_1)/2a} \frac{b}{l}\cos^2\theta\,\mathrm{d}\theta\,, \tag{1}$$

and

$$c_1(\varphi) = P(\varphi)/P(\varphi=0)\,.$$

Hence, by numerical integration, the value of $c_1(\varphi)$ may be determined for any value of φ.

3·2. *Calculation of* $c_2(\varphi)$. – Let $f_1(\alpha)\,\mathrm{d}\alpha$ be the probability that a given particle will be scattered through a total angle α to $\alpha+\mathrm{d}\alpha$. The projected angles φ and ψ are small and obey the relationship $\alpha^2=\varphi^2+\psi^2$.

Let $f_2(\alpha)\,\mathrm{d}\alpha$ be the distribution of α given by averaging the function $f_1(\alpha)\,\mathrm{d}\alpha$ over the momentum spectrum of the observed particles. Then, if there is no limitation on either φ or ψ the probability that angle φ to $\varphi+\mathrm{d}\varphi$ will be ob-

served is

$$(2) \qquad f_3(\varphi)\,\mathrm{d}\varphi = 4\int\limits_{\psi=0}^{\psi=\infty} \frac{f_2(\alpha = (\varphi^2+\psi^2)^{\frac12})}{2\pi(\varphi^2+\psi^2)^{\frac12}}\,\mathrm{d}\varphi\,\mathrm{d}\psi\,,$$

(where the factor 4 appears because four quadrants are considered and it is assumed that the solid angle $2\pi\sin\alpha\,\mathrm{d}\alpha$ may be written $2\pi\alpha\,\mathrm{d}\alpha$). Again geometry limits ψ as will be seen in Fig. 3 *b*). Thus for any particular position the probability distribution of the angles φ will be,

$$(3) \qquad f_4(\varphi)\,\mathrm{d}\varphi = \frac{2}{\pi}\,\mathrm{d}\varphi\left[\int\limits_0^{\psi_{c_1}} \frac{f_2(\alpha=(\varphi^2+\psi^2)^{\frac12})}{(\varphi^2+\psi^2)^{\frac12}}\,\mathrm{d}\psi + \int\limits_0^{\psi_{c_2}} \frac{f_2(\alpha=(\varphi^2+\psi^2)^{\frac12})}{(\varphi^2+\psi^2)^{\frac12}}\,\mathrm{d}\psi\right],$$

or, where the angle of incidence θ is such that the limiting angles ψ_{c_1} and ψ_{c_2} are in the same direction and $\psi_{c_2} > \psi_{c_1}$

$$(4) \qquad f_4(\varphi)\,\mathrm{d}\varphi = \frac{2}{\pi}\,\mathrm{d}\varphi\int\limits_{\psi_{c_1}}^{\psi_{c_2}} \frac{f_2(\alpha=(\varphi^2+\psi^2)^{\frac12})}{(\varphi^2+\psi^2)^{\frac12}}\,\mathrm{d}\psi\,.$$

For Molière's theory $f_2(\alpha)$ may be replaced at angles greater than 4°, with sufficient accuracy, by a function of the form R/α^3 ,where R is a constant. Hence

$$(5) \qquad f_4(\varphi)\,\mathrm{d}\varphi = \frac{R\,\mathrm{d}\varphi}{\pi\varphi^3}\left[\left(\mathrm{tg}^{-1}\frac{\psi_{c_2}}{\varphi} + \frac{\psi_{c_2}\varphi}{(\varphi^2+\psi_{c_2}^2)^{\frac12}}\right) \pm \left(\mathrm{tg}^{-1}\frac{\psi_{c_1}}{\varphi} + \frac{\psi_{c_1}\varphi}{(\varphi^2+\psi_{c_1}^2)^{\frac12}}\right)\right].$$

If there were no limits imposed on ψ_{c_1} and ψ_{c_2} then the distribution in φ would be $f_4(\varphi;\,\infty)\,\mathrm{d}\varphi$ which is given by

$$f_4(\varphi;\,\infty)\,\mathrm{d}\varphi = R\,\frac{\mathrm{d}\varphi}{\varphi^3}\,.$$

Then the correction is given for any set of values ψ_{c_1} and ψ_{c_2} by

$$(6) \qquad P(\varphi) = \frac{f_4(\varphi)}{f_4(\varphi;\,\infty)} = \frac{1}{\pi}\left[\left(\mathrm{tg}^{-1}\frac{\psi_{c_2}}{\varphi} + \frac{\psi_{c_2}\varphi}{(\varphi^2+\psi_{c_2}^2)^{\frac12}}\right) \pm \left(\mathrm{tg}^{-1}\frac{\psi_{c_1}}{\varphi} + \frac{\psi_{c_1}\varphi}{(\varphi^2+{}^{2}_{c_1}\psi)^{\frac12}}\right)\right].$$

The probability that a given set of values ψ_{c_1} and ψ_{c_2} will occur is the probability that a particle will be incident at an angle θ to $\theta+\mathrm{d}\theta$ in a distance

y to $y+dy$ along the scattering material and is given by $K_1(dy/h_1)\cos^2\theta\,d\theta$ where h_1 is the length of the scattering material in the plane considered. Thus the relative correction factor for any given values of ψ_{c_1} and ψ_{c_2} and hence for given values of y and θ is

$$K_1 P(\varphi; y, \theta)\,\frac{\cos^2\theta}{h_1}\,d\theta\,dy\,,$$

where $P(\varphi; y, \theta)$ is given by (6) with

$$\psi_{c_1} = \mathrm{tg}^{-1}\left(\frac{(h_2-h_1)/2+y}{L-a}\right)-\theta\,,$$

$$\psi_{c_2} = \mathrm{tg}^{-1}\left(\frac{(h_1+h_2)/2-y}{L-a}\right)+\theta\,.$$

The total correction function $c_2(\varphi)$ is given by

$$c_2(\varphi) = \frac{k_2}{h_1}\int\limits_{y=0}^{h_1}\;\int\limits_{\theta=0}^{\mathrm{tg}^{-1}(h_1+h)/2a} P(\varphi; y, \theta)\cos^2\theta\,d\theta\,dy\,, \tag{7}$$

where k_2 is a geometrical constant.

A numerical integration of equation (7) will give the value of $c_2(\varphi)$ for any specific value of φ.

Similarly the value of $c_2(\varphi)$ was calculated for Olbert's theory with $f_2(\alpha)$ approximated to the form R/α^7 but the difference between the value found for this form and that found for Molière's theory is negligible. As an indication of the numerical importance of this type of calculation values used in an arrangement by NASH and POINTON have been adopted in which $l=l_1=22.5$ cm, $l_2=41.5$ cm, $h=h_1=6.75$ cm, $h_2=10.5$ cm, $a=16.70$ cm and $L=106$ cm. The value of the correction factor $c_1(\varphi)c_2(\varphi)$ is shown in Fig. 4 as a function of φ both for a $\cos^2\theta$ distribution and for normal incidence ($\theta=0$).

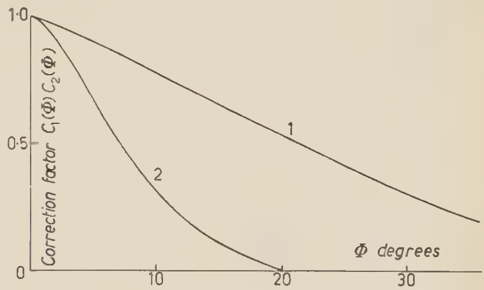

Fig. 4.

4. – Discussion.

The calculations would be most accurate if the actual value of « n » for each value of $p\beta$ was used. However, values of $c_1(\varphi)c_2(\varphi)$ have been calculated on the assumption that the total intensity varies with incident angle, θ, as $\cos\theta$, $\cos^3\theta$ and $\cos^6\theta$ and the results are shown in the following table, together with the results obtained above for a $\cos^2\theta$ distribution.

TABLE I.

φ	$c_1(\varphi)\, c_2(\varphi)$			
	$\cos\theta$	$\cos^2\theta$	$\cos^3\theta$	$\cos^6\theta$
0°	1	1	1	1
5	0.905	0.900	0.900	0.889
10	0.797	0.782	0.774	0.736
15	0.682	0.657	0.638	0.568
20	0.572	0.526	0.504	0.415

It is seen that any error introduced by the assumption of a $\cos^2\theta$ distribution is small if the actual variation of n with $p\beta$ is not appreciably greater than $\cos^3\theta$.

In the interpretation of previous experiments on the scattering of μ-mesons the incident angle has been assumed vertical for all particles. It would appear from Fig. 4 that previously used correction factors have underestimated the expected number of large angle scatters.

The effect of this correction on the interpretation of McDiarmid's experiments (1954-55) carried out at 26 m w.e. underground has been estimated. This would make the calculated Molière distribution for a point nucleus uncertain by an amount varying from 20% to 80% for angles in the range 6° to 15°. Even so, the experimental results are in good agreement with the recalculated theoretical distribution for a point nucleus.

GEORGE, REDDING and TRENT [3], working at a depth of 57 m w.e. underground, found that the measured distributions lie above that expected for a point nucleus. This is due to over correction of their theoretical distribution for loss of large angles in the apparatus. If the corrections are carried out as indicated above the experimental distributions agree with the theoretical predictions for a point nucleus.

* * *

The authors are grateful to Professor L. F. BATES, F.R.S., for the facilities of his laboratories and his continued interest and encouragement in this work.

Two of us (J.E.C. and A.J.P.) are indebted to the Department of Scientific and Industrial Research for the provision of maintenance grants.

RIASSUNTO (*)

L'interpretazione degli esperimenti eseguiti sotto terra per studiare lo scattering grand'angolare dei mesoni μ dipende dalla forma presunta dello spettro sotterraneo e dall'errore geometrico introdotto dal sistema selettivo di contatori. Si è ottenuta la forma della variazione angolare di intensità a 40 m a.e. Si discute l'effetto dell'introduzione di questo valore nel calcolo dei fattori geometrici di correzione. Si dimostra che i precedenti esperimentatori che hanno presunto l'incidenza normale di tutte le particelle hanno sottostimato il numero degli scattering grand'angolari.

(*) *Traduzione a cura della Redazione.*

IL NUOVO CIMENTO Vol. VI, N. 5 1° Novembre 1957

Field Operators and Retarded Functions.

V. Glaser

Institute « Rudjer Boskovic » - Zagreb

H. Lehmann

Institut für theoretische Physik, Universität Hamburg

W. Zimmermann

Max Planck-Institut für Physik - Göttingen

(ricevuto il 15 Luglio 1957)

Summary. — A formula for the expansion of field operators with respect to products of ingoing fields is derived. The coefficients in this expansion are the retarded functions introduced earlier. They fulfil a system of equations which turns out to be not only a necessary but also sufficient condition for such functions to yield a local field operator.

We discuss some consequences of a recent formulation of quantized field theories by means of retarded products (1). First we derive a formula for the expansion of field operators with respect to products of incoming fields which is not restricted to perturbation theory. The following section contains a system of equations for the retarded functions. It serves to state necessary and sufficient conditions for these functions, so that the general principles of field theory are fulfilled. Our results are valid only for theories without stable bound states. For the latter case we refer to a paper by Nishijima (2).

(1) H. Lehmann, K. Symanzik and W. Zimmermann: *Nuovo Cimento* (in press). In the following quoted as LSZ II.

(2) K. Nishijima: to be published.

1. – Expansions with respect to incoming fields.

HAAG [3] has shown under very general assumptions that a field operator $A(x)$ may be expanded in the following manner:

$$(1)\qquad A(k) = \delta(k^2+m^2)A_{\text{in}}(k) + \sum_{n=2}^{\infty}\frac{1}{n!}\int \mathrm{d}k_1 \dots \mathrm{d}k_n \frac{\delta(k-\sum k_i)}{k^2+m^2-i\varepsilon k_0}\cdot$$
$$\cdot g(k_1, \dots, k_n)\,\delta(k_1^2+m^2)\dots\delta(k_n^2+m^2) \colon A_{\text{in}}(k_1)\dots A_{\text{in}}(k_n)\colon,$$

$A(k)$ denotes the Fourier transform of $A(x)$:

$$(2)\qquad A(x) = \frac{1}{(2\pi)^{\frac{3}{2}}}\int \mathrm{d}k \exp[+ikx]A(k)\,.$$

The function $g(k_1, \dots, k_n)$ are defined only for $k_i^2+m^2=0$. We shall derive such an expansion using only the asymptotic condition at $t=-\infty$. Haag's functions $g(k_1, \dots, k_n)$ turn out to be closely related to the retarded functions [1]

$$(3)\qquad \begin{cases} r(x;x_1\dots x_n) = (\Omega, R(x;x_1\dots x_n)\Omega)\,, \\ R(x;x_1\dots x_n) = \\ \qquad = (-i)^n \sum \theta(x-x_1)-\theta(x_{n-1}-x_n)[\dots[A(x), A(x')]\dots, A(x_n)]\,. \end{cases}$$

We note first that any linear operator L, operating in the Hilbert space of the basis vectors $\{\Phi_{\text{in}}^{q_1\dots q_k}\}$, allows the expansion [4]

$$(4)\qquad L = \sum_{n=0}^{\infty}\frac{1}{n!}\int \mathrm{d}k_1 \dots \mathrm{d}k_n(\Omega, [\dots[L, A_{\text{in}}^*(k_1)]\dots A_{\text{in}}^*(k_n)]\Omega)\cdot$$
$$\cdot\varepsilon(k_1)\,\delta(k_1^2+m^2)\dots\varepsilon(k_n)\,\delta(k_n^2+m^2)\colon A_{\text{in}}(k_1)\dots A_{\text{in}}(k_n)\colon,$$

since both sides of this relation coincide for arbitrary matrix elements of the system $\{\Phi_{\text{in}}^{q_1\dots q_k}\}$. In the particular case that L is the field operator $A(x)$ terms with $n=0, 1$ are given by

$$(\Omega, A(x)\,\Omega) = 0\,,$$
$$\int \mathrm{d}k(\,\Omega, [A(x), A_{\text{in}}^*(k)]\,\Omega)\,\varepsilon(k)\,\delta(k^2+m^2)A_{\text{in}}(k) = A_{\text{in}}(x)\,.$$

---

(3) R. HAAG: *Dan. Mat. Fys. Medd.*, **29**, 13 (1955).

(4) The infinite sums in (4) and (5) do not lead to problems of convergence, since all matrix elements with respect to incoming states have only a finite number of non-vanishing terms.

Inserting the vacuum expectation value of eq. (35) of LSZ II for $m=0$

$$\varepsilon(k_1)\dots\varepsilon(k_n)(\Omega,[\dots[A(x),A^*_{\text{in}}(k_1)]\dots A^*_{\text{in}}(k_n)]\Omega)=$$
$$=\frac{1}{(2\pi)^{3n/2}}\int \mathrm{d}k_1\dots\mathrm{d}k_n \exp\left[i\,(k_1x_1+\dots+k_nx_n)\right]K_{x_1}\dots K_{x_n}r(x;x_1\dots x_n)$$

into (4), we obtain

$$(5)\qquad A(x)=A_{\text{in}}(x)+\sum_{n=2}^{\infty}\frac{1}{n!}\int \mathrm{d}x_1\dots\mathrm{d}x_n\,K_{x_1}\dots K_{x_n}r(x;x_1\dots x_n):A_{\text{in}}(x_1)\dots A_{\text{in}}(x_n):^{(4)}.$$

This is the desired expansion formula for the field operator. With the notation

$$(6)\qquad f(x;x_1\dots x_n)=K_xK_{x_1}\dots K_{x_n}r(x;x_1\dots x_n),$$

(5) becomes

$$(5')\quad A(x)=A_{\text{in}}(x)-\sum_{n=2}^{\infty}\frac{1}{n!}\int \mathrm{d}x'\mathrm{d}x_1\dots\mathrm{d}x_n\,\Delta_R(x-x')f(x';x_1\dots x_n):A_{\text{in}}(x_1)\dots A_{\text{in}}(x_n):$$

since it follows from the retarded character of the r-functions that

$$K_{x_1}\dots K_{x_n}r(x;x_1\dots x_n)=-\int \Delta_R(x-x')f(x';x_1\dots x_n)\,\mathrm{d}x'.$$

According to (6) $f(x;x_1\dots x_n)$ depends only on the differences $y_i=x-x_i$. f is symmetric in y_i and vanishes if at least one of the times $y_{i0}<0$.

To compare with Haag's expansion (1) we transform (5′) into momentum space:

$$(5'')\qquad A(k)=\delta(k^2+m^3)A_{\text{in}}(k)+\sum_{n=2}^{\infty}\frac{1}{n!}\int \mathrm{d}k_1\dots\mathrm{d}k_n\,\frac{\delta(k-\sum k_i)}{k^2+m^2-i\varepsilon k_0}\cdot$$
$$\cdot\tilde f(k_1,\dots,k_n)\,\delta(k_1^2+m^2)\dots\delta(k_n^2+m^2):A_{\text{in}}(k_1)\dots A_{\text{in}}(k_n):$$

with

$$f(x;x_1\dots x_n)=$$
$$=\frac{1}{(2\pi)^{3n/2+3/2}}\int \mathrm{d}k_1\dots\mathrm{d}k_n\exp\left[i(x-x_1)k_1+\dots+i(x-x_n)k_n\right]\tilde f(k_1,\dots,k_n).$$

The functions $\tilde f(k_1,\dots,k_n)$ coincide evidently with Haag's functions for $k_i^2+m^2=0$ and they form a particular extrapolation of $g(k_1,\dots,k_n)$ for arbitrary momenta.

Of course, this extrapolation does not affect the expansion of $A(x)$.

An expansion for $A_{\text{out}}(x)$ follows directly from (5′):

$$A_{\text{out}}(x) = A_{\text{in}}(x) + \sum_{n=2}^{\infty} \frac{1}{n!} \int dx'\, dx_1 \dots dx_n\, \Delta(x-x') f(x'; x_1 \dots x_n) \colon A_{\text{in}}(x_1) \dots A_{\text{in}}(x_n) \colon \text{[5]}. \tag{7}$$

Only the values of $\tilde{f}(k_1, \dots, k_n)$ on the «energy shell» $k_i^2 + m^2 = 0$ and $(\sum k_i)^2 + m^2 = 0$ are effective in (7).

Eq. (5) is a special case of general expansion theorem for R-products:

$$R(x; x_1 \dots x_k) = r(x; x_1 \dots x_k) + \sum_{n=1}^{\infty} \frac{1}{n!} \int dz_1 \dots dz_n\, K_{z_1} \dots K_{z_n} r(x; x_1 \dots x_k, z_1 \dots z_n) \colon A_{\text{in}}(z_1) \dots A_{\text{in}}(z_n) \colon . \tag{8}$$

To prove this relation we substitute $R(x; x_1 \dots x_n)$ for L in (4) and then proceed as above.

Eq. (8) contains a convenient expansion of the commutator

$$[A(x), A(y)] = R(x; y) - R(y; x) = r(x; y) + \sum_{n=2}^{\infty} \frac{1}{n!} \int dz_1 \dots dz_n K_{z_1} \dots K_{z_n} r(x; y, z_1 \dots z_n) \colon A_{\text{in}}(z_1) \dots A_{\text{in}}(z_n) \colon - (x \leftrightarrow y) . \tag{9}$$

We note finally that the expansion given here can also be derived by the methods developed in the appendix to LSZ I. The definition (LSZ II. (29)) of the functional $\mathfrak{R}\{x, J\}$ leads to the equation

$$\mathfrak{R}\{x, J\} = \colon \exp\left[-\int A_{\text{in}}(x') K_{x'} \frac{\delta}{\delta J(x')}\, dx'\right] \colon (\Omega, \mathfrak{R}\{x, J\}\, \Omega) , \tag{10}$$

which is the functional form of (8).

2. – Field operator and retarded functions [6].

As shown in LSZ II, $r(x; x_1 \dots x_n)$ is a retarded and Lorentz invariant function of the co-ordinate differences. However these properties do not characterize the r-functions completely. In addition they satisfy a system of

[5] The asymptotic condition at $t = +\infty$ has been used to prove that this formula does not depend on the order of integration. Compare LSZ II, footnote [14].

[6] A characterization of field theories in terms of a set of functions was first given by A. S. Wightman: *Phys. Rev.*, **101**, 860 (1956).

equations which couples the different functions. To derive these equations we note the operator identity

$$(11)\qquad R(x;\, y, x_1 \dots x_n) - R(y;\, x, x_1 \dots x_n) = \\ = \sum_{i_1 \dots i_n} \sum_{k=0}^{n} \frac{1}{k!\,(n-k)!} [R(x;\, x_{i_1} \dots x_{i_k}),\, R(y;\, x_{i_{k+1}} \dots x_{i_n})].$$

which may be verified directly or—more elegantly—be obtained from the functional equation (LSZ II, 29))

$$(12)\qquad \frac{\delta \mathfrak{R}\{x; J\}}{\delta J(y)} - \frac{\delta \mathfrak{R}\{y; J\}}{\delta J(x)} = -i[\mathfrak{R}\{x; J\}, \mathfrak{R}\{y; J\}]\,.$$

We take the vacuum expectation value of (11) and sum over intermediate states:

$$(13)\qquad r(x;\, y, x_1 \dots x_n) - r(y;\, x, x_1 \dots x_n) = \sum_{i_1 \dots i_n} \sum_{k=0}^{n} \frac{1}{k!\,(n-k)!} \cdot \\ \cdot \sum_{l=0}^{\infty} \sum_{\alpha_1 \dots \alpha_l} (\Omega,\, R(x;\, x_{i_1} \dots x_{i_k})\, \Phi_{\text{in}}^{\alpha_1 \dots \alpha_l})(\Phi_{\text{in}}^{\alpha_1 \dots \alpha_l},\, R(y;\, x_{i_{k+1}} \dots x_{i_n})\Omega) - (x \leftrightarrow y)\,.$$

According to eq. (34″) of LSZ II we have the relation

$$(14)\qquad (\Omega,\, R(x;\, x_1 \dots x_n) A_{\text{in}}^{\alpha_1 *} \dots A_{\text{in}}^{\alpha_k *} \Omega) = \\ = \int \mathrm{d}u_1 \dots \mathrm{d}u_k f_{\alpha_1}(u_1) \dots f_{\alpha_k}(u_k) K_{u_1} \dots K_{u_k} r(x;\, x_1 \dots x_n u_1 \dots u_k)\,.$$

Inserting this into (13) we obtain the system of equations:

$$(15)\qquad r(x;\, y, x_1 \dots x_n) - r(y;\, x, x_1 \dots x_n) = \\ = \sum_{i_1 \dots i_n} \sum_{k=0}^{n} \sum_{l=1}^{\infty} \frac{(-i)^l}{k!\,(n-k)!\,l!} \int \mathrm{d}u_1 \dots \mathrm{d}u_l\, \mathrm{d}v_1 \dots \mathrm{d}v_l\, K_{u_1} \dots K_{u_l} \cdot \\ \cdot r(x; x_{i_1}, \dots x_{i_k} u_1 \dots u_l) \Delta^+(u_1 - v_1) \dots \Delta^+(u_l - v_l) K_{v_1} \dots K_{v_l} r(y;\, x_{i_{k+1}} \dots x_{i_n} v_1 \dots v_l) - (x \leftrightarrow y)\,.$$

The connection between field operator and retarded functions may now be given completely. As was shown, the defining equation of the retarded function

$$(3)\qquad r(x;\, x_1 \dots x_n) = (\Omega,\, R(x;\, x_1 \dots x_n)\Omega)$$

is solved explicitely for the field operator $A(x)$ by the expansion formula

$$(5)\qquad A(x) = A_{\text{in}}(x) + \sum_{n=2}^{\infty} \frac{1}{n!} \int \mathrm{d}x_1 \dots \mathrm{d}x_n K_{x_1} \dots K_{x_n} r(x;\, x_1 \dots x_n) \colon A_{\text{in}}(x_1) \dots A_{\text{in}}(x_n) \colon .$$

This simple relationship forms the basis of the following two theorems. They contain necessary and sufficient conditions which the retarded functions have to satisfy in order that $A(x)$ fulfils all general physical principles.

Theorem I. Let a field operator $A(x)$ be given which satisfies the asymptotic conditions, Lorentz-invariance and the causality condition. If retarded functions are then defined by (3), eq. (5) follows and the functions $r(x; x_1 \dots x_n)$ satisfy the following conditions:

a) $r(x; x_1 \dots x_n)$ is a real, symmetric and invariant function of the variables $y_i = x - x_i$. It vanishes unless all co-ordinates y_i are in the forward light cone $y_{i0} \geqslant 0$, $y_i^2 \leqslant 0$.

b) The functions $r(x; x_1 \dots x_n)$ satisfy the equations (15).

c) If $\tilde{f}(k_1 \dots k_n)$ denotes the Fourier transform of

$$f(x - x_1, \dots, x - x_n) = K_x K_{x_1} \dots K_{x_n} r(x - x_1, \dots, x - x_n),$$

then $\tilde{f}(k_1, \dots, k_n)$ is finite on the energy shell $k_i^2 + m^2 = 0$, $(\sum k_i)^2 + m^2 = 0$ and does not depend on the order in which the $n+1$ limits $k_i^2 + m^2 \to 0$, $(\sum k_i)^2 + m^2 \to 0$ are taken.

Theorem II. Let arbitrary functions $r(x; x_1 \dots x_n)$ be given which satisfy the conditions *a*), *b*) and *c*) formulated in theorem I. If $A(x)$ is defined by (5), then eq. (3) follows and $A(x)$ satisfies the asymptotic conditions, Lorentz-invariance and the causality condition.

Condition *a*) and *b*) of Theorem I have already been proved. That the functions $\tilde{f}$ are finite on the energy shell (condition *c*)) follows from the existence of the matrix elements of $A(x)$ and $A_{\text{out}}(x)$, since it is a consequence of the asymptotic conditions that these operators may be expanded as in (5′) and (7). The continuity condition also contained in *c*) follows from the commutation relations of the incoming and outgoing fields (cf. LSZ II, footnote 14).

The proof of the second theorem will only be sketched:

The definition (5) of the field operator shows directly that $A(x)$ is Lorentz-invariant and fulfills the asymptotic condition at $t = -\infty$.

As a consequence of (15) and the retarded property of $r(x; x_1 \dots x_n)$ contained in *a*), the functions defined by $(\Omega, R(x; x_1 \dots x_n)\Omega)$ are identical with the given functions $r(x; x_1 \dots x_n)$.

Since $A(x)$ satisfies the asymptotic condition at $t = -\infty$, the commutator may be expressed by $r(x; x_1 \dots x_n)$ as in (9).

Hence

$$[A(x), A(y)] = 0 \quad \text{if} \quad (x - y)^2 > 0$$

because of the invariant retarded character of the r-functions.

Finally we have to prove the asymptotic condition at $t = +\infty$ and thereby the unitarity of the scattering matrix. From the definition (5) of $A(x)$ we obtain eq. (7), the expansion of the outgoing field (7). $A_{\text{out}}(x)$ satisfies the Klein-Gordon equation and the unitarity equations (15) imply the correct commutation relations

$$[A_{\text{out}}(x), A_{\text{out}}(y)] = i\Delta(x-y) .$$

(7) The interchange of the order of integration is permitted by the continuity conditions of $\tilde{f}(k_1, ..., k_n)$ contained in (c) (compare also footnote (5)).

RIASSUNTO (*)

Si deriva una formula per lo sviluppo degli operatori di campo rispetto ai prodotti dei campi entranti. I coefficienti di tale sviluppo sono le funzioni ritardate precedentemente introdotte. Essi soddisfano un'equazione che risulta essere una condizione non solo necessaria ma sufficiente affinchè dette funzioni forniscano un operatore di campo locale.

(*) *Traduzione a cura della Redazione*

IL NUOVO CIMENTO Vol. VI, N. 5 1° Novembre 1957

Renormalisation d'une théorie ne conservant pas la parité.

B. d'Espagnat et J. Prentki

CERN - Genève

(ricevuto il 21 Luglio 1957)

Summary. — The extension of the renormalization procedure to a parity non conserving theory is investigated. For the sake of definiteness a parity non conserving interaction term of the form eq. (1) is assumed, which means that a parity non conserving (but CP invariant) nucleon-hyperon-K interaction is postulated: CP invariance is here introduced so that the α/β ratio of terms with opposite parities could eventually be appreciable without violating known experimental data (absence of electric dipole moment for elementary particles) [6]. It is shown that the theory represented by eq. (1) is indeed renormalizable. In the proposed renormalization procedure a real physical nucleon has still a definite parity with respect to the bare nucleon. Effects of parity non conservation are then entirely contained in the renormalized vertex operators $\Gamma_r^{\pm}$ as well as in the renormalized baryon propagation function $S_r(p)$, which, however, tends to the same limiting form as the usual $S_r(p)$ of a parity conserving theory in the limit where p tends towards the four momentum of a real particle. It is considered that such a renormalization scheme is necessary if quantitative estimation of the maximum admissible α/β ratio compatible with experimental data is desired.

Afin d'étudier la possibilité de renormalisation d'une théorie qui ne conserve pas la parité considérons le Lagrangien $L = L_{\text{particules libres}} + L_{\text{int.}}$ avec

$$L_{\text{int.}} = \bar{Y}(\alpha + \beta\gamma_5)NK + \bar{N}(\alpha - \beta\gamma_5)YK^* \,, \tag{1}$$

(N = champ nucléonique, Y = champ hyperonique) et α et β réels si γ_5 hermitique (invariance sous C.P. produit de la conjugaison de charge et de la parité).

2989

Avec les notations habituelles (voir par exemple, réf. ([1-5])), on a

$$\Sigma^*(p) = A + BS(p)^{-1} + S(p)^{-2}\Sigma_f(p) + (B' + 2m\Sigma_f'(p))\varrho_\mu\gamma_\mu\gamma_5 , \tag{2}$$

$$\frac{1}{S'(p)} = \frac{1}{S(p)} - \Sigma^*(p) , \tag{3}$$

où, dans le dernier terme, B' est une constante infinie (au même titre que A et B) et $\Sigma_f'(p)$ une fonction finie de p (au même titre que $\Sigma_f(p)$). L'expression (2) ne contient pas de terme du type $A'\gamma_5$ en raison de l'invariance sous C.P. de la théorie. Un calcul au second ordre montre aisément que $B = (\alpha^2+\beta^2)U + v$, $B' - 2\alpha\beta U + w$, où U est une intégrale divergente et v et w des quantités finies de telle sorte que dans la limite d'une coupure infinie on a $B'/B = 2\alpha\beta/(\alpha^2+\beta^2)$, donc $B'/B =$ quantité finie. En fait cette dernière relation est vraie à n'importe quel ordre: le rapport des quantités exactes B et B' est un nombre fini. Posons comme d'habitude

$$\frac{\partial}{\partial p_\mu}\left(\frac{1}{S'(p)}\right) = \Gamma_\mu(p) = \gamma_\mu + \Lambda_\mu(p) , \tag{4}$$

$$\frac{1}{S'(p)} - \frac{1}{S'(p')} = \int_0^1 \mathrm{d}q_\mu \Gamma_\mu(q) = \int_0^1 \mathrm{d}\lambda (p_\mu - p'_\mu)\Gamma_\mu(p^\lambda) , \tag{5}$$

avec

$$p^\lambda = p\lambda + p'(1-\lambda) , \tag{6}$$

p' correspondant à un vecteur réel: on constate alors aisément que le terme $1/S'(p')$ peut être absorbé dans la renormalisation de masse habituelle: ceci permet de négliger les termes $1/S'(p')$ dans (5) et A dans (2).

Le passage aux quantités renormalisées se fait de la façon suivante: posons

$$S_r(p) = Z_2^{-1}(a - b\gamma_5)\, S'(p)(a + b\gamma_5) \tag{7}$$

$$\Gamma_{\mu r}(p) = Z_2\, (a - b\gamma_5)\Gamma_\mu(p)(a + b\gamma_5) \tag{8}$$

([1]) F. J. DYSON: *Phys. Rev.*, **75**, 1736 (1949).
([2]) A. SALAM: *Phys. Rev.*, **79**, 910 (1950).
([3]) J. C. WARD: *Phys. Rev.*, **84**, 897 (1951).
([4]) G. F. CHEW: *Phys. Rev.*, **94**, 1748 (1954).
([5]) J. M. JAUCH et F. ROHRLICH: *The Theory of Photons and Electrons* (Cambridge, Mass., 1955).

ce qui par (4) et (5) entraîne immédiatement

$$\Gamma_{\mu r}(p) = \frac{\partial}{\partial p_\mu}\left(\frac{1}{S_r(p)}\right), \tag{9}$$

$$\frac{1}{S_r(p)} = \int_0^1 \mathrm{d}\lambda(p_\mu - p'_\mu)\Gamma_{\mu r}(p^\lambda) . \tag{10}$$

Dans (7), (8) Z_2 a et b sont des nombres arbitraires et a et b sont en général finis et liés par $a^2 - b^2 = 1$. Bien que $\Gamma_\mu(p')$ soit d'après (2) et (3) de parité mixte (superposition d'un vecteur et d'un pseudo-vecteur), (8) permet d'imposer à $\Gamma_{\mu r}(p')$ d'être égal à un vrai vecteur, plus précisément d'imposer

$$\Gamma_{\mu r}(p') = \gamma_\mu. \tag{11}$$

(8) donne alors Z_2 a et b en fonction de B et B':

$$Z_2 = [(1-B)^2 - B'^2]^{-\frac{1}{2}} ; \qquad \begin{aligned} a &= Z_2^{-\frac{1}{2}}[(1-B+B')^{\frac{1}{2}} + (1-B-B')^{\frac{1}{2}}]/2 \\ b &= Z_2^{-\frac{1}{2}}[(1-B+B')^{\frac{1}{2}} - (1-B-B')^{\frac{1}{2}}]/2 . \end{aligned} \tag{12}$$

On voit que les quantités a et b sont finies en général même dans le cas d'une coupure infinie mais néanmoins, dans le cas d'une coupure finie, dépendent de la coupure. Notons cependant que ces quantités bien que finies n'apparaîtront pas dans les formules finales permettant de calculer un phénomène. Posant

$$\Lambda_{\mu r}(p) = Z_2(a - b\gamma_5)\Lambda_\mu(p)(a + b\gamma_5) , \tag{13}$$

il vient par (4) et (8)

$$\Gamma_{\mu r}(p) = Z_2(a - b\gamma_5)\gamma_\mu(a + b\gamma_5) + \Lambda_{\mu r}(p) , \tag{14}$$

d'où par (11)

$$\Gamma_{\mu r}(p) = \gamma_\mu + \Lambda_{\mu r}(p) - \Lambda_{\mu r}(p') . \tag{15}$$

(15) doit naturellement être considéré comme une équation intégrale en $\Gamma_{\mu r}(p)$, lequel intervient également dans l'expression pour $\Lambda_{\mu r}(p)$ qui reste à déterminer. Ceci se fait de la manière habituelle: si W est un certain diagramme de self énergie, par exemple celui du second ordre $\Lambda_\mu(p, W)$ est donné par l'expression bien connue

$$\Lambda_\mu(p, W) = g^2\Gamma^{(-)}S'\Gamma_\mu S'\Gamma^{(+)}D' , \tag{16}$$

où $\Gamma^{(+)}(p_2, p_1)$ et $\Gamma^{(-)}(p_2, p_1)$ sont les vertex $\alpha+\beta\gamma_5$, $\alpha-\beta\gamma_5$ modifiés par les corrections de vertex et $D'(k)$ la fonction de propagation du K modifiée. Posant

$$\Gamma^{(\pm)} = Z_1^{(\pm)-1}(a+b\gamma_5)\Gamma_r^{(\pm)}(a-b\gamma_5)\,; \qquad D'(k) = Z_3 D_r(k)\,, \tag{17}$$

il vient

$$\Lambda_\mu(p, W) = Z_2^{-1}(a+b\gamma_5)g_r^2\Gamma_r^{(-)}S_r\Gamma_{\mu r}S_r\Gamma_r^{(+)}D_r(a-b\gamma_5)\,, \tag{18}$$

avec

$$g_r = gZ_2Z_1^{(+)-\frac{1}{2}}Z_1^{(-)-\frac{1}{2}}Z_3^{\frac{1}{2}}\,, \tag{19}$$

d'où par (13)

$$\Lambda_{\mu r}(p, W) = g_r^2\Gamma_r^{(-)}S_r\Gamma_{\mu r}S_r\Gamma_r^{(+)}D_r\,, \tag{20}$$

c'est-à-dire que $\Lambda_{\mu r}(p, W)$ a la même expression formelle que $\Lambda_\mu(p, W)$ mais à condition que les quantités renormalisées soient utilisées partout. On constate bien aisément que ceci est généralement vrai quel que soit le diagramme W utilisé et par conséquent vrai aussi pour la somme $\Lambda_{\mu r}(p)$ de tous les $\Lambda_{\mu r}(p, W)$.

L'équation intégrale (15), pour $\Gamma_{\mu r}(p)$, qui, supposée résolue, donne $S_r(p)$ par (5) contient également $D_r(k)$ et $\Gamma_r^{(\pm)}(p_2p_1)$. Ces deux dernières quantités sont elles-mêmes données par des équations intégrales et on a donc, comme il est bien connu, affaire en fait à un système d'équations intégrales simultanées.

La renormalisation de la fonction de propagation $D'(k)$ ne donne lieu à aucune nouveauté, si du moins on néglige la diffusion des K par les K: ceci tient à ce que la fonction $W_\mu(k)$ definie par

$$W_\mu(k) = \frac{\partial}{\partial k_\mu}\left(\frac{1}{D'(k)}\right), \tag{21}$$

contrairement à ce qui se passe pour $\Gamma_\mu(k)$, est un vrai vecteur, même lorsque l'interaction ne conserve pas la parité (on ne peut définir un pseudovecteur à partir du seul vecteur k). Nous ne transcrirons donc pas la renormalisation de $D'(k)$ qui se fait exactement de la manière habituelle (noter que les diagrammes dits triangulaires sont interdits par la conservation de l'étrangeté).

En ce qui concerne les vertex, la renormalisation s'effectue d'une manière tout à fait analogue à celle qui a été décrite pour les self-énergies. Définissant

$$\Gamma^{(\pm)}(p_2, p_1) = \alpha \pm \beta\gamma_5 + \Lambda^{(\pm)}(p_2, p_1) \tag{22}$$

et

$$\Lambda^{(\pm)}(p_2, p_1) = Z_1^{(\pm)-1}(a+b\gamma_5)\Lambda_r^{(\pm)}(p_2, p_1)(a-b\gamma_5), \tag{23}$$

il vient

$$\Gamma_r^{(\pm)}(p_2, p_1) = \Gamma_r^{(\pm)}(p', p') + \Lambda_r^{(\pm)}(p_2, p_1) - \Lambda_r^{(\pm)}(p', p') . \tag{24}$$

On constate comme ci-dessus que, quel que soit le diagramme de vertex W, $\Lambda_r^{(\pm)}(p_1, p_1, W)$ est donné par la même expression que $\Lambda^{(\pm)}(p_1, p_1, W)$ mais avec des quantités renormalisées, il en va donc de même de leur somme $\Lambda_r^{(\pm)}(p_1, p_2)$. Enfin, grâce à l'arbitraire sur Z_1 on peut toujours donner à $\Gamma_r^{(\pm)}(p', p')$ l'expression finie

$$\Gamma_r^{(\pm)}(p', p') = u + v\gamma_5 ; \qquad u^2 - v^2 = 1 \tag{25}$$

u et v sont évidemment reliées aux quantités α et β et aussi aux quantités L et L' qu'il convient d'introduire lorsqu'on met $\Lambda(p_2, p_1)$ sous une forme correspondant à l'expression (2) pour $\Sigma(p^*)$. (24), compte tenu de (25), est l'équation intégrale pour $\Gamma_r^{(\pm)}(p_2, p_1)$. Les équations (15), (24) et l'équation correspondante pour $W_r(k)$ que nous n'avons pas écrite, donnent la solution du problème de rénormalisation étudié.

En vertu de (10) et (11), $S_r(p)$ tend vers un vrai scalaire lorsque $p \to p'$. Il en résulte, ainsi qu'il est facile de s'en convaincre, qu'un nucléon physique réel a dans cette théorie la même parité qu'un nucléon nu (*).

Il n'est bien entendu nullement prouvé qu'il y ait des interactions fortes qui ne conservent pas la parité: leur existence n'est cependant pas exclue pourvu qu'on leur impose d'une part de conserver le produit C.P., ceci à cause de l'absence de moment dipolaire des particules élémentaire [6,7] (+), d'autre part d'être de force moindre que l'interaction nucléon-nucléon habituelle: il se pourrait que l'interaction (1) réponde précisément à ce dernier critère. Bien entendu il n'est pas non plus exclu que l'interaction nucléon-nucléon-π elle-même comporte un petit terme ne conservant pas la parité: il faut toutefois remarquer que la combinaison des couplages scalaire et pseudoscalaire ne peut dans ce cas satisfaire à l'invariance sous C.P. et que les autres combinaisons ne sont manifestement pas renormalisables.

(*) Noter toutefois que (11) est une condition très naturelle mais nullement nécessaire. Autrement dit, l'absence d'une contrainte, à savoir la conservation de parité imposée à la théorie habituelle, entraîne ici une plus grande liberté dans le choix de la méthode de renormalisation. On pourrait donc manifestement se donner d'autres prescriptions de renormalisation en vertu desquelles le nucléon physique n'aurait pas une parité bien déterminée par rapport à celle du nucléon nu. Nous remercions le professeur Touschek pour une remarque à ce sujet.

(6) T. D. Lee et C. N. Yang: *Phys. Rev.*, **104**, 254 (1956).

(7) L. Landau: *Nuclear Physics*, **3**, 127 (1957).

(+) Noter que si P.C. est conservé le deutéron n'a pas non plus de moment dipolaire ainsi que nous l'a fait remarquer le professeur F. Villars.

Le fait de disposer d'une méthode pour renormaliser la théorie (1) doit permettre d'évaluer sans ambiguité, en fonction des paramètres α et β — ou plus exactement u et v — l'importance relative de manifestations éventuelles de la non conservation de la parité dans les interactions fortes, par exemple dans la diffusion des nucléons polarisés par les nucléons, ou des mésons π par les nucléons avec observation de la polarisation de l'état final, ou encore dans la production de mésons π. Ces calculs n'ont pas encore été effectués. Il semble toutefoir qu'il s'agisse dans la majorité des cas d'effets proportionnels à la vitesse et d'importance peu considérable qui, sous des hypothèses assez larges, auraient pu échapper à la détection.

* * *

Nous tenons à remercier les professeurs FERRETTI et VILLARS et le docteur OMNÈS pour de très interessantes discussions au sujet de ce problème.

RIASSUNTO (*)

Si esamina l'estensione della procedura di rinormalizzazione a una teoria non conservativa della parità. Per fissare le idee si assume un termine d'interazione non conservante la parità della forma dell'eq. (1), il che equivale a postulare un'interazione nucleone-iperone K non conservante la parità (ma CP invariante): si introduce qui l'invarianza CP affinchè il rapporto α/β dei termini con parità opposte possa essere eventualmente apprezzabile senza violare dati sperimentali noti (assenze di momento di dipolo elettrico per le particelle elementari) ([6]). Si dimostra che la teoria rappresentata dall'eq. (1) è in realtà rinormalizzabile. Nella procedura di rinormalizzazione proposta un nucleone fisico reale ha ancora una parità definita rispetto al nucleone nudo. Gli effetti della non conservazione della parità sono interamente contenuti sia negli operatori di vertice rinormalizzati $\Gamma_r^{\pm}$, sia nella funzione di propagazione dei barioni rinormalizzata $S_r(p)$, che, tuttavia, tende alla stessa forma limite del comune $S_r(p)$ di una teoria conservante la parità al limite in cui p tende al quadrimomento di una particella reale. Si considera che tale schema di rinormalizzazione sia necessario desiderando ottenere una valutazione quantitativa del massimo rapporto α/β compatibile con i dati sperimentali.

(*) *Traduzione a cura della Redazione.*

On the Q-Values of the Λ^0 and the θ^0 and on the Anomalous V^0-Decays.

C. D'Andlau, R. Armenteros, A. Astier, H. C. DeStaebler (*), B. P. Gregory, L. Leprince-Ringuet, F. Muller, C. Peyrou (+) and J. H. Tinlot (×)

Laboratoire de Physique de l'Ecole Polytechnique - Paris

(ricevuto il 29 Luglio 1957)

Summary. — A study of 161 V^0-decays observed in the momentum chamber of the Ecole Polytechnique at the Pic du Midi has been made. These events correspond to a strict choice based on the measurability of the momenta of both secondaries (better than 10%). The main results are: 1) No direct evidence for anomalous neutral hyperon decays. Upper limits (6 to 8%) can be placed on the existence of various hypothetical modes. 2) The Q-values for the Λ^0-decay: $Q_{\Lambda^0}=(37.9\pm0.4)$ MeV. 3) The direct identification of the π nature of both secondaries of the θ^0-decay-mode. 4) The Q-value for θ^0-decay: $Q_{\theta^0}=(217\pm4)$ MeV. 5) A direct proof of the non identity of the particles responsible for the θ^0-decay and the anomalous V^0-decays based on the significant difference between the number of slow and fast events of each category.

1. – Introduction and general results.

We report in this paper the results of an analysis of V^0-decays observed in the double cloud chamber experiment installed at the Pic du Midi. The main improvement in the installation since preceding experiments (1) has been an increase in the magnetic field from 2 500 to 5 000 gauss. A total of

(*) Now at Stanford University, USA.

(+) Now at CERN, Geneva, Switzerland.

( ) Now at Rochester University, USA.

(1) B. Gregory, A. Lagarrigue, L. Leprince-Ringuet, F. Muller and Ch. Peyrou: *Nuovo Cimento*, **11**, 292 (1954).

550 V^0-decays were observed and roughly measured during the first scanning of about 30 000 pictures.

1·1. *Selection of events.* – The original purpose of the work was to obtain information about anomalous decays. It was realized from the beginning that, for the study to be as meaningful as possible, a large sample of events would have to be selected according to some predetermined criterion. Since anomalous decays are defined as those which are incompatible with the known Λ^0 and θ^0 modes, high accuracy is required. The results of this paper are based on a restricted sample consisting of 161 V^0 for which both secondaries have sagittae equal to or greater than 1.5 mm. The corresponding errors in the Q-values lie between 5% and 20%.

To ensure that our sample was complete, a large number of events (about 200), chosen on a looser criterion, were completely measured. The restricted sample was then selected from these.

This selection method will allow us to discuss quantitatively such results as the absence of anomalous hyperon decays, the existence of anomalous decays with Q-values in the neighbourhood of the known θ^0 mode, and an important statistical result on the difference of nature between the particles responsible for the θ^0 and the anomalous modes of decay.

On the other hand since this choice has the effect of reducing the available time of flight, no attempt has been made to measure V^0-lifetimes.

1·2. *General results.* – For each of the 161 events ([2]), the electronic computer was programmed to give a $Q(\mathrm{p},\pi)$ and a $Q(\pi,\pi)$ together with their corresponding errors and also the following well known parameters:

$$P_t = \frac{P_+ P_- \sin\varphi}{P}\;; \quad |\boldsymbol{P}| = |\boldsymbol{P}_+ + \boldsymbol{P}_-|\;; \qquad \alpha = \frac{P_+^2 - P_-^2}{P^2}\,.$$

The general results are shown in an (α, p_t) plot in Fig. 1. Comparison of these data with those obtained in other laboratories ([3]) shows that our results are in qualitative agreement with the accepted general picture of V^0-decays, namely with the existence of the $\Lambda^0 \to \mathrm{p} + \pi + 37$ MeV and of the θ^0 decaying most probably into two π-mesons with a Q-value of 214 MeV, against a small background of anomalous decays.

Taking as starting point this knowledge, an iteration process has been followed to classify our data. Only the final step will be described in this

([2]) The lengthy tables giving the complete measurements are available at: Laboratoire de Physique, Ecole Polytechnique, 17 rue Descartes, Paris V^e, France.

([3]) R. W. THOMPSON: *Hyperons and Heavy Mesons*, in *Progress in Cosmic Ray Physics*, Vol. III, Chap. V (1955).

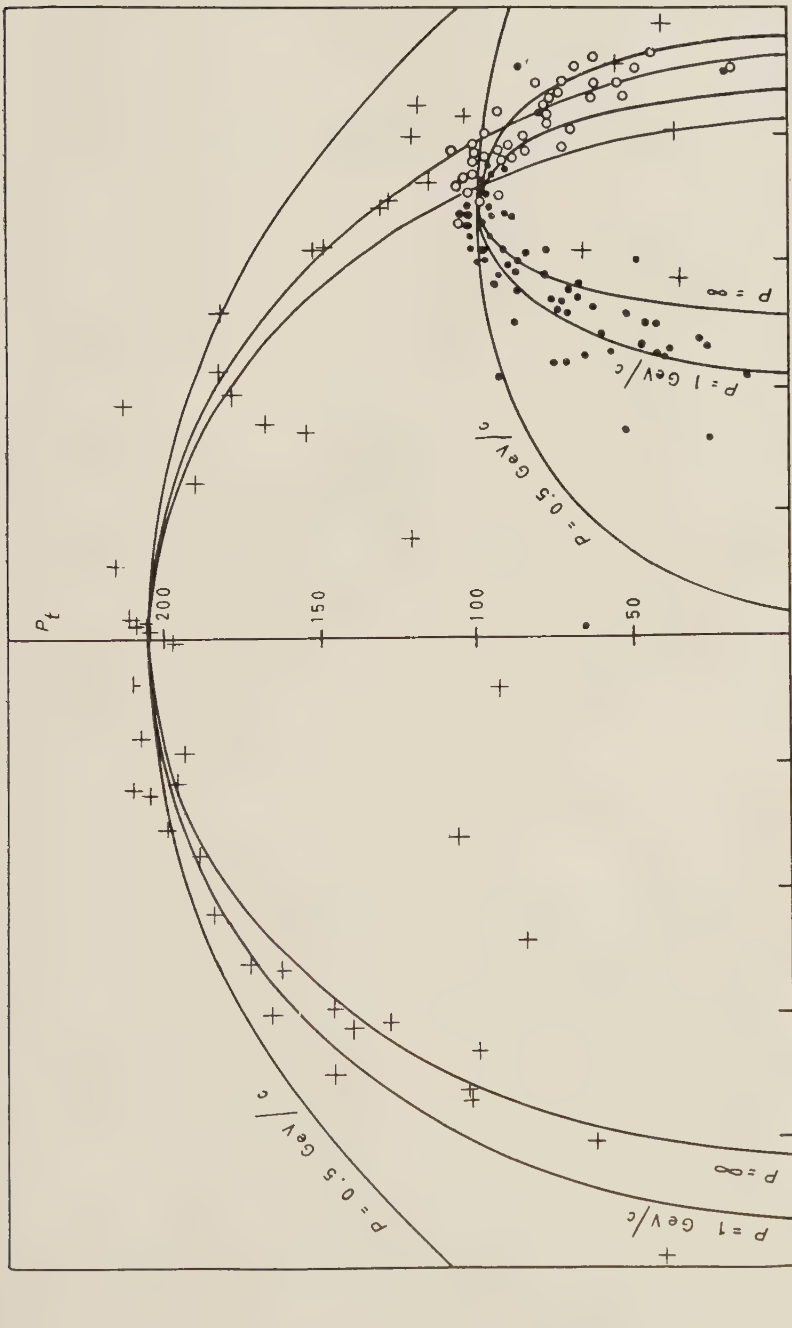

Fig. 1. – (α, p_t) representation for all the 161 V^0's. The ellipses drawn correspond to the θ^0 and Λ^0 modes for three momenta: $p=\infty$, $p=1$ GeV/c, $p=0.5$ GeV/c. The assumed Q-values were: 217 MeV for the θ^0 and 37.9 MeV for the Λ^0.

paper. For example the choice of events to be discussed as Λ^0 (Sect. 3 and 4) was made by eliminating all V^0's for which the $Q(\pi, \pi)$ was compatible within three standard deviations with the best value for θ^0 (217 MeV) obtained in Sect. 5.

1·3. *Errors*. – A description of the methods used in reducing the data and in estimating the errors is given in the appendix. Their main features are the following:

— The sagitta was taken as the Gaussian variable in estimating errors in momenta. All errors are standard deviations.

— The errors (σ_M) arising from the measurements were considered to be independent from track to track and were quadratically combined with the errors (σ_S) arising from multiple scattering.

— On the other hand gas distortion (σ_D) affects in a dependent way two neighbouring tracks. In calculating errors in Q-values, account was taken of this difference between dependent and independent errors.

— The maximum detectable momentum i.e. the momentum of a vertical track with a sagitta $\sigma = \sqrt{\sigma_M^2 + \sigma_D^2}$ on its useful length was found to be 27 GeV/c

— σ_M and σ_D were taken as constant whatever the length of the track.

— Events were classified as A events whenever the final error was essentially due either to scattering, or to the measurement of a long vertical track. Only those events were kept for the determination of Q-values.

2. – The problem of anomalous hyperon decays.

In Fig. 2, the $Q(p, \pi)$-distribution is shown for the V^0-decays belonging to the restricted sample whose $Q(\pi, \pi)$-values deviate by more than 3 standard deviations from that of the θ^0-particle ($Q_{\theta^0} = 217$ MeV, see Sect. 5).

Of the 81 events contributing to the histogram, 71 concentrate around a central value placed between 35 ÷ 40 MeV; all events for which the positive track is recognized as a proton (see Sec. 1 Appendix) belong to this group. On the other hand, 10 are clearly incompatible with this distribution; seven of them (no. 100, 167, 191, 194, 195, 196, 197) have positive secondaries which have masses below that of the proton; for the other 3 events (no. 50, 64, 82), no useful upper limit to the mass of the positive particle can be fixed. These 10 anomalous events are listed in Table I, together with event no. 33 for which the positive track is not a proton although the $Q(p, \pi)$ is compatible with a Λ^0-decay (36.3 ± 1.6) MeV.

It is clear from the histogram that this experiment provides no direct

evidence for the existence of hyperon decays different from the Λ^0. This is in agreement with the general accepted picture although some anomalous hyperonic decays have been reported in the literature ([4,5]). It seems never-

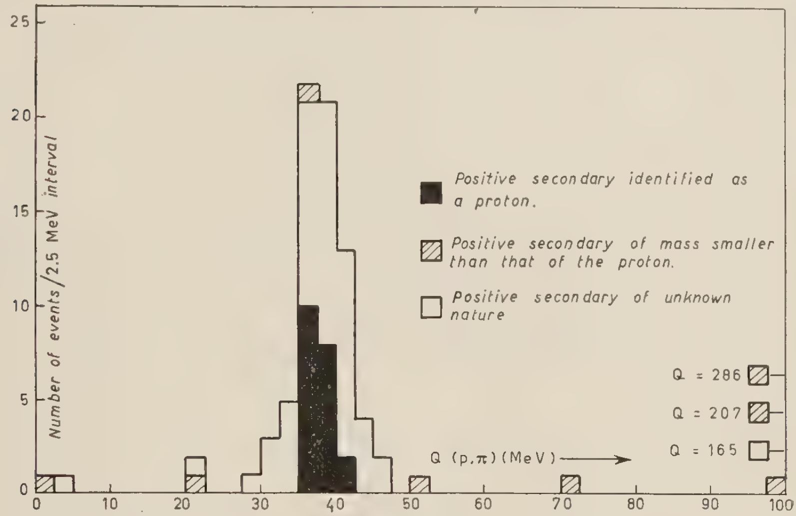

Fig. 2. – $Q(\mathrm{p}, \pi)$ histogram for non-θ^0-events.

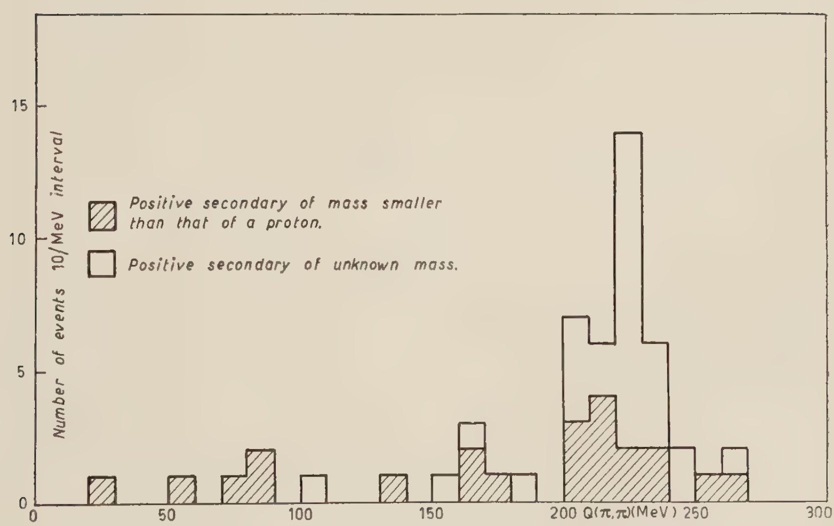

Fig. 3. – $Q(\pi, \pi)$ histogram for non-Λ^0-events.

([4]) R. B. Leighton, S. D. Wanlass and C. D. Anderson: *Phys. Rev.*, **89**, 148 (1953).

([5]) V. A. J. Van Lint, G. H. Trilling, R. B. Leighton and C. D. Anderson: *Phys. Rev.*, **95**, 295 (1954).

TABLE I. – *In this table are listed all the events discussed as anomalous in Sections* **2**, **4** *and* **5**.

No.	p^+ (MeV/c)	I/I_0	p^- (MeV/c)	φ (degrees)	p (MeV/c)	α	p_T (MeV/c)	$Q(\mathrm{p}, \pi)$ (MeV)	$Q(\pi, \pi)$ (MeV)	Class A
196 (1)	$176^{+4.4}_{-4.2}$	Min.	$56.3^{+0.82}_{-0.80}$	46.4 ± 0.14	218	0.58	32.8	$5.4\ ^{+0.2}_{-0.2}$	$25.57^{+1.11}_{-1.06}$	—
191 (2)	$227^{+5.1}_{-4.8}$	»	$181\ ^{+17.1}_{-14.4}$	74.4 ± 0.33	321	0.16	119.8	$70.3\ ^{+10.5}_{-8.8}$	$88.9\ ^{+7.07}_{-6.03}$	—
100	391^{+34}_{-29}	»	$122.0^{+5.4}_{-5.0}$	93.0 ± 0.23	403	0.85	118.1	$54.2\ ^{+3.9}_{-3.5}$	$165.6\ ^{+14.0}_{-12.0}$	—
197	$246^{+5.0}_{-4.8}$	»	$284\ ^{+18}_{-16}$	41.1 ± 0.25	497	−0.08	92.4	$109\ ^{+10.2}_{-9.1}$	$56.47^{+4.17}_{-3.79}$	—
194 (3)	$169^{+6.0}_{-5.6}$	»	$430\ ^{+16.9}_{-15.7}$	41.1 ± 0.28	567	−0.48	83.8	$207\ ^{+10.3}_{-9.6}$	$78.00^{+4.19}_{-3.92}$	A
195 (4)	588^{+52}_{-44}	»	$61.6^{+5.9}_{-5.0}$	68.5 ± 0.23	613	0.91	54.9	$22.6\ ^{+3.1}_{-2.6}$	$164.4\ ^{+14.9}_{-12.7}$	A
33 (5)	587^{+72}_{-58}	»	$152.4^{+3.2}_{-3.1}$	49.6 ± 0.25	693	0.66	97.9	$36.1^{+1.60}_{-1.62}$	$136.1\ ^{+18.2}_{-14.8}$	—
167	$363^{+11.8}_{-11.1}$	»	$682\ ^{+18}_{-17}$	26.0 ± 0.17	1022	−0.32	106.1	$286\ ^{+9.1}_{-8.7}$	$88.8\ ^{+3.26}_{-3.13}$	—
64 (6)	1010^{+108}_{-89}	»	$107.8^{+2.5}_{-2.4}$	18.0 ± 0.14	1109	0.81	30.1	$7.8\ ^{+2.7}_{-2.2}$	$158.4\ ^{+18.1}_{-15.8}$	A
82	1429^{+138}_{-116}	»	$338\ ^{+13.2}_{-12.3}$	13.7 ± 0.13	1759	0.62	64.8	$22.8\ ^{+4.4}_{-4.6}$	$108.7\ ^{+12.7}_{-10.7}$	—
50	1545^{+112}_{-98}	»	$727\ ^{+14.3}_{-13.8}$	25.1 ± 0.12	2208	0.37	213.5	$165\ ^{+5.1}_{-5.1}$	$269.9\ ^{+17.9}_{-15.8}$	—
63 (7)	$526^{+11}_{-10.6}$	»	$2574\ ^{+207}_{-177}$	13.1 ± 0.11	3008	−0.66	99.3	$847\ ^{+61}_{-52}$	$176.2\ ^{+14.7}_{-13.1}$	A
12 (7)	2263^{+301}_{-237}	»	$1113\ ^{+125}_{-103}$	11.9 ± 0.25	3324	0.33	154.0	$137\ ^{+25}_{23}$	$163.0\ ^{+22}_{-18}$	A

(1) The negative secondary of this event has an ionization $\geqslant 2 \times$ minimum.

(2) The positive secondary of this event stops in the 4th plate in the lower chamber. Its mass, calculated by ionization-momentum, is equal to $(290 \pm 19)\ \mathrm{m_e}$.

(3) The negative secondary of this event produces a nuclear interaction between the chambers.

(4) The ionization of the negative secondary of this event is minimum.

(5) Event 33 was ruled out as a Λ^0 by the ionization of the positive track.

(6) The positive secondary of this event goes through 4 plates in the lower chamber without producing an electronic shower.

(7) Events 63 and 12 are such that their $Q(\pi, \pi)$-values differ from the θ^0-value by less than three standard deviations. They are not included in the anomalous group but will be discussed in Sect. **5**. The $Q(\mathrm{p}^-, \pi^+)$ of event 63 is consistent with a Λ^0-decay.

Remark. – It may be noted that 8 events among the first 11 have a $Q(\pi, \pi) > 80$ MeV.

theless worth-while to investigate statistically the possible existence of anomalous hyperonic decays. Our strict choice of events will allow us to fix upper limits to the number of various assumed decay modes.

If we assume that alternate modes exist of the type:

$$(1)\qquad \begin{cases} \Lambda^0 \to p + \mu^- + \nu + 71 \text{ MeV} \\ \Lambda^0 \to p + e^- + \nu + 173 \text{ MeV} \end{cases}$$

then at most two of the three anomalous events with a positive secondary of undetermined mass can be explained in this way. (Event no. 50 gives $Q(p, e) > 177$ and $Q(p, \mu) > 80$ MeV). At the 95% confidence limit, this implies that no more than 8% of non-θ^0 decays observed can be of the above type.

If we assume the existence of a neutral decay of the type:

$$(2)\qquad Y^0 \to p + \pi + Q \neq 37 \text{ MeV},$$

in which the assumed Q-value lies outside the band of 25 to 50 MeV, no more than one of the three anomalous events can be explained in this way. At the 95% confidence limit this implies that no more than 6% of the non-θ^0-decays observed can be of type (2).

All anomalous V^0's could correspond to decays of a unique hypothetical hyperon according to the modes:

$$(3)\qquad \begin{cases} Y^0 \to p + \pi^- + \pi^0 + Q \\ Y^0 \to n + \pi^+ + \pi^- + Q \end{cases}$$

where the proton and neutron decays might be expected to have equal probability. The results of this experiment cannot rule out this possibility.

The simple result that no ionizing proton was recognized, although 8 of our anomalous events must be of the neutron type of decay, can well be due to the expected difference in momentum spectra between the π's and the nucleons in this decay. (Indeed, in our restricted sample, for a similar decay mode, the Λ^0, only 18% of the protons were recognized, whereas all the negative π's had a momentum smaller than 600 MeV/c).

On the other hand, the comparison between the spectra of positive and negative secondaries cannot lead to any conclusion, because the expected difference is smoothed out by our measurability criterion which tends to increase in our restricted sample the proportion of neutron to proton decays and to distort the spectra. We have attempted to clear up this problem by com-

bining our results with those of other observers; the conclusion is that, experimentally, decays exemplified by equation (3) cannot be ruled out.

Theoretically it has to be remarked that this hypothesis does not fit the present accepted picture for strange particles. On the other hand, the Columbia group (6,7) has given a convincing experimental proof that long lived anomalous V⁰'s exist and are K-particles. The hypothesis (3) must therefore be rejected if the anomalous decays observed near the producer in this cosmic ray experiment are of the same type as those observed by the Columbia group.

A search has been made for possible examples of the decay:

$$\overline{\Lambda}^0 \to p^- + \pi^+ + 37\ \text{MeV}\,. \tag{4}$$

Only four events are compatible with this mode of decay, but three of these are in excellent agreement with the θ^0 mode. The last (no. 63 see Table I) has a $Q(\pi, \pi)$ which lies 2.9 standard deviations below that obtained for the θ^0. We cannot therefore rule out the possibility that it is a θ^0 with large fluctuations; we can also consider this event as an anomalous K^0.

The conclusion is that although the presence of anomalous hyperon decays cannot be completely excluded, their contribution to V^0-decays is probably very small. From now on we shall assume that the anomalous decays are due to heavy mesons.

3. – The Q-value of the Λ^0.

The best Q-value for the Λ^0 was derived from a straight averaging of the values obtained by selecting from the total sample of 70 Λ^0's, 18 class A-events with errors $dQ \leqslant 2.2$ MeV. The reasons for restricting the choice to class A-events are indicated in the Appendix. The supplementary choice of $dQ \leqslant 2.2$ MeV allows us to neglect the effect of asymmetry in our errors. The numerical value of 2.2 MeV is arbitrary and arises from a convenient gap in the distribution of the individual dQ values. The final result is:

$$Q_{\Lambda^0} = (37.9 \pm 0.4)\ \text{MeV}\,.$$

The basic data on the 18 events are given in Table II (*). Other groupings of events, such as straight and weighted mean on the whole group of 70 events

---

(6) K. Lande, E. T. Booth, J. Impeduglia, L. M. Lederman and W. Chinowsky: *Phys. Rev.*, **103**, 1901 (1956).

(7) K. Lande, L. M. Lederman and W. Chinowsky: *Phys. Rev.*, **105**, 1925 (1957).

(*) See note added in proof at the end of the paper.

yield no significantly different results from the one quoted. Moreover the distribution of the 52 remaining events around the value of 37.9 MeV is in good agreement with that expected from the estimated individual errors.

TABLE II. – *Results on the* 18 Λ^0*'s of quality A selected for the final Q-value.*

N.	p_+ (MeV/c)	p_- (MeV/c)	φ (degrees)	$Q(\mathrm{p}, \pi)$ (MeV)
11	$766^{+17.5}_{-16.8}$	$283.0^{+3.47}_{-3.39}$	13.1 ± 0.13	$36.57^{+1.9}_{-1.9}$
13	$138^{+15.3}_{-12.9}$	$134.4^{+3.07}_{-2.94}$	56.8 ± 0.89	$38.89^{+1.71}_{-1.70}$
34	634^{+35}_{-31}	$143.1^{+4.7}_{-4.4}$	53.7 ± 0.07	$38.05^{+2.01}_{-1.98}$
45	417^{+13}_{-12}	$164\ ^{+4}_{-3.8}$	44.8 ± 0.18	$37.93^{+1.70}_{-1.62}$
47	968^{+30}_{-28}	$261\ ^{+5.65}_{-5.41}$	28.1 ± 0.11	$41.09^{+1.87}_{-1.80}$
72	401^{+11}_{-10}	$205.8^{+2.6}_{-2.6}$	10.6 ± 0.21	$37.96^{+1.6}_{-1.6}$
74	347^{+10}_{-9}	$181.0^{+2.8}_{-2.7}$	25.3 ± 0.13	$37.29^{+1.38}_{-1.35}$
80	$1\,181^{+35}_{-33}$	$286.0^{+4.2}_{-4.1}$	24.5 ± 0.12	$38.10^{+1.2}_{-1.2}$
83	857^{+26}_{-24}	$163.5^{+4.7}_{-4.4}$	42.7 ± 0.22	$35.86^{+1.82}_{-1.74}$
88	$1\,135^{+34}_{-32}$	$98.6^{+4.8}_{-4.4}$	45.9 ± 0.26	$39.02^{+1.93}_{-1.82}$
89	545^{+13}_{-12}	$215.8^{+4.4}_{-4.3}$	23.9 ± 0.17	$36.85^{+1.84}_{-1.79}$
125	365^{+21}_{-19}	$129.1^{+3.4}_{-3.2}$	65.7 ± 0.43	$37.41^{+1.84}_{-1.74}$
129	542^{+25}_{-23}	$221.3^{+2.83}_{-2.76}$	26.2 ± 0.15	$40.88^{+1.74}_{-1.81}$
135	$1\,146^{+42}_{-39}$	$297.2^{+4.0}_{-3.9}$	21.5 ± 0.16	$35.01^{+1.6}_{-1.6}$
141	$1\,237^{+56}_{-52}$	$290\ ^{+5.4}_{-5.2}$	23.7 ± 0.08	$36.75^{+1.55}_{-1.55}$
157	484^{+18}_{-17}	$199.6^{+4.0}_{-3.9}$	30.9 ± 0.21	$39.42^{+2.1}_{-2.1}$
162	$1\,066^{+59}_{-53}$	$234.1^{+4.7}_{-4.5}$	30.1 ± 0.14	$36.62^{+1.52}_{-1.45}$
163	$1\,227^{+79}_{-70}$	$271.9^{+4.4}_{-4.3}$	26.6 ± 0.15	$39.00^{+1.1}_{-1.1}$

The error quoted has the meaning of a standard deviation. The effect of possible systematic errors was found to be small compared to the statistical error quoted and was therefore neglected. Using the results obtained in the Appendix, the computed maximum effects on the Q-values are:

— magnetic field ($\Delta Q = \pm 0.3$ MeV),

— systematic gas distortion ($0 < \Delta Q < +0.25$ MeV),

— wrong interpretation ($\Delta Q = \pm 0.17$ MeV).

This last was estimated by assuming that one of the 18 events, displaced by two standard deviations from the mean, was not a Λ^0.

For comparison with previous work we refer to the review article (³) and

also to a more recent measurement [8]. The error quoted for the cloud chamber results in these papers are probable errors.

We note that our result lies 1 MeV above the well known emulsion group value [9] ($Q = 36.92 \pm 0.22$ MeV). Nevertheless these two measurements cannot be considered as incompatible, since they differ by two standard deviations.

4. – Difference in the primaries responsible for θ^0 and anomalous decays.

In this section and in the next, we consider all events deviating by three or more standard deviations from the Q of the Λ^0-particle. Following the conclusions of Sect. 2, we assume that all these 51 events represent decays of heavy mesons. The general results are summarized in a histogram (Fig. 3). Its general appearance is very much like that obtained by the Indiana group [10] when establishing the existence of the θ^0-particle. However, in our case there is an overlap between the events contributing to the θ^0 line and the background of anomalous cases. Eleven events differ by more than three standard deviations from the mean value of 217 MeV to be found later (see Sect. 5) for the θ^0 mode of decay. These events are the ones discussed in Sect. 2 and are listed in Table I.

The interpretation of the $Q(\pi, \pi)$ histogram given above is strenghtened and acquires a significant meaning when the distribution of Q-values as a function of « primary » momentum P (defined as $|\boldsymbol{P}| = |\boldsymbol{p}_+ + \boldsymbol{p}_-|$) is considered. This is done graphically in Fig. 4. A strong correlation between Q and P is clearly manifest in the diagram; thus, while for values of P smaller than 1.2 GeV/c the ratio of anomalous to the total number of decays is 9/12, this ratio is reduced to 2/39 for P greater than 1.2 GeV/c. These two ratios are clearly incompatible and we may conclude that the particles responsible for the normal and the anomalous decays have either a different lifetime or a different spectrum at production, or both.

This result may be criticized on the grounds that the Q-correlation has been made with respect to the « visible » momentum P which does not include the momentum carried by the neutral particle(s). We can estimate the momentum of the neutral secondary since all the three-particle decays that may be envisaged to account for the anomalous events will have secondaries either

---

[8] W. B. Fretter, E. W. Friesen and A. Lagarrigue: *Suppl. Nuovo Cimento*, **4**, 569 (1956).

[9] M. W. Friedlander, D. Keefe, M. G. K. Menon and M. Merlin: *Phil. Mag.*, **45**, 533 (1954).

[10] R. W. Thompson, F. R. Burwell and R. W. Huggett: *Suppl. Nuovo Cimento*, **4**, 286 (1956).

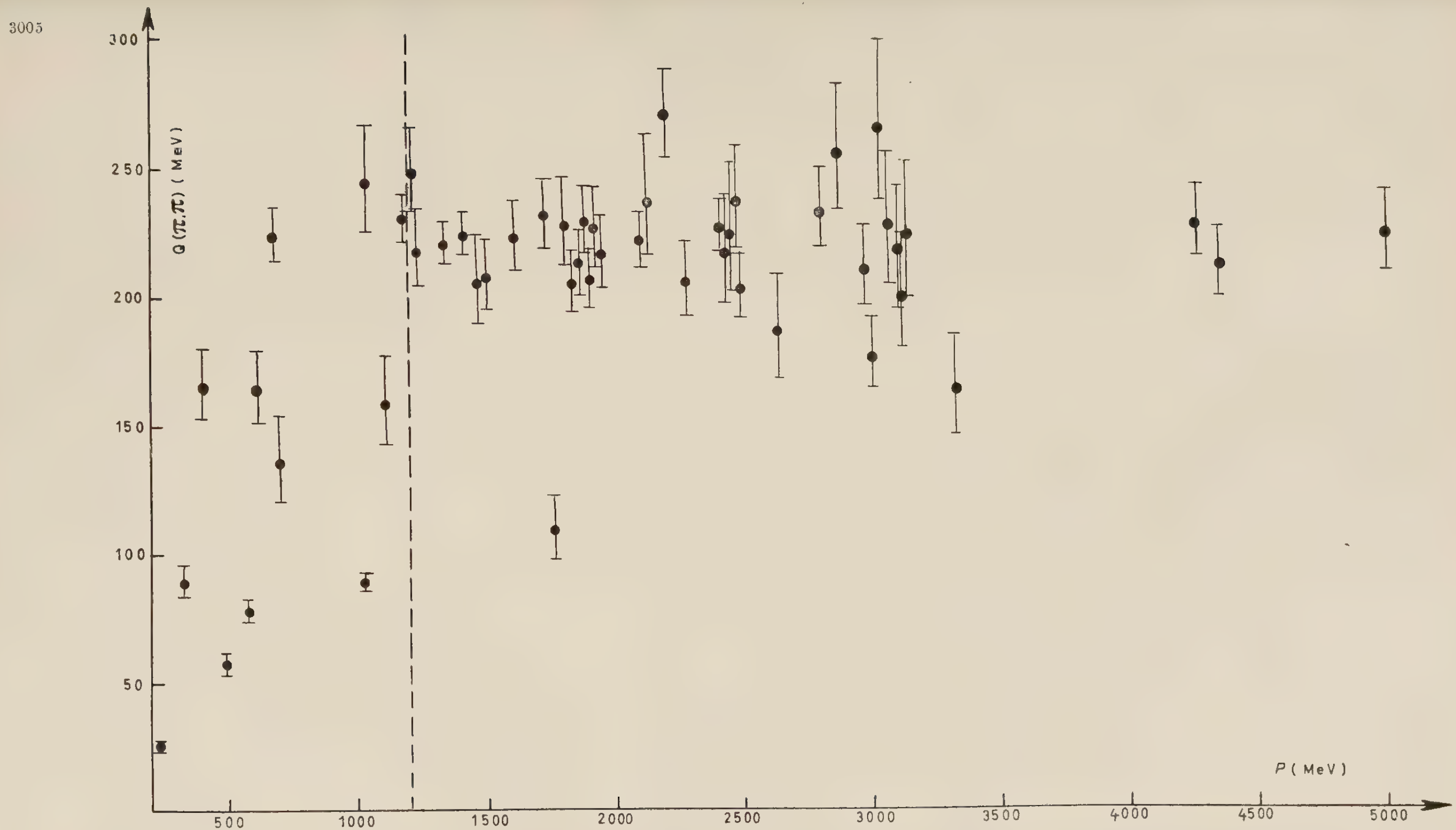

Fig. 4. – Distribution of $Q(\pi, \pi)$-values for non-Λ^0-events as a function of total longitudinal momentum $P = |\boldsymbol{p}_+ + \boldsymbol{p}_-|$.

with nearly equal masses or moving relativistically in the center of mass. In either case each secondary in the laboratory system will, on the average, contribute equally to the total primary momentum. A good approximation to the total momentum can consequently be obtained by multiplying P by 1.5. The correlation between Q's and momenta does not change significantly since the new ratios of anomalous to the total number of events below and above 1.2 GeV/c total momentum are 7/10 and 4/41 (the chance that this difference arises from a statistical fluctuation is smaller than 0.1%).

It has also to be noted that always under the assumption of a single particle being responsible for the non-Λ^0 group, the measurement criterion (see Sect. **1**) used to select the events may introduce a bias tending to increase the ratio under consideration, as the total primary momentum increases.

The significant difference found above proves that, as a group, anomalous events cannot be considered as alternate modes of decay of the particle responsible for the θ^0 mode of decay.

In a recent paper the same conclusion has been reached by the C.I.T. group [11] from the observation of a certain number of differences between θ^0 and anomalous events. There is also a direct and convincing evidence for the existence of a long lived K^0-meson [6,7] which decays in anomalous modes. The simplest interpretation of our result is therefore that the anomalous V^0-decays observed in cosmic rays immediately below a producer are of the type observed by the Columbia group at much longer times of flight. Compared to the results obtained by the Columbia group about the secondaries of anomalous V^0-decays our information is very meagre. This information is given in Table I. The example of an (e^-, π^+)-decay, previously reported [12] does not belong to our restricted sample.

5. – The Q-value of the θ^0 mode of decay.

The significant correlation between Q-values and primary momenta obtained in the last section will permit the selection, independently of Q-values, of a

---

[11] J. A. Kadyk, G. H. Trilling, R. B. Leighton and C. D. Anderson: *Phys. Rev.*, **105**, 1862 (1957).

One may note that 10 of the 18 V^0's considered in this paper as anomalous had a Q-value that differed from the θ^0 Q-value by less than two standard deviations, as can be seen from the raw data of Table I. This tends to reduce the statistical significance of these results.

[12] C. d'Andlau, R. Armenteros, A. Astier, H. C. DeStaebler, B. P. Gregory, L. Leprince-Ringuet, F. Muller, C. Peyrou and J. H. Tinlot: *Nuovo Cimento*, **4**, 917 (1956).

sample of events in which the θ^0-mode largely predominates. We will only consider in this section those V^0's which are not Λ^0's and for which the total momentum is larger than 1200 MeV/c (changing the cut-off to 1500 MeV/c does not affect the result appreciably).

39 events remain, of which only one (no. 82, $Q(\pi, \pi) = (109 \pm 12)$ MeV) is obviously anomalous. Three other events (Table I, no. 50, 63 and 12) have Q-values which deviate by 3 standard deviations or so from the mean. We cannot rule out the possibility that some of these three events are θ^0's in which, statistically, the error was large; but the probability for all three to be θ^0's is much less than 1%. Since among the three Q-values two are low and one high, and since it is not possible to decide which ones are anomalous, we shall not include them in our calculated mean. This procedure involves a supplementary error which will be considered later.

The final Q-value is now derived from a straight averaging of 22 events, belonging to class A and for which the individual error was smaller than 17 MeV (*). The reasons for this choice are similar to the ones discussed in Sect. 3. Moreover a weighted mean, in this case, would favour slower events which have a better chance of being anomalous (Sect. 4).

The final result is:

$$Q_{\theta^0} = (217.0 \pm 2.8)\ \text{MeV}\,.$$

The distribution of these 22 V^0's, listed in Table III gives an external dispersion corresponding to an error on the mean of 2.3 MeV.

The distribution of the remaining events around this mean is good if one excludes events no. 50, 63 and 12. If these are included, the χ test (less than 0.1% chance) shows again that some (or all) of these three events do not belong to the group.

The error quoted has the meaning of a standard deviation and does not include systematic errors. Using the results obtained in the Appendix, the computed maximum effects on the Q-values are:

— magnetic field: $\Delta Q = \pm 1.5$ MeV,

— systematic gas distortion: $\Delta Q = + 0.5$ MeV,

— wrong interpretation: $\Delta Q = \pm 3.5$ MeV.

This last was estimated by adding to the 22 events, first the two highest (no. 50 and no. 120 $Q = (249^{+18}_{-15})$ MeV), then the two lowest Q-values (no. 63 and n. 12).

(*) In the choice of these events, account was taken of the fact that the quoted error is a function of the actual measurement. This effect would tend to bias the choice towards low Q-values. Event 139 was included because, assuming a Q of 217 MeV, the recalculated error was smaller than 17 MeV.

TABLE III. – *Results on the 22 θ^0's of quality A selected for the final Q-value.*

N.	p_+ (MeV/c)	p_- (MeV/c)	φ (degrees)	$Q(\pi, \pi)$ (MeV)
5	$3\,026^{+275}_{-233}$	$1\,329^{+56}_{-51}$	11.0 ± 0.11	$210.5^{+14.5}_{-12.5}$
6	397^{+19}_{-17}	$1\,491^{+83}_{-75}$	27.1 ± 0.19	$213.2^{+11.9}_{-10.8}$
21	$1\,796^{+202}_{-176}$	881^{+41}_{-38}	16.4 ± 0.14	$186.1^{+17.9}_{-14.6}$
43	962^{+32}_{-30}	$1\,336^{+119}_{-101}$	19.9 ± 0.14	$204.7^{+14.8}_{-12.6}$
53	$1\,581^{+105}_{-93}$	$317^{+9.8}_{-9.2}$	28.7 ± 0.13	$229.6^{+13.7}_{-12.1}$
95	$1\,901^{+227}_{-182}$	$1\,111^{+83}_{-73}$	15.6 ± 0.17	$209.8^{+16.9}_{-13.5}$
116	$268^{+13.3}_{-12.0}$	$1\,555^{+97}_{-86}$	26.2 ± 0.12	$205.4^{+12.0}_{-10.7}$
119	$523^{+13.7}_{-13.0}$	$1\,585^{+97}_{-86}$	24.3 ± 0.13	$220.7^{+10.3}_{-9.3}$
123	$2\,106^{+226}_{-171}$	$2\,145^{+255}_{-207}$	11.4 ± 0.15	$226.8^{+15.1}_{-13.2}$
127	$1\,427^{+109}_{-95}$	556^{+15}_{-14}	25.1 ± 0.07	$216.3^{+15.7}_{-13.4}$
130	$1\,086^{+35}_{-33}$	296^{+20}_{-18}	38.2 ± 0.09	$220.8^{+8.4}_{-7.7}$
139	$1\,560^{+141}_{-119}$	$271^{+10.0}_{-9.0}$	29.4 ± 0.08	$227.9^{+18.7}_{-15.9}$
143	$1\,119^{+87}_{-76}$	$1\,338^{+96}_{-84}$	19.8 ± 0.08	$226.2^{+10.4}_{-9.4}$
144	$1\,172^{+83}_{-72}$	502^{+22}_{-20}	30.3 ± 0.14	$223.2^{+14.3}_{-12.6}$
153	701^{+18}_{-17}	$2\,092^{+182}_{-155}$	19.0 ± 0.06	$232.8^{+16.2}_{-14.4}$
154	488^{+20}_{-18}	$2\,087^{+147}_{-128}$	18.6 ± 0.11	$202.7^{+13.3}_{-11.5}$
170	$322^{+10.4}_{-9.8}$	$1\,217^{+96}_{-83}$	32.4 ± 0.20	$208.1^{+15.0}_{-13.0}$
178	513^{+23}_{-21}	$1\,274^{+85}_{-75}$	29.2 ± 0.1	$231.2^{+15.1}_{-13.5}$
181	$2\,552^{+322}_{-258}$	$2\,436^{+238}_{-199}$	9.6 ± 0.15	$222.3^{+16.7}_{-14.1}$
183	827^{+54}_{-48}	$1\,673^{+202}_{-163}$	19.9 ± 0.15	$224.2^{+18.3}_{-14.8}$
186	835^{+41}_{-38}	$1\,137^{+74}_{-65}$	24.9 ± 0.17	226.3^{+9}_{-8}
192	965^{+35}_{-33}	993^{+81}_{-69}	23.4 ± 0.08	$206.2^{+12.0}_{-10.8}$

Finally, we estimate the total error to be ± 4 MeV and our result is:

$$Q_{\theta^0} = (217 \pm 4)\ \text{MeV}\,.$$

Previous results were: (214 ± 5) MeV ([10]) and (222.6 ± 5.5) MeV ([8]). In the first case, the error includes possible systematic effects (the standard deviation statistical error was ± 4 MeV). In the second case, the error quoted in the original paper was a probable statistical error; for the sake of consistency, we have given the corresponding standard deviation.

6. – The π nature of the secondaries of the θ^0-decay mode.

It has been well established that the θ^0 decays into a $\pi^\pm$ and another particle of mass smaller than or equal to that of the π (see for instance refe-

rence [3]). The belief in the π-nature of both secondaries arises from various sources:

a) The analogy with the known decay $K^+ \to \pi^+ + \pi^0$.

b) Under the assumption that the production of the θ^0 in the collision of π^- on hydrogen is of the type: $\pi^- + p \to \theta^0 + \Lambda^0$, the θ^0 must be a boson.

c) A proof has been attempted [10], based on a careful analysis of the distribution of the θ^0-events in an (α, p_t) plot. Although the method used is correct and elegant, it is a very difficult one, depending on differentiation between very closely lying Q curves by means of experimental points, the errors of which are not in all cases small in comparison with the separation of the curves.

We wish to supplement this information by a very direct evidence of the π-nature of both secondaries of the θ^0 mode of decay obtained through the observation of the behaviour of the secondaries entering the multiplate chamber. In four events (no. 14 (*), 140, 181 and 209 (*)) both secondaries produce a nuclear interaction in the multiplate chamber and are therefore neither μ's nor electrons. These events are not Λ^0's and their $Q(\pi, \pi)$-values are all in good agreement with the θ^0-mode:

$$(213^{+34}_{-29})\ \text{MeV}\ ; \qquad (239^{+21}_{-20})\ \text{MeV}\ ; \qquad (222^{+17}_{-14})\ \text{MeV}\ ; \qquad (209^{+44}_{-32})\ \text{MeV}\ .$$

Since it is already established that the θ^0 decays into a π and another particle of mass smaller than or equal to that of the π, we may conclude that the decay mode of the θ^0 is directly established to be:

$$\theta^0 \to \pi^+ + \pi^-\ .$$

We may note that for geometrical reasons the observation of secondaries in the bottom chamber presents a strong bias toward the more energetic events. The four events considered above have total momenta around 4 GeV/c. 21 secondaries of the 51 V^0's belonging to the non-Λ^0 group were directed towards the multiplate chamber. None were electrons and the number of nuclear interactions observed (16) confirms our previous analysis that most of the fast V^0's in this group are θ^0's decaying into two π's.

(*) These two events do not belong to the restricted sample.

APPENDIX

Measurements and errors.

1. *Measurements.* – The final measurements were made on full size projections of the 3 photographs taken of the momentum chamber. The radii of curvature were measured by adjusting to the trajectories arcs of circles of known curvature; the standard procedures were followed to convert these radii into momenta.

The space co-ordinates of each event were calculated (*) from measurements made on drawings of the same projections. The co-ordinates, in the conical projections, of four points on each track as well as those of the V^0 apex were measured; from these, the spatial co-ordinates were calculated after correcting for the effects due to the presence of the magnetic field and of the chamber expansion. The directions of the secondaries and thence the angle φ of the V^0 were obtained by a least squares fit.

Rough mass estimates have been made by combining the measured momenta with visual estimates of ionization. A check on the validity of the ionization estimates—used only when a mass differentiation can be made through a difference between the minimum of ionization and an ionization $\geqslant 2.5 \times$ minimum—is obtained from the fact that we very seldom fail to recognize a proton whose range in the multiplate chamber corresponds to an ionization $\geqslant 2 \times$ minimum in the upper chamber. Using this criterion, a particle of momentum $\leqslant 600$ MeV/c is classified as protonic or not protonic depending on whether the ionization is estimated to be different from the minimum or not. These estimates have only been used occasionally and do not play a very important part in the results of this paper.

2. *Statistical errors in momentum.* – The curvature is essentially derived from a measurement of a sagitta. Other sources of error (scattering and distortion) also affect directly the sagitta. In considering the momentum errors the sagitta will therefore be taken as the random variable.

The measurement is affected both by statistical and systematic errors. For the purposes of an analysis of Q-values, it is necessary to divide the statistical errors into two classes: dependent and independent, the division being determined by the way in which they affect the Q-value calculation.

Thus the errors due to scattering and those inherent to the measurement will affect each secondary of a given V^0 independently, while a more or less complete dependance will exist in those arising from the chamber distortions. An account follows on how these errors have been estimated.

(*) We wish to thank here the Compagnie des Machines Bull who graciously let us have free use of one of their « Γ » computers. We are particularly grateful to MM. Dreyfus, Lescaut and Cauderlier for the kind help they always gave us during the working out and checking of the programme as well as during the carrying out of the calculations.

Independent errors: In each case the r.m.s. error introduced by the multiple scattering (σ_S) of the particle in the gas of the chamber was computed using the standard formula [13]. The total independent error was a quadratic combination of σ_S and a somewhat less well defined measurement error (σ_M) due to ion diffusion, uncertainty of measurement, etc. which was estimated in the following manner.

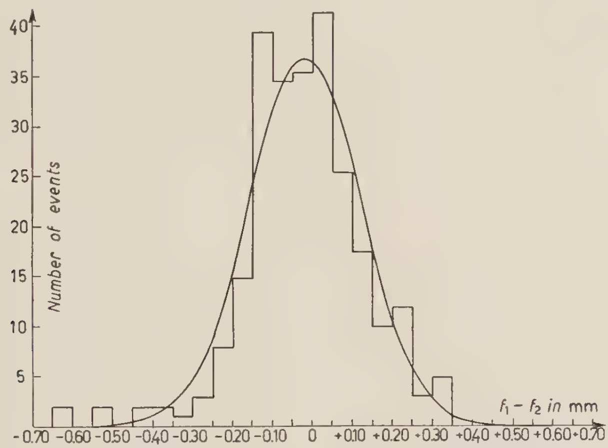

Fig. 5. – Histogram of the difference between two measurements f_1 and f_2 of a track. The best adapted Gaussian curve has a standard deviation: $\sigma = \sqrt{\langle(f_1 - f_2)^2\rangle} = 0.14$ mm.

Each track has been measured independently by two different persons on at least one of the 3 views. The distribution of the differences $(f_1 - f_2)$ in the two measures of sagittae, shown in the histogram of Fig. 5, allows us to calculate the measurement error. The experimental distribution is well fitted by a Gaussian distribution centered at $\langle f_1 - f_2 \rangle = 0$ and with a standard d-viation of 0.14 mm. Since each track has been measured on three views, the standard deviation—assuming complete independence in the measurements—of each complete measurement would be $\sigma_M = 0.14/\sqrt{6} = 0.06$ mm. A considerable contribution to the error must be due to ion diffusion, so that the condition of complete independence is not fulfilled. We can take the extreme view that this ultimate limit has been reached in our measurements and then $\sigma_M = 0.14/\sqrt{2} = 0.10$ mm. Since a calculation such as that suggested by BLACKETT [14] of the error due to diffusion cannot be made reliably under our experimental conditions, we have finally taken an intermediate value $\sigma_M = 0.08$ mm to represent the standard error in the measurement of sagitta. The track-length measured—especially in the cases used for the final Q-values estimations—being fairly constant no account has been taken on the possible variation of this error with measured length.

(13) B. ROSSI: *High Energy Particles*, p. 72.
(14) P. M. S. BLACKETT: *Suppl. Nuovo Cimento*, **2**, 264 (1954).

3011

Dependent errors: Chamber distortions have been measured by comparing the calculated and the measured sagittae of 58 tracks of protons which after passing through the magnetic chamber stopped in the multiplate chamber.

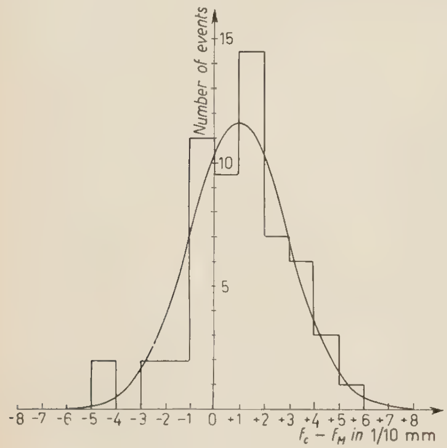

Fig. 6. – Histogram of the differences between the calculated sagitta of a proton (f_C) and the measured sagitta (f_M). The drawn Gaussian has a mean value of 0.1 mm and a standard deviation of 0.2 mm.

In Fig. 6 the distribution of the quantity $\Delta f = f_C - f_M$ is shown; f_M is the measured sagitta and f_C that calculated for the same track length (45 cm on the average) on the assumption that the track was that of a proton of known residual range. To the experimental histogram the best Gaussian distribution that can be adapted is characterized by a mean value $\langle \Delta f \rangle = (0.1 \pm 0.03)$ mm and a standard deviation $\sigma = 0.2$ mm.

The contribution of a gas distortion can now be obtained by subtracting quadratically the contributions due to the uncertainty on the exact range of the proton in the plate chamber, the multiple scattering in the momentum chamber and the measurement error estimated above. The standard deviation for gas distortion (σ_D) is found to be:

$$\sigma_D = 0.14 \text{ mm}.$$

Although this number has been obtained for long vertical tracks, we have applied it to all our measurements disregarding track-length and position. In order to determine Q-values, only those events in which the measurements corresponded to long vertical tracks were used (unless the main error was due to scattering).

3. *Systematic errors in momentum.* – In the preceding section an estimate was made of the random error to be attributed to our individual measurements. Since a large number of events were measured, systematic errors may represent an important contribution to the uncertainty on the final result. We have therefore estimated what we believe to be upper limits to the systematic error arising from different causes.

Systematic gas distortion: In Fig. 6 we observe that the mean value of the measured proton sagittae is slightly lower than the calculated one. The displacement was $\langle \Delta f \rangle = (0.1 \pm 0.03)$ mm. This deviation could be due to various causes among which the most important are: systematic gas distortion, and the failure to detect nuclear interactions of the protons at the end of their range. This last cause of error is difficult to estimate, but could explain the measured difference. We therefore conclude that our method of calibration is not well suited to a measurement of systematic gas distortion. Nevertheless our final measurements can be used to estimate this error. An assumed systematic gas distortion will change the true Q-value of each Λ^0- and θ^0-event by an amount dQ which is in first approximation a linear function of the

distortion sagitta. This dQ calculated for a given distortion will have a different magnitude and sign from event to event. In Fig. 7 we have plotted for Λ^0's and θ^0's the measured Q-values as a function of the calculated dQ assuming a $+0.1$ mm systematic distortion. In both cases no systematic effect is observed. Limits may be set by drawing extreme lines compatible with the data. The corresponding extreme values for a systematic gas distortion expressed in sagitta would be between 0 and $+0.1$ mm.

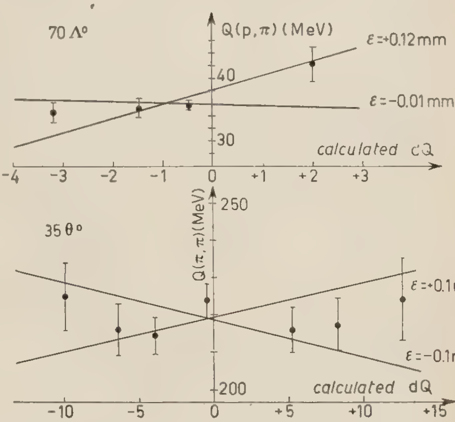

Fig. 7. – Effect of an assumed systematic distortion on the Q-values of Λ^0 and θ^0. The abscissa corresponds to a calculated dQ assuming a 0.1 non-systematic distortion. Each point corresponds to a group of events for which the errors in the Q-values are of the same magnitude. The slopes ε of the lines drawn give the limits on the possible systematic distortion.

M a g n e t i c f i e l d c a l i b r a t i o n: Absolute measurements of the magnetic field at the centre of the chamber have been made for different intensities of coil current; these measurements were made at the beginning and at the end of the run, using the magnetic resonance method (*). Three ammeters—two of which are photographed immediately after the expansion of the chambers— were thus calibrated. The consistency of their relative readings has been verified at frequent intervals.

The field variation over the volume of the chamber was measured with a flux-meter. The variation is very small—it never exceeds 5% of the value at the centre—but allowance has been made for it by taking as effective field the homogeneous equivalent field for vertical tracks distributed at random in the chamber. This effective field differs by 0.7% from that at the centre of the chamber.

The uncertainty in the magnetic field knowledge has been estimated to be smaller than $\pm 0.5\%$; this value is arrived at by adding together an uncertainty of $\pm 0.2\%$, representing the dispersion of the readings in the two series of calibration measurements, and an estimated uncertainty smaller than 50% in the correction made to arrive at the effective field.

W r o n g i n t e r p r e t a t i o n o f e v e n t s: We have considered in each case an upper limit to the error introduced by a possible contamination of events which do not correspond to the type studied.

4. *Error in Q-values.* – Assuming a two body decay into a positive and a negative particle of known masses the three measurements of momenta (p_+, p_-) and total angle (φ) allow a calculation of the Q-value. We have calculated for

---

(*) We wish to thank M. LECOMTE of the CEA for the care and interest with which he carried out this calibration.

3013

all events $Q(\mathrm{p}, \pi)$ and $Q(\pi, \pi)$ in which the assumed masses are indicated. p stands for proton of mass 938.2 MeV and π for a charged meson of mass 139.5 MeV. The errors for each Q may be computed as a function of the momenta and angle errors. Since the error in angle due to recontruction uncertainties is always very small we have not discussed the method used to compute it.

Whenever the two tracks have similar lengths and appear in the same region of the chamber we have assumed full correlation for dependent errors; the total error was then:

$$\mathrm{d}Q^2 = \mathrm{d}Q^2_{\mathrm{p}+\,\mathrm{ind.}} + \mathrm{d}Q^2_{\mathrm{p}-\mathrm{ind.}} + (\mathrm{d}Q_{\mathrm{p}+\,\mathrm{dep}} + \mathrm{d}Q_{\mathrm{p}-\mathrm{dep}})^2 + \mathrm{d}Q^2_{\varphi}\,.$$

For the other extreme case in which the two secondaries are in very different regions we have assumed no correlation and in this case:

$$\mathrm{d}Q^2 = \mathrm{d}Q^2_{\mathrm{p}+} + \mathrm{d}Q^2_{\mathrm{p}-} + \mathrm{d}Q^2_{\varphi}\,.$$

For intermediate cases we have assumed partial correlation.

Finally two classes of events were considered; class A for which the error was essentially due either to a momentum measurement of a long vertical track (similar to the reference protons) or to scattering. We feel that a good external check of the error exists for these events. Although no external check is available for the other events, we have observed that their r.m.s. deviation from the mean (obtained for A events) is in good agreement with that calculated using the estimated errors.

Note added in proof.

It was pointed out to us by Professor THOMPSON that our value for the Q_{Λ^0} might be affected by our method of selecting non-θ^0-events.

The effect of this bias can be estimated by an iteration process in determining the so-called non-θ^0-events and is negligible in our case. See for details the *Proceedings of the International Conference on Mesons and recently discovered particles* (Padua-Venice, September 1957).

RIASSUNTO (*)

Si è fatto uno studio di 161 decadimenti V^0 osservati nella camera doppia dell'École Polytechnique installata al Pic-du-Midi. Questi eventi corrispondono a una scelta rigorosa basata sulla misurabilità dei momenti dei due secondari (superiore al 10%). I risultati principali sono: 1) Nessuna prova diretta di decadimenti anomali di iperoni neutri. All'esistenza di vari modi ipotetici di decadimento si possono porre limiti superiori (6 a 8%). 2) I valori di Q per il decadimento Λ^0: $Q_{\Lambda^0} - (37.9 \pm 0.4)$ MeV. 3) L'identificazione diretta della natura π di ambi i secondari del modo di decadimento θ^0. 4) Il valore di Q per il decadimento θ^0: $Q_{\theta^0} = (217 \pm 4)$ MeV. 5) Una prova diretta della non identità delle particelle responsabili del decadimento θ^0 e dei decadimenti V^0 anomali basata sulla differenza significativa tra il numero di eventi lenti e rapidi delle due categorie.

(*) *Traduzione a cura della Redazione.*

IL NUOVO CIMENTO Vol. VI, N. 5 1° Novembre 1957

A Multiplate Cloud Chamber Study of Unstable Particles (*) (+).

M. Annis (×), N. F. Harmon (†) and R. D. Sard

Washington University - St. Louis, Missouri

(ricevuto il 31 Luglio 1957)

Summary. – A multiplate cloud chamber has been operated at mountain altitude under a penetrating shower selector. The distribution of scattering angles of penetrating secondaries is used to determine jointly the exponent γ of their differential momentum spectrum and the noise level, σ_1, of the chamber. γ is 2 to 2.5, and σ_1 is less than $0.8\cdot 10^{-2}$ radians, corresponding to a maximum detectable momentum (standard error) of more than 2 GeV/c. Several unusual decays in flight have been found. In one, a charged V-decay gives rise to a photon, recognized by the electron shower it produces. The event is interpreted as $K_{\pi 2}\to\pi+\pi^0$, the π^0 decaying in its normal (2γ) mode). In another, a V^0-decay gives an interacting penetrating particle and a particle producing an electron shower in the first plate it strikes. The event is dynamically compatible with $\theta^0\to\pi+\pi+214$ MeV, but the charge exchange that must then be postulated is very improbable. A more likely interpretation is β-decay: $K^0_\beta\to\pi+e+?^0$. From the observed energy release the neutral particle must be massless if K^0_β has the same mass as the other K-particles. Finally, a case is reported that appears to be a cascade decay of a neutral V into a charged one. The charged V decays into an interacting light particle, probably a π-meson. The most likely interpretation in terms of presently known particles is $V^0\to\Sigma^\pm+\pi^\mp$; $\Sigma^\pm\to\pi^\pm+n$, with a mass of at least 1390 MeV ($Q_{\Sigma\pi}\geqslant 60$ MeV).

(*) Supported by the joint program of the ONR AND AEC and by a grant from the Research Corporation.

(+) The present article is based on a thesis presented by N. F. Harmon to the Board of Graduate Studies of Washington University in Setember 1955 in partial fulfillment of the requirements for the degree of Doctor of Philosophy. The results have been presented at the Monterey meeting of the American Physical Society, Dec. 27, 28, 1956 (*Bull. Am. Phys. Soc.*, **1**, 377, 386 (1956)).

(×) Now at Allied Research Associates, Inc., Boston, Mass.

(†) Salt Lake City, Utah.

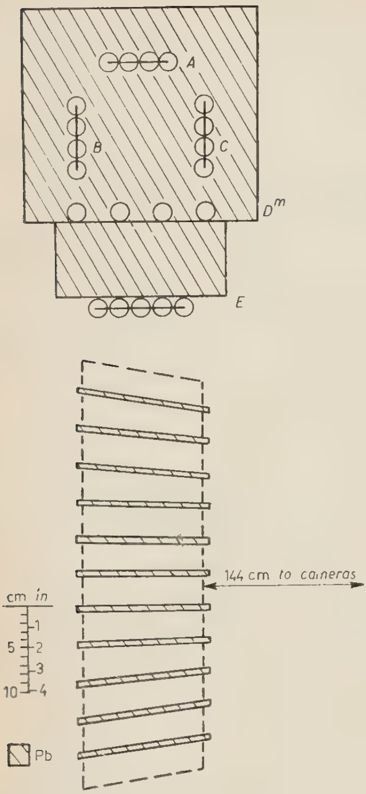

Fig. 1. – The arrangement of material.

1. – Introduction.

The present experiment was undertaken several years ago as a contribution to the study of the properties of the new unstable particles. In the time that has elapsed before completion of our analysis, a good deal of progress has been made in this field. Our contribution is therefore limited to several unusual cases of decay in flight (1), and to a statistical study of the scattering of penetrating shower particles from which it has been possible to determine jointly the momentum spectrum of these particles and the « noise level » scattering of our chamber.

The sample studied consists of 3 000 events photographed at Berthoud Pass, Colorado (2) (altitude 3 400 m) in the late summer of 1952. The arrangement of material is shown in Fig. 1. The triggering arrangement was a multiple Geiger tube penetrating shower selector. During most of the run it required BCD^2E, i.e. one or more tubes discharged in group B, one or more in group C, two or more in group D, and one or more in group E. For the rest of the time, a pulse from group A was also required.

The cloud chamber (3), of illuminated volume 50 cm × 50 cm × 13 cm, contained eleven lead plates of 0.63 cm thickness (7.2 g cm^{-2}). It was filled with argon and 65 – 35 ethyl al ohol-water vapor to a total pressure of 76 cm Hg at 26.7 °C. Four photographs of the chamber were taken at each event, two being a binocular pair, for convenience in preliminary scanning, and two wide-angle views, at ± 16° off axis, that permitted more precise localization in the chamber.

(1) An early example of a τ-decay in flight has already been reported: M. Annis and N. F. Harmon: *Phys. Rev.*, **88**, 1202 (1952).

(2) We are indebted to Messrs. Piccioni and Cool and their colleagues at the Brookhaven National Laboratory for making it possible for us to use their cabin at Berthoud Pass.

(3) E. J. Althaus: *Washington University Thesis*, 1950; E. J. Althaus and R. D. Sard: *Phys. Rev.*, **91**, 373 (1953).

The scanning and measuring were carried out on a viewing table of the type used previously by one of us (4). The wide-angle views were projected side by side, at $1.25\times$ full size. The positions of blobs were determined analytically from rectangular co-ordinate measurements on the table. The angles of V's were computed from such position determinations.

Measurements of scattering in the plates were made on the table with a special protractor, reading to $1\cdot10^{-3}$ radians. The true scattering angles, orthogonally projected on two mutually perpendicular planes, were computed rigorously (5) from the measurements on the conically projected views. For a particle penetrating all eleven plates, we thus had twenty-two statistically independent cells. The standard theory of sampling from a normal distribution and Molière's formulation of the multiple scattering distribution were used to estimate the momentum times velocity of the particle (6).

The energies of photon-induced showers were estimated from number of track segments and size at the maximum according to Bender's calibration (7) which used the same set of pictures.

2. – Noise level and momentum spectrum.

The multiplate cloud chamber can be used to estimate the momentum times velocity ($\Pi = p\beta c$) of a particle (6,8) if the scattering angles in the plates are sufficiently large relative to the experimental errors and if the number of plates traversed is sufficient to give a statistically significant sample of scattering angles.

It is convenient to specify the experimental errors, resulting both from the cloud chamber behavior (ion diffusion, δ-ray scattering, gas motion, etc.) and from measuring errors, by the standard deviation, σ_1, of the noise angle distribution, or « noise level ». Instead of estimating from a set of pictures obtained with a special triggering arrangement, we estimate it from its effect in our data on the apparent momentum spectrum of the penetrating particles from locally produced penetrating showers. It appears to be possible to make a joint determination of the exponent of this spectrum and of the noise level.

(4) M. Annis: *Mass. Inst. of Technology Thesis*, 1951.

(5) R. J. Safford: private communication.

(6) S. Olbert: *Phys. Rev.*, **87**, 319 (1952); M. Annis, H. S. Bridge and S. Olbert: *Phys. Rev.*, **89**, 1216 (1953).

(7) P. Bender: *Nuovo Cimento*, **2**, 980 (1955).

(8) M. Annis, W. B. Cheston and H. A. Primakoff: *Rev. Mod. Phys.*, **25**, 818 (1953).

Assume that the prior probability that Π lie in $\mathrm{d}\Pi$ is

$$(1) \qquad P(\Pi)\,\mathrm{d}\Pi = \begin{cases} 0, & \text{for } \Pi < \Pi_{co} \\ N_\pi \Pi^{-\gamma}\,\mathrm{d}\Pi, & \text{for } \Pi > \Pi_{co}, \end{cases}$$

where Π_{co} specifies the lower limit of acceptance of the detecting apparatus. Assume a Gaussian noise-angle distribution, of variance, σ_1^2, and a Gaussian distribution for the real scattering angles, of variance GQ, where these quantities are as defined in Olbert's adaptation [6] of the Molière scattering expressions to multiplate chambers. With our method of selecting tracks for this sample (see below) the assumption of a Gaussian multiple scattering distribution is a good approximation. If t_2 is the root-mean-square of the n observed scattering angles of a particle, its expected distribution [9] is

$$(2) \qquad G(\sigma_1, \gamma; t_2)\,\mathrm{d}t_2 = N_{t_2} t_2^{n-1}\,\mathrm{d}t_2 \int \frac{\mathrm{d}\Pi\,\Pi^{-\gamma}}{((A^2/2\Pi^2) + \sigma_1^2)^{n/2}} \exp\left[\frac{-nt_2^2}{2((A^2/2\Pi^2) + \sigma_1^2)}\right],$$

where $A^2 = \Pi^2\, 2\, GQ$ and N_{t_2} is a normalization factor. Our procedure is to determine a histogram of t_2's for an appropriate sample, and to compare this histogram with $G(t_2)$ computed numerically according to (2) for various assumed values of σ_1 and γ. Comparison of the histogram and the computed curves allows us to estimate both σ_1 and γ.

The histogram shown in Fig. 2*a* and 2*b* results from measurements on forty-nine particles selected according to the following criteria:

1) The particle traverses all eleven plates in the well-illuminated region of the chamber, with ionization not noticeably above minimum.

2) No particular scattering angle exceeds thrice the r.m.s. value of the other scattering angles, to stay within the limits of the Gaussian approximation.

3) The track is accompanied by at least one other penetrating one, to ensure that it is part of a locally produced penetrating shower. Scatterings in the top and bottom plate were not measured, so $n = 18$ rather than 22. The penetration requirement (1) sets a lower limit, $\Pi_{co} = 250$ MeV, for π-mesons. The cut-off is actually not sharp, however, because the small-scattering requirement (1) introduces a bias against small values of Π. It is thought that this bias accounts for the falling-off of the histogram for $t_2 > 1 \cdot 10^{-2}$ radians. We base our estimates of σ_1 and γ entirely on the observed distribution at smaller values of t_2.

---

[9] We proceed as in ref. [8], eq. (10)–(15).

Fig. 2a shows the curves calculated for $\gamma = 3$ and $\sigma_1 = 0.3 \cdot 10^{-2}$ radians and $0.8 \cdot 10^{-2}$ radians. Lower values of σ_1 than $0.3 \cdot 10^{-2}$ gave essentially the

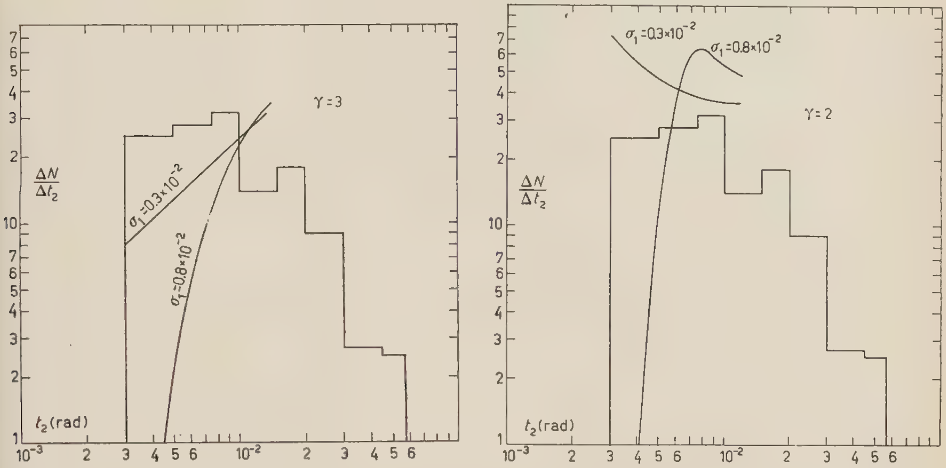

Fig. 2. – Comparison of observed scattering distributions with the curves expected (Eq. (2)) for various σ_1 and γ. 2a): $\gamma=3$, $n=18$; 2b): $\gamma=2$, $n=18$.

same slope in the region of interest. We conclude that $\gamma < 3$, as $\gamma = 3$ gives too rapid a fall of the momentum spectrum at high momenta. Fig. 2b shows the corresponding curves for $\gamma = 2$. The curve for $\sigma_1 = 0.8 \cdot 10^{-2}$ is again too steep as well as displaced; that for $0.3 \cdot 10^{-2}$ radians slopes the wrong way. A momentum exponent of 2 to 2.5 seems most likely, with σ_1 between $0.3 \cdot 10^{-2}$ and $0.8 \cdot 10^{-2}$ radians. The former estimate is in excellent agreement with a direct magnet cloud chamber determination ([10]),

$$\gamma = 2.5 \pm 0.3 \, ,$$

having Π_{co} in the range $500 \div 1000$ MeV. The lower limit on σ_1 happens to correspond to the precision with which the scattering protractor can be set on a typical track segment. The upper limit, which is certainly too high, corresponds to an apparent Π of 1.9 GeV. We conclude that in this batch of pictures momentum-velocity estimates from scattering measurements in nine plates (18 cells) are meaningful for $\Pi < 2$ GeV. In general ([8]), for n cells, $\Pi_{max} \sim 2(n-\gamma)^{-\frac{1}{2}}$.

([10]) K. H. Barker and C. C. Butler: *Proc. Phys. Soc.*, A **64**, 4 (1951).

3. – A charged V-decay with an associated electron shower.

Fig. 3 shows a decay in flight of a charged particle with en electron shower apparently produced by a photon from the point of decay. A minimum ionizing particle enters the chamber above Pb-1 near *e* (it is obscured by a jet in the view shown), traverses two plates, and suffers a deflection of $(90 \pm 7)^\circ$ in the gas at *a*. The charged decay product, *ac*, traverses at least 37 g cm^{-2} Pb in going up through the second plate before leaving the illuminated region of the chamber. At *b*, under the third plate there appears an electron cascade shower whose energy is estimated to be (350 ± 90) MeV. The other electrons in the chamber do not appear to be associated with the decay. The shower at *b* re-projects to *a*; it makes an angle of $(17 \pm 4)^\circ$ with the path of the primary.

The shortness of the segment of the primary under the second plate makes it impossible to estimate its ionization; it is certainly not noticeably above minimum above the plate. The secondary track is directed forward in the chamber. A conservative estimate of its ionization above the second plate, considering its inclination, indicates that it is at least $1.5 \times$minimum.

If the charged secondary, *ac*, is a proton, its penetrating power requires a momentum (equal to the transverse momentum) of at least 560 MeV/c, too high to be consistent with the $\Sigma \to$p-decay process. If it is a π-meson, its momentum at emission is greater than 170 MeV/c. The decay observed can therefore not be interpreted as $\tau' \to \pi + 2\,\pi^0$, in which the transverse momentum is less than 133 MeV/c. The increased ionization in the second compartment sets an upper limit on the momentum of the secondary at emission. Thus, for a π-meson, $170 < pc < 220$ MeV; for a μ-meson, $140 < pc < 175$ MeV.

The transverse momentum of the shower at *b* is only (98 ± 32) MeV; so that a third particle is required to balance transverse momentum. The event may be interpreted then as a three-body decay into a photon, an L-meson, and another neutral particle. As the shower core is in the plane of primary and secondary, the third particle must also be in that plane. The possibility that the neutral particle is as heavy as a π^0-meson would imply a mass value for the primary well above 966 m_e. In effect, the Q-value of a three-body decay is always greater than the apparent Q calculated on the assumption of a two-body decay. In this case $Q(\mu^\pm, \gamma) = (300 \pm 36)$ MeV, $Q(\pi^\pm, \gamma) = (326 \pm 42)$ MeV. If the third particle is a π^0-meson, the primary mass is at least (90 ± 40) MeV above 494 MeV.

A more reasonable interpretation in the light of present knowledge is that the third neutral particle is a photon, the two photons resulting from the decay of a π^0-meson produced at *a*. The event would then be a decay in flight of the particle variously designated as χ, θ, and $K_{\pi 2}$, the π^0 decaying in its

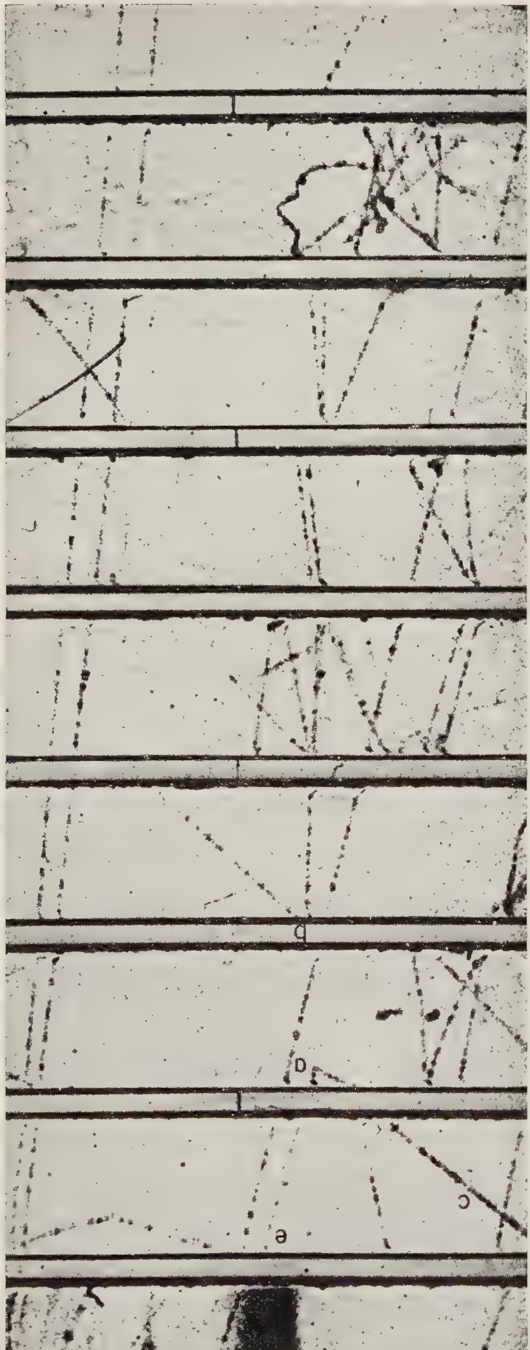

Fig. 3. – A charged-V decay with an associated electron shower.

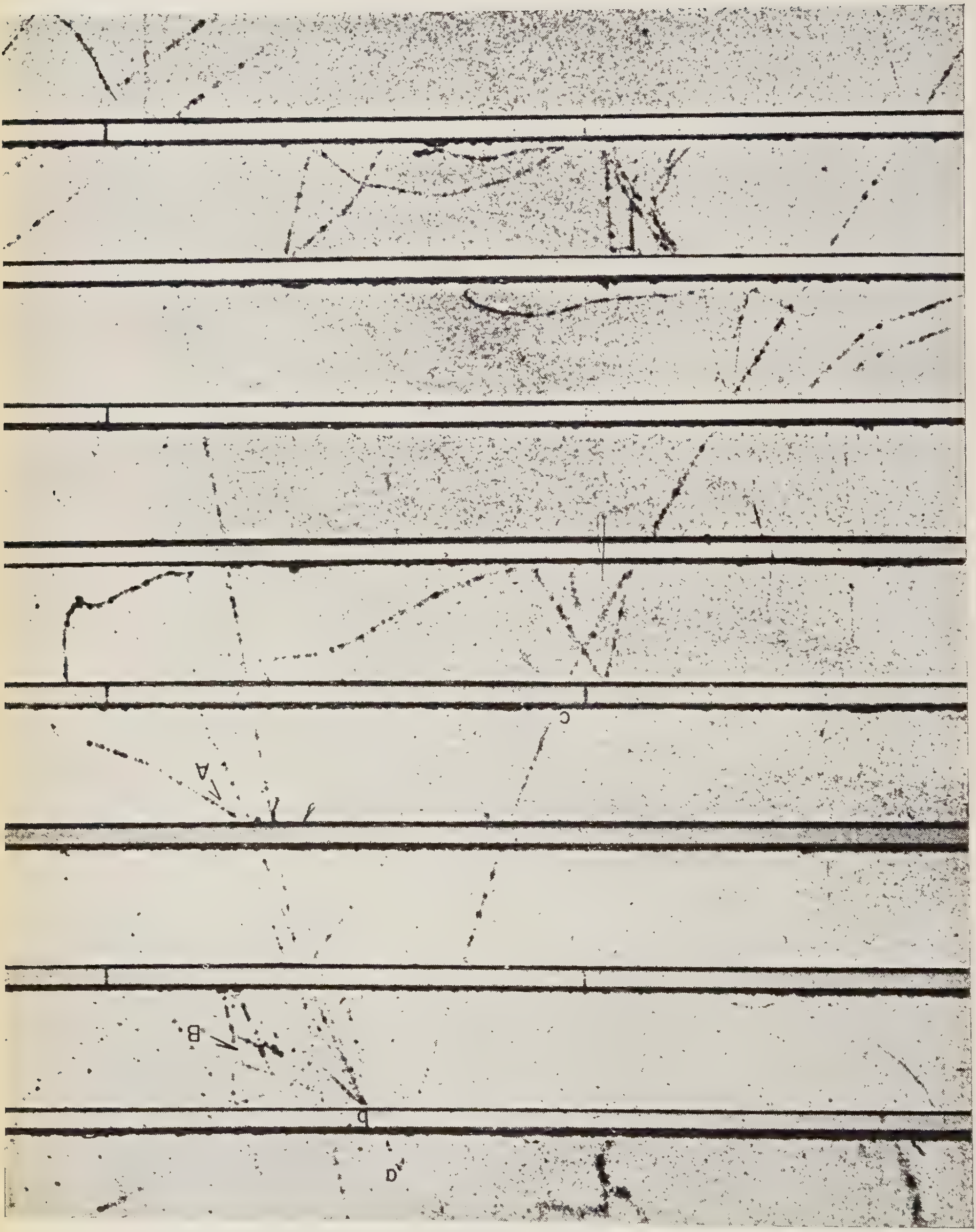

Fig. 4. – A neutral-V decay producing an electron shower.

most probable mode. The energy of the unobserved photon can be calculated from the conservation of energy and momentum in the two decay processes. There are two solutions. One calls for a 1.3 GeV photon given off at an angle of only 5° to the line of flight of the primary. This photon would then be required to traverse the remaining nine lead plates of the chamber without materializing. This is most improbable, so we rule it out. The other solution calls for a photon of (120 ± 55) MeV at an angle of about 57° to the primary. The π^0-meson parent to the two photons was, then, given off at an angle of $(25 \pm 7)°$ to the primary with a momentum of (450 ± 110) MeV/c.

With this information we obtain a $Q(\pi, \pi^0)$ of (300 ± 100) MeV, in agreement with the accepted value of 219 MeV corresponding to mass 494 MeV/c^2.

This event could also be a decay in flight of an upward directed θ^0-meson produced at b. However, the association of the three other penetrating particles with ea makes it more likely that it is a charged K-particle produced in the same event as these other particles.

The event seems then to represent a clear-cut case of the decay in flight

$$K^{\pm}_{\pi 2} \to \pi^{\pm} + \pi^0 + 219 \text{ MeV},$$

the π^0-meson decaying in the normal mode. A decay in flight in which the π^0-meson decays in a very improbable mode ($\pi^0 \to 4e$) has previously been reported ([11]). Our event gives further evidence that some of the observed charged V-decays are due to known K-mesons ([12]).

4. – K^0-decay producing an electron shower.

Fig. 4 shows an unusual V^0-decay occurring at a, above the top lead plate. The included angle is $(72 \pm 4)°$. One of the secondaries penetrates all eleven plates, undergoing a scattering of about 11° in the fourth plate at c. The other gives rise to an electronic shower at b, whose energy we estimate as (280 ± 100) MeV.

The penetrating secondary has a range exceeding 84 g cm^{-2}. Its ionization is not noticeably above minimum. If it is a π-meson or proton, it is much more likely that the scattering at c is due to a nuclear interaction than to Rutherford scattering. In any case the small deflection indicates negligible energy loss, and it is permissible to estimate the initial value of Π from the

(11) A. L. Hodson, J. Ballam, W. H. Arnold, D. R. Harris, R. R. Rau, G. T. Reynolds and S. B. Treiman: *Phys. Rev.*, **96**, 1089 (1954).

(12) R. Armenteros, A. Astier, C. D'Andlau, B. Grégory, A. Hendel, J. Hennessy, A. Lagarrigue, L. Leprince-Ringuet, F. Muller, Ch. Peyrou and R. R. Rau: *Suppl. Nuovo Cimento*, **4**, 541 (1956).

small-angle scatterings in the other eight plates between the top and bottom ones. The value found is (560 ± 100) MeV. If the particle is a π-meson, its momentum is then (575 ± 100) MeV/c, well above the minimum value of 240 MeV/c required by the observed penetration. If it is a proton, $pc = (840 \pm 100)$ MeV, not much more than the value of 740 Me Vrequired for the penetration. In this case the ionization would range from 2.5 to 3 times minimum in the last three compartments. We conclude that the penetrating decay product, *ac*, is lighter than a proton.

The electron shower produced by the other decay product at b is not associated with any heavily ionizing or penetrating particles. The particle *ab* must then be either an electron or a strongly interacting particle producing a π^0-meson in the plate. With regard to the latter possibility, there is indeed a suggestion of a double core structure, indicated by B and A on the figure, but the wide-angle electrons B may simply be low-energy electrons scattered off at wide angles. If the shower does result from π^0-decay at b, the estimated energy of (280 ± 100) MeV gives a lower limit for the energy of the particle *ab*.

The $\Lambda^0 \to \pi + p + 37$ MeV decay is very unlikely on dynamical grounds, because of the high secondary energies and large angular opening. Even if we take for the energy of *ac* the lower limit set by its penetration and for the energy of *ab* the lower limit given by the shower energy of (280 ± 100) MeV, we find $Q(\pi, p) > (130 \pm 13)$ MeV if *ac* is the π-meson and *ab* the proton. We have seen already that penetration, ionization, and scattering argue strongly against *ac* being a proton. If nevertheless we consider the possibility that *ac* is a proton and *ab* a π-meson, we find (130 ± 75) MeV for our very conservative lower bound on $Q(p, \pi)$. The process $\theta^0 \to \pi + \pi + 214$ MeV is, on the other hand, a distinct possibility. The extreme lower limit is in this case $Q(\pi, \pi) > (120 \pm 50)$ MeV. This interpretation involves a charge-exchange scattering of one of the π-mesons at b. In view of the uncertainty as to the angle between the two photons in the subsequent $\pi^0 \to \gamma + \gamma$ decay and the energy of the second photon, we do not attempt a closer estimate of $Q(\pi, \pi)$. We can, however, use the known mass of the θ^0 (494 MeV) [13], the momentum of *ac* ((575 ± 100) MeV/c), and the opening angle $(72 \pm 4)^\circ$ to calculate the energy of the π-meson *ab*. The result is (226 ± 50) MeV total energy, which is not inconsistent with the size of the visible showers. The interpretation of this V^0 as a θ^0-decay runs into a difficulty, however, when we calculate the probability of the postulated charge exchange and subsequent pair production. The interaction cross-section for a π-meson of this energy with a Pb nucleus

(13) R. W. Thompson, A. V. Buskirk, L. R. Etter, C. J. Karzmark and R. H. Rediker: *Phys. Rev.*, **90**, 1122 (1953).

is indeed «geometric» ($2.15 \cdot 10^{-24}$ cm^2) [14], corresponding to a probability of $5.0 \cdot 10^{-2}$ in the Pb plate. It is known [15] that the interactions result only rarely in charge-exchange scatterings, and that when this does occur the scattering is predominantly in the backward direction. On the basis of a recent study of 85 MeV kinetic energy π^+-meson interactions with deuterons, we can set $2.3 \cdot 10^{-2}$ as a conservative upper limit on the probability that the interaction leads to a charge-exchange scattering with a deflection of less than 60°. Finally, the probability that a decay photon will be converted is 0.7. Multiplying the various probabilities, we find that the probability that a θ^0-decay will give rise to the event seen is less than $8 \cdot 10^{-4}$. As the number of V^0-decays seen in the whole experiment was only 40, of which less than 25% are expected to be θ^0-decays [17], the probable number of events of the type hypothesized is less than $8 \cdot 10^{-3}$. While probability considerations such as these are not absolutely compelling, it can be said that the θ^0 interpretation is very unlikely.

A more likely one is β-decay:

$$K^0_\beta \to \pi + e + ?^0$$

Using (280 ± 100) MeV for the electron energy and (575 ± 100) MeV/c for the π-meson momentum, we find $Q(\pi, e) = (350 \pm 100)$ MeV. If the lower limit on the momentum of *ac* set by its penetration is used (240 MeV/c), $Q(\pi, e) \geqslant (225 \pm 60)$ MeV.

Strong evidence for a decay process of this type has recently been found in a magnet cloud chamber event from the Ecole Polytechnique [18]. One product of the V^0-decay is identified as a π^+-meson by its $\pi^+ \to \mu^+$ decay and the other is identified as being lighter than a μ-meson from momentum and ionization; the $Q(\pi^-, e^-)$ is 82 or 105 MeV. Three other less clear-cut cases have been reported: the similar event of COWAN [19] gives $Q(\pi^+, e^-) = 225$ MeV, buth the negative particle may be of near-protonic mass; the two Duke events [20] give $Q(\pi^-, e^+) = 18$ and $Q(\pi^+, e^-) = 48$ MeV, although both cases

[14] G. BERNARDINI, E. T. BOOTH, L. M. LEDERMAN and J. H. TINLOT: *Phys. Rev.*, **82**, 105 (1951).

[15] J. O. KESSLER and L. M. LEDERMAN: *Phys. Rev.*, **94**, 689 (1954) and references therein.

[16] K. C. ROGERS and L. M. LEDERMAN: *Phys. Rev.*, **105**, 247 (1957).

[17] H. S. BRIDGE, CH. PEYROU, B. ROSSI and R. J. SAFFORD: *Phys. Rev.*, **91** 362 (1953).

[18] C. D'ANDLAU, R. ARMENTEROS, A. ASTIER, H. C. DESTAEBLER, B. GRÉGORY, L. LEPRINCE-RINGUET, F. MULLER, CH. PEYROU and J. H. TINLOT: *Nuovo Cimento*, **4**, 917 (1956).

[19] E. W. COWAN: *Phys. Rev.*, **94**, 161 (1954).

[20] M. M. BLOCK, E. M HARTH and M. E. BLEVINS: *Phys. Rev.*, **100**, 959A (1955).

may be electron pairs. If one assumes that any two of the five cases represent β-decay of the same particle, the spread in Q-values indicates that there are more than two decay products. It is tempting to identify the particle as a neutral counter-part of the charged K_β found in emulsion research ([21]). $Q(\pi, e)$ gives, of course, a lower limit on the energy release in the many-body disintegration. If the K^0_β mass is 494 MeV/c², our high Q-value indicates, within the estimated error, that the neutral products are massless, as in that case $0 < Q(\pi, e) < 354$ MeV. If a few more cases of this type can be obtained in a multiplate chamber, it will be possible to decide whether the neutral particle is a photon. For the present, we interpret our case as evidence for

$$K^0_\beta \to \pi + e + \left\{ \begin{matrix} \nu \\ \text{or} \\ \gamma \end{matrix} \right\}.$$

LEDERMAN and his coworkers ([22]) have recently reported evidence for a long-lived K^0-particle decaying into more than two particles. There is some dynamical evidence for the mode (π, e, ν or γ), but direct identification of the electron has not yet proved possible. In this respect our observation of shower production is unique, as it pins down the mass more closely than is possible by comparison of momentum and ionization in a magnet cloud chamber.

5. – A possible new type of cascade decay.

Fig. 5 shows a V^0-decay at *a* giving rise to the tracks *abc* and *ad*. The remarkable feature of this event is the apparent deflection of *abc* near *b*, 5 mm from the apex. By far the most likely interpretation of this deflection is as a decay in flight. The picture would then represent the first evidence for a cascade decay in which a neutral unstable particle disintegrates into a charged unstable particle heavier than a π-meson ([23]).

Analysis of the deflection is made difficult by the presence near by of other

([21]) M. W. FRIEDLANDER, D. KEEFE, M. G. K. MENON and L. VAN ROSSUM: *Phil. Mag.*, **45**, 1043 (1954).

([22]) K. LANDE, E. T. BOOTH, J. IMPEDUGLIA, L. M. LEDERMAN and W. CHINOWSKY: *Phys. Rev.*, **103**, 1901 (1956); K. LANDÉ, L. M. LEDERMAN and W. CHINOWSKY: *Phys. Rev.*, **105**, 1925 (1957).

([23]) M. S. SINHA and S. N. SENGUPTA: *Nuovo Cimento*, **5**, 1153 (1957)) have recently reported two apparent neutral V-charged V cascades. In both cases the change of direction interpreted as a charged V-decay takes place inside a plate. The arguments against interpreting the deflections as interactions are not convincing.

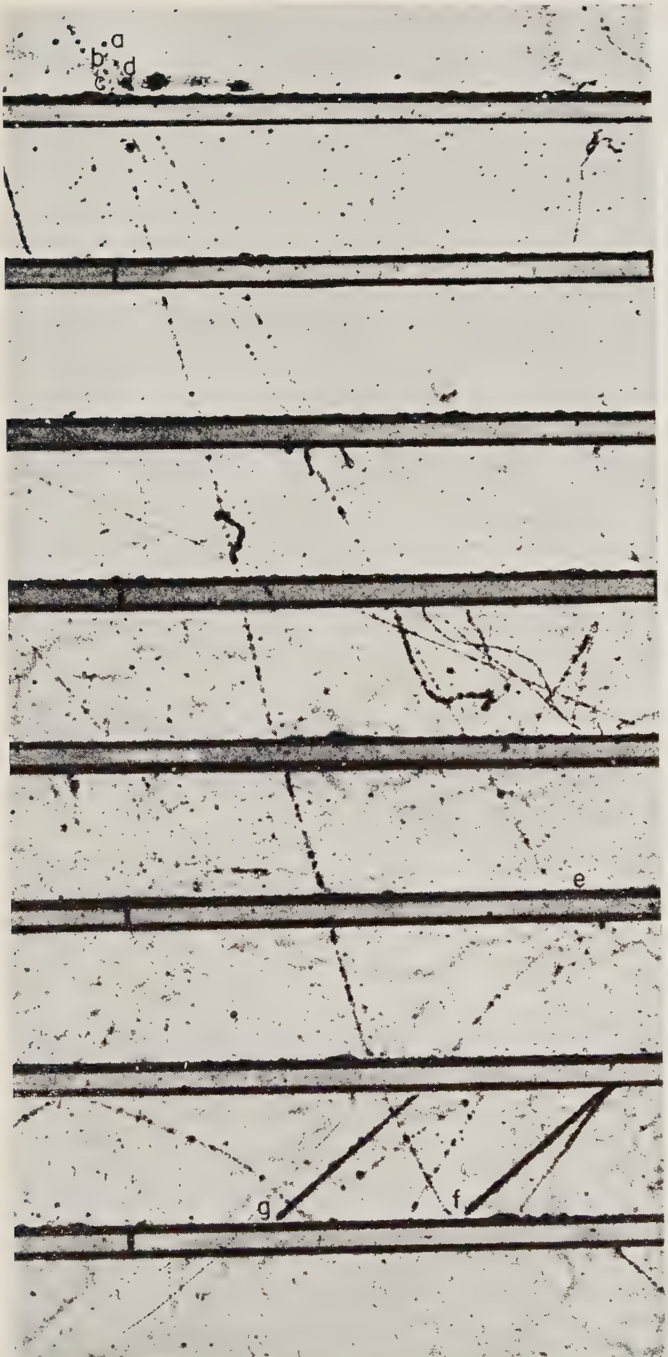

Fig. 5. – A possible neutral V-charged V^0 cascade.

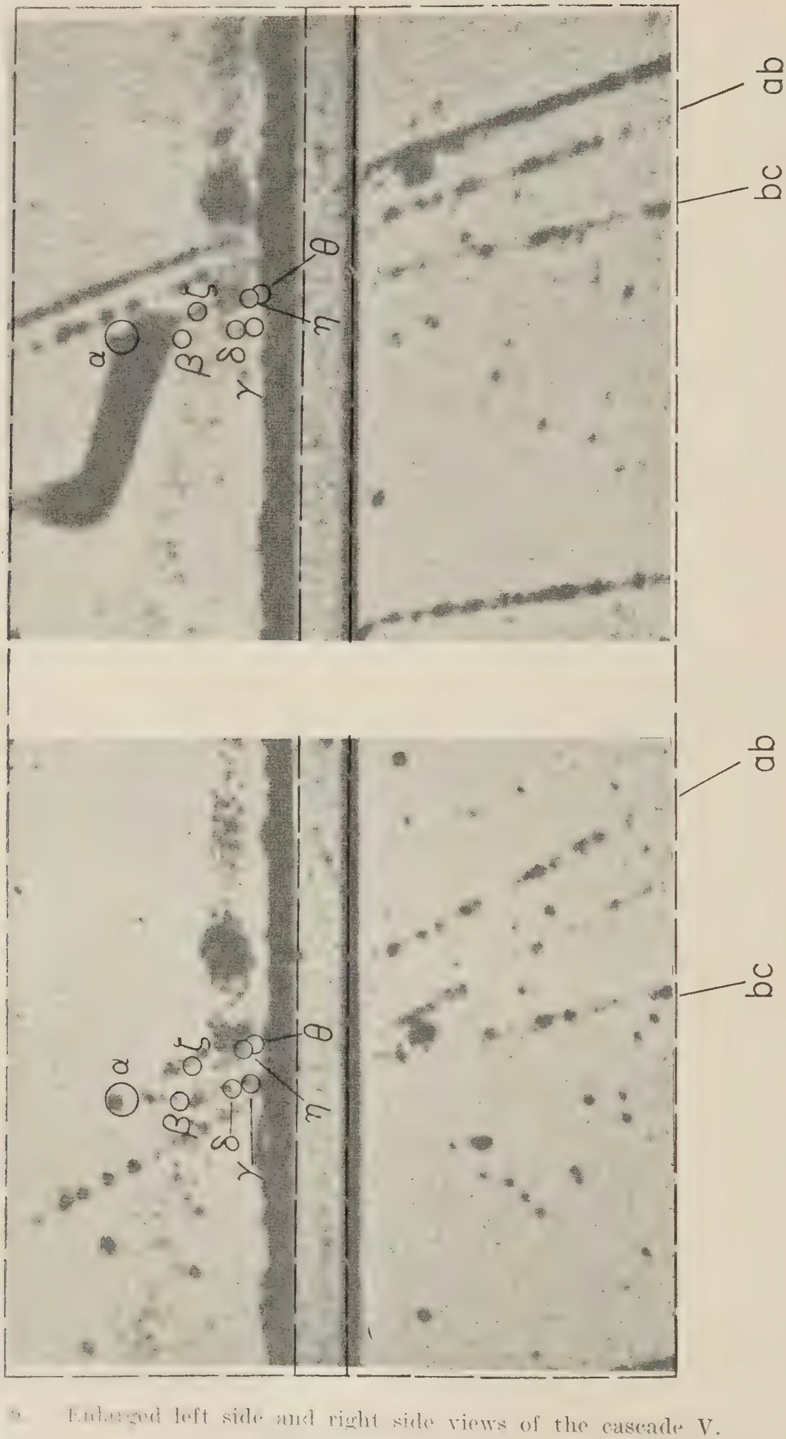

Fig. [illegible]. Enlarged left side and right side views of the cascade V.

counter-age tracks and a smear of pre-expansion tracks. There are, fortunately, four views of the event—left side view, seeing *abc* at $-11°$ to the axis, the two stereo views, seeing it at $+3°$ and $+5.5°$, and the right side view, at $+19°$. Any two of them suffice for determining the co-ordinates of a blob, and the mutual consistency of these determinations then provides a control on the assignment of images in the negatives to a particular blob in the chamber. The difference in appearance between old and counter-age blobs is also of help in sorting out the different tracks. In our analysis we only make use of blob images that can be identified on all four views, that give consistent co-ordinates in space and that appear to be of counter age. We assume that the particle's path is contained somewhere in the blob.

Fig. 6 shows magnified prints of the left side and right side views, with the key blob images identified. The large blob α is the vertex of the V^0. The charged V-decay occurs very near the small blob β. The left side and stereo views show two blobs between α and β that appear to belong to the charged V primary, but because of their size they could not contribute to defining its direction. The secondary of the charged-V is defined by the straight line $\beta\gamma\delta$. The fact that δ is in line with $\beta\gamma$, as well as the straightness of the near-by penetrating tracks, indicate that there is little distortion near the plate. Even without localizing the V^0-vertex within α by means of the other V^0-decay track *ad*, we see that there is a deflection in *ac* at *b*, for on the right side view a straight line through, β, γ, δ cannot be made to touch α. The deflection is at least 5°. On *ad* we can identify the blobs ζ, η, θ; they are collinear on a line through the right side of α. We can now localize the V^0-vertex more closely, with the result: a deflection at *b* of $(12 \pm 3)°$, and a V^0-angle at *a* of $(25 \pm 4)°$.

The decay product *ad* traverses three plates while in the well-illuminated region, with scattering too small to measure, implying $\Pi > 1$ GeV. In the poorly illuminated region it traverses two more plates and interacts very near the front edge of the sixth plate at *e*, *eg* being a product of this interaction. It penetrates 45 g cm^{-2} Pb before interacting. This corresponds to a momentum of at least 600 MeV/c if it is a proton or 180 MeV/c if it is a π-meson. The particle *bcf* traverses seven Pb plates and interacts in the eighth at *f*; its initial range was at least 55 g cm^{-2} Pb. Its ionization is not noticeably above minimum. The observed scattering angles in the six middle plates give a Π of (350 ± 80) MeV. For a proton this corresponds to an ionization of $(2.5^{+0.5}_{-0.5})$ times minimum. The particle is therefore most likely lighter than a proton. Since it interacts at *f*, it is not a μ-meson. We conclude that it is probably a π-meson; it could be a K-meson.

If the apparent deflection at *b* is spurious—resulting from a freakish conjuncture of unrelated blobs—or if the deflection there is due to a scattering in the gas, the V^0-decay at *a* is consistent with either the Λ^0- or θ^0_1-scheme,

3025

the latter giving a somewhat better fit with the momentum estimates from multiple scattering.

It is very unlikely that the deflection is a scattering in the gas. The geometric nuclear cross-section corresponds to a probability per 25 cm of gas (the length of visible track between the vertex of the V^0 and the eight plate) of $5 \cdot 10^{-4}$, and only a small fraction of the interactions in the gas will fail to give other tracks. The probability of a single Coulomb scattering of more then 5° in 25 cm is $6 \cdot 10^{-5}$. In our sample of 40 V^0's the expected numbers of such scatterings are 0.025 and 0.003 respectively.

Various possible interpretations of the cascade decay come to mind, such as

(*a*) [24]
$$V^0 \to \pi^{\pm} + K^{\mp}, \quad K^{\mp} \to \pi^{\mp} + ?^0$$

(*b*)
$$V^0 \to \pi^{\pm} + \Sigma^{\mp}, \quad \Sigma^{\mp} \to \pi^{\mp} + n$$

(*c*)
$$V^0 \to \pi^{+} + \Xi^{-}, \quad \Xi^{-} \to \pi^{-} + \Lambda^0 .$$

The first scheme would be the neutral counterpart of the heavy charged hyperon reported by EISENBERG [25]. It seems unlikely in our case, because of the long mean lives of the known K-particles [26]. In addition the orientation of the charged V-decay is such that a π^0-meson from the K_π-decay could hardly fail to produce a visible shower. For the second scheme a lower limit on the mass of the hyperon can be calculated by using for the momentum of the π-meson, p_π, the minimum value, 180 MeV/c, corresponding to its observed penetration and for the momentum of the Σ-hyperon, p_Σ, the longitudinal component of the minimum momentum of its decay π-meson, 200 MeV/c. The result is 1390 MeV, corresponding to a minimum Q of 60 MeV. A more likely estimate can be made by using the known dynamics of the $\Sigma \to \pi + n$ decay scheme to calculate p_Σ from the decay π-meson momentum (372 ± 77) MeV/c and the decay angle $(12 \pm 3)°$, and by taking for p_π the value 1000 MeV/c corresponding to the noise level for $n = 6$. It turns out that $p_\Sigma = (810 \pm 320)$ MeV/c or (7.1 ± 1.1) GeV/c. The former corresponds

(24) R. B. LEIGHTON, S. D. WANLASS and C. D. ANDERSON: *Phys. Rev.*, **89**, 148 (1953).

(25) Y. EISENBERG: *Phys. Rev.*, **96**, 541 (1954); *Suppl. Nuovo Cimento*, **4**, 484 (1956).

(26) L. W. ALVAREZ, F. S. CRAWFORD, M. L. GOOD and M. L. STEVENSON: *Phys. Rev.*, **101**, 503 (1956); V. FITCH and R. MOTLEY: *Phys. Rev.*, **101**, 496 (1956); E. L. ILOFF, G. and S. GOLDHABER, J. E. LANNUTTI, F. C. GILBERT, C. E. VIOLET and M. WIDGOFF: *Phys. Rev.*, **102**, 927 (1956).

to an ionization of $(2.3^{+2.4}_{-0.6})$ times minimum for the track *ab*, but the track is so short that one could not distinguish such an ionization from minimum. It gives a minimum mass of (1700 ± 100) MeV/c², or $Q(\Sigma, \pi) \geqslant (370 \pm 100)$ MeV. The large root gives a minimum mass for the neutral hyperon of (1760 ± 130) MeV/c², or $Q(\Sigma, \pi) \geqslant (430 \pm 130)$ MeV. These masses are much larger than that of the presumed counterpart, $\Xi^- \to \Lambda^0 + \pi^- + 65$ MeV. For the third scheme a similar calculation gives for a likely estimate of the lower limit on the V^0 mass 1.9 GeV, or $Q(\Xi^-, \pi^+) \geqslant 0.4$ GeV.

No interactions in the gas were observed in our sample, so the likelihood that the apparent V^0-decay is actually an interaction in the gas must indeed be very small. The possibility must nevertheless be considered. A fast neutron belonging to the shower could produce a Σ and a K. Or, even less probable but still possible, a θ^0 could interact to produce a Σ and a π, as suggested by FRY [27]. A kinetic energy of the order of 1 GeV is required. Evidently other cases of cascade decays of the type reported will have to be found before the existence of a neutral super-hyperon can be considered established.

---

(27) W. F. FRY, private communication, Padua, 1957.

RIASSUNTO (*)

Si è fatta funzionare in alta montagna una camera a nebbia, sotto un selettore di sciami penetranti. Si usa la distribuzione degli angoli di scattering dei secondari penetranti per determinare congiuntamente l'esponente γ del loro spettro differenziale dei momenti e il livello σ_1 del disturbo della camera. γ è 2 a 2.5 e σ_1 è meno di $0.7 \cdot 10^{-2}$ radianti, corrispondenti a un momento osservabile massimo (errore standard) di oltre 2 GeV/c. Si sono trovati alcuni decadimenti in volo inconsueti. In uno, il decadimento di una V carica genera un fotone, riconosciuto dallo sciame elettronico che produce. L'evento è interpretato come $K_{\pi 2} \to \pi + \pi^0$, il π^0 decadendo nel suo modo normale (2γ). In un altro, un decadimento V^0 da una particella penetrante interagente e una particella che produce uno sciame elettronico nella prima piastra che colpisce. L'evento è dinamicamente compatibile con $\theta^0 \to \pi + \pi + 214$ MeV ma lo scambio di carica che in tal caso occorre postulare è molto improbabile. Una interpretazione più verosimile è un decadimento β: $K^0_\beta \to \pi + e + ?^0$. Dalla liberazione d'energia osservata la particella neutra deve essere priva di massa se K^0_β ha la stessa massa delle altre particelle K. Si registra finalmente un caso che appare essere un decadimento in cascata di una V neutra in una carica. La V carica decade in una particella leggera interagente, probabilmente un mesone π. L'interpretazione più probabile in termini delle particelle attualmente note è: $V^0 \to \Sigma^\pm + \pi^\mp$; $\Sigma^\pm \to \pi^\pm + n$, con una massa di almeno 1390 MeV ($Q_{\Sigma\pi} \geqslant 60$ MeV).

(*) *Traduzione a cura della Redazione.*

Production of Strange Particles by 4.3 GeV π^- in Emulsion.

C. Besson, J. Crussard, V. Fouché, J. Hennessy,
G. Kayas, V. R. Parikh and G. Trilling
Ecole Polytechnique, Laboratoire de Physique - Paris

(ricevuto il 13 Agosto 1957)

Summary. — A large stack of emulsion has been exposed in the 4.3 GeV π^- beam of the Berkeley Bevatron. 317 K^+ and 96 K^- stopping in the stack have been observed; 184 K^+ and 66 K^- have been followed back to an originating star made by a beam π^-. The origins of K^+ are larger than those of K^-, as far as the numbers of black and grey prongs are concerned, and the emission of the K^- is more concentrated in the forward direction than that of the K^+. Charged Σ of moderate energy have been observed in the origin of K^+; their frequency is $0.17^{+0.12}_{-0.06}$ per star. The mean free paths for production of K^+ and K^- of energy < 150 MeV in emulsion are (4700 ± 1200) cm and (24000 ± 7000) cm respectively. The majority of the K^+ stopping in the stack are probably produced in secondary collisions in the nucleus of pions resulting from the first impact of the incoming π^-. A larger fraction of the K^- is probably produced in the first collision. Approximate values of the production cross-sections of strange particles by the collisions of 4.3 GeV π^- with nucleons can be deduced from the study of suitably selected small origins of K^+ and K^-. The cross-section for the production of K^+ is ~ 0.7 mb. For K^-, it is probably $\geqslant 0.3$ mb. It thus appears that as the pion energy increases from 1 to 4 GeV, there is no pronounced increase in the total cross-section for strange-particle production. The K K production becomes a substantial fraction of the total, and the direct hyperon production probably remains about constant or decreases.

Introduction.

Some data on the production of strange particles by 4.3 GeV π^- ([1-3]) have already been obtained.

(1) G. Maenchen, W. M. Powell, G. Saphir and R. W. Wright: *Phys. Rev.*, **99**, 1619 (1955).
(2) M. Schein, D. K. Haskin and R. G. Glasser: *Nuovo Cimento*, **3**, 131 (1956).
(3) B. F. Edwards, A. Engler, M. W. Friedlander and A. Z. Kamal: *Nuovo Cimento*, **5**, 1188 (1957).

Further investigation of this problem has been carried out with a stack of 95 stripped Ilford G-5 emulsions (25 cm $\times$ 35 cm $\times$ 600 μm) exposed to the 4.3 GeV π^- beam of the Berkeley Bevatron. The stack was placed at 18 m from the target, the beam pions being parallel to its 25 cm dimension. The exposure lasted $\sim$ 11 hours. The energy and intensity of the beam vary somewhat in the various parts of the stack (see Appendix II); we estimate that $\sim 22 \cdot 10^6$ pions entered the stack.

The stack was scanned for stopping strange-particles, most of which were followed back to the parent star. These were of the following types:

a) Stars with a minimum ionization primary in the direction of the beam (« beam sources »).

b) Stars with no apparent primary (« neutral sources »). These were carefully checked: in particular, if a prong was less ionizing than the outgoing K, it was always followed to make sure that it was not the primary.

c) Stars with a « grey » primary. These are mere interactions of the K in flight, as no « grey » particle is energetic enough to create strange particles.

d) Stars with a minimum-ionization primary at an angle to the beam (« false sources »). Such a primary can be a fast pion, a proton or the K itself coming from a previous interaction.

Whenever possible, apparent primaries of sources of types *c*) and *d*) were followed back to the real source.

In addition, a number of K-mesons originated outside the stack, and a certain number were not followed.

The results are summarized in Table I.

TABLE I.

Type	Number found	Type of source				From outside not found	Not followed
		a	*b*	*c*	*d*		
K_L, τ', $K_{\mu 3}$	247	147	10	4	16	35	35
τ	70	37	8	3	4	12	6
K^-	96	66	5	1	4	17	3
Σ	24	13	2	0	2	0	7

The rest of this work, except for Sect. 3, is entirely limited to K^+ mesons coming from origins of type *a*).

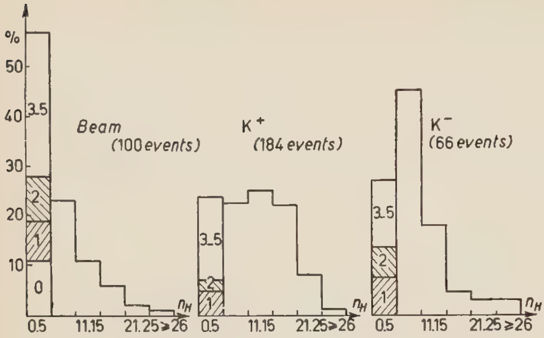

Fig. 1. – Distribution of heavy prongs.

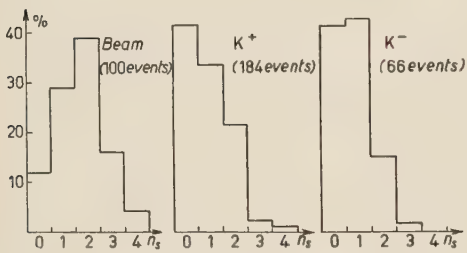

Fig. 2. – Distribution of shower prongs.

1. – Results.

1·1. *Types of stars.* – In Fig. 1 and 2 are shown the prong distributions of K^+ origins, K^- origins and 100 interactions observed by scanning along beam tracks. All prongs of grain density < 1.2 times plateau are considered as shower prongs, and all others, including short recoils are considered as heavy prongs. The beam track length followed to obtain the 100 interactions yields an interaction m.f.p. (exclusive of diffraction scattering) of (36.4 ± 3.3) cm, for 4.3 GeV π^- in emulsion, in agreement with other measurements [2,4,5].

The average multiplicities found are the following:

$$\text{for } K^+ \text{ origins:} \quad \begin{cases} \langle n_H \rangle = 11.5 \pm 0.5 \\ \langle n_S \rangle = 0.9 \pm 0.1 \end{cases}$$

$$\text{for } K^- \text{ origins:} \quad \begin{cases} \langle n_H \rangle = 8.9 \pm 0.7 \\ \langle n_S \rangle = 0.8 \pm 0.1 \end{cases}$$

$$\text{for « beam stars »:} \quad \begin{cases} \langle n_H \rangle = 6.5 \pm 0.6 \\ \langle n_S \rangle = 1.7 \pm 0.1 \end{cases}$$

It will be noticed that,

i) The K origins have, on the average, one shower track less than the

---

(4) A. Marques, N. Margem and G. A. B. Garnier: *Nuovo Cimento*, **5**, 290 (1957).
(5) J. O. Clarke and J. V. Major: *Phil. Mag.*, **2**, 37 (1957).

beam stars. This is easily accounted for by the extra energy involved in producing strange particles.

ii) The K^+ origins are substantially larger than the beam stars.

iii) The K^- origins are also larger than the beam stars but somewhat smaller than the K^+ origins. The latter difference has already been noticed in emulsions exposed to cosmic rays [6].

1·2. *Corrections to the number of* K-*mesons observed.*

a) Scanned area. All analyses which follow have been made taking into account only the K-mesons found in the central part of the stack. The K found elsewhere have been discarded (see Appendix I and II)). The purpose of this was to simplify the calculations involved in the geometrical corrections.

The total numbers of K-mesons found in the «scanned area» are: 48 τ, 201 K^+, 72 K^-, of which respectively 26, 111 and 53 had «beam» sources.

b) We have rejected all K that interact between the origin and the stopping point. This is because we do not have an accurate measurement of their energy, nor do we know whether they would have stopped in the scanned area had they not interacted. An appropriate correction is made at the proper time (see Sect. **1·4**).

c) Scanning biases. It is evident that the total number of K-mesons that stop in the scanned area is larger than the number found. In order to get a corrected figure, the following biases must be evaluated.

i) K^+ missed. The proportion of τ-decays (Table I) is much too large, since recent data [7] indicate a τ proportion of $5.5 \pm 0.4\,\%$ of all K^+ decays. Hence we appear to miss a great many of the minimum secondaries. This is not surprising, since, in the present stack, plateau ionization is ~ 16 to 20 grains/100 μm, a rather low figure. Based on 90 % efficiency for τ-detection, the number of K^+ (not including τ-decays) stopping in the «scanned area» should be 915 ± 155, of which 201 were seen, the scanning efficiency for K^+ excluding τ is thus $(22.0 \pm 3.3)\,\%$.

ii) K^- missed. We miss those K^- absorptions where the K^- gives nothing (K_ϱ), only one light track (taken for a K^+), a few very short tracks, one slow proton, or on the contrary a very large star. From an estimation

---

(6) M. W. Friedlander, Y. Fujimoto, D. Keefe, M. G. K. Menon, M. Ceccarelli, M. Grilli, M. Merlin, A. Salandin and B. Sechi: *Suppl. Nuovo Cimento*, **4**, 428 (1956).

(7) R. W. Birge, D. H. Perkins, J. R. Peterson, D. H. Stork and M. N. Whitehead: *Nuovo Cimento*, **4**, 834 (1956).

made on K^- capture stars from the K^- beam ([8]), the proportion of such absorptions is:

K_0	$(14 \pm 0.8)\%$	These we would not detect ($\sim 34\%$)
1 light track	$(8 \pm 0.6)\%$	
Very short tracks / One slow proton . . .	$\sim 8\ \%$	
Large stars	$\sim 4\ \%$	
Other stars	$\sim 66\ \%$	For these, we estimate the scanning efficiency about 80%

(from the compared results of different scanners).

Furthermore, we discard all the K^- stopping in the upper and lower 30 μm of the plates, for which the scanning efficiency is certainly reduced. The scanning efficiency for K^- is thus $(0.66)\,(0.8)\,(0.9) = 48\%$.

iii) *Steep K-tracks.* A detailed study of the distribution of dip angles of the observed K has shown that for all $K^\pm$ except τ the scanning efficiency becomes poorer when the dip angle is greater than 30°. The τ's, on the other hand, seem to be found with an efficiency independent of their dip angle.

d) In view of the above considerations the following procedures were adopted in the analysis of the data.

i) In the study of the angular and energy distribution of K^+ and K^-, only those events in which the K had a dip angle of less than 30° were considered.

ii) In the calculation of production cross-sections for K^+, all events were counted and the results were corrected using the figures of paragraph *c*-i) of this Section. It is clear that since the τ scanning efficiency is independent of dip angle, and since the result of paragraph *c*-i) is based on the observed K^+/τ ratio, no further correction due to inefficiency in seeing K^+ with large dip angles is necessary.

iii) In the calculation of production cross-sections for K^-, only events with dip angles $\leqslant 30°$ were counted. The results were then corrected by adding the expected number of events of dip angle $\geqslant 30°$, and the number of events missed for the reasons discussed in paragraph *c*-ii) of this Section.

([8]) M. CECCARELLI: Private communication.

1·3. *Angular and energy distribution.* – Fig. 3 gives the laboratory angular distributions for K^+ and K^- of range ≥ 1 cm; it will be noticed that the K^- distribution is more concentrated forward than that for K^+.

Fig. 4 gives the energy distribution for K^+ and K^-. There is a tendency in the K^- stars in favour of low energies ($E < 40$ MeV: 30% of total against 18% for K^+). This might be an indication in favour of a nuclear potential (attractive for K^-, repulsive for K^+) of order 20 MeV, in agreement with a recent hypothesis [9-13].

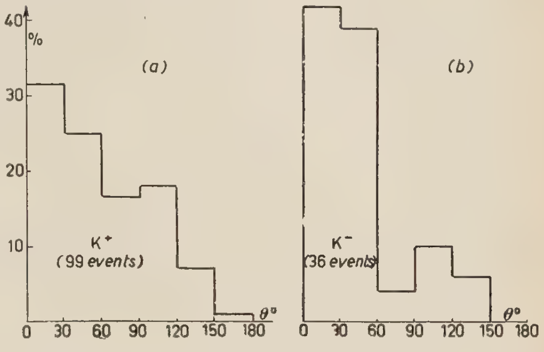

Fig. 3. – Angular distribution $R_K \geq 1$ cm.

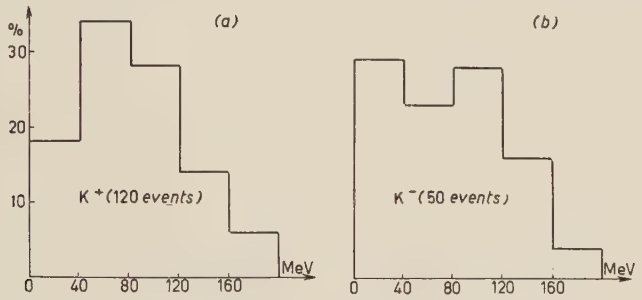

Fig. 4. – Energy distributions.

1·4. *Geometric corrections. Mean free path for production of slow* K-*particles.* – It is possible to calculate the mean free path for the production in emulsion of $K^\pm$ of energy ≤ 150 MeV (range ≤ 10 cm). In this calculation it is necessary to take into account:

1) the detection biases previously discussed;

(9) N. N. BISWAS, L. CECCARELLI-FABBRICHESI, M. CECCARELLI, K. GOTTSTEIN, N. C. VARSHNEYA and P. WALOSCHEK: *Nuovo Cimento*, **5**, 123 (1957).

(10) M. BALDO-CEOLIN, M. CRESTI, N. DALLAPORTA, M. GRILLI, L. GUERRIERO, M. MERLIN, G. A. SALANDIN and G. ZAGO: *Nuovo Cimento*, **5**, 402 (1957).

(11) G. COSTA and G. PATERGNANI: *Nuovo Cimento*, **5**, 448 (1957).

(12) G. COCCONI, G. PUPPI, G. QUARENI, A. STANGHELLINI: *Nuovo Cimento*, **5**, 172 (1957).

(13) W. ALLES, N. N. BISWAS, M. CECCARELLI and J. CRUSSARD: in print.

2) the variation in the beam intensity throughout the stack (measured directly by counting beam tracks at various places at the entrance in the stack, and assuming an attenuation length of 30 cm);

3) the effects of stack geometry, discussed in Appendix I.

The result is:

$$\text{For } K^+ \qquad \lambda = 4\,900 \text{ cm},$$
$$\text{For } K^- \qquad \lambda = 27\,000 \text{ cm}.$$

Errors and necessary corrections are the following:

i) Statistical error: $\begin{cases} 10.5\,\% & \text{for } K^+, \\ 15\ \ \% & \text{for } K^-. \end{cases}$

ii) Uncertainty on beam intensity $\sim 20\,\%$.

iii) Uncertainty on τ/K^+ ratio and K^+ scanning efficiency 13 %.

iv) Uncertainty on K^- scanning efficiency $\sim 15\,\%$.

v) A certain number of slow $K^\pm$ that have been discarded because they interact, would have stopped in the scanned area anyway. Taking the interaction m.f.p. for K^+ as 95 cm [14] and for K^- as 27 cm [15], the λ's of K^+ and K^- must be decreased by $\sim 5\,\%$ and $\sim 20\,\%$ respectively.

vi) Possible K^- contamination in the pion beam (see Appendix II). The m.f.p. for K^- production should be increased by $\sim 10\,\%$.

The final figures are then:

$$\lambda_+ = (4\,700 \pm 1\,200) \text{ cm},$$
$$\lambda_- = (24\,000 \pm 7\,000) \text{ cm}.$$

Remark on K^-/K^+ ratio. This K^-/K^+ ratio of the order of $\frac{1}{5}$ is much higher than the corresponding results in the K-beams of the bevatron ($\sim 1/100$ [16]) or in emulsion exposed to 6.2 GeV protons ($\sim 1/50$, corrected [17]); it is more like the ratio obtained in cosmic ray observations.

---

(14) J. E. LANNUTTI, W. W. CHUPP, G. GOLDHABER, S. GOLDHABER, E. HELMY and E. L. ILOFF: *Phys. Rev.*, **101**, 1617 (1956).

(15) W. H. BARKAS, W. F. DUDZIAK, P. C. GILES, H. H. HECKMAN, F. W. INMAN, C. J. MASON, N. A. NICHOLS and F. M. SMITH: *Phys. Rev.*, **105**, 1417 (1957).

(16) W. W. CHUPP, S. GOLDHABER, W. R. JOHNSON and F. WEBB: *Suppl. Nuovo Cimento*, **4**, 359 (1956) (Pisa Conference).

(1) J. CRUSSARD, V. FOUCHÉ, J. HENNESSY, G. KAYAS, L. LEPRINCE-RINGUET, D. MORELLET and F. RENARD: *Nuovo Cimento*, **3**, 731 (1956).

This can be explained by geometrical considerations without invoking a very large difference between K^-/K^+ ratios at production in π^--nucleon and proton-nucleon collisions: K beams are emitted at 90°, and in the emulsions exposed to 6.2 GeV protons the K are also observed at rather large angles. Comparison of the angular distributions of K^+ and K^- show that at large angles the K^-/K^+ ratio should be much smaller than the average value.

1·5. *Associated hyperons in* K^+ *production.* – A number of black, grey, and minimum prongs have been followed in 196 origins of K^+ and τ, in order to detect strange particles associated with K^+.

Two hyperfragments (non-mesonic decays) and 9 charged Σ's have been found: one Σ^+ decay at rest (a black track at production) and 8 $\Sigma^- \to n+\pi^-$ decays in flight (all grey tracks at production). No $\Sigma^+ \to n+\pi^+$ decays have been observed on minimum tracks.

From this the proportion of charged Σ hyperons emitted in K^+ origins has been estimated, as described in Appendix III. The result is $0.17^{+0.12}_{-0.06}$ per K^+ origin star.

It is worth mentioning that most of the Σ seem to be grey tracks of ionization ~ 1.5 to 3 times minimum. The fast Σ (minimum tracks), if any, are rare. If the number of Σ^0 it equal to half of the number of $\Sigma^{\pm}$, the total proportion of Σ is $0.25^{+0.18}_{-0.09}$ per star. This figure agrees with the 0.21 ratio found in the G-stack for cosmic rays stars ([18]).

It is not possible to derive from this result any valid estimate of the $\Sigma/(\Lambda^0+\overline{K})$ ratio in π^--nucleon collision producing K^+ at 4.3 GeV, because of the complexity of the production process. This question will be considered further in the discussion.

2. – Discussion.

From the experimental results one can try to deduce some information on the mechanism of production of K^+ and K^- in nuclei. This must account for the main features of the data, which can be summarized in the following way:

i) The origins of $K^{\pm}$ stopping in the stack are larger than the « normal » stars made by 4.3 GeV π^-; furthermore, the K^+ stars are larger than the K^--stars.

ii) The angular distribution of the K^- is more concentrated in the forward direction than that of the K^+.

([18]) D. F. Falla, M. W. Friedlander, F. Anderson, W. D. B. Greening, S. Limentani, B. Sechi-Zorn, C. Cernigoi, G. Iernetti and G. Poiani: *Nuovo Cimento*, **5**, 1203 (1957).

iii) In $\sim \frac{1}{4}$ of the origins of K^+ there are Σ hyperons, mostly of moderate energy.

There are two principal production mechanisms:

A) The K particles are produced in the first collision of the incoming π^- with a nucleon.

B) The first collision creates a certain number of pions; one of these or the scattered nucleon produces the K in a secondary interaction.

Obviously the K particles produced may or may not interact before leaving the nucleus.

Mechanism *B* will be discussed first.

2·1. *Mechanism B.* – Some information on pion production in π^--nucleon collisions at 4.3 GeV and on K^+ production by pions of energy $\leqslant 1.5$ GeV is now available. This has enabled us to investigate in some detail mechanism *B* for K^+ production.

This has been done by a Monte Carlo calculation based on a somewhat crude model described in Appendix IV.

The results for 1370 incident π^- are the following:

a) The angular distribution of the K^+ is given by Fig. 5. Though it is more concentrated in the forward direction than the experimental distribution of Fig. 4-*a*, we think that there is no significant disagreement: the introduction of the Fermi momentum of the nucleon in the second collision, a slightly different excitation function for K^+ production favoring somewhat more high values of the pion energy as compared to the low values, and a possible anisotropy of the K^+ in the c.m. could probably, bring both distributions in agreement. A more refined model would probably not lead to any definite conclusion on the angular distribution, and was therefore not attempted.

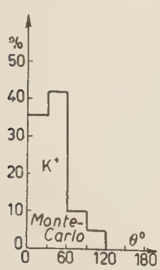

Fig. 5. – Angular K^+ distribution calculated by Monte Carlo.

b) More interesting is the information on the number of K^+ produced in this process which should be observed in the scanned area. This has been calculated from the result of the Monte Carlo (all corrections being made for scanning biasses and stack geometry) assuming that half of the produced K are K^+ and half K^0; it is found that ~ 130 K^+ produced by model *B* should have been observed. The actually observed number is 137. The agreement between calculated and observed numbers is certainly fortuitous, in view of the crude assumptions used in

the calculations. One can only conclude that mechanism B is probably responsible for a substantial fraction of the observed K^+.

This could explain very well the large size of many origins of K^- by a selection of central collisions of the incident π^- in which many secondary pions interact again.

A similar investigation of K^- production by mechanism B does not seem to be possible, in the absence of sufficient data on the production cross-section at different energies and on the probabilities of reabsorption of the created K^-.

Σ hyperons and mechanism B. If the Σ's are generally produced by secondary pions of 1 to 2 GeV, (this is the energy of most pions in the Monte Carlo calculation of model B), it can be understood why the observed Σ are grey tracks. We have tried to check this point by assuming that the observed Σ-K pairs are produced by secondary pions in the reaction π + nucleon $\to \Sigma^\pm + K^+$. It is then possible to calculate for each pair the longitudinal Fermi momentum of the nucleon necessary to satisfy the conservation laws. The results are listed in Table II.

TABLE II.

Event	Type of star	$\theta_{\Sigma^-\text{-beam}}$	p_F longitud. (*) (MeV/c)
τ_{48}	$17+0\ \pi^-$	5°	~ -100
K_1	$27+0\ \pi^-$	6°	~ 0
τ'_6	$2+2\ \pi^-$	7° 5	~ 0
τ_3	$9+0\ \pi^-$	15°	~ -100
τ'_2	$9+1\ \pi^-$	25°	~ 0
K_{150}	$8+2\ \pi^-$	22°	~ 0
K_{130}	$14+1\ \pi^-$	71°	~ -200
K_{24}	$6+1\ \pi^-$	41°	~ -500
K_{41}	$11+1\ \pi^-$	80° 5	~ -500

(*) a negative p_F means that the nucleon moves toward the pion, in the laboratory system.

The first 6 events are quite reasonable, the last two are absurd. Notice that the angle of the Σ in the last three is much larger, which may indicate a secondary interaction of the hyperon itself inside the nucleus.

The number of observed Σ (25%) is also consistent with the assumption that mechanism B accounts for a large fraction of the observed K^+.

2'2. *Mechanism A.* – Although the previous discussion has shown that most of the observed K^+ are produced in secondary collisions, it seem reason-

able to assume that by selecting only very small origins, we can have a sample of K produced predominantly according to mechanism A. We have selected the following categories:

a) π^--proton collisions. Some K^+ may originate in collisions of beam pions on hydrogen nuclei of the emulsion: these stars must fit the reactions

$$\pi^- + p \to \Sigma\,(\Lambda) + K^+ + n\pi$$
$$\to \text{nucleon} + K^+ + \overline{K} + n\pi$$

with different sign possibilities for Σ, nucleon, $\overline{K}$ and π.

They must have no black prongs or blobs, 1 or possibly 2 grey tracks (including the K) and an even number of prongs.

b) π^--neutron collisions. Some stars look like interactions on an isolated neutron (no black tracks or blobs, odd number of tracks, $\leqslant 2$ grey tracks). Those are probably examples of collisions on edge neutrons.

c) In the same spirit, we have selected stars of the two preceding types presenting in addition a blob or a few short evaporation tracks ($\leqslant 1$ black track of range $> 20\ \mu m$, plus any number of tracks $\leqslant 20\ \mu m$).

None of these stars is compatible with a pure $\pi^- + p \to \Sigma^- + K^+$ reaction, all involving at least 3 particles in the final state.

The angular distribution of K^+ and K^- from these stars is given in Fig. 6-*a* (the results concerning K^+ and K^- are quite similar, and have been put together). It is compared with distributions calculated under the following assumptions:

i) The distribution of p^*, the momentum of the K in the center of mass of the collision, is derived from phase space considerations ([19,20]). To

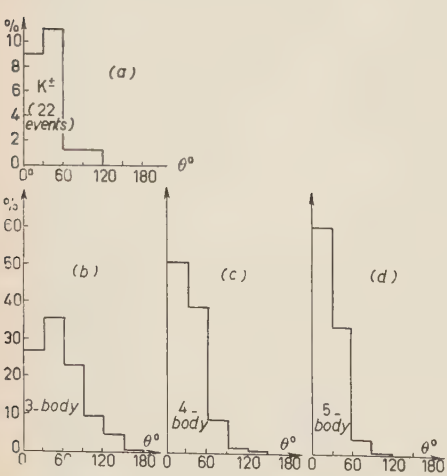

Fig. 6. – *a*) angular distribution of $K^\pm$ observed in small stars; *b*) angular distribution calculated for 3-body reaction; *c*) angular distribution calculated for 4-body reaction; *d*) angular distribution calculated for 5-body reaction.

([19]) M. M. BLOCK: *Phys. Rev.*, **101**, 796 (1956).
([20]) G. E. A. FIALHO: *Phys. Rev.*, **105**, 328 (1957).

a very good approximation it depends only on the number of particles in the final state. Only reactions producing three particles ($\Sigma K\pi$ or $K\bar{K}$ Nucleon), four particles ($\Sigma K\pi\pi\varphi$ or $K\bar{K}$ Nucleon $\pi\varphi$) or five particles ($\Sigma K\pi\pi\pi$, or $K\bar{K}$ Nucleon $\pi\pi$) are considered.

ii) The angular distribution of the K in the center of mass system is assumed to be isotropic in the limited backward solid angle corresponding to K stopping in the stack ($\sim 4\pi/10$).

The distributions calculated under the above assumptions are corrected for stack geometry and scanning inefficiency, as discussed in Appendix I, the result being the calculated histograms of Fig. 6 *b*, *c* and *d*.

It is seen that the agreement with the calculated distributions is good, especially if a 4 body reaction is chosen. This agrees with the observation in the diffusion chamber at Berkeley [21] in which the observed cases of strange particle production are accompanied by at least one secondary pion.

Cross-sections. Assuming the validity of mechanism A for these small stars it is possible to calculate production cross-sections in π^--nucleon collisions at 4.3 GeV (see Appendix I), assuming a 3, 4 or 5 body reaction and isotropy of the K in the center of mass. This calculation requires the mean free path for the production of small stars as defined above, whether or not origins of K. This is deduced from the number of small stars (« small » being defined by the previously given criteria) observed in the scanning along beam tracks already discussed in Sect. **1**·1, and from the length of beam track followed. The resulting mean free path for the production of small stars is (121 ± 21) cm. From this figure, from the known total π^--nucleon cross-section at 4.3 GeV of (25 ± 2.5) mb [21,22], and from the number of K observed to originate from small stars, cross-sections for K^+ production by π^--nucleon collision (i.e. $[(Z\sigma_{\pi^- p} + (A - Z)\sigma_{\pi^- n})/A]$ averaged over emulsion nuclei) can be calculated and are shown in the first row of Table III. From the angular distributions (see previous paragraph), the best values are probably those corresponding to 4 or 5 body reactions.

It must be emphasized that, strictly speaking, this experiment only measures the values of $d\sigma/d\Omega$ ($\theta \approx 180°$) and that the cross-sections in Table III are really values of $4\pi(d\sigma/d\Omega)(180°)$: their interpretation as true total cross sections depends on the validity of the assumption of isotropy of the K^+-production in the center of mass.

(21) G. Maenchen: *Thesis UCRL*, 3730 (1957).
(22) F. Wikner: *Thesis UCRL*, 3639 (1957).

3039

The second row of Table III gives the cross-sections obtained when all K origins, rather than just the very small ones, are included in the calculation. The larger values obtained reflect the important role played by secondary interactions in the larger origins.

TABLE III.

	K^+		K^-	
	3 body	4 or 5 body	3 body	4 or 5 body
only small stars	(1.1 ± 0.4) mb	(0.7 ± 0.3) mb	(0.5 ± 0.25) mb	(0.3 ± 0.15) mb
all K origins	(3.5 ± 1.0) mb	(2.3 ± 0.7) mb	$(0.9 \pm 0.3\ )$ mb	(0.5 ± 0.15) mb

The fact that the difference between these values and the cross-sections obtained from the small stars is less marked for K^- than for K^+ suggests (without proving it, though) that the fraction of slow K produced by mechanism A is higher for K^- than for K^+. This could also explain the smaller size of the origins of K^- and their angular distribution more concentrated in the forward direction, when compared to K^+.

Very little can be said on the role played by the secondary interactions of the K. It is probably unimportant when small origins of K^+ are considered, but in addition to the small origins of K^- there might be a few other interactions on edge nucleons in which the K^- is reabsorbed, thus giving a larger star. Therefore the cross-sections given in Table III for K^- production must probably be considered as lower limits.

3. – « Neutral » origins.

As mentioned before (see Introduction), 18 origins of K^+, 5 of K^- and 2 of Σ^+ definitely have a neutral primary. All of these, except 3 origins of K^+ and one of K^-, are small stars with visible energy (the K or Σ not being counted) < 300 MeV; 14 have visible energy < 100 MeV and 4 have no other charged prongs than the K (or Σ).

It can be proved that only a small fraction of these stars ($\sim \frac{1}{5}$ at the most) are likely to have been originated by fast neutrons.
This is derived from a combination of the following data:

a) The density of ordinary stars with neutral primaries as a function of the number of minimum prongs, determined by an area scanning made in different places in our stack.

b) The observations made at Rochester [23] on the types of stars produced in emulsion by 3 GeV protons (in particular, the shower prong distributions of such stars).

The majority of these neutral origins can probably be attributed to charge-exchange interactions of neutral strange particles. This explanation agrees with the facts that the stars are generally small and that their number (25) is of the same order as the number of origins with a grey primary or a minimum primary not parallel to the beam (34).

From the θ_1^0, θ_2^0 point of view [24], it may seem surprising that such a low K^-/K^+ ratio is found in these charge-exchange stars. Even if only the interactions of particles produced as θ^0 are considered, one would expect them to give rise to an important $\bar{\theta}^0$ component, because the average path length in the stack is longer than the average decay length of the θ_1^0. If n and $\bar{n}$ are the frequencies of interactions of θ^0 and $\bar{\theta}^0$ respectively in the central part of the stack, $\bar{n}/n$ can be estimated by a calculation similar to the analysis made by CASE [25] of the Pais-Piccioni experiment [26]; taking 90 cm and 30 cm for the interaction m.f.p. of θ^0 and $\bar{\theta}^0$ respectively, one finds that $1 < \bar{n}/n < 3$ (the indetermination comes from a phase term, related to the mass difference between θ_1^0 and θ_2^0, which is unknown). In fact, there are also interactions of particles produced as $\bar{\theta}^0$, for which $\bar{n}/n$ is larger, and of Λ^0 (for which $n = 0$). The expected $\bar{n}/n$ should then be definitely greater than 1.

However, this conclusion is not in disagreement with the observed $(5\,K^- + 2\,\Sigma)/18\,K^+$ ratio, because a large part of the interactions of $\bar{\theta}^0$ and Λ^0 can yield hyperons which are not detected in the scanning (Λ^0, Σ^0, $\Sigma^\pm$ decaying in flight).

These results also agree with previous observations on the interactions in emulsion of long lived strange particles [27].

4. – Conclusions.

It is possible to give a picture of the production of slow K^+ in emulsion nuclei by 4.3 GeV π^-. A large fraction of the K^+ ($\gtrsim \frac{1}{2}$ of those with energy < 150 MeV) is produced in secondary collisions of pions, or possibly nucleons, resulting from the first interaction of the beam pion. These K^+ are probably associated mostly with hyperons (Λ^0 or Σ), and perhaps a few $\bar{K}$.

---

[23] T. F. HOANG: Private communication.
[24] M. GELL-MANN and A. PAIS: *Phys. Rev.*, **97**, 1387 (1955).
[25] K. M. CASE: *Phys. Rev.*, **103**, 1449 (1956).
[26] A. PAIS and O. PICCIONI: *Phys. Rev.*, **100**, 1487 (1955).
[27] R. LEVI-SETTI: *7th Rochester Conference* (1957).

At 4.3 GeV, about 3% of the π^--nucleon collisions produce K^+ ($\sigma \sim 0.7$ mb out of a total of 25 mb). If the production cross-section of K^0 is not very different from that of K^+ (a rather natural assumption if several π are also produced in the reaction) the total cross-section for strange particle production is ~ 1.5 mb ($1 \div 2$ mb). It thus appears that there is no spectacular rise of this cross-section as the π energy increases from 1 to 5 GeV, the cross-section of $1 \div 1.5$ GeV being already ~ 1 mb ([28]). This conclusion is invalidated if, for pion energy around 4 GeV, the K^+ are emitted very predominantly forward in the center of mass, for in this case they would evidently not be detected in this experiment.

Insofar as the K^- are concerned, the situation is much less clear. It is evident that the predominant K^+ mechanism namely

$$\begin{aligned}\pi^- + \text{Nucleon} \rightarrow \text{Nucleon} + \pi + \pi + \dots \\ \quad \longrightarrow + \text{Nucleon} \rightarrow \Sigma \ \ (\text{or } \Lambda^0) + K^+\end{aligned}$$

is not allowed for K^- because of the strangeness selection rules. Hence the existence of differences between K^+ and K^- origins both as to star size and as to K angular distribution can be understood without any more detailed knowledge of K^- production mechanisms. It does seem likely, however, because of the higher threshold for K^- production, that a larger fraction of the K^- are produced in the initial interaction than is the case for K^+. The observed differences between K^+ and K^- origins are not in disagreement with this assumption.

From the number of small origins of K^-, the production cross-section of K^- at $4 \div 5$ GeV in π^--nucleon interactions is ~ 0.3 mb, as compared to ~ 0.7 mb for K^+. This would imply a $K\overline{K}/KY$ branching ratio of ~ 1.

However this result is very approximate because of large statistical errors and because the proportion of reabsorbed K^- cannot be evaluated. If the latter is important, $K\overline{K}$ reactions can well be the predominant ones at 4 GeV.

Thus it appears that the cross-section for hyperon production in π-nucleon collisions probably does not increase between 1 and 5 GeV, and may even decrease.

* * *

We are very grateful to Professor E. J. LOFGREN who arranged the exposure of the stack and to the members of the Bevatron staff who realized it in perfect conditions.

([28]) R. G. GLASSER: *7-th Rochester Conference* (1957).

We also thank Professor L. LEPRINCE-RINGUET for his constant help and encouragement, Mr. WALLER for the fabrication of the stack, and Mmes R. FAIST, J. J. SEROPIAN, J. VITA, Mlles M. DUCROS, M. LEPLÉ and M. M. RANÇON for their considerable and efficient scanning work.

APPENDIX I

Calculation of geometrical corrections.

We define:

I: beam intensity (variable).

n: number of beam interactions per cm^3 of emulsion excluding diffraction scattering).

$\lambda = I/n$ = m.f.p. of π^- in emulsion ($= (36.4 \pm 3.3)$ cm. See Sect. **1**·1).

$N(R, \theta)\,\mathrm{d}R\cdot\mathrm{d}\theta$: number of $K^\pm$ of range between R and $R + \mathrm{d}R$, angle between θ and $\theta + \mathrm{d}\theta$ stopping per cm^3 of emulsion scanned.

$g(R, \theta)\,\mathrm{d}R\cdot\mathrm{d}\theta$: Probability that a $K^\pm$ has a range between R and $R + \mathrm{d}R$ and angle between θ and $\theta + \mathrm{d}\theta$.

$\mathrm{d}V$: element of volume scanned V.

ξ: ratio of $K^\pm$ producing stars to total stars (constant).

φ: azimuthal angle of K-beam plane.

Obviously:

$$N(R, \theta)\,\mathrm{d}R\cdot\mathrm{d}\theta\cdot\mathrm{d}V = g(R, \theta)\,\mathrm{d}R\cdot\mathrm{d}\theta\cdot\mathrm{d}V \int \xi\cdot n\,\frac{\mathrm{d}\varphi}{2\pi}, \tag{1}$$

$$= g((R, \theta)\,\mathrm{d}R\cdot\mathrm{d}\theta\cdot\mathrm{d}V\cdot\frac{\xi}{\lambda}\int I\,\frac{\mathrm{d}\varphi}{2\pi},$$

where $I(R, \theta, \varphi)$ is taken at the point of coordinates R, $\pi - \theta$, $\varphi + \pi$ from point scanned.

The total number of such K's in the scanned region will be:

$$\mathrm{d}R\cdot\mathrm{d}\theta\cdot\int_V N(R, \theta)\,\mathrm{d}V = g(R, \theta)\cdot\mathrm{d}R\cdot\mathrm{d}\theta\cdot\frac{\xi}{\lambda}\cdot\int_V\int_\varphi \mathrm{d}V\cdot I\cdot\frac{\mathrm{d}\varphi}{2\pi}. \tag{2}$$

The ratio: mesons stopping in the scanned area to total mesons produced,

will be proportional to:

$$L(R, \theta) = \iint \mathrm{d}V \cdot I \cdot \frac{\mathrm{d}\varphi}{2\pi} \cdot$$

This depends on the volume scanned; it is therefore more convenient to « normalize » it, thus getting an expression approximately independent of scanned volume, if the region scanned is not too large. We can take:

$$P(R, \theta) = \frac{L(R, \theta)}{L(0, \theta)}, \tag{3}$$

where $L(0, \theta)$ is obviously equal to the total length $\mathcal{L}$ of beam tracks traversing the scanned region.

Taking into account stack geometry, beam intensity and the position of the scanned region, it is possible to calculate $P(R, \theta)$. Then substituting in (2), we get:

$$\mathrm{d}R \cdot \mathrm{d}\theta \cdot \int N(R, \theta) \cdot \mathrm{d}V = g(R, \theta) \cdot \mathrm{d}R \cdot \mathrm{d}\theta \cdot \frac{\xi}{\lambda} \cdot \mathcal{L} \cdot P(R, \theta)\,. \tag{4}$$

The total number of particles stopping in the scanned volume is therefore:

$$\mathcal{N} = \iiint N(R, \theta) \cdot \mathrm{d}V \cdot \mathrm{d}R \cdot \mathrm{d}\theta = \frac{\xi}{\lambda} \cdot \mathcal{L} \cdot \int_0^\infty \int_0^\pi g(R, \theta) \cdot P(R, \theta) \cdot \mathrm{d}R \cdot \mathrm{d}\theta\,. \tag{5}$$

In the calculation of angular distributions such as those given in Fig. 6 b, c, d, the quantity $g(R, \theta)$ is evaluated from the assumed model of production and then the right side of (4) is integrated with respect to R. Once $g(R, \theta)$ is known, ξ can be evaluated from (5) and, from it, a production cross-section can be derived (Table III).

It is possible to obtain a production cross-section or mean free path for slow K without any hypothesis as to a production model (Sect. **1**·4), for in this case the behavior of $g(R, \theta)$ in the range of values of R of interest can be inferred from the experimental observations. In particular if one confines oneself to K for which $P(R, \theta)$ is not too small, i.e. $R \lesssim 10$ cm, equation (5) can be approximated by:

$$\mathcal{N} = \frac{\xi}{\lambda} \cdot \mathcal{L} \cdot \frac{\mathcal{N}}{\sum\limits_{i=1}^{\mathcal{N}} \dfrac{1}{P(R_i, \theta_i)}}\,,$$

or:

$$\xi = \frac{\lambda}{\mathcal{L}} \cdot \sum_{i=1}^{\mathcal{N}} \frac{1}{P(R_i, \theta_i)}\,. \tag{6}$$

The mean free path for the production of slow K is then λ/ξ or:

$$\lambda^{K} = \frac{\lambda}{\xi} = \frac{\mathcal{L}}{\sum_{i=1}^{\mathcal{N}} \frac{1}{P(R_i, \theta_i)}} . \tag{7}$$

The statistical error in λ^K is easily shown to be:

$$\frac{\Delta\lambda^{K}}{\lambda^{K}} = \frac{\sqrt{\sum_{i=1}^{\mathcal{N}} \left(\frac{1}{P(R_i, \theta_i)}\right)^2}}{\sum_{i=1}^{\mathcal{N}} \frac{1}{P(R_i, \theta_i)}} . \tag{8}$$

Appendix II

Possible K^- contamination in the π^- beam.

This has been investigated by two methods.

a) Information supplied by the Berkeley Laboratory (29) and derived from other experimental data gives an upper limit for the percentage of K^- in the beam of $\sim 0.7\%$ at the entrance to our stack, if the K^-/π^- ratio at production is assumed to be not greater at 4.3 GeV/c than at 0.9 GeV/c.

Assuming that (i) high-energy π^- and K^- have the same interaction mean free path, (ii) at least half the K^- change into K^0 or hyperons after interacting, (iii) the energy and angular distributions of K^- resulting from the interactions of K^- in the beam are the same as those of K^- produced by beam pions, one gets an upper limit for the number of beam K^- stopping in the scanned area after interaction of about 20% of the observed number of K^-.

b) To check further, we took advantage of the fact that the momentum of the beam pions is not uniform at the stack entrance, but varies between ~ 3.8 GeV/c and ~ 4.8 GeV/c from one end to the other (29).

A rough phase-space calculation of the production of K^- by 6.2 GeV protons in the target shows that it is much more difficult to produce a K^- at 4.8 GeV/c than at 3.8 GeV/c. This of course, is also true of π^-, but to a much lesser degree. We can expect the fraction of K^- in the beam to vary by a factor ~ 5 or more from one end of the stack to the other. On the other hand, the τ/π^- ratio will remain constant.

We therefore made a fast scanning at both ends of the stack, noting espe-

(29) E. J. Lofgren and W. W. Chupp: Private communication.

cially the τ and K^-. If there are many K^- in the beam, the K^-/τ ratio should decrease strongly from one end to the other and be intermediate in the « scanned area ». The results are shown in Table IV.

TABLE IV.

	4.8 GeV/c end	Scanned area	3.8 GeV/c end
K^-	12	72	10
τ	13	48	7
K^-/τ	0.95 ± 0.4	1.50 ± 0.3	1.4 ± 0.7

Methods *a*) and *b*), then, agree to indicate that at most $\lesssim 20\%$ of the observed K^- are produced by K^- in the beam. We have taken 10% for our calculations.

APPENDIX III

Proportion of associated hyperons.

a) First, a correction must be made for the $\Sigma^{\pm}$ decays missed even though they occur on the observed parts of the tracks: $\Sigma^+ \to p+\pi^0$ in flight (confusion with scattering of proton), and those of the Σ^- captures at rest which do not give a visible star (this is assumed to be half of the captures at rest).

It has been assumed that there is an equal number of Σ^+ and Σ^- and that the $(\Sigma^+ \to p)/(\Sigma^+ \to \pi^+)$ ratio is 1. From this, 75% of the $\Sigma^{\pm}$ decaying at rest or in flight in the observed parts of the tracks are detected.

b) Certain prongs of the 196 stars studied for associated hyperons have not been followed or have been observed on only part of their total range. The proportion of tracks followed being different for black, grey and minimum, the estimated percentage of Σ depends on the assumed energy distribution of the Σ. This makes a rigorous calculation impossible. In order to reduce this uncertainty, the calculation has been done separately for black, grey and minimum prongs.

For grey prongs for instance, the total number of « grey » Σ decays which would be observed if there were one grey $\Sigma^{\pm}$ in each star having grey prongs is,

$$A = 0.75 \sum_1^N \left(1 - \frac{\sum_1^n \exp[-t/\tau]}{n}\right),$$

where N is the number of stars with grey prongs ($N < 196$),
n is the number of grey prongs in each star,
t is the time of flight corresponding to the observed length of a prong ($t = \infty$ for a track followed to its end),
τ is the mean life of the $\Sigma^\pm$.

The result is very insensitive to the valué of τ, because the tracks were followed on sufficient lengths ($\gtrsim 5$ cm). We have taken $\tau = 1.2 \cdot 10^{-10}$ s.

The proportions ϱ of $\Sigma^\pm$ of each kind (black, grey and minimum) per K^+ star is then given by:

$$\varrho = \frac{N}{196}\,\frac{m}{A}\,,$$

m being the number of actually observed Σ decays. The result is

Black tracks	$N = 184$	$A = 83$	$m = 1$	$\varrho = 0.01 \pm 0.01$
Grey tracks	$= 178$	$= 47$	$= 8$	$\varrho = 0.16 \pm 0.06$
Minimum tracks	$= 124$	$= 10$	$= 0$	$\varrho = 0\,^{+0.1}_{-0}$
			Total:	$\varrho = 0.17\,^{+0.12}_{-0.06}$

Appendix IV

Monte Carlo calculations of mechanism *B*.

The assumptions are the following:

a) The mean free path of the incoming 4.3 GeV π^- and of the secondary pions in nuclear matter is $2.5 \cdot 10^{-13}$ cm.

b) The target nucleon is at rest, in the first and in the second collision.

c) The multiplicity of pions created in the first collision is derived from calculations made by A. I. Nikishov ([30]) based on a statistical model and on the results of the diffusion chamber at Berkeley ([1]). These are not in disagreement with more recent data of the diffusion chamber ([21]).

d) The c.m. energy spectrum of the pions is calculated from phase-space considerations ([19,20]). The c.m. angular distribution is isotropic.

e) The cross section for production of strange particles is constant and equal to 1 mb from $E_\pi = 840$ MeV up to about 2.5 GeV (*). This assumption of a flat excitation function is suggested by recent results summarized at the 7th Rochester Conference ([28]), added to former data of the diffusion chamber

---

([3]) A. I. Nikishow: *Żurn. Ėxp. Theor. Fiz.*, **30**, 990 (1956).

(*) The probability of getting secondary π of energy > 2.5 GeV and the low corresponding detection probability of K make the results insensitive to the excitation function above 2.5 GeV, unless it happens to rise very sharply.

at Brookhaven (31). In the $2\div 2.5$ GeV region the 1 mb value is possibly inaccurate, but the corresponding fraction of the events is quite small, because a large proportion of the pions have energies $\leqslant 1.5$ GeV and because the probability for the K to stop in the stack decreases very rapidly when E_π increases.

f) The c.m. energy of the K depends uniquely on the energy of the incident secondary pion and is calculated in the following way: for $E_\pi < 1.4$ GeV, it corresponds to the $\pi^- + \text{nucleon} \to \Sigma + K$ reaction;

for $E_\pi = 2.5$ GeV, it corresponds to the maximum of the phase space distribution for $\pi^- + \text{nucleon} \to \Sigma + K + \pi$.

for intermediate energies, the energy is obtained by interpolation.

g) The c.m. angular distribution of the K^+ is isotropic.

The calculation has been done separately in heavy (Ag, Br) and light (C, N, O) nuclei.

Note added in proof.

N. B.: Re ent results given at the Venice/Padua Conference 1957 indicate that the cross-section assumed in *e*) is somewhat high and should be about halved. This does not c ange essentially the conclusions.

(31) W. B. Fowler, R. P. Shutt, A. M. Thorndike and W. L. Whittemore: *Phys. Rev.*, **98**, 121 (1955).

RIASSUNTO (*)

Un grosso pacco di emulsioni è stato esposto al fascio di π^- di 4.3 GeV del bevatrone di Berkeley. Si sono osservati 317 K^+ e 96 K^- arrestati nel pacco. 184 K^+ e 66 K^- sono stati seguiti all'indietro fino a una stella originaria prodotta da uno dei π^- del fascio. Le origini dei K^+ sono più ampie di quelle dei K^- per quanto riguarda il numero di rami neri e grigi e l'emissione dei K^- è più concentrata in avanti di quella dei K^+. All'origine dei K^+ si sono osservati Σ carichi di moderata energia; la loro frequenza è $0.17^{+0.12}_{-0.06}$ per stella. I cammini liberi medi per la produzione di K^+ e K^- di < 150 MeV in emulsione sono rispettivamente (4700 ± 1200) cm e (24000 ± 7000) cm. La maggioranza dei K^+ arrestati nel pacco sono probabilmente prodotti in collisioni nucleari secondarie dei pioni risultanti dal primo urto dei π^- incidenti. Una frazione maggiore dei K^- è probabilmente prodotta nella prima collisione. Valori approssimati delle sezioni d'urto di produzione di particelle strane nella collisione dei π^- di 4.3 GeV coi nucleoni si possono dedurre dallo studio di ristrette origini di K^+ e K^- opportunamente scelte. La sezione d'urto per la produzione di K^+ è ~ 0.7 mb. Per i K^- è probabilmente $\geqslant 0.3$ mb. Appare pertanto che, crescendo l'energia dei pioni da 1 a 4 GeV, non si ha un aumento pronunciato della sezione d'urto totale per la produzione di particelle strane. La produzione $K\bar{K}$ risulta essere una sostanziale frazione del totale e la produzione diretta di iperoni resta probabilmente costante o decresce.

(*) *Traduzione a cura della Redazione.*

3048

IL NUOVO CIMENTO Vol. VI, N. 5 1° Novembre 1957

Effect of the Spin-Orbit Potential on the Magnetic Moment of the Deuteron (*).

J. J. Swart, R. E. Marshak and P. S. Signell
University of Rochester - Rochester, New York

(ricevuto il 3 Settembre 1957)

Summary. — It is shown that at the present stage the contribution to the magnetic moment of the deuteron does not pose a serious dilemma for the spin-orbit potential explanation (in addition to the Gartenhaus potential) of the high energy nucleon-nucleon scattering (up to 150 MeV).

In a recent paper, two of us have shown that the addition of a strong short range attractive spin-orbit potential (in the $J = L + 1$ state) to the Gartenhaus potential gives an excellent charge-independent fit of all the available two-nucleon scattering data up to 150 MeV (1). Gammel and Thaler (2) have independently shown that a certain combination of central, tensor and spin-orbit Yukawa forces with repulsive cores will yield a good explanation of the p-p scattering data up to 310 MeV and a somewhat poorer but still reasonable fit of the n-p scattering data up to the same energy. Recently, Feshbach (3) has calculated the consequences of the SM and GT spin-orbit potentials for the magnetic moment of the deuteron along the lines first suggested by Blanchard et al (4).

(*) This work was supported in part by the Atomic Energy Commission.

(1) P. S. Signell and R. E. Marshak: *Phys. Rev.*, **106**, 832 (1957).

(2) J. L. Gammel and R. M. Thaler: *Proc. of Seventh Rochester Conference on High Energy Physics* (1957).

(3) H. Feshbach: to be published. We are indebted to Prof. Feshbach for sending us a preprint of his work.

(4) F. H. Blanchard, R. Avery and R. G. Sachs: *Phys. Rev.*, **78**, 292 (1950).

In his calculation, Feshbach neglets the effects of the D state wave function for the deuteron and uses an approximate S state wave function. He finds that the additional contribution to the magnetic moment of the deuteron, $\Delta\mu$, is -0.056 n.m. for the SM potential and -0.036 n.m. for the GT potential, both numbers exceeding in magnitude the difference, -0.0224 n.m., between the magnetic moment of the deuteron and the sum of the magnetic moments of the neutron and proton. Such a large value for $\Delta\mu$ implies a negative value for p_D, the D state probability in the deuteron. Feshbach feels that his calculation poses a serious dilemma for a two-nucleon spin-orbit interaction of the type utilized by SM and GT to fit the scattering data.

We wish to point out that at this stage of our understanding of the two-nucleon interaction, the dilemma of the magnetic moment of the deuteron is really not so serious. Apart from the continuing uncertainty in the mesonic and relativistic corrections (5) to the deuteron magnetic moment, it seems that Feshbach has overestimated the magnetic moment contribution of the spin-orbit force. If one uses a more realistic ground state wave function for the deuteron, e.g. the wave function predicted by the Gartenhaus potential (6), the contribution of the SM spin-orbit potential to the magnetic moment is reduced in magnitude. We find that

$$\Delta\mu = (-0.029 + 0.007 - 0.002)\ \text{n.m.} = -0.024\ \text{n.m.}$$

where the first term is the contribution of the S state, the second of the S-D interference and the third of the D state. Using the Gartenhaus ground state wave function, the GT spin-orbit potential gives a contribution of -0.017 n.m. to the magnetic moment of the deuteron. Feshbach's approximate ground state wave function for the deuteron thus overestimates the magnetic moment contribution of the spin-orbit potential by more than a factor of 2.

While the situation is much improved by the use of a more accurate deuteron wave function, it is still not too satisfactory. The value of p_D predicted by the Gartenhaus potential (6) (which constitutes the central plus tensor part of the SM potential) is 6.8% and this is too large to reconcile with the $\Delta\mu$ contributed by the SM potential-even if allowance is made for the uncertain mesonic and relativistic effects. However, there is an additional avenue of escape which is readily available at the present time. In deducing the consequences of the SM potential, it must be remembered that the spin-orbit

---

(5) Cfr. M. Sugawara: *Progr. Theor. Phys.*, **14**, 535 (1955) for the latest estimates. Sugawara's calculations are based on the Tamm-Dancoff method which is certainly unreliable for treating pion effects.

(6) S. Gartenhaus: *Phys. Rev.*, **100**, 900 (1955). We are indebted to Dr. Gartenhaus for sending us a table of the deuteron wave function.

part is purely phenomenological and permits of an isotopic spin dependence which has not been fully exploited. In particular, we can show that the fits of the n-p scattering data up to 150 MeV obtained with the SM potential will be only slightly affected by changes in the spin-orbit potential which completely eliminate the spin-orbit contribution to the magnetic moment of the deuteron.

As one illustration, we report the results of reversing the sign of the tail of the spin-orbit potential beyond $r = 1.4$ fermi in even parity states only (isotopic spin $T = 0$). In odd parity states ($T = 1$), the spin-orbit potential is left unchanged. This is equivalent to an isotpic spin dependence of the spin-orbit potential. As shown in Fig. 1, the new unpolarized n-p cross section at 150 MeV changes very little. The new n-p polarization curve 150 MeV matches experiment as well as before and, of course, the p-p predictions are completely unaffected. With the new spin-orbit potential in the $T = 0$ state [7], $\Delta\mu$ becomes negligible, namely -0.001 n.m. The minor changes in the n-p scattering cross sections up to 150 MeV despite the obliteration of the magnetic moment contribution to the deuteron are a consequence of the relative unimportance of the tail of the spin-orbit potential for the scattering in this energy region.

Other choices of the $T = 0$ spin-orbit potential are possible, such as eliminating it completely, without serious modification of the n-p scattering predictions up to 150 MeV [8] and, of course with no change in the p-p predictions. We therefore

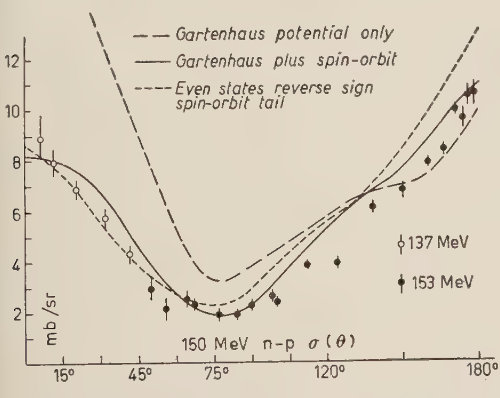

Fig. 1. – Comparison of potential predictions with experimental n-p scattering cross-section at 150 MeV. The dashed line represents the Gartenhaus prediction, the solid line the prediction of the SM potential and the dotted line the prediction of the SM potential except that the spin-orbit potential in the $T = 0$ state has a reversed tail beyond $r = 1.4$ f (see text).

---

(7) The reversed tail which we are considering introduces a discontinuity into the $T = 0$ spin-orbit potential at $r = 1.4$ f. This discontinuity simplifies the reprogramming of the calculation but is of no physical consequence; a continuous spin-orbit potential which reverses sign would do just as well.

(8) The Gartenhaus potential itself is, of course, not sacred. The assumptions underlying the derivation of the Gartenhaus potential (cfr. ref. (6)) imply that the potential should not be taken too seriously at small distances (of the order of the nucleon Compton wave length). As a matter of fact, major modifications of the Gar-

conclude that a combination of phenomenological spin-orbit plus Gartenhaus potential can be chosen so as to match the scattering data up to 150 MeV without posing a dilemma for the magnetic moment of the deuteron. We agree with Feshbach (3) that the magnetic moment of the deuteron places a valuable restriction (9) on the spin-orbit potential in the $T=0$ state of the n-p system. However, we believe that the available data on the two-nucleon interaction do not require us to abandon the spin-orbit potential as an important component of this interaction and to invoke more complicated and less plausible hypotheses (3).

---

tenhaus potential at small distances do not hurt agreement with experiment up to 150 MeV provided the spin-orbit potential is retained in the $T = 1$ state (see forthcoming paper by SIGNELL and MARSHAK). We regard the Gartenhaus potential as a reasonable representation of the central plus tensor parts of the total charge-independent two-nucleon interaction. Preliminary investigation shows that one can probably get good fits to the n-p scattering data by elimination of the $T = 0$ spin-orbit potential with simultaneous enhancement of the triplet even central (Gartenhaus) potential in the core region ($\mu r < 0.35$).

(9) The same statement can be made about the binding energy of the deuteron. Indeed, the same recipes which help with the magnetic moment are also favorable for the binding energy. For example, the SM potential, as it stands, yields a repulsive spin-orbit contribution in the ${}^3D_1$ state. A reversed tail on the spin-orbit potential would help to bring the binding energy back toward the Gartenhaus (correct) value, and elimination of the $T=0$ spin-orbit potential completely would of course give the deuteron parameters derived by Gartenhaus (6).

RIASSUNTO (*)

Si dimostra che attualmente il contributo al momento magnetico del deutone non pone un serio dilemma alla spiegazione del potenziale spin-orbita (in aggiunta al potenziale Gartenhaus) dello scattering nucleone-nucleone ad alta energia (fino a 150 MeV).

(*) *Traduzione a cura della Redazione.*

3032

IL NUOVO CIMENTO Vol. VI, N. 5 1° Novembre 1957

Hilbert Spaces in Quantum Field Theories.

S. Albertoni

Istituto di Matematica del Politecnico - Milano
Laboratori CISE - Milano

F. Duimio

Istituto di Scienze Fisiche dell'Università - Milano
Istituto Nazionale di Fisica Nucleare - Sezione di Milano

(ricevuto il 23 Settembre 1957)

Summary. — One examines the structure of the Hilbert space spanned by the states of a quantized field. A hypothesis is made concerning the possibility of a physical interpretation of various subspaces of it, and connections with some « pathological » results derived by several authors, are indicated.

1. – Introduction.

The various difficulties and inconsistencies, which appear in quantum field theories, have stimulated a number of researches on the mathematical basis of such theories.

In this paper we shall briefly review the main features of these studies. In particular, we shall emphasize the following items:

1) The infinite direct product of Hilbert spaces introduced by von Neumann (1) as the most natural frame for the development of quantum field theories.

2) The possible representations of field operators (2-5).

(1) J. v. Neumann: *Compositio Math.*, **6**, 1 (1939).
(2) K. O. Friedrichs: *Mathematical aspects of the quantum theory of fields* (New York, 1953).
(3) L. Garding and A. Wightman: *Proc. Acad. Nat. Sci.*, **40**, 617 (1954).
(4) A. Wightman and S. Schweber: *Phys. Rev.*, **98**, 812 (1955).
(5) R. Haag: *Dan. Mat. Fys. Medd.*, **29**, no. 12 (1955).

In order to make as clear as possible the basis of the considerations we are going to develop, let us briefly recall the usual procedure generally adopted in field quantization.

1) One introduces field operators $\Phi_\lambda(x)$, i.e. a set of operators associated to every space point, at a given time (or, more generally, defined on a space-like surface σ). They are supposed to satisfy given commutation rules, and their evolution in time (in a Heisenberg picture) is determined by differential equations (equations of motion).

2) The Hamilton operator, from which te equations of motion are derived, is divided in two parts:

$$H = H_0 + H_I ,$$

where H_0 is the free field hamiltonian (whose essential feature is the time invariance of the equations of motion derived from it). H_I is the interaction hamiltonian.

3) The eigenstates of H_0 are generally determined in an occupation number representation. There is a complete equivalence between the set of such eigenstates and the eigenstates of an assembly of infinite oscillators. The interaction hamiltonian H_I causes transitions between these states.

4) A physical interpretation of the eigenstates of H_0 is built up in terms of free particles, obtaining in such a way equivalence between a free field theory and a many (free) particle theory.

However, where the interaction is introduced, the very meaning of the mentioned equivalence becomes obscure: it can be established only in particular cases, such as the non-relativistic theory [6] or the Dirac theory without positron interpretation, with external forces [7-10].

In this connection it is not useless to remind that the definition of a « physical particle » when the interaction is present, is not simple, because, for example, « a single electron », cannot be understood as a single quantum of a Dirac field, but as a complex system composed of such a quantum together

---

(6) W. HEISENBERG: *I principi fisici della teoria dei quanti* (Torino, 1953).

(7) W. FURRY and J. R. OPPENHEIMER: *Phys. Rev.*, **45**, 245, 343 (1934).

(8) R. BECKER and G. LEIBFRIED: *Phys. Rev.*, **69**, 34 (1946); *Zeits. f. Phys.*, **125**, 347 (1948).

(9) M. GUNTHER: *Phys. Rev.*, **88**, 1411 (1952).

(10) P. BOCCHIERI and A. LOINGER: *Nuovo Cimento*, **2**, 314 (1955).

with a « cloud » of photons and pairs. This phenomenon produces essential changes on the physical properties of the electron.

2. – Let us now introduce a free field and, for the sake of simplicity, we assume it to be enclosed in a cubic box, with volume V. Such a system, in accordance with 3) of Sect. **1**, is equivalent to a denumerable infinity of oscillators with frequencies $\omega_k (k = 1, 2, 3, ...)$. Consequently its Hamiltonian can be written in the following form (omitting the zero-point energy):

$$H_0 = \sum_K H_K = \sum_K \omega_K a_K^* a_K \,, \tag{1}$$

where a_K and a_K^* are the usual (annihilation and creation) operators introduced by Dirac in his treatment of the armonic oscillator (*). The eigenstates of H_0 can be classified wtih the help of an infinity of « quantum numbers » j_k, each of them defining the state of an oscillator. The most useful choice for the j_k is the one obtained using as « spectral variables » the eigenvalues of the number operator $N_k = a_K^* a_K$.

It follows that, if we denote with $\mathcal{H}^{(k)}$ the Hilbert space spanned by the eigenstates $|N_k'\rangle$ of the k-th oscillator, an eigenstate $|\xi_{H_0}\rangle$ of H_0 is heuristically representable with the infinitely multiple ket [11],

$$|\xi_{H_0}\rangle = |N_1'\rangle \cdot |N_2'\rangle \dots |N_k'\rangle \dots \,. \tag{1'}$$

It is natural at this point to try to investigate the rigorous connections between the space $\mathcal{H}$ to which the states (1′) belong and the various $\mathcal{H}^{(k)}$. This problem has been thoroughly analysed by von Neumann [1]. According to him the space $\mathcal{H}$ is nothing but the infinite direct product space

$$\mathcal{H} = \prod_K \otimes \mathcal{H}^{(k)} \,.$$

We report in appendix a rather detailed description of the properties of this space. However we stress here the fact that $\mathcal{H}$ is not separable (a simple $\mathcal{H}^{(k)}$ *is* separable!), and it can be decomposed with the help of some separable subspaces (which we shall call « bundles »), $\prod_k^{\sigma} \otimes \mathcal{H}^{(k)}$, called « incomplete infinite direct product » belonging to the equivalence class σ.

(*) Eventual labels for spin, isotopic spin, etc. are supposed to be enclosed in the k-index.

(11) P. A. M. Dirac: *Quantum mechanics*, third edition (Oxford, 1947).

Of particular importance is the « bundle » $\prod\limits_k^{(0)} \otimes \mathcal{H}^{(k)}$, the one which contains the vacuum state, i.e. the state of the type (1′) with $N_k^{'} = 0$ for every k. Only the states belonging to this « bundle » can be interpreted as describing (free) particles.

All the other states usually are not considered « physical » because they should correspond to states with an actual infinity of particles.

But, when interacting fields are considered, it is possible that, for particular choices of the interaction, transitions take place from states $\in \prod\limits_k^{(0)} \otimes \mathcal{H}^{(k)}$ to states not contained in it. Now however the eigenstates of $H_0 \in \prod\limits_k^{(0)} \otimes \mathcal{H}^{(k)}$ refer to situations with a finite number of « bare » particles, i.e. unobservable quantities; so we cannot assume as a « physicity » criterium, the finiteness of the number of such « bare » particles.

As a consequence we cannot *a priori* reject states with an actual infinity of bare particles (« myriotic fields » (*)): more precisely we cannot exclude in the development of the eigenstates of H in terms of eigenstates of H_0 the appearence of states of the mentioned « myriotic » type.

It comes out to be natural to investigate the possibility of a physical interpretation of those states, and moreover whether they can be useful in the fundamental problem concerning the diagonalization of the total hamiltonian H.

In this connection we quote the results obtained by VAN HOVE [12,13] and MIYATAKE [14], according to which H_I and H (+), for certain classes of field theories with point interaction, do not possess any domain in $\prod\limits_k^{(0)} \otimes \mathcal{H}^{(k)}$. They show that

$$\|H_I\,|n\rangle\|^2 = \infty\,,$$

$$\|H\;|n\rangle\|^2 = \infty\,,$$

when $|n\rangle$ is any state $\in \prod\limits_k^{(0)} \otimes \mathcal{H}^{(k)}$.

(*) Quot. [2] Sect. **19**.

(12) L. VAN HOVE: *Acad. R. Belgique, Bull. Cl. des Sciences* (Dec. 1951).

(13) L. VAN HOVE: *Physica*, **18**, 145 (1952).

(14) O. MIYATAKE: *Journ. Inst. of Polytechnics Math. series Osaka Univ.*, **2**, 89 (1951); **3**, 145 (1952).

(+) Obviously, any operator has to be considered as an « extended operator » in $\mathcal{H}$ as explained in the Appendix.

3. – In this section we expose an interesting fact, which only recently has been brought to the attention of physicists [4,5]: the problem of the representation of the q_K and q_K^* operators.

As it is well known these operators are completely determined (up to unity transformations) by the commutation relations, when they refer to a system with a finite number n of degrees of freedom.

But when $n \to \infty$, infinite non-equivalent representations appear. Between them the particular case of the Jordan-Wigner canonical representation, is obtained when the existence of a « vacuum » state $|0\rangle$, defined by

$$a_k|0\rangle = 0\,, \tag{2}$$

for every k, is assumed.

An explicite example has been given by HAAG [5].

Following this procedure we assume for the a_K operators the commutation rules

$$\left\{\begin{aligned} &[a_k, a_{k'}^*] = \delta_{kk'} \\ &[a_k, a_{K'}] = [a_k^*, a_{K'}^*] = 0\,. \end{aligned}\right. \tag{3}$$

Then, we introduce a set of operators

$$\left\{\begin{aligned} b_k &= \cosh\varepsilon\cdot a_k + \sinh\varepsilon\, a_k^*\,, \\ b_k^* &= \sinh\varepsilon\cdot a_k + \cosh\varepsilon\, a_k^*\,, \end{aligned}\right. \tag{4}$$

for which the commutation relations are unchanged.

If we assume that the number of the a_k's infinite, (i.e. $k = 1, 2, \ldots, n$), unitary transformation $V^{(n)}$ exists [15,16], such that

$$\begin{aligned} b_k &= V^{(n)} a_k V^{(n)*}\,, \\ b_k^* &= V^{(n)} a_k^* V^{(n)*}\,. \end{aligned}$$

$V^{(n)}$, as it is easy to check, has the form

$$\left\{\begin{aligned} V^{(n)} &= \exp\,[i\varepsilon T^{(n)}]\,, \\ T^{(n)} &= \frac{i}{2}\sum_1^n{}_k\,[a_k^* a_k^* - a_k a_k]\,. \end{aligned}\right. \tag{6}$$

([15]) J. v. NEUMANN: *Math. Ann.*, **104**, 570 (1931).

([16]) F. RELLICH: *Nachr. Akad. Wiss. Göttingen*, **2**, 107 (1946).

3057

In the case of field theories, where the a_k's are infinite in number, we are obviously interested in a limit process, $n \to \infty$. But this process gives raise to the following pathological features:

$$T = \lim_{n\to\infty} T^{(n)} \tag{7a}$$

has no domain in $\prod_k^{(0)} \otimes \mathcal{H}^{(k)}$,

$$\lim_{n\to\infty} \langle p | V^{(n)} | q \rangle = 0 \tag{7b}$$

for any $|p\rangle$ and $|q\rangle \in \prod_k^{(0)} \otimes \mathcal{H}^{(k)}$.

4. – The various considerations exposed in the preceeding section leaves us to formulate the following hypothesis. If $V^{(n)}$ are the quantities defined in Sect. 3, or quantities analogously introduced through relations of the type (4), with consequences similar to (7), the operator defined as

$$U = \lim_{n\to\infty} V^{(n)} \tag{8}$$

exists and is unitary (in $\mathcal{H}$).

Then it follows that, for any $|q\rangle \in \prod_k^{(0)} \otimes \mathcal{H}^{(k)}$ an uniquely determined state $|q\rangle = U|q\rangle$ exists in $\mathcal{H}$. Obviously, for 7 b), it does not belong to $\prod_k^{(0)} \otimes \mathcal{H}^{(k)}$.

The correspondence $|q\rangle \rightleftarrows |q\rangle$ is a one to one mapping of the space $\prod_k^{(0)} \otimes \mathcal{H}^{(k)}$ on a certain subspace of $\mathcal{H}$. Remembering the « bundle properties » (Appendix) we can conclude that the mentioned subspace forms a « bundle » different from $\prod_k^{(0)} \otimes \mathcal{H}^{(k)}$.

As an illustration of the above hypothesis, we consider now a case, where a transformation of the type of Sect. 3 appears in connection with a physical problem, i.e. in the well known (and soluble) theory of a neutral scalar field in interaction with a fixed source.

In this theory the hamiltonian is given by

$$\left\{\begin{aligned} H &= H_0 + H_I\,, \\ H_0 &= M_0 + \sum_k \omega_k a_k^* a_k\,, \\ H_I &= \frac{g}{\sqrt{V}} \sum_k \frac{f(k)}{\sqrt{2\omega_k}} [a_k + a_k^*]\,, \end{aligned}\right. \tag{9}$$

3058

with M_0, the energy of the source (mass of the « bare » nucleon),

$$u_k = \sqrt{\mu^2 + k^2}, \quad (\mu \text{ is the mass of mesons}),$$

$f(k)$ a cut-off function.

Adopting the preceeding notation, the space $\mathcal{H}$ is defined as the space spanned by *all* the eigenstates of H_0. The subspace $\mathcal{H}^{(0)} = \prod_k^{(0)} \otimes \mathcal{H}^{(k)}$ is spanned by the eigenstates of H_0 with a finite number of mesons, in presence of the « bare » nucleon.

In order to solve the eigenvalue problem associated with the total hamiltonian H, we can use the following transformation by means of which H is diagonalized [17]:

$$W = \exp\left[g \sum_k \gamma(k)(a_K^* - a_K)\right], \tag{10}$$

where $\gamma(k)$ is a function to be determined.

Then:

$$H' = WHW^{-1} = M_0 + \sum_K \omega_k a_k^* a_k + g^2 \sum_K \gamma^2(k)\omega_k - g \sum_K \gamma(k)[a_k + a_k^*] + \\ + \frac{g}{\sqrt{V}} \sum_K \frac{f(k)}{\sqrt{2\omega_K}} [a_K^* + a_K - 2g\gamma(k)]\,. \tag{11}$$

Assuming

$$\gamma(k) = \frac{1}{\sqrt{2V}} \frac{f(k)}{\omega_K^{\frac{3}{2}}}\,, \tag{12}$$

we obtain the diagonalized form for H'

$$H' = M_0 + \sum_k \omega_K a_k^* a_k - \frac{g^2}{2V} \sum_k \frac{f^2(k)}{\omega_K^2}\,. \tag{13}$$

H' results equal in form to H_0, if M_0 is substituted by the « renormalized mass »

$$M = M_0 - \frac{g^2}{2V} \sum_k \frac{f^2(k)}{\omega_K^2}\,.$$

Then, apart from a shift of the energy scale, we can write for the eigenstates

---

[17] E. Arnous: *Nuovo Cimento*, 5, 483 (1957); for a rigorous treatment see 2) Sect. **14**.

$|\boldsymbol{p}\rangle$, $|p\rangle$ of H, H_0 respectively, the following connection:

$$|p\rangle = W|\boldsymbol{p}\rangle \, . \tag{14}$$

For example, in the case of the vacuum state $|0\rangle$, which is the state of minimum energy of H_0 (equal to M_0), i.e. the state with the bare nucleon and no mesons, we have

$$\left\{\begin{aligned} &|\boldsymbol{0}\rangle = W^{-1}|0\rangle = N\left\{|0\rangle + \frac{g}{\sqrt{2V}}\sum_K \frac{f(k)}{\omega_K^{\frac{3}{2}}}|k\rangle + \ldots\right\},\\ &N = \exp\left[-\frac{g^2}{4V}\sum_K \frac{f^2(k)}{\omega_K^3}\right].\end{aligned}\right. \tag{14'}$$

In the development (14') states with one, two, ... mesons are denoted by $|k\rangle$, $|k_1k_2\rangle$, ...

The state $|\boldsymbol{0}\rangle$ describes the « clouded » nucleon, which is the state of minimum energy of H (equal to M).

It is apparent that the above development is mathematically consistent only if the quantity $A = \sum_k (f^2(k)/\omega_k^3)$ has a finite value. When it happens to be divergent we should be faced with a case similar to the one examined in Sect. **3**. In particular for the transformation W we should have

$$\lim_{A\to\infty} \langle p|W|q\rangle = 0 \, ,$$

with $|p\rangle$, $|q\rangle \in \mathcal{H}^{(0)}$.

With the help of our hypothesis of Sect. **4**, the operator W would assume a definite meaning also in the limit $A\to\infty$ (which is obviously the case for the point interaction, for which $f(k)=1$), with the following consequences, which now can be better understood for their physical meaning:

a) The eigenstates of H, belong to $\mathcal{H}$, but not to $\mathcal{H}^{(0)}$; they are in fact orthogonal to every state of $\mathcal{H}^{(0)}$. This shows the impossibility of a perturbation treatment [13].

b) They belong to a « bundle » $\mathcal{H}^{(g)}$, different from $\mathcal{H}^{(0)}$ and essentially determined by the coupling constant g (and naturally by the form of the interaction and of the cut-off function). In fact it is easy to see that the « bundle » $\mathcal{H}^{(g')}$, obtained in the same way as before with the only change of g by g', is orthogonal to $\mathcal{H}^{(g)}$ [13].

c) The isomorphism of $\mathcal{H}^{(0)}$ and $\mathcal{H}^{(g)}$ is explicitely given by the following application:

$$|k_1k_2\ldots k_l\rangle \longleftrightarrow |\boldsymbol{k}_1\boldsymbol{k}_2\ldots\boldsymbol{k}_l\rangle \, ,$$

where

$$|k_1 k_2 \dots k_l\rangle = \frac{1}{\sqrt{l!}} a^*_{k_1} \cdot a^*_{k_2} \dots a^*_{k_l} |0\rangle ,$$

is a state $\in \mathcal{H}^{(0)}$ obtained from the vacuum state of $\mathcal{H}^{(0)}$ by application of a finite number of creation operators, and

$$|k_1 k_2 \dots k_l\rangle = \frac{1}{\sqrt{l!}} a'^*_{k_1} a'^*_{k_2} \dots a'^*_{k_l} |0\rangle ,$$

is a state of $\mathcal{H}^{(g)}$ obtained from the physical vacuum $|0\rangle$ of $\mathcal{H}^{(g)}$ by application of a finite number of operators

$$a'_k = W^* a_k W .$$

The latter are the so called « modified operators » introduced by FRIEDRICHS [18].

d) From relation (2), we obtain

$$a'_k |0\rangle = 0 \qquad \text{for every } k.$$

So we can conclude that a representation of the Jordan-Wigner type for the « modified operators » a'_k, in the space $\mathcal{H}^{(g)}$ is possible.

e) If we calculate the expectation value in the physical vacuum state of the number operator $N = \sum_K a^*_K a_K$, we have

$$\langle 0|N|0\rangle = \frac{g^2}{2V} \sum_K \frac{f^2(k)}{\omega_K^3} = A .$$

For A divergent this result confirms the « myriotic » character of the states of $\mathcal{H}^{(g)}$.

We should like to notice that the simplicity of the present example is due to the fact that the spectra of H_0 and H have essentially the same structure.

It seems probable that, for more complex cases, other phenomena, connected with the structure of the extended operators and their action in the bundles of $\mathcal{H}$, which have been analysed by VON NEUMANN [1], play an important role.

We conclude remarking that some results of this section and particularly the point *d*) can be an indication of a close connection between the structure

---

(18) K. O. FRIEDRICHS: loc. cit. Part III.

(19) H. WEYL: *The theory of groups and quantum mechanics*, english translation (New York, 1931).

of the space $\mathcal{H}$ and the existence of many inequivalent representations of the a_K operators.

In the following appendix we have estimated opportune and useful to expose with some details the mathematical concepts which form the background of this paper.

Appendix

1-A. – For a better understanding of the constructive procedure of the « infinite direct product » of Hilbert spaces, we give some elementary considerations on the direct product of two m, n dimensional (real) Hilbert spaces $\mathcal{H}^{(m)}$ and $\mathcal{H}^{(n)}$. The most natural definition has been given by WEYL ([19]) who defines the product $\mathcal{H}^{(m)} \otimes \mathcal{H}^{(n)}$ as the $m \times n$ dimensional variety generated by elements of the type

$$a \otimes b \equiv (a_1, a_2, ..., a_m) \otimes (b_1, b_2, ..., b_n) = \tag{1}$$

$$= (a_1 b_1, a_2 b_1, ..., a_m b_1;\ a_1 b_2, a_2 b_2, ..., a_m b_2;\ a_1 b^n, a_2 b_n, ..., a_m b_n),$$

where a_i and b_j are the components of $a \in \mathcal{H}^{(m)}$ and $b \in \mathcal{H}^{(n)}$.

From (1), we can associate, for example, to the product $a \otimes b$ the matrix

$$\|a_i b_j\| \equiv T\ ; \qquad (i = 1, 2, ..., m;\ j = 1, 2, ..., n). \tag{2}$$

The scalar product (Tx, y) for any $x \in \mathcal{H}^{(m)}$, $y \in \mathcal{H}^{(n)}$, and whose value is given by

$$(a, x) \cdot (b, y)\ , \tag{3}$$

can be understood as the linear functional in x and y, corresponding to T, which « represents » the element $a \otimes b \in \mathcal{H}^{(m)} \otimes \mathcal{H}^{(n)}$. Then, for the generalization to infinite products

$$\mathcal{H}^{(1)} \otimes \mathcal{H}^{(2)} \otimes ... \otimes \mathcal{H}^{(k)} \otimes ...\ , \tag{4}$$

it is reasonable to follow a similar procedure. It is clear that in this case, convergence difficulties will appear.

2-A. – VON NEUMANN (*) introduces at first some convergence considerations on the quantities

$$\prod_{\alpha \in I} z_\alpha\ , \qquad \sum_{\alpha \in I} z_\alpha\ ; \qquad (z_\alpha \text{ real or complex}).$$

(*) In this work the general case is treated where the labels 1, 2, 3, ... of (4) can be substituted by a label $\alpha \in I$, I being an arbitrary set. We are interested only in the case of a denumerable set.

Because of the fact that $\prod_{\alpha\in I}|z_\alpha|$ can be convergent when $\prod_{\alpha\in I} z_\alpha$ is not (for possible strong oscillations of $\arg z_\alpha$), it is said « quasi-convergent » if $\prod_{\alpha\in I}|z_\alpha|$ is convergent, and its value is assumed to be;

i) the value of $\prod_{\alpha\in I} z_\alpha$ if it is convergent too,

ii) 0 if $\prod_{\alpha\in I} z_\alpha$ is not convergent.

Then a sequence $\{b_\alpha\}$ of vectors $f_\alpha \in \mathcal{H}^{(\alpha)}$, $\alpha \in I$, is called a C-sequence if and only if $\prod_{\alpha\in I}\|f_\alpha\|$ is convergent ($\|f_\alpha\|^2 = (f_\alpha, f_\alpha)$). It follows that if $\{f_\alpha\}$ and $\{g_\alpha\}$ are two C-sequences, $\prod_{\alpha\in I}(f_\alpha, g_\alpha)$ is quasi-convergent.

Let

(5) $$F[\{f_\alpha\};\ \alpha\in I]$$

be any functional defined on the totality of the C-sequences, antilinear with respect to every elements $f_{\bar\alpha}$ of $\{f_\alpha\}$.

The set of the functionals (5) form a linear space

(6) $$\prod_{\alpha\in I} \bigcirc\, \mathcal{H}^{(\alpha)}.$$

Consider now those elements of the space (6) generated by the particular functionals defined by

(7) $$F_{\{f^0_\alpha\}}[\{f_\alpha\};\ \alpha\in I] = \prod_{\alpha\in I}(f^0_\alpha, f_\alpha)\,,$$

where $\{f^0_\alpha\}$ is any fixed C-sequence. It is apparent that they are the generalization of the functionals (3) of Section **1-A**. The space

(8) $$\prod_{\alpha\in I}{}' \otimes \mathcal{H}^{(\alpha)}$$

is defined as the linear space of all the functionals (7) and their finite sums

(9) $$\sum_1^p{}_i\, F_{\{f^{0,i}_\alpha\}}[\{f_\alpha\};\ \alpha\in I]\,; \quad (\{f^{0,i}_\alpha\} \text{ are fixed } C\text{-sequences})$$

with the linear inner product

$$(F, G) = \sum_1^p{}_i \sum_1^q{}_j\, (f^{0,i}_\alpha, g^{0,j}_\alpha)\,; \qquad (\|F\|^2 = (F, F))$$

where F, G have form (9).

In such a way any functional (7) belonging to (8) can be assumed to define an element

(10) $$\prod_{\alpha\in I}\otimes f^0_\alpha\,,$$

which is the generalization of the element $a \otimes b$ considered in **1-A.**

Finally, the « *complete direct product space* »

$$\prod_{\alpha\in I} \otimes \mathcal{H}^{(\alpha)} = \mathcal{H} \tag{11}$$

is defined as the completion of the space (8), with the consideration of functionals $F \in \prod_{\alpha\in I} \otimes \mathcal{H}^{(\alpha)}$ obtained as « limits » of functional $F_r \in \prod_{\alpha\in I} \otimes \mathcal{H}^{(\alpha)}$ in the following sense:

$$F[\{f_\alpha\};\ \alpha\in I] = \lim_{r\to\infty} F_r[\{f_\alpha\};\ \alpha\in I] \tag{1}$$

for all C-sequences $\{f_\alpha\}$,

$$\lim_{r,s\to\infty} \|F_r - F_s\| = 0\ . \tag{11}$$

This $\mathcal{H}$ is a non-separable space.

3-A. – To investigate the structure of the space $\mathcal{H}$ the notion of C_0-sequence is given as a sequence for which

$$\sum_{\alpha\in I} \big|\, \|f_\alpha\| - 1 \,\big|\, ,$$

is convergent.

Any C-sequence is a C_0-sequence, but the converse does not always hold.

Two C_0-sequences are equivalent $\{f_\alpha\} \approx \{g_\alpha\}$ if

$$\sum_{\alpha\in I} |(f_\alpha, g_\alpha) - 1|$$

is convergent.

This equivalence is reflexive, symmetric and transitive and decomposes the set of all C_0-sequences into mutually disjoint equivalence classes $\sigma(f_\alpha;\ \alpha\in I)$ composed of the C_0-sequences $\approx \{f_\alpha\}$. The set formed by these equivalence classes σ is denoted by Γ.

If a C_0-sequence $\{f_\alpha\}$ differs from another one $\{g_\alpha\}$ only for a finite number of elements, it follows $\{f_\alpha\} \approx \{g_\alpha\}$.

The space $\prod^{\sigma}_{\alpha\in I} \otimes \mathcal{H}^{(\alpha)}$ obtained in the same way as in Sect. **2-A.** using only the C_0-sequences of a given equivalence class σ, is called the « *incomplete direct product* ».

Of particular interest are the following properties of the spaces $\prod^{\sigma}_{\alpha\in I} \otimes \mathcal{H}^{(\alpha)}$:

a) $\prod^{\sigma}_{\sigma\in I} \otimes \mathcal{H}^{(\alpha)}$ is the closed linear set determined by all C_0-sequences $\{f_\alpha\}$ for which $f_\alpha \neq f^0_\alpha$ occurs for a finite number of elements only, where $\{f^0_\alpha\}$ is a C_0-sequence (always existent in σ) with the property $\|f^0_\alpha\| = 1$.

b) Two spaces $\prod^{\sigma}_{\alpha\in I} \otimes \mathcal{H}^{(\alpha)}$ and $\prod^{\sigma'}_{\alpha\in I} \otimes \mathcal{H}^{(\alpha)}$ corresponding to different equivalence classes σ, σ' are orthogonal.

c) Each $\prod_{\alpha\in I}^{\sigma} \otimes \mathcal{H}^{(\alpha)}$ has the same dimension and is a separable space.

d) The linear closed set determined by all $\prod_{\alpha\in I}^{\sigma} \otimes \mathcal{H}^{\alpha}$; $\sigma \subset \Gamma$, is the complete space $\mathcal{H}$.

4-A. – After the definition of the space $\mathcal{H}$ it is necessary to know the relationship between operators in the various $\mathcal{H}^{(\alpha)}$, $\alpha \in I$, to those in $\mathcal{H}$. If B_α is the ring (*) of all bounded operators in $\mathcal{H}^{(\alpha)}$ and $B_\otimes$ the ring of those in $\mathcal{H}$, given $A_{\alpha_0} \in B_{\alpha_0}$ then there exists a unique operator $\bar{A}_{\alpha_0} \in B_\otimes$, such that for all C-sequences $\{f_\alpha\}$,

$$\bar{A}_{\alpha_0} \cdot (\prod_{\alpha\in I} \otimes f_\alpha) = (\bar{A}_{\alpha_0} \cdot b_{\alpha_0}) \otimes \prod_{\substack{\alpha\in I\\ \alpha\neq\alpha_0}} \otimes f_\alpha \,.$$

The operator $\bar{A}_{\alpha_0}$ is called the extension of A_{α_0}.

The set, B_{α_0}, of all $\bar{A}_{\alpha_0}$, is a ring $\subset B_\otimes$ and containing the unity operator 1.

The ring generated by all $\bar{B}_{\alpha_0}$ is denoted by $B^{\#}$. Obviously $B^{\#} \subset B_\otimes$ and in general $B^{\#} \neq B_\otimes$.

An arbitrary operator A in $\mathcal{H}$ belongs to $B^{\#}$ if and only if it commutes with all projectors $P(\sigma)$ into the incomplete products $\prod_{\alpha\in I}^{\sigma} \otimes \mathcal{H}^{\alpha}$, $(\sigma \subset \Gamma)$ and with the operator $U(z_\alpha;\, \alpha \in I)$ (certainly existent) with the property

$$U \prod_{\alpha\in I} \otimes f_\alpha = \prod_{\alpha\in I} \otimes z_\alpha f_\alpha \,; \qquad (|z| = 1)$$

for every C_0-sequence f_α (+).

(*) Algebrically, a set of operators is called ring if with the operators A, B, it contains also A, A^*, $A+B$ and AB.

(+) It is clear that an operator of the type we have used in Sect. **4** form. (8) cannot belong to $B^{\#}$.

RIASSUNTO

Si esamina la struttura dello spazio hilbertiano degli stati di un campo quantizzato, si fa un'ipotesi circa la possibilità di interpretazione fisica di vari suoi sottospazi, e si indicano connessioni con risultati « patologici » segnalati da diversi autori.

A p, γ Coincidence Method for the Measurement of π^0 Photoproduction.

W. JOHN and G. STOPPINI (*)

Physics Research Laboratory, University of Illinois - Urbana, Ill.

(ricevuto il 15 Luglio 1957)

Summary. — A method has been developed to measure differential cross-sections for photoproduction of neutral pions from hydrogen below 260 MeV incident photon energies. Tye recoil protons are detected in coincidence with one of the decay γ-rays of the pion. The proton counter telescope utilizes a proportional gas counter as transmission counter. A lead glass Čerenkov counter detects the γ-rays. A thin liquid hydrogen target with Mylar walls is used. Some cross-sections measured at 90° in the center of mass are presented.

The measurement of the angular distribution for the photoproduction of neutral pions from hydrogen is complicated by the continuous energy spectrum of the incident photon beam and by the two γ-decay of the π^0. So far the most direct measurements of the differential cross section have involved the detection of the energy and angle of the recoiling proton. The Caltech group has used a magnet to select the protons in one experiment (1) and in another experiment (2) a proton telescope in coincidence with a γ telescope which detected one of the decay γ of the π^0. The Caltech measurements extend down to 260 MeV incident photon energy. Recently YAMAGATA (3) has obtained some cross-sections down to 240 MeV using a magnet and MCDONALD *et al.* (4) have obtained cross-sections down to 260 MeV using emulsions. Measure-

(*) Fulbright Scholar From Rome, Italy.

(1) D. C. OAKLEY and R. L. WALKER: *Phys. Rev.*, **97**, 1283 (1955).

(2) R. L. WALKER, D. C. OAKLEY and A. V. TOLLESTRUP: *Phys. Rev.*, **97**, 1279 (1955).

(3) T. YAMAGATA: *Ph.D. Thesis*, University of Illinois, November, 1956.

(4) W. S. MCDONALD, V. Z. PETERSON and D. R. CORSON: *Phys. Rev.*, **107**, 577 (1957).

ments at lower energies require a detector for the low energy protons and a thin target. We have developed a p, γ coincidence method to extend the measurements to lower incident photon energy because of the current interest in the photopion production near threshold ( ).

In our method the decay γ of the π^0 is detected by a total absorption Čerenkov counter ([3]) whose efficiency is very nearly 100%. This eliminates the uncertainty in the efficiency of the γ detector used in previous experiments. The recoiling protons are detected by a proton telescope. The telescope has the advantage over a magnet of allowing the simultaneous collection of data for all energies in the bremsstrahlung spectrum. We have developed a low energy proton telescope consisting of a proportional gas counter followed by a plastic scintillation counter. The thin proportional gas counter gives a pulse height essentially proportional to $\mathrm{d}E/\mathrm{d}x$ of the particle, with a negligible energy loss for the protons; the thick scintillation counter stops the particle and gives a pulse height proportional to the energy. Thus the combined pulses from the two counters serve to identify the particle.

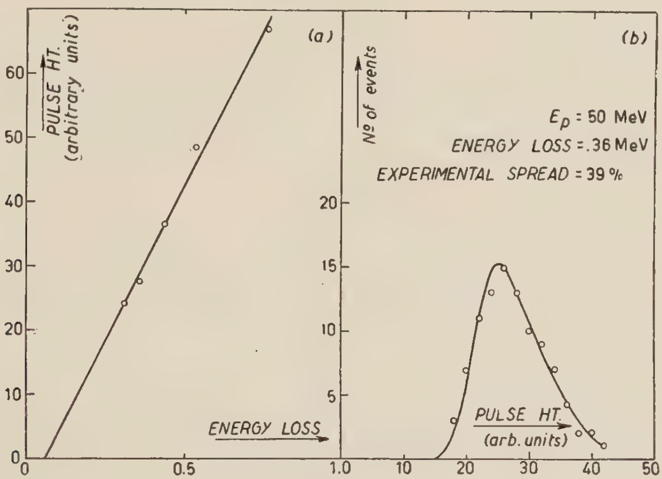

Fig. 1.

The proportional gas counter is 4 cm in diameter and 20 cm long. The protons travel parallel to the axis of the counter. This geometry introduces a discrimination against random background particles. The 0.013 cm tungsten wire anode is supported at the ends by radial nylon rods. The end windows of the counter are a sandwich of 0.025 mm Mylar and 0.025 mm aluminum. The counter was filled with 40 cm Hg of xenon and 8 cm Hg of methane (total thickness ∼ 60 mg/cm²). Xenon was chosen to reduce the efficiency of the counter for low energy background neutrons. The counter was operated with a high multiplication (∼ 20) to insure that the output pulse would show

([5]) N. M. Kroll and M. A. Rudermann: *Phys. Rev.*, **93**, 233 (1954).

3067

little dependence on the distance of the path of the protons from the anode. The counter pulse was differentiated at the input of the pre-amplifier by a 0.5 μs time constant. Background electrons act like a source of random noise pulses upon which the larger proton pulses are superimposed. The pulse

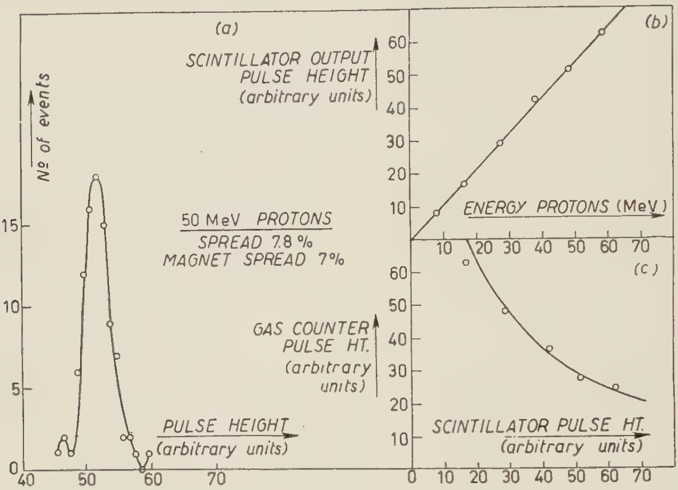

Fig. 2.

height due to a proton is distorted by electron background pulses but under the conditions of our experiment the distortion was less than the Landau spread. The counter was tested with an X-ray crystal spectrometer using the 17.4 keV K_α line of molybdenum. The distribution of pulse heights was Gaussian and the width of the spread was in exact agreement with the results reported by HANNA *et al.* (6) confirming their finding that the gas multiplication introduces less spread than the theoretical prediction (7). The counter was also tested with protons in the energy range 15 to 60 MeV. In Fig. 1 (*a*) the output pulse height is plotted as a function of the energy loss in the counter. In Fig. 1 (*b*), the observed Landau spread for 50 MeV protons is shown.

The stopping scintillation counter consists of a cylinder of plastic scintillator 4 cm in diameter and 4 cm in length viewed end-on by a RCA 6810 photo-multiplier. The scintillator is optically coupled by oil to an aluminum foil reflector.

The performance of the entire proton telescope was tested by counting mono-energetic protons between 15 and 60 MeV obtained by magnetically analyzing photoprotons from a lead target. Background electrons were seen to be clearly separated from the protons by the telescope. The energy resolution of the stopping counter is roughly 2%, full width at half maximum.

(6) G. C. HANNA, D. H. W. KIRKWOOD and B. PONTECORVO: *Phys. Rev.*, **75**, 985 (1949).

(7) U. FANO: *Phys. Rev.*, **72**, 26 (1947).

In Fig. 2 is shown (*a*) the stopping counter pulse height distribution for 50 MeV protons; (*b*) the stopping counter pulse height as a function of the proton energy and (*c*) the gas counter pulse height versus the stopping counter pulse height compared with the expected $\mathrm{d}E/\mathrm{d}X \propto 1/E$ curve. The magnet test showed that some protons were scattering out of the stopping counter. The effect amounted to 10% in the worst case and can be corrected by placing a collimator in front of the stopping counter.

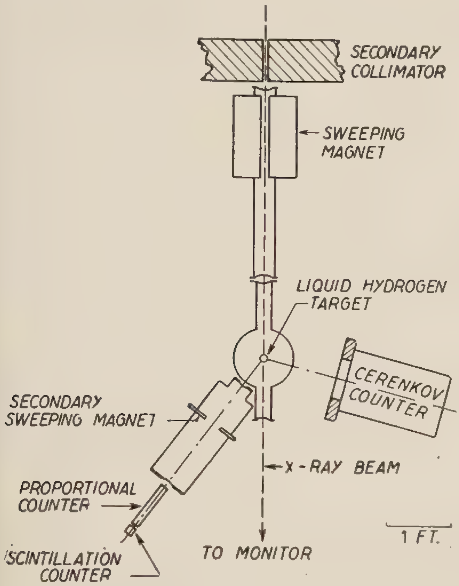

Fig. 3.

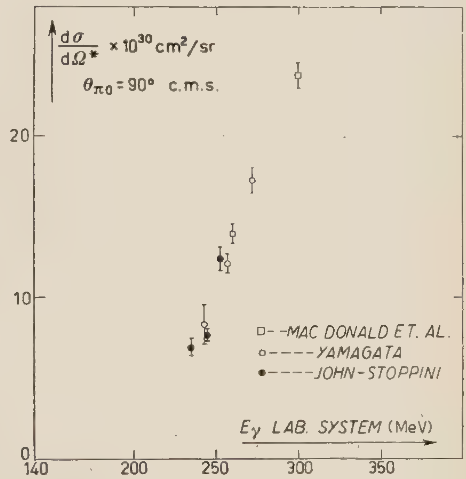

Fig. 4.

We have had a preliminary run to measure the differential cross sections for the neutral pion photoproduction in hydrogen at 90° in the C.M. system. The experimental apparatus is shown in Fig. 3. The γ-ray beam of the 300 MeV betatron is collimated to 2 cm diameter. The liquid hydrogen target consists of a cylindrical « appendix » 3 cm in diameter with 0.0038 cm Mylar walls. The proton telescope was set at 37° in the lab. system. A fast (50 mμs) coincidence between the stopping scintillation counter and the Čerenkov counter triggers an oscilloscope trace. The gas counter pulse and the scintillation counter pulse stretched to a length of 0.5 μs are displayed. The bias of the Čerenkov counter was set at 80 MeV. The discrimination of the arrangement used was excellent as shown by a low accidental rate (2.5%), the vanishing of good counts below the meson threshold and the low empty target rate (2%). Thus the photoprotons from the carbon in the Mylar appendix were effectively eliminated by the coincidence with the Čerenkov counter. The only other process which is also counted by our arrangement is the proton Compton effect which, however, has a cross section at least 100 times smaller than the photopion cross section ( ).

The proton energy spectrum was converted to differential cross sections by using a dynamical efficiency calculated by the Illiac ([3]). The calculation included energy losses of the protons in the target. The Schiff spectrum was

used for the incident photon spectrum. The results are shown in Fig. 4. The errors are statistical only. For comparison the results of YAMAGATA (3) and MC DONALD *et al.* (4) are shown. The minimum γ-ray energy was determined by the minimum proton energy which could leave the target.

A thinner target is being developed which will allow us to extend the measurements to lower energies. Another limitation to the lowest energy attainable is imposed by multiple scattering of the protons in the gas counter. However, the energies which can be reached should permit a valuable determination of the S-wave in the photoproduction.

* * *

We wish to acknowledge many helpful discussions with Prof. G. BERNARDINI. Mr. H. TOMASHKE gave valuable assistance with the experimental work. Dr. T. YAMAGATA carried out the Illiac calculation. The staff of the laboratory gave helpful cooperation. This work was sponsored by the Office of Naval Research.

RIASSUNTO

Viene descritto un apparato di coincidenze p, γ per lo studio del processo $\gamma+p\to\pi^0+p\,(\to 2\gamma+p)$ per energie del fotone incidente minori di 260 MeV. Il telescopio per la rivelazione e misura dell'energia del protone di rinculo, consiste di un sottile contatore proporzionale di trasmissione (per la misura di $\mathrm{d}E/\mathrm{d}x$) e di un contatore proporzionale ad assorbimento totale (per la misura di E). Il contatore di trasmissione è un contatore a Xe ($\sim\frac{1}{2}$ atm) e permette la selezione e misura dell'energia di protoni fino a 5 MeV. Il rivelatore di fotoni è un contatore di Čerenkov ad assorbimento totale. Sono presentate alcune preliminari determinazioni delle sezioni d'urto differenziali a 90° nel sistema del baricentro.

IL NUOVO CIMENTO Vol. VI, N. 5 1° Novembre 1957

The Behaviour of Phase-Sensitive Detectors (*).

M. B. Palma-Vittorelli, M. U. Palma and D. Palumbo
Istituto di Fisica dell'Università - Palermo

(ricevuto il 3 Agosto 1957)

Summary. — After an introduction to the problem, an analysis is made of the output of different types of phase detectors for any given input. Expressions are given for the frequencies present in the output (for any given input) and for the related amplitudes and phases. Such expressions agree with and analytically define the well known result that a noise figure close to unity may be reached using phase-detection.

1. – Introduction.

It is well known that a modulated wave consists of a frequency spectrum which in any case is a Fourier spectrum, although in general the frequencies are not all multiples of the same « fundamental » frequency (1).

We shall be concerned with the problem of the detection of an A.M. wave in the presence of an outweighing level of noise, and we shall examine the advantages offered in such a case by the use of a phase-sensitive detector (P.D.) compared with conventional linear or square-law detectors.

A P.D. (or lock-in detector) is an essentially linear detector, in which the modulated wave is in some way mixed with a « reference » continuous wave, the fundamental component of which has the same frequency as, and a constant phase relationship with, the carrier of the A.M.-wave (2). A number of harmonics of the carrier may be present in the « reference » continuous wave (C.W.). Different types of P.D. may be obtained, according to the different ways in which the mixing is accomplished; the main types will be taken into

(*) This work forms part of a program of research undertaken with the financial support of the Consiglio Nazionale delle Ricerche, through the Comitato Nazionale per la Fisica, for which the Authors wish to express their sincere gratitude.

(1) J. Favard: *Les fonctions presque périodiques* (Paris, 1933).

(2) A. G. Emslie: *R.L. Rep.* (*M.I.T.*) No. 103-5, May 16, 1944.

consideration in Sect. 3: we will see that it is necessary to have a linear response of the detector to the signal which carries the information, in order to obtain the best conditions of detectability of signal in noise.

Throughout this paper (if not otherwise specified) we will mean by signal any one of the sine waves present in the spectrum of the time-dependent input variable (noise excluded); by amplitude, a quantity proportional either to the voltage or to the current, having the dimensions of the square root of a power; by average the one taken over an ensemble of identical instruments (which is known to be in general different from the time average). We will call S the signal amplitude and by $N=\sqrt{W_N}$ the R.M.S. noise amplitude, equal to the square root of the mean noise power. We will mean by signal-to-noise ratio, the ratio S/N.

As it will be seen in detail in Sect. 2, a conventional square-law or even a linear detector gives, in the case of $S/N \ll 1$, an output signal amplitude proportional to S^2/N, i.e. a second-order effect which severely impairs the signal-to-noise ratio, whereas the P.D. has the outstanding feature of giving an output signal amplitude proportional to S, i.e. a first-order effect which may in principle leave S/N unaffected. In Sect. 2 we will also show that any kind of « first » linear detector behaves much in the same way as a P.D., as far as S/N is concerned, provided that the local oscillator (L.O.) amplitude is large enough.

In Sect. 3 the behaviour of a mechanical-switch type P.D. will be analysed and it will be shown that the results which will be given hold for (or may be easely extended to) different types of P.D.

Expressions will be given for the amplitudes of the different Fourier components of the output for any given input, and for the related phase-shifts, which are of importance when the P.D. has to be used in feedback loops.

These expressions will evidence the behaviour of P.D. also as far as their noise figure is concerned.

2. – Minimum detectable signal.

Let us make the usual assumption that the noise has a gaussian distribution, and that all the noise may be ascribed to a single noise source, located at the input of the circuit (we will analyse this assumption further). Let the information be carried by an amplitude-modulated wave:

$$(S_0 + S_1 \cos \omega_1 t) \cos \omega_0 t \tag{1}$$

and imagine that first both modulated wave and noise go through a device having a bandwidth $2\,\Delta f$ centred on $f_0=\omega_0/2\pi$ and a constant gain within this bandwith; let $W_{2\Delta f}$ be the mean noise power at the output terminals of such a device. Let us assume the noise to be periodic, with period $T=2\pi/\omega$, very long compared with all periods occurring in the system, and which we may let approach infinity. Then the noise may be written [3]

$$A_N(t) = \sum_K (a_K \cos K\omega t + b_K \sin K\omega t)\,, \tag{2}$$

---

[3] LAWSON and UHLENBECK: *Threshold Signals*. R.L.S. No. 24 (New York, 1950).

where the sum must be taken over those values of K which pertain to $2\Delta f$. Obviously we may write:

$$A_N(t) = X_N(t)\sin\omega_0 t + Y_N(t)\cos\omega_0 t\,, \tag{3}$$

where

$$\begin{cases} X_N(t) = \sum\limits_K [a_K \sin(K\omega - \omega_0)t + b_K \cos(K\omega - \omega_0)t \\ Y_N(t) = \sum\limits_K [a_K \cos(K\omega - \omega_0)t + b_K \sin(K\omega - \omega_0)t \end{cases} \tag{4}$$

and

$$S(t) + A_N(t) = X_N(t)\sin\omega_0 t + [Y_N(t) + S_0 + S_1\cos\omega_1 t]\cos\omega_0 t\,, \tag{5}$$

$X_N(t)$ and $Y_N(t)$ are obviously functions of the time, containing frequencies ranging from zero up to the order of Δf.

Since the R.M.S. output amplitude from a linear detector is proportional to

$$\sqrt{X_N^2(t) + [Y_N(t) + S_0 + S_1\cos\omega_1 t]^2} \tag{6}$$

and since the mean values of X_N and Y_N vanish, expression (6) becomes for the case $S/N \ll 1$:

$$\simeq \sqrt{W_{2\Delta f}} + \frac{1}{2}\frac{(S_0 + S_1\cos\omega_1 t)^2}{\sqrt{W_{2\Delta f}}}\,. \tag{7}$$

This shows that the output signal amplitude is of the second order, compared with the input amplitude, so that the measurement of a second-order effect is needed in this case. It follows a drastic limitation of the minimum detectable signal, defined as the one which gvies a deflection of the order of magnitude of the square root of the fluctuation.

If we now inject into the linear detector a second signal $S_R\cos(\omega_0 t + \varphi)$, being now $S_R/N \gg 1$, the term due to the cross-product between signal and reference becomes outweitghing among the ones given by the signal and the same procedure as above gives an output proportional to

$$S_R + (S_0 + S_1\cos\omega_1 t)\cos\varphi + \frac{W_{2\Delta f}}{2S_R}\,, \tag{8}$$

which shows that now one has to deal with a first-order instead of a second-order effect.

Finally, let us suppose the reference frequency to be $\omega_R/2\pi$, no longer equal to the carrier frequency (heterodyne case). In this case the input amplitude to the linear detector in the case of a signal $S\cos\omega t$ is $S_R\cos\omega_R t + S\cos\omega t + N(t)$, and the above procedure gives, instead of eq. (7):

$$\sqrt{X_N^2 + Y_N^2 + S_R^2\left[1 + \frac{S}{S_R}\cos(\omega_R - \omega)t\right]^2 + S^2\sin^2(\omega_R - \omega)t} \simeq \tag{9}$$

$$\simeq S_R + \frac{W_N}{2S_R} + S\cos(\omega_R - \omega)t\,,$$

which shows that any « first » linear detector yields the same advantage as a P.D. as far as S/N is concerned, provided that the L.O. amplitude is much larger than N. Beside the signal-to-noise ratio considerations, the usefulness of a large L.O. amplitude is a well recognized one [4,5]. In fact eq. (9) holds for $S/S_R = h \ll 1$; if h is no longer very small the amplitude of the wave having a frequency $(\omega_R - \omega)/2\pi$ (sec. eq. (9)) is proportional to [4]

$$S\left(1 - \frac{h^2}{2^3} - \frac{h^4}{2^6} - \frac{5h^6}{2^{10}} \ldots\right), \tag{10}$$

and this indicates one extra requirement for a large L.O. amplitude.

Both the P.D. and the linear heterodyne « first » detector, when they include suitable filters, behave as frequency converters, as it will be seen in detail in Sect. 3. In both cases, the presence of a C.W. reference, makes the system give a linear instead of a quadratic response, in the case of a large C.W.-to-noise ratio.

In a linear or square-law detector, without the injection of a C.W., the minimum detectable signal as defined above, is given by [3]

$$\frac{S_{\min}^2}{W_N} = \frac{A}{\sqrt{n}}, \tag{11}$$

where A is a constant of the order of unity, n the number of observations on which the average is taken, and W_N the average noise power. For the energy $E_{\min}$, associated with the minimum detectable signal, eq. (11) gives [3]

$$E_{\min} \simeq \sqrt{n}\, K T_{\text{eff}}, \tag{12}$$

where T_{eff} is the effective temperature of the whole system. But the absolute theoretical limit of the minimum detectable energy is KT_{eff}, which is the real uncertainty in the energy. The efficiency of a linear or quadratic detector differs therefore from the absolute limit by a factor $\sqrt{n}$ [3].

When a coherent C.W. is injected into a linear detector, eq. (11) becomes

$$\frac{S \cos\varphi}{\sqrt{W_N}} = \frac{A}{\sqrt{n}}, \tag{13}$$

which gives, as an order of magnitude, for $\cos\varphi = 1$

$$E_{\min} \simeq nS^2 \simeq KT_{\text{eff}}. \tag{14}$$

One may easily see that this relationship holds also for any signal contained in the side-bands of the modulated carrier. In these cases therefore one may in principle reach the absolute limit for the minimum detectable signal.

---

[4] H. J. Reich: *Theory and Application of Electron Tubes* (New York, 1944).
[5] R. Pound: *Microwave Mixers*, R.L.S., No. 16 (New York, 1948).

3. – Phase-detector analysis and discussion.

Our purpose is now to analyse the behaviour of a mechanical (vibrating reed) full-wave P.D. followed by a low-pass filter, synthetized with two resistances r, R in series, and a capacitor C in parallel with R (the output being at the terminal of C). It is clear that such a P.D. makes a periodical inversion of the sign of the input, at a frequency equal to $\omega_R/2\pi$, thus multiplying the input voltage by a square wave (of unitary amplitude), the fundamental frequency of which is equal to $\omega_R/2\pi$ and the Fourier expansion of which we will indicate by $Q(t)$. The behaviour of any other kind of P.D. will be later deduced from this case.

Let V_{in} be the voltage at the input terminals of the system, comprehensive of P.D. and filter, V the voltage at the input to the filter, and V_{out} the output voltage from the whole system. Let us use the variable $x = \omega_R t$, and let be:

$$\alpha = \frac{1}{r\omega_R C}, \qquad \lambda = \frac{1}{\omega_R C}\left(\frac{1}{R} + \frac{1}{r}\right) = \frac{1}{\varrho\omega_R C}.$$

The equation of the filter may be written:

$$\lambda V_{out} + \frac{\mathrm{d}V_{out}}{\mathrm{d}x} = \alpha V,$$

which gives

$$V_{out}(x) = V' \exp[-\lambda x] + \alpha \exp[-\lambda x]\int_0^x \exp[\lambda x]V(x)\,\mathrm{d}x, \tag{15}$$

where V' is a constant which has no importance when one is concerned with stationary solutions.

If $V_{in}(x)$ is a continuous function of time, $V(x)$ may not have more than a finite number of discontinuities in any finite time interval, and $V_{out}(x)$ will be a continuous function at any time point, and derivable at any time point except the discontinuity points of $V(x)$.

Let us assume a sinusoidal input, of frequency $\omega/2\pi$

$$S_{in}(x) = S\sin(kx+\varphi) \qquad \text{with } k = \omega/\omega_R,$$

so that

$$V(x) = S_{in}(x)Q(x) = \frac{4}{\pi} S\sin(kx+\varphi)\sum_{0}^{\infty}{}_n \frac{\sin(2n+1)x}{2n+1}, \tag{16}$$

Eq. (15) gives

$$V_{out}(x) = V'\exp[-\lambda x] + \alpha S\exp[-\lambda x]\int_0^x \exp[\lambda x]\sin(kx+\varphi)Q(x)\,\mathrm{d}x. \tag{20}$$

3075

Since both functions $Q(x)$ and $\exp[\lambda x]\sin(kx+\varphi)$ are integrable and have a limited variation in any finite interval, by a theorem on the Fourier series [6], we get [7]

$$V_{out}(x) = V'\exp[-\lambda x] +$$
$$+\frac{4}{\pi}S\alpha\exp[-\lambda x]\sum_0^\infty {}_n\frac{1}{2n+1}\int_0^x \sin(kx+\varphi)\sin(2n+1)x\exp[\lambda x]\,dx\,,$$

or, for the stationary case:

$$V_{out}(x) = \frac{2}{\pi}S\alpha\cdot \tag{18}$$
$$\cdot\left\{\sum_0^\infty {}_n\frac{\lambda\cos[(2n+1-k)x-\varphi]+(2n+1-k)\sin[(2n+1-k)x-\varphi]}{(2n+1)[\lambda^2+(2n+1-k)^2]}-\right.$$
$$\left.-\sum_0^\infty {}_n\frac{\lambda\cos[(2n+1+k)x+\varphi]+(2n+1+k)\sin[(2n+1+k)x+\varphi]}{(2n+1)[\lambda^2+(2n+1+k)^2]}\right\}.$$

Let us now consider the two cases: k rational, and k irrational. In the first case, eq. (18), because of the absolute and uniform convergence of x second term, represents the Fourier expansion of the output voltage, which is a periodic function. In fact, if $k=p/q$, with p and q integers having no common factor, and $\Omega=\omega_R/q$, all the time-dependent terms of the angles of the trigonometric functions in eq. (21), are integral multiples of x/q, namely Ωt. Hence one has only to order the terms, which is allowed by the absolute convergence of the series. In the second case (k irrational) the different frequencies in eq. (16), are no longer multiples of the same fundamental frequency. The output voltage $V_{out}(x)$ is now a quasi-periodic function, and eq. (18) represents its Fourier series [1]. In any case, the frequencies present in the output voltage are given by $(2n+1\pm k)\omega_R/2\pi$, the amplitudes and phases of which are respectively

$$\frac{2}{\pi}S\alpha\frac{1}{(2n+1)[\lambda^2+(2n+1\pm k)^2]^{\frac{1}{2}}}\,, \tag{19a}$$

and

$$\psi=\mathrm{tg}^{-1}\frac{\lambda}{2n+1\pm k}\pm\varphi\,. \tag{19b}$$

A d.c. component will be present in the output only if $k=2n+1$, and its amplitude will be

$$\frac{2}{\pi}\frac{\varrho}{r}\frac{\cos\varphi}{2n+1}S\,. \tag{19c}$$

---

(6) L. TONELLI: *Serie Trigonometriche* (Bologna, 1928).

(7) M. B. PALMA-VITTORELLI, M. U. PALMA and D. PALUMBO: *Atti Acc. Sci. Lett. Arti Palermo* (in print).

The previous results still apply to the case of an input wave which is not sinusoidal but contains a spectrum of frequencies. In such case, obviously, the output is the sum of the contributions of the different sinuosidal input components: for each contribution eqs. (18) and (19) hold.

The above results show that, as far as the d.c. output component is concerned, since the response is of a δ-function type, the case is similar to the one of the interference phenomenon given by a diffraction grating having an infinite number of slits and thus an infinite resolving power. But this discontinuity in the response is only a fictitious one because, actually, the device that follows the P.D. cannot have vanishing bandwith Δf. If $k \neq 2n+1$, and if

$$(2n + 1 - k)\frac{\omega_R}{2\pi} \leqslant \Delta f\,, \tag{20}$$

an a.c. component will be present in the output and will not be filtered; its frequency will vary continuously between 0 and Δf as k varies continuously between the limits given by eq. (20). This specifies the frequency conversion operated by the P.D. and indicates that the well known circuits of « speach scramblers » widely used in communication engineering ([8]) are nothing but P.D. Eqs. (19) show further that for a phase change of π in the input signal, an equal phase change in the output a.c. components occurs, together with a sign reversal in the d.c. component if any due to the signal. This fact renders the P.D. a most important tool for the detection of a.c. error signals in automatic control loops, and in general when one wants to use the whole information carried by a bidirectionally modulated wave. Making $\varphi = \pi/2$ renders the system carrier-balanced.

The above results hold (beside a d.c. steady component) for any switch-type, full-wave P.D., both mechanical and electronic the internal resistance of the P.D. may be thought of as part of r, while a not perfect square-wave, or a not vanishing flight-time, somewhat affect the coefficients of the Fourier expansion of the square wave: since in such cases is $\Delta f \ll f$, it may be easily shown that the deviations from the previous « ideal » results are not significant.

For those types of P.D. in which reference and signal are first added and then injected into a linear detector, the reference usually is a sine wave. In this case, since the reference amplitude S_R is much larger than the signal amplitude S, the sum may be written:

$$S_R\left[1 + \frac{S}{S_R}\cos(\omega_R - \omega)t\right]\sin\omega_R t\,. \tag{21}$$

The term in square bracketts being always positive, the action of a full-wave linear detector on the wave represented by expression (21), is to substitute to $\sin\omega_R(t)$ its absolute value, i.e. to multiply expression (21) by $Q(\omega_R t)$, which proves that eqs. (18) to (20) still hold.

If a half-wave linear detector is used, we may in any case symbolise its

---

([8]) N. Carrara: *Suppl. Nuovo Cimento*, **4**, 1001 (1956).

action by a multiplication by a square wave, whose values are now 0 and 1; this gives a constant term in the Fourier expansion of the square-wave, and eq. (16) becomes:

$$V(x) = S \sin(kx+\varphi)\left[\frac{1}{2}+\frac{2}{\pi}\sum_0^\infty{}_n \frac{\sin(2n+1)x}{2n+1}\right], \tag{22}$$

which shows that half of the signal goes unaffected through the detector and half is detected in the usual way.

In another type of P.D., the reference wave is injected into grid No. 3 of a suitable tube, whereas the signal(s), is injected into grid No. 1. In this case, the tube transconductance is periodically varied at the reference frequency and may be expressed as a function of the reference (8).

When the reference is a square-wave the signal is multiplied by a square-wave, as one may easily see considering that any analytical function of a square-wave is a linear function of the latter. Such a square-wave is not centered on zero and has in general an amplitude different from unity. Thus the results obtained for the half-wave P.D. hold, beside of the presence of two different factors in the two terms in square bracketts of eq. (22). Let us now have in the same circuit a sinusoidal reference: if the response is linear also for the latter, n must be taken as equal to zero in eqs. (18) to (20). In eq. (18) the sum then gives only the first term. If, on the contrary, the response to the reference is not linear, all harmonics appear (8): $(2n+1\pm k)$ has now to be replaced by $(n\pm k)$ in eqs. (18) to (20), and the coefficients $1/(2n+1)$ have to be replaced by the coefficients given by the series expansion of the transcharacteristic related to the electrode considered.

All the P.D. until now considered give an essentially linear response to the signal, even if $S/N \ll 1$, as it is shown by eqs. (19). This means that they always give a first-order response to the signal, also when the reference is not added to the signal carrying the information, as it was assumed for the derivation of eqs. (8), (13), (14). This proves that the equations concerning the minimum detectable signal hold also for the switch-type P.D.

A possible non-linearity in the response to the signal may make the P.D. responsive to the subharmonics of ω_0 and, furthermore, may give rise to cross-modulation of signal and noise, which may severely impair the signal-to-noise ratio, according to the fact that eqs. (8), (13), (14) no longer hold.

At microwave frequencies a P.D. may be made with two crystal diodes, one in each side arm of a magic T, as it appears evident on considering the low-frequency equivalent circuit of the latter. In fact many microwave circuits used in the laboratory (8) or in engineering (frequency stabilization, Moving Target Indicator, etc.) are phase-detectors. Here we have in any case the difficulty that the detectors are either non-linear or very noisy (9,10).

Finally a discriminator used in standard F.M. radio receivers (4) may be considered as a special type of P.D. in which a portion of the signal itself is used as reference: this means that, even if the two diodes are linear detectors, eq. (12) rather than eq. (14) holds: in any case, interference between the input signals gives rise, at the output terminals, to a modulation-frequency signal.

---

(9) TORREY and WHITMER: *Crystal Rectifiers* (New York, 1948).

(10) G. R. NICOLL: *Proc. I.E.E.*, **101**, 317 (29, Sept. 1954).

4. – The use of filters in phase-detection.

We now investigate the output from a P.D., when the input is the amplitude modulated wave, represented by eq. (1) (where f, is equal to the frequency of the reference signal in the P.D.) together with the noise represented by eq. (2) and having a gaussian distribution.

a) If the bandwith Δf of the whole system is arbitrarily large, the signal-to-noise ratio deteriorates, but not severely: in fact, in the case of a full-wave P.D., the power, given by the input modulated wave is distributed after detection as follows: for the carrier, into a d.c. term and into terms having frequencies $2nf_0$, and for the side-frequency signals, into the modulation frequency f_1 and the frequencies $f_1 \pm 2nf_0$. Since the whole information is usually given by the d.c. and f_1 terms, the extra frequencies may be thought of as a non-gaussian noise. The noise, on the other hand undergoes only frequency conversions. The signal-to-noise ratio is somewhat lowered and may be computed using eqs. (18) and (19). Under these conditions, the possible noise generated by the P.D. itself may be ascribed to an input noise source. In the case of a half-wave P.D. eq. (22) shows that the amplitude of the signal which carries the information is reduced by a factor $\frac{1}{2}$ compared with the full-wave case. The rest of the input signal (which passes unchanged through the P.D.) may be thought of as an extra non-gaussian noise. Beside this, the considerations made for the full-wave case still hold.

b) If the phase detector is followed by and RC low-phase filter the bandwidth of which is Δf, as was assumed in Sect. 3, the output noise arises from noise located within an infinite number of bandwidths $2\Delta f$ centered on f_0 and its odd harmonics: one may easily see from eqs. (18) and (19) that, if the noise is assumed to have a gaussian distribution and a constant spectral density, the overall output N is equal to that present in any one of the bandwidths. It follows that the whole R.M.S. noise amplitude N, reduces to $N_{2\Delta f}$, namely to the one contained in the bandwidth $2\Delta f$. In the case of a half- wave detector, again any signal splits in two equal parts, one of which passes unaffected, and the other undergoes frequency conversion. It follows that the converted signal output amplitude is reduced by $\frac{1}{2}$ compared with before, whereas the output N is reduced by a factor $\frac{3}{4}$ ($\frac{1}{2}$ being contributed by the bandwidths $2\,\Delta f$ centred on f_0 and its odd harmonics, and $\frac{1}{4}$ being contributed by the bandwidth between zero and Δf).

c) One gets similar results using, instead of a low-pass filter after detection, a device of bandwidth $2\,\Delta f$ centred on f_0 and located before the detector. The noise comes from one single bandwidth, and is spread out in frequency. The same considerations as in *b*) hold for the noise and the signal-to-noise ratio in the case of a full-wave detection. If we use a half-wave detector, the only differences are in the reduction of the converted signal by a factor $\frac{1}{2}$ and in the presence of the half non-converted signal, as a non-gaussian noise. The possible noise generated by the P.D. itself may no longer (as far as their frequency distribution is concerned) be ascribed to an input source.

d) Finally, if filters are used both before and after the detector, signal

and noise are both always reduced in the same ratio. As long as saturation effects are negligible, the input bandwidth $2\Delta f_{\text{in}}$ is unimportant until $\Delta f_{\text{in}} < 2f_R - \Delta f_{\text{out}}$, i.e. until no contribution comes from the bandwidths centred on the next odd harmonic of the carrier. Apart from the noise introduced by the phase-detector, which again may be ascribed to an input source, this is the best one may achieve.

It seems worthwhile to note that in order to obtain before detection a bandwidth as narrow as one can get using a low-pass filter after detection, one has to use a non-minimum-phase-shift network ([11-13]) or networks having a very fast drop in their gain characteristic and a considerable related phase-shift. This should be born in mind when using P.D. as circuit elements in feedback loops. For such a case, it may be of interest to make the following observation: assume that two side-signals given by the same modulating signal, have undergone phase-shifts before detection. If, as usual, we are interested in the output signal having the modulating-signal frequency, the only terms having $n=0$ and containing $(1-k)$ in eqs. (18) (19) need to be considered. It may be shown from eqs. (19) that such a signal (due to the side-signals which recombine), has an extra phase-shift equal to $(\alpha_2-\alpha_1)/2$, which means that, only if $\alpha_1=\alpha_2$, they cancel in the P.D.

In conclusion, the above considerations about the P.D. noise figure, together with eqs. (19) show that one may closely approach the condition expressed by eq. (14). Nothing can be said in general in the case of a non-linear response of the system to the signal, if one does not specify the response; anyway one has to remember that, as we have seen, a departure from linearity always deteriorates the signal-to-noise ratio.

* * *

We wish to express our gratitude to Prof. M. SANTANGELO for his continued interest and stimulating discussions, and to Prof. N. CARRARA for his appreciated constructive and stimulationg criticism and help.

([11]) VALLEY and WALLMAN: *Vacum Tube Amplifiers* (New York, 1948).

([12]) H. W. BODE: *Network Analysis and Feedback Amplifier Design* (New York, 1945).

([13]) J. G. THOMASON: *Linear Feedback Analysis* (London, 1955).

RIASSUNTO

Dopo una introduzione al problema del minimo segnale rivelabile, per il caso di un'onda modulata in ampiezza, viene studiata la risposta dei diversi rivelatori sensibili alla fase (phase-sensitive detectors, lock-in detectors), per una qualsiasi tensione d'ingresso. Vengono fornite le espressioni che danno le frequenze (e le relative ampiezze) presenti all'uscita; tali espressioni definiscono analiticamente il noto risultato, che la rivelazione sensibile alla fase permette di raggiungere una cifra di rumore prossima all'unità. Inoltre vengono fornite le espressioni degli sfasamenti rispetto all'entrata, che interessano nel caso, per esempio, di circuiti di controllo automatico.

Velocity-Dependent Nuclear Interaction.
II. - Level Schemes.

W. E. Frahn and R. H. Lemmer
Nuclear Physics Division of the National Physical Research Laboratory, C.S.I.R., Pretoria - South Africa

(ricevuto il 25 Marzo 1957)

1. – In a previous paper [1] a general single-particle equation with non-local interaction has been studied in the effective mass approximation. In this approximation a wave equation is obtained which has the form of a Schrödinger equation with local potential $V(r)$, but which contains a spatially variable effective mass $M(r)$ appearing in a generalized kinetic energy operator.

In the present paper we shall investigate the eigenvalue spectrum of the single-particle wave equation (I.12), using the isotropic harmonic oscillator potential. In the Mayer-Jensen shell model the overall nuclear potential is usually assumed intermediate between the harmonic oscillator and the square well potentials, representing approximations for light and heavy nuclei, respectively.

Recently, Ross, Lawson and Mark [2] have calculated nucleon energy levels, starting from a single-particle equation similar to (I.12), but which does not contain the fully symmetrized form of the kinetic energy operator. The potential $V(r)$ used by these authors is the diffuse well potential proposed by Woods and Saxon, for which they earlier carried out shell model calculations in the static case [3]. In a sense, therefore, the present investigation may be considered complementary to that of Ross, Lawson and Mark in the region of lighter nuclei. It must, however, be noted that the non-static effects change the spectra of both static potentials towards greater resemblance, so that a close similarity of the results may be expected.

2. – The eigenvalues of (I.12) for the isotropic oscillator potential have been derived in I and were given by

$$E_{nl} = - V_0 + \left(N + \frac{3}{2}\right) \hbar\omega^* - \frac{\varkappa^2}{2}\left[N(N+3) + l(l+1) + \frac{9}{2}\right], \tag{1}$$

(1) W. E. Frahn and R. H. Lemmer: *Nuovo Cimento*, **5**, 1564 (1957), referred to as I.
(2) A. A. Ross, R. D. Lawson and H. Mark: *Phys. Rev.*, **104**, 401 (1956).
(3) A. A. Ross, H. Mark and R. D. Lawson: *Phys. Rev.*, **102**, 1613 (1956).

($N = 2n + l = 0, 1, 2, \ldots$), with

$$\omega^* = \left(\frac{M_0}{M^*}\right)^{\frac{1}{2}} \omega\,; \qquad \frac{M_0}{M^*} = 1 + \frac{a^2 V_0}{2\hbar^2} M_0\,; \qquad \varkappa^2 = \frac{1}{8} M_0 \omega^2 a^2\,. \tag{2a, b, c}$$

The normalized eigenfunctions, obtained by a first order perturbation calculation, are

$$u_{nl}(r) = u_{nl}^{(0)}(r) + \frac{\varkappa^2}{4\hbar\omega^*}\left\{\left[n(n-1)\left(n+l-\frac{1}{2}\right)\left(n+l+\frac{1}{2}\right)\right]^{\frac{1}{2}} u_{n-2,l}^{(0)}(r) - \right.$$
$$\left. - \left[(n+1)(n+2)\left(n+l+\frac{3}{2}\right)\left(n+l+\frac{5}{2}\right)\right]^{\frac{1}{2}} u_{n+2,l}^{(0)}(r)\right\}, \tag{3}$$

where $u_{nl}^{(0)}(r)$ denotes the normalized radial oscillator wave function (I.29).

In order to discuss the main effects of the velocity dependence, we compare the oscillator potential

$$V(r) = -V_0 + \tfrac{1}{2} M_0 \omega^2 r^2\,, \tag{4}$$

with that of the corresponding static model defined by

$$V_s(r) = -V_{0,s} + \tfrac{1}{2} M_0 \omega_s^2 r^2\,. \tag{5}$$

The expectation values of r^2 for the single-particle states are

$$\langle r^2 \rangle = \frac{\hbar}{M^* \omega^*}\left(N + \frac{3}{2}\right); \qquad \langle r^2 \rangle_s = \frac{\hbar}{M_0 \omega_s}\left(N + \frac{3}{2}\right). \tag{6 a, b}$$

If the nuclear radius, $R = r_0 A^{\frac{1}{3}}$, is to be the same in the static and non-static cases, we have

$$\frac{\omega^*}{\omega_s} = \frac{M_0}{M^*}\,, \tag{7}$$

and from (2a):

$$\omega^* \omega_s = \omega^2\,. \tag{8}$$

In order to bind the same number of particles, the potential well depths must be related by $V_0 = (M_0/M^*) V_{0,s}$. Thus we obtain

$$V(r) = \frac{M_0}{M^*} V_s(r)\,. \tag{9}$$

The static oscillator level spacing, following from the connection between the occupation numbers and the nuclear radius, is given by [4]

$$\hbar\omega_s = \left(\frac{2}{3}\right)^{\frac{1}{3}} V_{0,s} A^{-\frac{1}{3}} = \frac{5}{4}\left(\frac{3}{2}\right)^{\frac{1}{3}} \frac{\hbar^2}{M_0 r_0^2} A^{-\frac{1}{3}}\,. \tag{10}$$

With $r_0 = 1.2 \cdot 10^{-13}$ cm we have $\hbar\omega_s = 41 A^{-\frac{1}{3}}$ MeV.

---

[4] V. F. WEISSKOPF: *Nucl. Phys.*, 3, 423 (1957).

Both empirical and theoretical evidence ([1,5]) lead consistently to the value $M^*/M_0 = 0.5$ for the nucleon mass reduction at the centre of the nucleus. This value will be assumed throughout the following calculations. The level spacing of the velocity-dependent oscillator is then given by $\hbar\omega^* = 2\hbar\omega_s = 82A^{-\frac{1}{3}}$ MeV, which is in accordance with the requirements from the nuclear photoeffect ([6]). From (10) we further obtain $V_{0s} = 47$ MeV and we thus have $V_0 = 94$ MeV. From (2b) and (10) then follows for the non-local range parameter

$$a = \frac{2}{\sqrt{5}}\left(\frac{2}{3}\right)^{\frac{1}{3}} r_0 = 0.94\cdot 10^{-13}\ \text{cm}\ . \tag{11}$$

The main effects of the velocity-dependence are thus an increase in the level spacing and the well depth by a factor two. Besides that, the non-static interaction removes the (n, l)-degeneracy of the oscillator levels so that the higher angular momentum states are more strongly bound than the lower l-states. This feature makes the velocity-dependent oscillator potential a suitable starting point for the construction of shell model level schemes.

3. – In order to obtain proper shell structure, we add a spin-orbit coupling term of the Thomas type to the interaction Hamiltonian, with a phenomenological parameter λ:

$$H_{\text{s.o.}} = -\lambda\frac{\hbar^2}{4M_0^2c^2}\left(\frac{1}{r}\frac{\partial V}{\partial r}\right)(\boldsymbol{\sigma}\boldsymbol{l})\ . \tag{12}$$

For the oscillator potential (4) we get

$$E_{\text{s.o.}} = -\lambda\frac{(\hbar\omega)^2}{4M_0c^2}\cdot\begin{cases} l & (j = l + \frac{1}{2}),\\ -(l+1) & (j = l - \frac{1}{2}).\end{cases} \tag{13}$$

Fig. 1 shows the neutron level schemes, calculated from (1) and (13) as functions of the mass number A, to which $\hbar\omega$ is related by $\hbar\omega = \sqrt{2}\hbar\omega_s = 57.8\cdot A^{-\frac{1}{3}}$ MeV. The spin-orbit coupling parameter is assumed to be $\lambda = 25$.

The general features of the level schemes, as regards the effects of the velocity dependence, show a close similarity to those obtained by ROSS, LAWSON and MARK ([2]) for the diffuse well potential. The improvement of the non-static model over the corresponding static one is seen particularly well in the case of the harmonic oscillator, where a proper shell structure is not obtained until the (n, l)-degeneracy of the static case is removed by the velocity-dependent interaction. The shell formation is still unsatisfactory in the region of higher A-values, where the lower partners of the (j, l)-doublets of higher l are too weakly bound; however, for smaller A-values these levels are strongly depressed until they eventually join the correct

---

([5]) K. A. BRUECKNER: *Phys. Rev.*, **97**, 1353 (1955); M. H. JOHNSON and E. TELLER: *Phys. Rev.*, **98**, 783 (1955); M. A. MELKANOFF, S. A. MOSZKOWSKI, J. NODVIK and D. S. SAXON: *Phys. Rev.*, **101**, 507 (1956); R. J. BLIN-STOYLE: *Nucl. Phys.*, **2**, 169 (1956); W. E. FRAHN: *Nuovo Cimento*, **4**, 313 (1956); W. E. FRAHN and R. H. LEMMER: *Nuovo Cimento*, **5**, 523 (1957).

([6]) D. H. WILKINSON: *Proc. Glasgow Conference* (1954), p. 161; S. RAND: *Phys. Rev.*, **99**, 1620 (1955); F. FULLER and H. HAYWARD: *Phys. Rev.*, **101**, 692 (1956).

shells. In the region of heavy nuclei the oscillator potential should be replaced by the more realistic diffuse well potential for which Ross, Lawson and Mark have already obtained satisfactory level schemes from the non-static model.

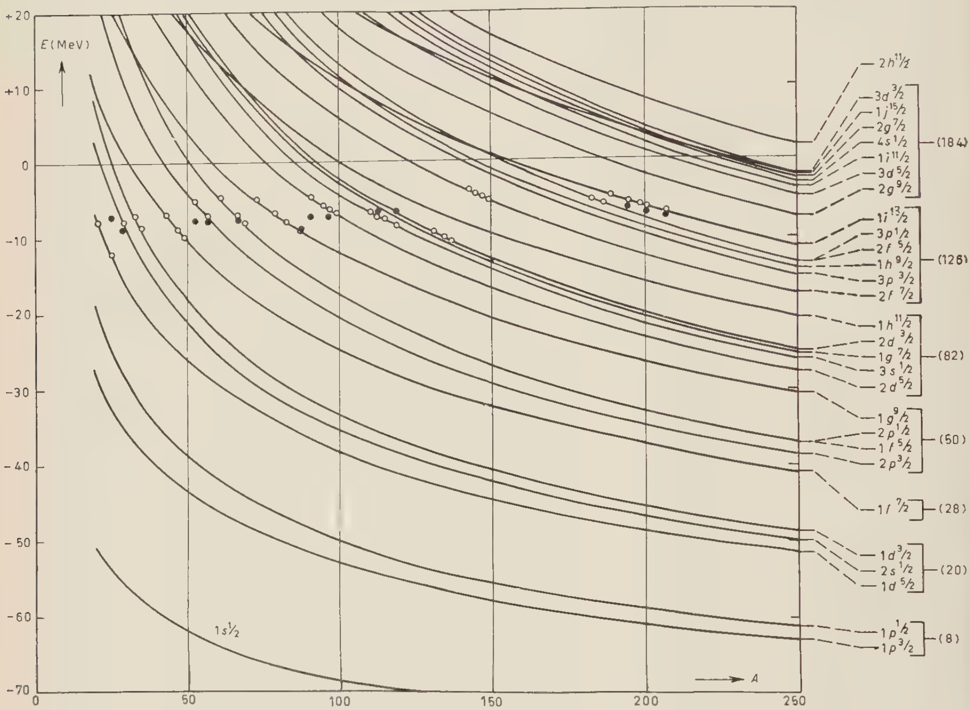

Fig. 1. – Neutron energy level schemes, calculated from (1) and (13) with the parameters: $V_0 = 94$ MeV, $r_0 = 1.2 \cdot 10^{-13}$ cm, $\lambda = 25$. The open circles denote the top neutron levels for odd-neutron nuclei, the full circles give the empirical values of (γ, n)-thresholds.

The positions of the last neutron in a level are indicated in Fig. 1 by open circles. Some empirical (γ, n)-thresholds [7] for odd-neutron nuclei are given by the full circles. It is seen that the general trend of the binding energies is reasonably well represented.

In conclusion, it may be said that although the velocity-dependent interaction studied here might still be a poor approximation to the full non-local interaction required by the many-body problem, it seems to provide a definite improvement over the corresponding static interaction.

* * *

This paper is published with permission of the South African Council for Scientific and Industrial Research.

---

(7) J. A. Harvey: *Phys. Rev.*, **81**, 353 (1951); R. Sher, J. Halpern and A. K. Mann: *Phys. Rev.*, **84**, 387 (1951).

IL NUOVO CIMENTO Vol. VI, N. 5 1° Novembre 1957

On the Thermodynamical Theory of Thermal Conduction of Dielectrics Under Electric Fields.

R. Fieschi

Istituto di Scienze Fisiche dell'Università - Milano
Istituto Nazionale di Fisica Nucleare - Sezione di Milano

(ricevuto il 4 Luglio 1957)

In a recent paper (1), by means of the methods of the thermodynamical theory of irreversible processes (2), the following expression has been derived for the thermal conductivity of dielectrics in the presence of a longitudinal electric field:

$$k = k_0 + \frac{(\sigma - \sigma_0)\theta}{(\theta_s - \theta)^2} V^2 . \tag{1}$$

The conclusions drawn by the author, that k does not depend on the sign of the field and that the dependence of k on V is quadratic, however do not hold since $\Delta\sigma = \sigma - \sigma_0$ depends on the re ltive orientation of thermal and electrical potential gradients. Indeed from the phenomenological equations it follows:

$$\Delta\sigma\,(V, \operatorname{grad}\theta) = -\,\Delta\sigma\,(-V, \operatorname{grad}\theta) = L_{12}\frac{\theta_s - \theta}{\theta V}, \tag{2}$$

hence, from (1)

$$\Delta k\,(V, \operatorname{grad}\theta) = -\,\Delta k\,(-V, \operatorname{grad}\theta) = L_{12}\frac{V}{\theta_s - \theta}, \tag{3}$$

(see Fig. 1 and 2).

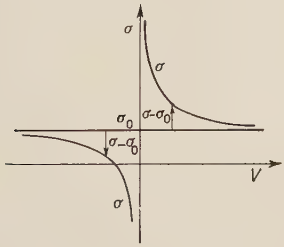

Fig. 1.

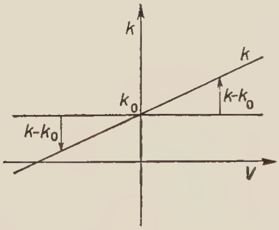

Fig. 2.

The correspondence with Dr. Mascarenhas is acknowledged.

(1) S. Mascarenhas *Nuovo Cimento*, **5**, 1118 (1957).
(2) See, for instance, S. R. De Groot: *Thermodynamics of Irreversible Processes* (Amsterdam, 1951).

3085

Radiative Beta Decay of the Pion.

J. C. Taylor

Imperial College of Science and Technology - London

(ricevuto il 5 Luglio 1957)

Theoretical estimates of the probability of the decay mode $\pi^+ \to e^+ + \nu + \gamma$ now definitely disagree with experiment (1). The theory uses only the known value of the tensor term, g_T, in the β decay of the neutron, and makes no assumption about a universal Fermi interaction. In this letter it is shown that the disagreement is removed if the pion-nucleon interaction is assumed to be pseudo-vector rather than pseudoscalar. There are no reasons against this assumption, except that the gradient coupling theory is not renormalisable.

According to Treiman and Wyld (2), whose notation we use, the matrix element chiefly responsible for the radiative β decay has the form

$$AeGg_T(\bar{\psi}_e\gamma_5\boldsymbol{\epsilon}\boldsymbol{k}\psi_\nu)\,.$$

Here $\boldsymbol{k}$ and $\boldsymbol{\epsilon}$ are the photon momentum and polarisation, and A is a dimensionless number, assumed to be of order unity. In the gradient coupling theory, the matrix element must vanish with the pion momentum, P; and so, because of gauge invariance, must have one of the forms

$$Be(G/2M)g_TP^2(\bar{\psi}_e\gamma_5\boldsymbol{\epsilon}\boldsymbol{k}\psi_\nu)\,,$$

and

$$B'e(G/2M)g_T\cdot$$
$$\cdot[k\cdot P(\bar{\psi}_e\gamma_5\boldsymbol{\epsilon}\boldsymbol{P}\psi_\nu) - \varepsilon\cdot P(\bar{\psi}_e\gamma_5\boldsymbol{k}\boldsymbol{P}\psi_\nu)]\,.$$

$G/2M$ is the gradient coupling constant equivalent, in the sense of the low-energy-limit theorems, to the pseudoscalar constant, G. B and B' have the dimensions of an inverse mass, and are assumed to be of order $1/M$ (2). Thus, in either term, the probability is reduced by a factor $(P^2/M^2)^2 \sim 10^{-3}$. This reduces the estimate (1) of the branching ratio, ϱ, of radiative to normal decay, from $\varrho \sim 10^{-3}$ to $\varrho \sim 10^{-3}$, which is consistent with present experiments (1) ($\varrho < 10^{-5}$).

The reason for this difference is clear. Although the pseudo-scalar and derivative interactions are equivalent for low energy p-wave processes, they differ in their efficacy as pair producers. In fact, it is to just such processes as pion decay that we should look to distin-

---

(1) J. M. Cassels, M. Rigby, A. M. Wetherell and J. R. Wormald (to be published).

(2) S. B. Treiman and H. W. Wyld: *Phys. Rev.*, **101**, 1552 (1956).

guish between them. The gradient coupling would make no difference to π^0 decay, however, since the usual form of the interaction, $\varphi \varepsilon_{ijkl} F_{ij} F_{kl}$, already vanishes with the pion momentum.

If neutron β decay should turn out to have a vector term, it would, on the present theory, give the dominant contribution to the radiative decay of the pion. The value of ϱ would be the same as in the pseudo-scalar theory (²) for the vector term, $\varrho \sim (P^2/M^2) \cdot 10^{-3} \sim 10^{-5}$, which, is uncomfortably close to the experimental limit.

IL NUOVO CIMENTO Vol. VI, N. 5 1° Novembre 1957

Pinched Discharge and Thermonuclear Reactors.

J. W. Gardner

Atomic Power Division, English Electric Co., Ltd. - Whetstone, Leics. - England

(ricevuto il 9 Agosto 1957)

One of the main obstacles to the production of useful thermonuclear power is the containment of the reacting gas at a temperature of 10^8 or 10^9 degrees absolute. The self-constricted discharge has been widely discussed as a possible means of achieving this end. [See, for example, recent reviews by Post (1) and by Thompson (2)]. However it is well known that an ionized gas confined by a magnetic field is subject to many instabilities and, as Thompson has pointed out (2), further progress depends, among other things, on a thorough mathematical analysis of these instabilities, including the search for stable configurations. The purpose of the present note is to indicate a possible analytical approach to the study of one of these instabilities, namely the «kinking» of the pinched discharge.

Some years ago the present writer had occasion to examine the problem of confining charged particles by cylindrical and toroidal magnetic fields (3). For the purpose in hand it proved unnecessary to work out the detailed motions of the particles: an examination of the form of the Lagrangian was sufficient to disclose the conditions of initial projection and magnetic field strength under which the motion would be confined. However, in an unpublished extension to this work (4) the detailed particle motions in the cylindrical field were obtained by an approximate method which treated the cylindrical field as a perturbation of a uniform field. Briefly the procedure was as follows. Coordinates x', y', z' were introduced which were related to a particle's cylindrical coordinates (r, θ, z) by $x' = r - a$, $y' = z$, $z' = a\theta$, a being the time average of r; the magnetic field H was then expanded in powers of x'/a and corresponding expansions introduced for x', y', z'. Substituting these expansions in the Lorentz equations of motion and equating terms of the same order on the right and left sides yielded an infinite family of equations, the zero order equation representing motion in a truly uniform field and the higher order equations representing perturbations from

(1) R. F. Post: *Rev. Mod. Phys.*, **28**, 338 (1956).

(2) W. B. Thompson: *Nature*, **179**, 886 (1957).

(3) J. W. Gardner: *Proc. Phys. Soc.*, B **62**, 300 (1949).

(4) J. W. Gardner: *M. Sc. Thesis* (Birmingham University, 1948).

3088

this motion due to the (cylindrical) non-uniformity of H. The first and second order equations were solved and gave results (e.g. for self-confinement and drift velocity) consistent with the exact treatment. Moreover the perturbation theory yielded a result which would have been unobtainable from the exact theory, without laborious numerical integration. This result is a relation between the total current and thermal energy in the pinched discharge, namely:

$$I^2 \propto NkT ,$$

where I is the current in e.m.u., N is the number of particles per cm length, k is Boltzmann's constant and T absolute temperature. The proportionality constant was shown to be of the order of, but somewhat greater than, unity; as is well known the conventional derivation of this relation, using the balance between kinetic and magnetic pressures assigns the value 2 for the proportionality constant.

The very reasonable results obtained by treating the cylindrical field as a perturbation of a uniform field encourage one to hope for some success in representing a local toroidal field as a perturbation of a cylindrical field; such a treatment would yield more detailed, albeit approximate, information about the particle motions than can be extracted by the approach of reference [3]. Now, when a pinched discharge « kinks » the self-magnetic field changes locally from cylindrical to toroidal: it is suggested therefore that the perturbation treatment of a toroidal field may well prove a useful tool for the theoretical analysis of this instability, which at present obstructs the exploitation of the pinched discharge as the principle of a thermonuclear reactor.

IL NUOVO CIMENTO Vol. VI, N. 5 1° Novembre 1957

μ-Meson Decay in the Theory of Individual Mass Reversal and in the Two Component Theory of Neutrino.

H. Segawa and S. Hori (*)

Faculty of Liberal Arts - Fukui University
(*) *Institute for Theoretical Physics - Kanazawa University*

(ricevuto il 22 Agosto 1957)

In a previous paper (¹), one of the authors proposed the theory of Individual Mass Reversal, based on the assumption that every existing interaction does not allow to measure signs of masses of all elementary particles. The theory predicts almost the same results for β- and π-μ decays as the two component theory of neutrino (²). Thus the muon emitted in π-μ decay undergoes complete polarization also in our theory, the only difference being that in contrast to the two component theory the muon can have either spirality right or left (in our theory) independently of the observed anisotropy in the β-decay experiments (³).

Possible forms of the μ-e decay interaction in our theory are classified into the following mutually excluding four types (¹):

$$\mathcal{H}_{\mu e} = \sum_i g_i[\bar{\mu}(1 \mp \gamma_5)O^i e](\bar{\nu}O^i\nu)\,, \tag{1}$$

(1a) (I) upper sign, $g_V = g_A = 0$,

(1b) (II) upper sign, $g_S = g_T = g_P = 0$,

(1c) (III) lower sign, $g_V = g_A = 0$,

(1d) (IV) lower sign, $g_S = g_T = g_P = 0$.

When the muon has right-hand spirality and decays with emission of one neutrino and one antineutrino, the distribution function for the μ-decay at rest is

$$w^{\mathrm{II}} \sim [3 - 2x - (2x - 1)\cos\theta]x^2\,\mathrm{d}x\,\mathrm{d}\Omega\,, \tag{2}$$

(¹) S. Hori and A. Wakasa: *Nuovo Cimento* (to be published).
(²) T. D. Lee and C. N. Yang: *Phys. Rev.*, **105**, 1671 (1957).
(³) C. S. Wu, E. Ambler, R. E. Hayward, D. D. Hoppes and R. P. Hudson: *Phys. Rev.*, **105**, 1415 (1957).

for the case II. This is equivalent to what was obtained in the two component theory, though $\xi = 1$ in our theory independently of the coupling constants and is not inconsistent with the experiment ([4]). The μ-decay can occur also through S, T, P interactions in our theory. For the case III,

$$(3)\quad w^{\mathrm{III}}(x,\theta) \sim \left[3(1-x) + 2\varrho(\tfrac{4}{3}x - 1) - \tfrac{1}{3}[2\varrho(5-4x) - 9(1-x)]\cos\theta\right] x^2\,\mathrm{d}x\,\mathrm{d}\Omega\,,$$

where the Michel parameter $\varrho = 6|g_T|^2/|g_S|^2 + |g_P|^2 + 6|g_T|^2$. For $\varrho = \frac{3}{4}$, w^{III} coincides with w^{II}.

In the case of emission of two identical neutrinos, only the case II is consistent with the experiment and the distribution (2) remains valid also in this case. The μ decay through S, T, P interactions is ruled out in this case simply because they give $\varrho = 0$.

When the muon has left-hand spirality, we have only to replace the case II by IV and III by I.

Another very important difference between our theory and the two component theory is polarization of the emitted positron. In our theory the emitted positron (electron) is completely polarized in the direction of its line of flight. For instance, in the case II the probability of the positron emitted with right hand or left hand spirality is given by

$$(4)\qquad w_R(x,\theta) = w^{\mathrm{II}}\,, \qquad w_L(x,\theta) = 0\,.$$

whereas

$$(5)\qquad \begin{cases} w'_R(x,\theta) \sim \frac{1}{2}|f_V + f_A|^2[3 - 2x - (2x-1)\cos\theta]x^2\,\mathrm{d}x\,\mathrm{d}\Omega\,, \\ w'_L(x,\theta) \sim \frac{1}{2}|f_V - f_A|^2[3 - 2x + (2x-1)\cos\theta]x^2\,\mathrm{d}x\,\mathrm{d}\Omega\,, \end{cases}$$

in the two component theory. Thus our case II gives the same results as the two component theory with $f_V = f_A$. Measurement of polarization of the emitted positron will be important also for the determination of relative magnitude and phase of the coupling constants in the two component theory.

([4]) R. L. Garwin, L. M. Lederman and M. Weinrich: *Phys. Rev.*, **105**, 1415 (1957).

Search for Mass-500 Particle as a K^+ Decay Product (*).

G. Harris, J. Orear and S. Taylor
Columbia University - New York

(ricevuto il 26 Agosto 1957)

If the mass-500 particle (1) is a decay product of a known particle, the only possibilities for the parent are the K-meson and the Ξ-hyperon. The K-meson decay is energetically more favorable by at least 100 MeV. For the K-meson there are two feasible cases.

Case 1.

The mass-500 particle is a lepton (μ' in our notation) with the decay modes

$$K \to \mu' + \nu$$

$$\mu' \to \begin{cases} e + 2\nu \\ \mu + 2\nu \end{cases}$$

Case 2.

The mass-500 particle is a boson (π' in our notation) with the decay modes

$$K \to \pi' + \pi^0$$

$$\pi' \to \begin{cases} e + \nu \\ \mu + \nu \end{cases}$$

In either Case 1 or 2 the mass-500 secondary would usually appear quite similar to the secondary of a $K_{\mu3}$ and could easily be misclassified as a $K_{\mu3}$ decay in nuclear emulsion. Using mass limits of 540 ± 50 electron masses (1), the secondary range in Case 1 would be $1.3\ \text{cm} < R_{\mu'} < 3.3\ \text{cm}$. For Case 2 the limits would be $0.4\ \text{cm} < R_{\pi'} < 1.4\ \text{cm}$.

In a systematic study of K^+-endings with secondaries heavier than 1.25 times minimum (2) we found 32 events with secondaries between 0.4 and 3.3 cm range which were originally classified as μ^+ secondaries. These were from a total sample of about 5000 K^+ endings. We have now re-examined these 32 secondaries by carefully grain counting them at the K-ending and find them all still consistent with the muon mass. A mass-500 particle would give a grain density about 40% higher than that expected for a muon of the same range.

We conclude that in our sample of 5000 K-endings, there is not one case of a mass-500 particle as a decay product.

(*) Research supported by the Office of Naval Research, the U. S. Atomic Energy Commission, and a research grant from the National Science Foundation.

(1) Alikhanian *et al.*: *Žur. Èksp. i Teoret. Fiz.*, **31**, 955 (1956).

(2) J. Orear, G. Harris and S. Taylor: *Phys. Rev.*, **104**, 1463 (1956), and S. Taylor, G. Harris and J. Orear: *Bull. Am. Phys. Soc.*, **2**, 20 (1957).

3092

Additional Remarks and Errata Corrige to a Paper on the Theory of Spin 2 Particles.

T. Regge

Istituto Nazionale di Fisica Nucleare - Sezione di Torino

(ricevuto il 6 Settembre 1957)

We apologize here for some misprints which appeared on a recent paper (1) by the author. A list of them is given at the end of this letter. At the same time we thought it useful to point out some additional properties of the γ_μ matrices, discovered after the paper was published. These properties considerably simplify the calculation of useful quantities like traces of products of several γ_μ matrices. To show them we follow here the same kind of algorithm already used in (1) and to which the reader is referred. In the following A_μ, B_μ etc. are any completely commutable vectors. We define barred operators as $\mathfrak{A} = A_\mu \gamma_\mu$, etc.

Then from the definition of the (p. 328) and a rather easy but lengthy calculation one can prove the following identities:

$$\mathfrak{A}\mathfrak{B}\mathfrak{C} + \mathfrak{B}\mathfrak{C}\mathfrak{A} + \mathfrak{C}\mathfrak{A}\mathfrak{B} = \mathfrak{B}\mathfrak{A}\mathfrak{C} + \mathfrak{C}\mathfrak{B}\mathfrak{A} + \mathfrak{A}\mathfrak{C}\mathfrak{B} \, , \tag{1}$$

$$(\mathfrak{A}\mathfrak{B} - \mathfrak{B}\mathfrak{A})\mathfrak{C}(\mathfrak{D}\mathfrak{E} - \mathfrak{E}\mathfrak{D}) = 0 \, . \tag{2}$$

They are consistent with the trace of six γ_μ matrices (see p. 331).

Finally we give here the list of the misprints:

page	instead of:	read:
327	$(\frac{3}{2}, \frac{1}{2})\ \frac{1}{2}, \frac{3}{2})(\frac{1}{2}, \frac{1}{2})$	$(\frac{3}{2}, \frac{1}{2})(\frac{1}{2}, \frac{3}{2})(\frac{1}{2}, \frac{1}{2})$
327	to formula (4) add	$\lvert \mu\mu\nu \rangle = 0.$
327-8	to formula (5) add	$\langle \mu\lambda \lvert \rangle = 0 \quad \langle \mu\lambda\nu \lvert \rangle = 0 \quad \langle \mu\lambda\nu \lvert \varrho \rangle = 0$
328	$L = -\overline{\Psi}(\eth + m)\Psi$	$L = -\overline{\Psi}(\eth + m)\Psi$ where $\eth = \partial_\mu \gamma^\mu$
329	$\langle v^\varrho_\sigma \lvert v^P_\tau \rangle$	$\langle v^P_\sigma \lvert v^P_\tau \rangle$

(1) T. Regge: *Nuovo Cimento*, **5**, 325 (1957).

page	instead of:	read:
329	$(\mathfrak{P}^4 = im\mathfrak{P}^3)/2m^4$	$(\mathfrak{P}^4 - im\mathfrak{P}^3)/2m^4$
	$(\mathfrak{P}^4 + im\mathfrak{P}^3)/em^4$	$(\mathfrak{P}^4 + im\mathfrak{P}^3)2m^4$
329	$K = \sum_{\tau\sigma} \lvert\langle v^P_\sigma \lvert A \rvert v^Q_\tau\rangle\rvert^2$	$K = \sum_{\sigma\tau} \lvert\langle v^P_\sigma \lvert A \rvert v^Q_\tau\rangle\rvert^2$
330	$10\lambda_1 + 4\lambda_2$	$10\lambda_2 + 4\lambda_1$
332	$\ldots \frac{13}{45} P^2Q^2[P^2(QE)^2 + Q^2(PE)^2]$	$\ldots \frac{13}{90} P^2Q^2[P^2(QE)^2 + Q^2(PE)^2]$
	$- \frac{1}{18} (PQ)^2 \cdot [P^2(QE)^2 + Q^2(PE)^2]$	$+ \frac{1}{36} (PQ)^2[P^2(QE)^2 + Q^2(PE)^2]$
333	$\frac{1}{5} \sum_{\sigma\tau} \lvert\langle v^{P_i}_\sigma \lvert \mathfrak{E} \rvert v^{P_f}_\sigma\rangle\rvert^2$	$\frac{1}{5} \sum_{\sigma\tau} \lvert\langle v^{P_i}_\sigma \lvert \mathfrak{E} \rvert v^{P_f}_\tau\rangle\rvert^2$
	$= \frac{1}{2m^8} \langle \ldots - m^2\mathfrak{P}^3_i\mathfrak{E}\mathfrak{P}_f\mathfrak{E}^3\rangle$	$= \frac{1}{2m^8} \langle \ldots - m^2\mathfrak{P}^3_i\mathfrak{E}\mathfrak{P}^3_f\mathfrak{E}\rangle$
334	$\langle P_1\overline{P}_2P_3 \lvert \varepsilon\mathfrak{P} : \varepsilon \rvert \mathrm{B}_1\mathrm{B}_2\mathrm{B}_3\rangle$	$\langle P_1\overline{P}_2P_3 \lvert \varepsilon\mathfrak{P}^4_i\varepsilon \rvert \overline{P_1P_2}P_3\rangle$

IL NUOVO CIMENTO VOL. VI, N. 5 1° Novembre 1957

The Principle of the Minimum Number of States at Weak Interactions.

G. MARX

Institute for Theoretical Physics of Eötvös University
Central Research Institute for Physics, Department of Atomphysics - Budapest

(ricevuto il 10 Settembre 1957)

In the years past two attempts have been made to restrict the possibilities allowed by the « classical » theory of weak interactions:

1) *The conservation of the fermion charge,* suggested (simultaneously but independent of each other in 1952-1953) by G. MARX [1], YA. B. ZELDOVICH [2] and by E. KONOPINSKI and H. M. MAHMOUD [3] (*).

2) *The neutrino theory of Majorana* which — conserving the P (space inversion) and C (charge conjugation) invariance — reduces the neutrino states to half their former number.

Generalizing the basic idea of Majorana it seems to be obvious to introduce the following hypothesis: *the number of the states of an elementary particle existing in Nature is minimum; when determining the minimum number of states the invariance requirements of its interactions have of course to be taken into account.* Formulating this mathematically: Every elementary particle is described by a field quantity corresponding to an *irreducible* representation of *all* the symmetry transformations of interactions.

This idea is accepted generally for the proper Lorentz transformations (*). Experience confirms that the field quantity describing any of the elementary particles transforms according to an irreducible representation of the Lorentz group. (The same is true for the isotopic transformation character of hot part-

(1) G. MARX: *Acta Phys. Hung.*, **3**, 55 (1953); *Zeits. f. Naturfor.*, **9a**, 1051 (1954).

(2) A. B. ZELDOVICH: *Dokl. Akad. Nauk SSSR*, **91**, 1317 (1953).

(3) E. KONOPINSKI and H. M. MAHMOUD: *Phys. Rev.*, **92**, 1045 (1953).

(*) Considering that the behaviour of baryons at weak interactions (β-decay etc.) is very similar to that of leptons, it may be assumed that « switching out » the strong interactions the difference between baryons and leptons would be resolved. Thus it seems to be more resonable to use the first suggested designation « conservation of the fermion charge » instead of « conservation of lepton charge » which has kept spreading recently.

(*) The mimimnm postulate seems to appear at first in an early work of H. WEYL. The author is indebted to Prof. T. D. LEE for having called his attention to this fact.

icles). In contradiction to the Dirac neutrino the Majorana neutrino belongs *to an irreducible representation of the charge conjugation symmetry group.*

As experimental information on the double β-processes (*) has been accumulating, there is growing evidence for the conservation law of fermion charge. At the same time the Majorana hypothesis as well as the principle of the minimum number of states (in the case of the C transformations) seem to be contradicted. This is very surprising for thus the C transformation would be distinguished as compared to the symmetry transformations of the coordinate and isotopic spin space (+). However, recent experiments on β and μ decay have shown that (in contradiction to the Majorana hypothesis) the weak interactions are not invariant under P and C transformations, but probably are invariant under the $L=P\cdot C$ transformation. Thus the number of states of the Dirac neutrino can be reduced by half in such a way that the coordinate or the L transformation transforms the remaining state system in itself. Using this reduction the Weyl-Salam-Landau-Lee-Yang theory of the neutrino is obtained. Thus if the principle of the minimum number of states and the invariance of weak interactions under the proper Lorentz group and L transformation is accepted the two-component theory of the neutrino can be obtained directly. At the same time there will no longer be contradiction between the conservation law of fermion charge and the principle of minimum number of states (*).

Now we are going to investigate the principle of the minimum number of states in connection with other particles. The number of states of photons is minimum as permitted by the Lorentz, L and gauge groups. The reduction of the states of charged leptons in a way similar to this used for neutrinos, is forbidden by the gauge invariance. For hot particles in addition to the symmetry transformation mentioned above, also the transformations of the isotopic spin space must be taken into consideration. Really the hot particles form irreducible isotopic multiplets. The particles and antiparticles are described by multiplet pairs of identical transformation properties.

At baryons the distinction between particle and antiparticle multiplets is required by the invariance under the phase transformation which is related to the conservation of the baryon number.

The K-mesons form an isotopic doublet, while the $\overline{\text{K}}$-mesons form an other doublet. Identification of these two doublets is forbidden by the invariance requirement with respect to the rotations of the isotopic space and by the gauge invariance.

Identification of π and $\overline{\pi}$ triplets is,

(*) Here we are thinking of the lack of $2n \to 2p + 2e$ (4), $\bar{\nu} + n \to p + e$ (5) processes.

A further evidence is supported by the fact that the decay processes of the type $K^+ \to \pi^- + \mu^+ + e^+$ and $\pi^+ \to \mu^+ + \bar{\nu}$ [instead of $\pi^+ \to \mu^+ + \nu$ (6)] has not been observed yet.

(4) M. Awschalom: *Phys. Rev.*, **101**, 1041 (1956).

(5) R. Davies: *Bull. Am. Phys. Soc. Ser. II*, **1**, 219 (1956).

(6) C. N. Yang: preprint.

(+) According to a suggestion of F. Károlyházi the Dirac neutrino can be made to an irreducible representation if one takes the following symmetry transformations into account: Lorentz, P, C transformations and a constant phase tranformation (1) connected with the conservation of the fermion charge, too.

(*) From the above mentioned facts it follows that the « maximal asymmetry » of the decay will be realized. However, as is well known, this theory does not give a cogent explanation for the asymmetry of the μ-meson decay (7). It may be assumed, however, that only the one neutrino processes exist in nature. In this case the old assumption must be renewed according to which the μ-decay (perhaps even also the β-decay) takes place by the interaction of a boson K via the direct interaction $(\mu\nu) \leftrightarrow K \leftrightarrow (e\nu)$ (8). The elementary processes do not conserve the parity, thus the resulting processes must be also of the same type.

(7) B. F. Touschek: *Nuovo Cimento*, **5**, 1281 (1957).

(8) See e.g. Y. Tanikawa: preprint.

however, not forbidden by these transformations. Indeed the experiment indicates that the π-mesons form the only charge multiplet which under charge conjugation is transformed into itself.

To sum up we can say, that the principle of the minimum number of states is a postulate of universal validity for elementary particles. There does not exist a particle for which the number of observed states would exceed the minimum (such a particle would be e.g. an anti-neutrino polarized in the forward direction, a $\bar{\pi}^0$-meson or a K-meson parity doublet). It must be emphasized, of course, that before adopting this principle the proper symmetry transformations of the particle interactions must be well known. Inversely: symmetry transformations of interactions may be determined by counting the particle states.

LIBRI RICEVUTI E RECENSIONI

M. HAÏSSINSKY – *La chimie nucléaire et ses applications* (Masson et Cie, 120 boulevard, St. Germain Paris VI), pp. VI-625, figg. 136, tavole 17.5 × 25, prezzo 5 000 Frf.

Con un'elegante veste tipografica è comparsa, nel corso di quest'anno, edita a Parigi dalla casa Masson et Cie l'interessante opera di M. HAÏSSINSKY, dal titolo « La chimie nucléaire et ses applications ».

Il termine « chimica nucleare » è molto recente e si è venuto affermando man mano che l'opera della chimica si è allargata ed ha preso nuovi indirizzi nell'ambito delle complesse attività di studio e di ricerca sbocciate con l'avvento dei reattori nucleari, con la produzione in laboratorio di nuovi elementi artificiali e con la scoperta degli ultimi elementi naturali.

Per analogia con la definizione di « chimica molecolare », la chimica tradizionale che studia le reazioni e le trasformazioni delle molecole, si è inteso chiamare chimica nucleare quella che si occupa delle trasformazioni e trasmutazioni dei nuclei.

Da ciò si può comprendere quanto il chimico nucleare tenda sempre più ad essere uno stretto parente del fisico nucleare.

Nel libro in oggetto, alla chimica nucleare propriamente detta sono dedicati otto dei venticinque capitoli che lo compongono, mentre larga parte è dedicata agli elementi radioattivi ed allo studio dei fenomeni chimico fisici di quantità imponderabili di materia, alle radiazioni ed ai loro effetti ed infine agli indicatori radioattivi e isotopici.

Come si vede è stato coperto un campo vastissimo e non è stato trascurato un capitolo introduttivo in cui vengono passate in rassegna le principali tappe compiute dagli scienziati, praticamente dalla fine del secolo scorso fino ad oggi, nello studio della radioattività, della fisica e della chimica nucleari.

L'interesse di questa opera risiede soprattutto nella possibilità, che uno studioso ha, di aggiornarsi rapidamente sugli argomenti che lo interessano, dei quali sono messi in luce con chiarezza, oltre che i fondamenti, anche i legami con altre materie correlate.

La vastità e la diversità delle nozioni non generano confusione perchè gli argo-

menti sono trattati con buona sistematica e, nella sua veste sintetica, l'opera risulta sempre di piacevole consultazione. Capitoli o gruppi di capitoli sono a sè stanti e possono essere letti e compresi separatamente.

Si può dire che lo sforzo dell'autore di fornire un'opera che, in modo sintetico, costituisce la messa a punto delle innumerevoli nozioni accumulate fino ad oggi nel campo delle trasformazioni della materia su scala nucleare, sia stata coronata da successo.

Il recensore ha trovato particolarmente interessanti i capitoli riguardanti le separazioni isotopiche e l'azione chimica delle radiazioni ionizzanti: in questi capitoli infatti, oltre essere descritte le fondamentali tecniche in uso e i principali risultati raggiunti, sono riportate numerose tabelle che possono essere di notevole interesse per lo sperimentale.

Di particolare pregio è infine il fatto che tutti i principali lavori compiuti dai ricercatori in ciascuno dei campi toccati, sono stati dal prof. M. Haïssinsky, accuratamente vagliati e citati, cosicchè in tutto il libro la bibliografia assomma a circa tremila voci.

E. Cerrai

T. Pearcey – *Tavole dell'integrale di Fresnel a 6 decimali.* Cambridge, University Press, 1956, 63 pp. Pr. 12s., 6d.

Le tavole forniscono i valori, tabellati di 0.01 in 0.01 con 7 cifre decimali nell'interval o $0 \leqslant x \leqslant 1$, e con 6 cifre decimali nell'intervallo $1 \leqslant x \leqslant 50$, delle due funzioni

$$C\left(\sqrt{\frac{2x}{\pi}}\right) = \frac{1}{\sqrt{2\pi}}\int_0^x \frac{\cos t}{\sqrt{t}}\,\mathrm{d}t\,,$$

$$S\left(\sqrt{\frac{2x}{\pi}}\right) = \frac{1}{\sqrt{2\pi}}\int_0^x \frac{\sin t}{\sqrt{t}}\,\mathrm{d}t\,.$$

Per l'interpolazione, sono riportate le differenze seconde centrali là dove le differenze terze sono $\geqslant 1$. Una tabella ausiliaria, in fondo al volume, ne facilita l'uso.

La compilazione delle tavole è stata effettuata per subtabulazione, a partire da quelle fornite da Lommel e citate in Watson, *Theory of Bessel Functions*, 2ª ed. (1944), p. 744.

E. Aparo

Prof. Dr. Gerhard Heber, Oberassistent Dr. Gerhard Weber; – *Grundlagen der modernen Quantenphysik* – B. G. Teubner Verlagsgesellschaft, Leipzig, 1956 (I vol.: pagg. VI – 146, 24 figure; II vol.: pagg. VI – 138, 20 figure).

La fisica quantistica dal « dualismo della luce » fino alla teoria della rinormalizzazione della massa e carica nella elettrodinamica e nella teoria mesonica è trattata in due volumetti con complessivamente circa 280 pagine di testo.

Ci si aspetta una certa semplicità, e non si rimane delusi. Il primo volume tratta della teoria quantistica delle particelle, il secondo della teoria dei campi. Secondo gli autori lo scopo dell'opuscolo è di dare un quadro delle nozioni fondamentali sperimentali e teoriche. Non mi sembra che tale scopo venga raggiunto. È ben noto che la questione della larghezza delle linee ottiche è stato il problema base che dal « principio della corrispondenza » ha condotto alla teoria di Heisenberg. Questo problema viene discusso soltanto nella parte che tratta della matrice S. Nel primo volume, in cui viene discusso il problema della emissione di radiazione da parte di atomi eccitati, gli autori ci informano (vol. I, pag. 97) che il processo della emissione spontanea non è descrivibile nell'ambito della meccanica ondulatoria. Una generale mancanza del presente

3099

libro è la spiccata preferenza per i concetti ondulatori. Risulta che la teoria delle trasformazioni non è menzionata, fatto che impedisce al lettore di capire il vero significato delle funzioni d'onda.

L'introduzione della equazione di Dirac, basata sulle vecchie e sbagliate dicerie che suggeriscono che l'equazione di Schrödinger-Gordon è in contraddizione con generali concetti della teoria quantistica, è poco convincente. Il fatto che questa equazione serve benissimo per la descrizione di mesoni non turba gli autori nella compilazione del I volume.

Più del primo, il secondo volume assume la forma di una compilazione di formule. Manca ogni cenno sulla necessità della 2ª quantizzazione che quindi si presenta come un passatempo matematico. Non si trova nessuna spiegazione quanto alla necessità di usare regole di anti-commutazione per i fermioni. In accordo con la mancanza dell'uso di concetti della teoria delle trasformazioni il II volume trascura nel modo più assoluto la proprietà di simmetria e le leggi di conservazione che risultano dalla invarianza relativistica.

Non si può negare che lo studio del presente volume conduce ad una certa familiarità con alcune manipolazioni della teoria dei campi, familiarità che, d'altra parte, si acquista anche leggendo le già esistenti ed eccellenti presentazioni di questa materia.

B. F. TOUSCHEK

Direttore responsabile: G. POLVANI

Tipografia Compositori - Bologna

Questo fascicolo è stato licenziato dai torchi il 28-X-1957

NICOLA ZANICHELLI, EDITORE - BOLOGNA

Alcune pubblicazioni di Matematica, Fisica, Fisica matematica, Fisica tecnica e Storia della scienza.

Estratto dal Catalogo Generale 1956

MATEMATICA

CHISINI, Oscar - *Lezioni di geometria analitica e proiettiva.*
In 8°; pag. VI + 490; (1939) . . . . L. 3 000

CHISINI, Oscar - *Esercizi di geometria analitica e proiettiva.*
In 8°; pag. VI + 296; (1945) . . . . L. 2 000

ENRIQUES, Federigo - *Le superficie algebriche*
In 8°; pag. XIV + 464; (1949) . . . . L. 3 000

LORIA, Gino - *Curve sghembe speciali algebriche e trascendenti*
Volume II; in 8°; pag. 254 (1925) . . . . L. 800

RIMINI, Cesare - *Fondamenti di analisi matematica con applicazioni*
Volume I; in 8°; pag. XVIII + 550; (1948) . . . . L. 4 000
Volume II; in 8°; pag. XVI + 704; (1951) . . . . L. 6 000

SANSONE, Giovanni - *Equazioni differenziali nel campo reale*
Volume I; in 8°; pag. XVIII + 400; (1948) . . . . L. 3 000
Volume II; in 8°; pag. XVI + 476; (1949) . . . . L. 4 000

SEGRÈ, Beniamino - *Lezioni di geometria moderna*
Volume I; in 8°; pag. 196; (1948) . . . . L. 1 500

TRICOMI, Francesco - *Funzioni ellittiche*
In 8°; pag. X + 344; (1951) . . . . L. 4 500

TRICOMI, Francesco - *Funzioni analitiche*
In 8°; pag. VIII + 134; (1946) . . . . L. 1 500

(segue)

FISICA, FISICA MATEMATICA E FISICA TECNICA

BORDONI, Ugo - *Fondamenti di fisica tecnica*
Volume I; in 8°; pag. VIII + 398 . . . . L. 5 000

BRONZI, Goffredo - *La tecnica dei radiotrasmettitori*
In 8°; pag. XX + 404; (1949) . . . . L. 4 000

FINZI, Bruno - *Meccanica razionale*
Volume I; in 8°; pag. XII + 344; (1955)
Volume II; in 8°; pag. XII + 426; (1955) . . . . L. 6 000

FINZI, Bruno e PASTORI, Maria - *Calcolo tensoriale e applicazioni*
In 8°; pag. VIII + 428; (1949) . . . . L. 2 000

FOÀ, Emanuele - *Fondamenti di Termodinamica*
In 8°; pag. VIII + 256; (1951) . . . . L. 3 000

LEVI-CIVITA, Tullio e AMALDI, Ugo - *Lezioni di Meccanica razionale*
Volume I: Cinematica, Principi e Statica.
In 8°; pag. XVIII + 816; (1950) . . . . L. 5 000
Volume II: Dinamica dei sistemi con un numero finito di gradi di libertà.
Parte I; in 8°; pag. XII + 510; (1951) . . . . L. 4 000
Parte II; in 8°; pag. VI + 672; (1952) . . . . L. 5 000

LEVI-CIVITA, Tullio e AMALDI, Ugo - *Compendio di Meccanica razionale*
Volume I: Cinematica, Principi e Statica.
In 8°; pag. XII + 424; (1938) . . . . L. 2 000
Volume II: Dinamica. Cenni di Meccanica dei sistemi continui.
In 8°; pag. VIII + 310; (1938) . . . . L. 2 000

PERSICO, Enrico - *Introduzione alla Fisica Matematica, a cura di Tino Zeuli*
In 8°; pag. XVI + 434; (1941) . . . . L. 4 000

RIMINI, Cesare - *Elementi di Elettrotecnica generale e di Teoria delle macchine*
In 8°; pag. XX + 806; (1951) . . . . L. 4 000

RIMINI, Cesare - *Fondamenti di Radiotecnica generale*
In 8°; pag. XX + 784; (1948) . . . . L. 4 500

TORALDO DI FRANCIA, Giuliano - *Onde elettromagnetiche*
In 8°; pag. XIV + 286; (1953) . . . . L. 3 000

(*segue*)

NICOLA ZANICHELLI, EDITORE - BOLOGNA

Estratto dal Catalogo Generale 1956

RACCOLTE DI SCRITTI DI MATEMATICI E FISICI

BURGATTI, Pietro - *Memorie scelte*
In 8°; pag. VI + 354; (1951) . . . . L. 2 500

CASTELNUOVO, Guido - *Memorie scelte*
In 8°; pag. X + 588 (1937) . . . . L. 1250

LEVI-CIVITA, Tullio - *Opere matematiche. Memorie e note pubblicate a cura dell'Accademia Nazionale dei Lincei.*
Volume I; dal 1893 al 1900.
In 8°; pag. XXXII + 564; (1954) . . . . L. 8 000

MELLONI, Macedonio - *Opere pubblicate sotto gli auspici dell'Università di Parma e della Società Italiana di Fisica, a cura di G. Polvani e G. Todesco*
Volume I - La Thermochrôse ou la Coloration calorifique.
In 8°; pag. [z] + XXXII + 358 + tavola fuori testo; (1954) . . . . L. 5 000
(In preparazione i Volumi successivi)

RIGHI, Augusto - *Scelta di scritti, pubblicati sotto gli auspici della Società Italiana di Fisica, a cura di G. C. Dalla Noce e G. Valle*
In 8°; pag. 374; (1951) . . . . L. 4 000

TORRICELLI, Evangelista - *Opere edite, col concorso del Comune di Faenza da Gino Loria e Giuseppe Vassura.*
Volume I: Geometria.
Parte I; in 8°; pag. XXXVIII + 407; (1919).
Parte II; in 8°; pag. 482 + 2 tavole fuori testo; (1919).
Volume II: Lezioni accademiche. Meccanica. Scritti vari.
In 8°; pag. 320 + 4 tavole fuori testo; (1919).
Volume III: Racconto di alcuni problemi. Carteggio scientifico.
In 8°; pag. 521; (1919).
Volume IV: Documenti alla vita. Documenti alle opere. Appendice.
In 8°; pag. 436 + 5 tavole fuori testo (1944).
Complessivamente, tutti e quattro i volumi . . . . L. 2 500

VOLTA, Alessandro - *Epistolario, Edizione Nazionale sotto gli auspici dell'Istituto Lombardo di Scienze e Lettere e della Società Italiana di Fisica*
Volume I: dal 1761 al 1780.
In 4°; pag. XVII + 518 + 16 tavole fuori testo; (1949) . . . . L. 5 000
Volume II: dal 1780 al 1788.
In 4°; pag. XXIV + 568 + 16 tavole fuori testo; (1951) . . . . L. 5 000
Volume III: dal 1788 al 1800.
In 4°; pag. XXII + 576 + 17 tavole fuori testo; (1953) . . . . L. 5 000
Volume IV: dal 1800 al 1805.
In 4°; pag. XXII + 578 + 16 tavole fuori testo; (1954) . . . . L. 6 000
Volume V: dal 1805 al 1827.
In 4°; pag. XXV + 564 + 16 tavole fuori testo; (1955) . . . . L. 6 000
(In preparazione un Volume di *Aggiunte alle Opere e all'Epistolario*)

STORIA DELLA SCIENZA

ENRIQUES, Federigo e DE SANTILLANA, Giorgio - *Compendio di storia del pensiero scientifico*
In 16°; pag. VI + 482; (1937) . . . . L. 900

ENRIQUES, Federigo e MAZZIOTTI, Manlio - *Le dottrine di Democrito d'Abdera*
In 8°; pag. XXII + 340; (1938) . . . . L. 1 500

DOMUS GALILÆANA

PISA - VIA S. MARIA, 18

EDIZIONI PROPRIE

- SCRITTORI ITALIANI DI SCIENZE FISICHE E MATEMATICHE.

O. F. MOSSOTTI - *Scritti raccolti da* LUIGI GABBA † *e* GIOVANNI POLVANI.

Volume I: *Scritti di Astronomia, Geodesia e Matematica.*
Pisa, 1942; pag. VI + 448 . . . . L. **3 000**

Volume II:
Tomo primo: *Scritti di Fisica, Meteorologia e vari.*
Pisa, 1951; pag. VI + 444 . . . . L. **4 000**

Tomo secondo: "*Nuova teoria degli Stromenti ottici*„
Pisa, 1954; pag. VIII + [h] + 308 . . . . L. **4 000**

Tutta l'opera completa (cioè il Volume I e i due Tomi del Volume II) . . . . L. **10 000**

- STUDI DI STORIA DELLE SCIENZE FISICHE E MATEMATICHE.

G. POLVANI - *Alessandro Volta.*
Pisa, 1942; pag. X + 488 . . . . L. **2 500**

- QUADERNI DI STORIA E CRITICA DELLE SCIENZE

R. GIACOMELLI - *Galileo Galilei giovane e il suo "De Motu„*
Pisa, 1949; pag. 108 . . . . L. **600**

A. AGOSTINI - *Le prospettive e le ombre nelle opere di Leonardo da Vinci.*
Pisa, 1954; pag. 48 . . . . L. **550**

E. TORRICELLI - "*De infinitis spiralibus*„ - *Introduzione, riordinamento, revisione del testo sul manoscritto originale, traduzione e commento a cura di* ETTORE CARRUCCIO.
Pisa, 1955; pag. 78 . . . . L. **700**

EDIZIONI ALTRUI
SOTTO GLI AUSPICI DELLA DOMUS GALILÆANA

GALILEO GALILEI - "*Sidereus Nuncius*„ - *Traduzione con testo a fronte, prefazione e note di* MARIA TIMPANARO CARDINI
Firenze (Editore Sansoni), 1948; pag. XVIII + 92 . . . . L. **700**